Myeloid Differentiation of Resident Vascular Stem Cells (mVSCs) into Macrophage-Like Cells (MLCs) in Response to Ox-LDL and Cholesterol

A dissertation for the degree of M.Sc
by
Muhayla Alanazi, BSc

Under the supervision of
Prof Paul A. Cahill

School of Biotechnology
Dublin City University

August 2024

Pre-examination Copy 01-11-2023

Declaration

I hereby certify that this material, which I now submit for assessment on the programme of study leading to the award of MSC is entirely my own work, and that I have exercised reasonable care to ensure that the work is original, and does not to the best of my knowledge breach any law of copyright, and has not been taken from the work of others save and to the extent that such work has been cited and acknowledged within the text of my work

Name: Muhayla Alanazi **Student number** :18212662

SIGNATURE: DATE: 27-08-2024

Acknowledgements

I heard one day that women cannot be independent! ..in the stage of her early life she depends on her father, when she gets married, depends on her husband and then when she is old depends on her sons, so I decided to not be like that and show that many females are strongly capable of independency, and also can be the master of our destiny, the only way to achieve this by being educated.

I am writing to express my heartfelt gratitude to those who are part of my journey for the unwavering support and encouragement I have received during my study period. Your guidance and assistance have played an indispensable role in helping me reach this significant milestone in my academic journey.

First and foremost, I would like to extend my deepest appreciation to my family. Your unwavering belief in me, your sacrifices, and your enduring support have been my pillars of strength throughout this endeavor. Your love and encouragement have been my constant motivation, and I am profoundly grateful for everything you have done to make my educational aspirations a reality. Special thanks to my parent who supported me from the beginning in this journey and have given me the full confidence to chase my dreams.

Next, I am so thankful to my country for giving me this opportunity and provide me and thousands of other students with all support and facilities in order to be success and professionally qualified to lead our country to more prosperity and growth.

To my great supervisor Prof Paul Cahill, I want to express my sincere gratitude for your mentorship, expertise, and dedication to my academic and professional growth which has been invaluable. Your guidance has not only enriched my knowledge but has also inspired me to strive for excellence. I am fortunate to have had the opportunity to learn from you, and I am deeply thankful for your support throughout my research. I will be grateful forever to you and will never forget all the support and encouragement you provided. You kept reminding me always that I am capable of achieving my master's and I am strong enough to go further in this journey. You have always been there to address my troubles and frustrations during this time. Thank so much.

To my friends Roya, Imen and Yousef, your camaraderie and collaboration has been instrumental in creating a positive and enriching learning environment. I am grateful for the camaraderie we shared, the insights we exchanged, and the collective efforts that made our academic journey more enjoyable and rewarding. I would also like to extend my thanks to you for all provided assistance, advice, and encouragement during my study period. Your contributions, no matter how big or small, have made a difference in my academic pursuits. To my soulmate Manal, thank you too for being with me on this journey, I never felt that there is a such great distance between us.

As I embark on the next chapter of my life, I carry with me the knowledge, experiences, and relationships I have gained during this period of study. Your support has been a source of strength, and I am deeply appreciative of your role in my academic success.

Table of Contents:

acknowledgements ..... **III**

Abbreviations ..... ERROR! BOOKMARK NOT DEFINED.

Units ..... **Ix**

List Of Figures: ..... **X**

List Of Tables: ..... **Xiv**

Abstract **1**

Chapter 1 ..... **2**

1.1 Cardiovascular Disease (Cvd), A Worldwide Killer. ..... ERROR! BOOKMARK NOT DEFINED.

1.2 Vascular Structure (What's Inside The Blood Vessels) ..... ERROR! BOOKMARK NOT DEFINED.

1.3 Subclinical Arteriosclerosis: Model Systems For Investigation ..... ERROR! BOOKMARK NOT DEFINED.

1.4 Arteriosclerosis **12**

1.5 The Neointima, The Key To Detecting Asymptomatic Atherosclerosis. **15**

1.6 Macrophages……..……..**22**

1.7 Aims And Objectives……..…… **53**

Chapter 2 ..... **55**

Materials & Methods **55**

2.1 Biological Materials **56**

2.2 Methods: **64**

2.3 Cell Characterisation **75**

2.4 Myeloid Inductive Stimuli **83**

2.5 Data Analysis And Management **84**

Chapter 3 ..... **85**

The Effects Of Myeloid Induction Stimuli On Myeloid Differentiation Of Mouse Vascular Smooth Muscle Cells (Vsmcs) And Resident S100β Stem Cells (Mvscs) **85**

3.1 Introduction: **86**

3.2 Methods **89**

3.3 Results **92**

3.4 Summary **119**

3.5 Discussion **120**

Chapter 4 ..... **126**

The Effects Of Myeloid Induction Stimuli On Myeloid Differentiation Of Human Vascular Smooth Muscle Cells (Hsmcs) And Hipsc-Derived S100β Stem Cells (Sneps) **126**

4.1 Introduction: **127**

4.2 Methods: **128**

4.3 Results **132**

4.4 Summary **162**

4.5 Discussion **163**
Chapter 5 ..... **167**
General Discussion **167**
5.1 General Discussion **168**
5.2 Conclusion **172**
5.3 Future Work **172**
Bibliography **175**

Abbreviations

ACS	Acute coronary syndromes
BAT	Brown adipose tissue
BMD-SC	Bone Marrow Derived Stem Cell
BSA	Bovine Serum Albumin
cDNA	Complementary DNA
CHD	Coronary heart disease
Cnn1	Calponin1
CO2	Carbon Dioxide
CVD	Cardiovascular Disease
DAPI	4',6-diamidino-2-phenylindole
DEPC	Diethylpyrocarbonate
DMEM	Dulbecco's Modified Essential Medium
DMSO	Dimethyl Sulfoxide
DNA	Deoxyribose Nucleic Acid
DPBS	Dulbecco's Phosphate Buffered Saline
ECs	Endothelial Cells
ECM	Extracellular Matrix
EMEM	Eagle's Minimum Essential Medium
FBS	Fetal Bovine Serum
FGF	Fibroblast Growth Factor
GAPDH	Glyceraldehyde 3-phosphate dehydrogenase
GEO	Gene Expression Omnibus
HAND2	Heart and Neural Crest Derivatives Expressed 2
HBSS	Hank's balanced salt solution
HF	Heart failure
HiPSC	Human induced Pluripotent Stem Cells
HPRT	Hypoxanthine phosphoribosyltransferase 1
HRP	Horseradish Peroxidase

hPSCs	Human Pluripotent stem cells
IgG	Immunoglobulin
iECs	Induced endothelial cells
iPSC	Induced Pluripotent Stem Cells
ISR	In-stent restenosis
KLF4	Krüppel-like factor 4
LB	Lysis buffer
LCA	Left carotid artery
Lpl	Lipoprotein lipase
mAA-vSC	Mouse Aortic Arch Vascular Stem Cell
IMT	Medial intimal thickening
MSC	Mesenchymal Stromal Stem Cell
MV	Matrix vesicles
mVSC	Multipotent Vascular Stem Cell
MM1	Maintenance Medium 1
mRNA	Messenger RNA
Myh11	Myosin Heavy-chain 11
MLC	Macrophage like cell
MYOCD	Myocardin
NICD	Notch Intracellular Domain
NGS	Next-generation sequencing
NECD	Notch Extracellular Domain
Ox-LDL	Oxidized low density lipoprotein
PMA	Paramethoxyamphetamine
P/S	Penicillin-Streptomycin
PBS	Phosphate Buffer Saline
PCR	Polymerase Chain Reaction
PDGF	Platelet Derived Growth Factor
PSCs	Pluripotent stem cells
PTMs	Post-translational modifications
RT-qPCR	Quantitative Reverse Transcriptase Polymerase Chain Reaction

RCA	Right carotid artery
RCP	Rolling circle product
RNA	Ribonucleic Acid
RIPA	Radioimmunoprecipitation assay
RT	Reverse transcriptase
RT	Room Temperature
S100β	S100 calcium-binding protein β
Sca-1	Stem Cell Antigen-1
SiRNA	Short interfering RNA
SM22α	Smooth Muscle 22 alpha
SMC	Smooth Muscle Cell
SMMHC	Smooth Muscle Myosin Heavy Chain
SNEPs.	HiPSC-derived Spontaneous Neuroectoderm Progenitor Stem Cells
SRF	Serum Response Factor
TDA	Thymine-DNA glycosylase
TET	Ten-eleven-translocation
TGF-β	Transforming Growth Factor Beta
vSC	Vascular Stem Cell
VEGF	Vascular Endothelial Growth Factor
vSMC	Vascular Smooth Muscle Cell
MDM	Monocyte Derived Macrophages
TRM	Tissue-Resident Macrophages

Units

°C Degrees Celsius
cm centimetre
g grams
hr hour
L liter
M molar
mg milligram
min minute
mL millilitre
mM millimolar
nm nanometre
nM nanomolar
rpm revolutions per minute
sec second
µL microliter
µg microgram
µm micrometre
µM micromolar

List of Figures:

Figure 1.1 A cross section of a healthy arterial wall.

Figure 1.2. Arterial architecture in normal vessels compared with arteriosclerotic (without lipid) and atherosclerotic (with lipid) vessels with lesions.

Figure1.3 Origin of neointimal vSMCs.

Figure1.4 Macrophage Subtypes in Atherosclerosis.

Figure 1.5 Macrophages polarization.

Figure 1.6 Overview of phagocytosis mechanisms by macrophages.

Figure 1.7 Uptake of LDL into Macrophages.

Figure 1.8 Overview of macrophage function during each stage of atherosclerosis.

Figure 1.9 The origin of macrophages within arteriosclerotic lesions.

Figure 1.10 Overview of monocyte-endothelial cell interaction and transmigration.

Figure 1.11 Schematic to illustrate strategy to address whether mVSCs and vSMCs undergo myeloid differentiation *in vitro*.

Figure 2.1 Overview of vascular smooth muscle cells (vSMCs), de-differentiated SMCs and resident multipotent vascular stem cells (mVSCs) used in this study.

Figure 2.2 Removal of the adventitial layer following enzymatic treatment.

Figure 2.3 Tissue pieces on a CellStart pre-coated 6-well plate.

Figure 2.4 Schematic illustration of the sequential seeding step on a CellStart™ pre-coated 6-well plate after cell enzymatic dissociation.

Figure 2.5 Schematic illustration of the seeding steps of the modified enzymatic dispersion protocol.

Figure 2.6 Morphological changes in cells following treatment with myogenic inductive stimuli.

Figure 2.7 Morphological changes in THP-1 monocytes before and after PMA to induce myeloid differentiation

Figure 2.8 Schematic of Cryopreservation Protocol

Figure 2.9 Schematic of immunocytochemistry (ICC) Protocol.

Figure 2.10 Confirmation of macrophage marker, MacII in J774A-1 cells, SMC marker, Cnn1 in MOVAS and S100β in mVSC cells using ICC.

Figure 2.11 Steps for RNA Isolation from cells

Figure 2.12 Schematic of RT-qPCR Protocol.

Figure 2.13 Real time Polymerase Chain Reaction RT-PCR

Figure 2.14 Schematic of representation of histochemical staining of lipid with Oil Red O stain

Figure 2.15 Gating strategy for flow cyto metery.

Figure 3.1 Characterization of mVSC and MOVAS SMCs by ICC.

Figure 3.2 Characterization of J774A-1 macrophages

Figure 3.3 Morphological changes in cells following treatment with myeloid inductive stimuli.

Figure 3.4 Lipid uptake in cells in cells following treatment with myeloid inductive stimuli.

Figure 3.5 The expression of myeloid genes *Cd68, MacII* and *F4/80* in (A) MOVAS SMCs and (B) S100β mVSCs following treatment with myeloid differentiation inductive stimuli.

Figure 3.6 Comparison of the expression of myeloid genes (A) *Cd68, (B) MacII* and (C) *F4/80* between MOVAS SMCs and S100β mVSCs following treatment with myeloid differentiation inductive stimuli.

Figure 3.7 Myeloid differentiation of Mouse Aortic Smooth Muscle Cells (MOVAS SMCs) into macrophage-like cells (MLCs).

Figure 3.8 Myeloid differentiation of Mouse Aortic Smooth Muscle Cells (MOVAS) into macrophage-like cells (MLCs).

Figure 3.9 Myeloid differentiation of S100β mVSCs into macrophage-like cells (MLCs).

Figure 3.10 Myeloid differentiation of S100β multipotent vascular stem cells (mVSCs) into macrophage-like cells (MLCs).

Figure 3.11 Comparison of the number of MACII and CD68-PE positive cells in MOVAS and S100β mVSC following treatment with myeloid inductive stimuli.

Figure 3.12 Flow cytometric analysis of Cd68 expression in MOVAS SMCs before and after treatment with myeloid inductive stimuli.

Figure 3.13 Flow cytometric analysis of Cd11b expression in MOVAS SMCs before and after treatment with myeloid inductive stimuli.

Figure 3.14 Flow cytometric analysis of F4/80 expression in MOVAS SMCs before and after treatment with myeloid inductive stimuli.

Figure 3.15 Flow cytometric analysis of Cd68 expression in S100β mVSCs before and after treatment with myeloid inductive stimuli.
Figure 3.16 Flow cytometric analysis of Cd11b expression in S100β mVSCs before and after treatment with myeloid inductive stimuli.
Figure 3.17 Flow cytometric analysis of F4/80 expression in S100β mVSCs before and after treatment with myeloid inductive stimuli.
Figure 3.18 Immunophenotyping of mouse macrophage cell line, J774A.1 compared to MOVAS SMCs and mouse S100β mVSCs by Amnis™ Cellstream Flow Cytometry.
Figure 3.19 Comparison of the expression of Cd68, Cd11b and F4/80 in MOVAS-SMC vs S100β mVSCs before and after treatment with myeloid inductive stimuli.
Figure 4.1 Characterisation of hiPSC-derived SNEPs by ICC
Figure 4.2 Characterisation of hiPSC-derived smooth muscle cells (hSMC) by ICC.
Figure 4.3 Morphological changes and Oil Red O lipid uptake in THP-1 monocytes before and after PMA induced myeloid differentiation.
Figure 4.4 Phenotypic changes in THP-1 monocytes before and after PMA-induced myeloid differentiation by ICC.
Figure 4.5 Lipid uptake in hSMCs before and after treatment with myeloid inductive stimuli.
Figure 4.6 Lipid uptake in S100β SNEPS before and after treatment with myeloid inductive stimuli.
Figure 4.7 The expression of myeloid genes *CD68, MACII* and *EMR1* in (A) hSMCs and (B) S100β SNEPs before and after treatment with myeloid inductive stimuli.
Figure 4.8 Comparison of the expression of myeloid genes (A)*CD68, (B) MACII* and (C) *EMR1* between hSMCs and S100β SNEPs before and after treatment with myeloid inductive stimuli.
Figure 4.9 Characterization of hiPSC-derived hSMCs transition into macrophage-like cells before and after treatment with myeloid inductive stimuli.
Figure 4.10 Characterization of hiPSC-derived hSMC transition into macrophage-like cells before and after treatment with myeloid inductive stimuli.
Figure 4.11 Characterization of hiPSC-derived S100β SNEP transition into macrophage-like cells before and after treatment with myeloid inductive stimuli.

Figure 4.12 Characterization of hiPSC-derived S100β SNEP transition into macrophage-like cells before and after treatment with myeloid inductive stimuli.
Figure 4.13 Comparison of the number of MACII and CD68 positive cells between hSMC and SNEP before and after treatment with myeloid inductive stimuli.
Figure 4.14 Immunophenotyping human PMA-induced THP-1 macrophages compared to hiPSC derived hSMCs and hiPSC-derived S100β NE progenitor cells (S100β SNEPs) by Amnis™ Cellstream Flow Cytometry.
Figure 4.15 Flow cytometric analysis of CD68 expression in hSMCs before and after treatment with myeloid inductive stimuli.
Figure 4.16 Flow cytometric analysis of CD11b expression in hSMCs before and after treatment with myeloid inductive stimuli.
Figure 4.17 Flow cytometric analysis of F4/80 expression in hSMCs before and after treatment with myeloid inductive stimuli.
Figure 4.18 Flow cytometric analysis of CD68 expression in S100β SNEPs before and after treatment with myeloid inductive stimuli.
Figure 4.19 Flow cytometric analysis of CD11b expression in S100β SNEPs before and after treatment with myeloid inductive stimuli.
Figure 4.20 Flow cytometric analysis of F4/80expression in S100β SNEPs before and after treatment with myeloid inductive stimuli.
Figure 4.21 Comparison of the expression of CD68, CD11b and F4/80 in hSMC vs S100β SNEPs before and after treatment with myeloid inductive stimuli
Figure 5.1 schematic of Arterial architecture in normal vessels and atherosclerotic vessels with lesions.

List Of Tables:

Table 2.1: Commercial cell lines & tissue-derived cells

Table 2.2: growth medium

Table 2.3: primers from IDT

Table 2.4: antibodies

Table 2.5: Chemical and biological agents

Table 2.6: plasticware

Table 2.7: CellStart Dilution for a 6-well plate

Abstract

Myeloid Differentiation of Resident Vascular Stem Cells (mVSCs) into Macrophage-Like Cells (MLCs) in Response to Ox-LDL and Cholesterol

Muhayla Alanazi

A hallmark of subclinical atherosclerosis is the build-up of vascular smooth muscle cell (SMC)-like cells and non-SMC cells, particularly macrophage-like cells (MLCs), which cause intimal medial thickening (IMT), lipid buildup, plaque development and blood flow restriction that can lead to a heart attack or stroke.

Previous cell fate mapping studies have implicated a putative role for SMCs and resident S100β vascular stem cells (mVSCs) in promoting lesion formation, prior to plaque development. The specific aim of this study was to assess whether murine and human S100β vascular stem cells are capable of myeloid differentiation to MLCs when exposed to atherogenic stimuli cholesterol, oxidized LDL (ox-LDL) *in vitro* before their response was compared to murine and human SMCs.

MLC phenotype was determined by morphological changes, immunocytochemical and immunophenotyping of macrophage surface markers using flow cytometry, in addition to histochemical analysis of lipid droplets and real-time PCR analysis of macrophage phenotypic markers.

The data reveal that murine and human SMC-like cells exposed to atherogenic stimuli *in vitro* increased their expression of myeloid phenotypic markers, typical of MLCs. Moreover, S100β vascular stem cells were also capable of myeloid differentiation but to a greater extent than SMCs in culture in response to the same atherogenic stimuli *in vitro*.

These data suggest that S100β vascular stem cells may represent a novel target for therapeutic intervention to reduce the number of MLCs in atherosclerotic lesions.

Chapter 1

Introduction

1.1Cardiovascular disease (CVD), a worldwide killer.

According to the World Health Organization (WHO), cardiovascular diseases (CVD) represent a group of diseases that affect the heart and blood vessels leading to a heart attack or stroke. Diseases affecting the heart and peripheral vasculature are collectively referred to as cardiovascular disease (CVD). Oftentimes, myocardial infarction and stroke happen unexpectedly, before help arrives. For this reason, a lot of therapy approaches are either palliative or ineffective. Modifiable physiological variables and lifestyle choices are the main causes of the widespread prevalence of CVD. Risk factor adjustments have been linked to lower rates of death and morbidity, particularly in those with either diagnosed or undiagnosed cardiovascular disease (CVD) (De Backer et al., 2003). These conditions can arise and worsen in those who have a hereditary susceptibility or after atherosclerotic lesions form over the course of a lifetime (M. C. Fishbein & Fishbein, 2015). Diabetes and uncontrolled hypertension are the two main CVD risk factors that are dominated by age(Heidenreich et al., 2011).

The primary cause of morbidity and death is CVD. This is especially true in industrialized nations(Yusuf et al., 2001)(C. J. Murray et al., 1996). Despite this progress, CVD remains the leading cause of death and disability in the United States and around the world, affecting 85.6 million Americans and accounting for one in every six healthcare dollars spent. Over the past 50 years, there has been remarkable and unprecedented progress in addressing CVD, as evidenced by a significant and ongoing reduction in CVD-related mortality(McClellan et al., 2019). Every year, CVD claims the lives of more women than males in several nations, including the United States of America(Rosamond et al., 2007)(Shaw et al., 2006). According to data from the National Health and Nutrition Examination Survey, which covered the years 2015 to 2018, the overall prevalence of CVD (which includes heart failure (HF), stroke, heart disease (CHD), and hypertension) in adults ≥20 years of age was 49.2% (126.9 million in 2018), and it increased with age in both males and females. Among those with CVD (CHD, HF, and stroke alone), the prevalence is 9.3% overall (26.1 million in 2018) when hypertension is excluded(Virani et al., 2021). Because of the rise in collagen and fall in elastin levels that come with aging, the aortae may stiffen(C. P. Johnson et al., 2001). Systolic pressure rises in proportion to stiffness, as well as reflected waves(Asmar et al., 1988).

1.2 Vascular structure (What's inside the blood vessels)

The vascular system is a network of blood vessels that connect the heart to all other organs and tissues in the body(Black & Garbutt, 2002). It supplies oxygenated blood and nutrients from the heart to organs and tissues through arterial and arteriolar transport، and also carries deoxygenated blood back to the heart through venule and venous transport (Black & Garbutt, 2002). Capillaries have the function of exchanging gases and transporting nutrients between blood and tissues. There are a total of five classes of blood vessels, all of which have been described: (i) Arteries have strong blood vessel walls because they transport blood under high pressure; (ii) Arterioles connect arteries and capillaries. They also have strong walls that can touch and expand many times, thus altering blood flow; (iii) Capillaries are the smallest type of blood vessel. Their walls are very thin and have many small permeable capillary pores water and other molecules; (iv) Veins act as blood reservoirs, carrying low-pressure blood from the venules to the heart (Black & Garbutt, 2002). Compared to arteries, their walls are much thinner, but they have enough muscle to stretch and contract. Finally (v) venules collect blood from capillaries and transport it to veins. Many venules can join into one vein (Black & Garbutt, 2002).

Blood vessels, except for capillaries, are composed of three layers: the intima, the media, and the adventitia (Figure 1.1). As mentioned earlier, arteries and veins differ in thickness, so the composition of these layers differs between the two. Each region contains different amounts of vascular smooth muscle cells (vSMCs) and elastin(Waller et al., 1992) (D. Wang et al., 2017). The innermost and thinnest layer, the intima, is composed of a single layer of endothelial cells that covers the subendothelial layer of the basement membrane and is supported by the inner elastic lamina. Endothelial cells secrete many bioactive substances that control thrombosis, prevent platelet and leukocyte adhesion, regulate vascular tone, and act as selective diffusion barriers (Waller et al., 1992) (D. Wang et al., 2017). The inner elastic membrane separates the intima from the media, which consists of elastic fibres. In humans, the sub endothelium is composed of Vascular Smooth Muscle cells (vSMC) and an extracellular matrix. These cells have a low proliferation rate and are phenotypically stable. Elastic fibres and cell layers increase towards the media. When stimulated by atherogenic factors such as tumour necrosis factor-alpha (TNF-α),

oxidized lipid (ox-LDL) and interleukin-1 beta (IL-1β), vSMCs are thought to proliferate and generate large amounts of extracellular matrix (ECM) causing pre-pathological intima thickening (PIT). Thickening occurs before PIT (Cheng et al., 2019)(Milutinović et al., 2020). The medial layer contains mainly vSMCs and elastin fibres, ECM, collagen, and proteoglycans. This layer is much thicker in arteries than in veins. The composition of the fibres also varies and includes fibres with low elasticity. In larger arteries, these layers are more organized due to their function and important role in moving large volumes of blood. An external elastic layer is also common in this region and provides structural support (Tellides & Pober, 2015). The vSMCs in the media typically consist of up to 40 layers arranged in a spiral or circle. Finally, there is the adventitia, the outermost layer of the blood vessel. It is composed entirely of fibroelastic connective tissue, which consists of fibroblasts, the main cells of the adventitial connective tissue. Progenitor and immune cells such as macrophages, T cells, B cells, and dendritic cells are also present (K. A. Campbell et al., 2012) (Waller et al., 1992) (D. Wang et al., 2017). It is also surrounded by an adipose tissue that helps anchor the blood vessels to the surrounding tissue. This layer is thicker in veins to prevent vessel collapse (Pugsley & Tabrizchi, 2000). The adventitia is involved in cell trafficking across arterial walls and in signalling between vSMCs, endothelial cells, and surrounding tissue. This layer is also responsible for luminal size regulation, inner and outer wall remodelling responses, and repair mechanisms in response to injury (Milutinović et al., 2020). In response to stress or injury, adventitial fibroblasts begin to proliferate, differentiate into myofibroblasts, and migrate toward the intima (F. Xu et al., 2007). They regulate endothelial cell and vSMC growth through secreted factors and recruit progenitor and inflammatory cells to blood vessels (F. Xu et al., 2015)

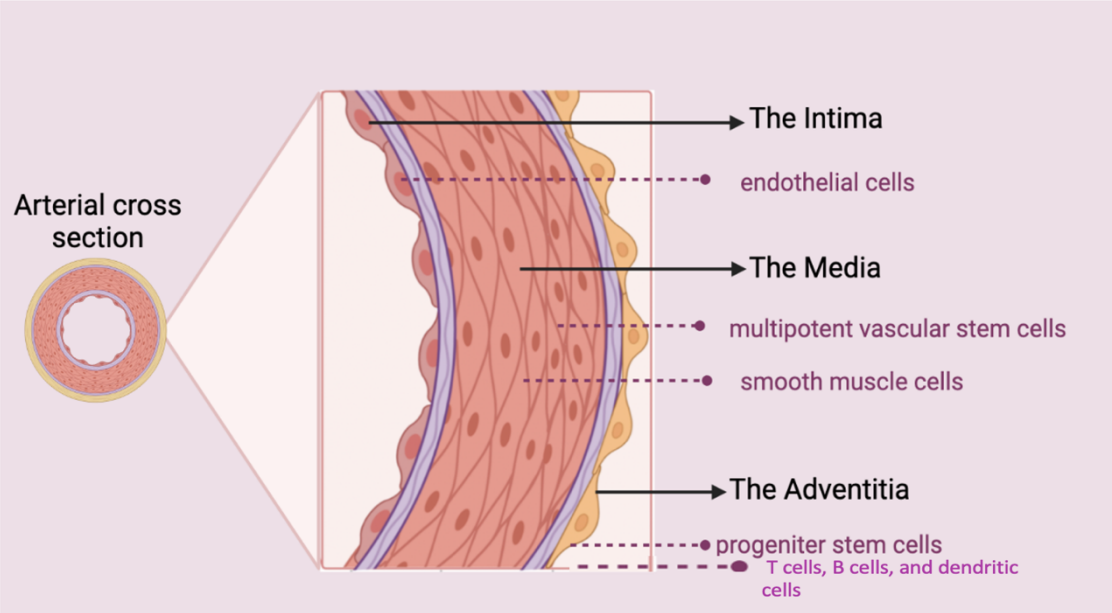

Figure 1.1. A cross section of a healthy arterial wall. Structural composition of healthy arterial walls and their diverse resident cell populations. The innermost layer, the intima, houses a single layer of ECs known as the endothelium. The middle layer, the media, contains differentiated vSMCs that give the artery its structural function through its ability to contract. The outermost layer, the adventitia, houses multiple cell populations, including fibroblasts, immune cells, and adventitial progenitor stem cell populations. Created with Biorender.

1.2.1 The tunica intima

The artery's innermost layer is called the tunica intima. It is made up of a sub-endothelial support structure and a monolayer of endothelial cells that encircles the lumen. Endothelial cells, which are the point of contact between the artery and the blood, have several properties that help to preserve healthy blood flow and ward off the onset of disease. For instance, the frictionless blood flow through the channel made possible by the smooth, flat nature of these cells lessens the shear stress placed on vascular cells(Gimbrone Jr. et al., 2000). Furthermore, it is well known that endothelial cells respond to variations in blood flow dynamics by expressing large levels of anti-inflammatory and anti-thrombotic proteins (Berk et al., 2001).

The basal elastic lamina of the tunica medium, which contains extra collagen, proteoglycans, and glycans necessary for endothelial support and function, is attached to the endothelial cells. Because

they are in close touch with the lumen and are consequently exposed to blood flow forces and interactions with blood components, these endothelial cells constitute an essential part of the vasculature. Because of this, endothelial cells have special abilities to cope with their changing surroundings. For example, they encourage anti-thrombotic and anti-inflammatory events and are phenotypically flat to lower blood flow resistance and minimize friction(Schwartz et al., 1995)(Catravas et al., 1999).

1.2.2 The Tunica Media

The internal elastic lamina, which is made up of elastic fibers and connective tissue, divides the intimal layer from the tunica media(Roostalu et al., 2018). The majority of the vascular smooth muscle cells (vSMCs) that make up the middle layer, or tunica media, contract to restrict the lumen and produce pressure for blood flow. Within this layer, SMCs are divided into other layers by elastic lamina, which creates a fibrous structure that gives the media stiff support. But within the medial layer, a tiny population of stem cells has been found. The medial layer also includes a modest population of resident stem cells, pericytes, and proteoglycans in addition to these SMCs (Potter et al., 2014; Z. Tang et al., 2012).

1.2.3 The Tunica Adventitia

Adipose tissue envelops the exterior elastic lamina, which divides the tunica media from the outermost layer. The adventitia, a collagen matrix rich in stem cells, perivascular nerves, adventitial macrophages, foam cells that are macrophages specific to fatty deposits on blood artery walls. They devour low-density lipoproteins and accumulate lipids, which gives the deposits a frothy look (X.-H. Yu et al., 2013), T cells, microvascular endothelial cells, and adipocytes, is less stiff than the other vascular layers. It is significant to remember that the adventitia's intricate network of interacting cells and biological components has led to its involvement in a variety of vascular diseases(Majesky et al., 2011).

1.3 Subclinical Arteriosclerosis: Model Systems for Investigation

Many people consider atherosclerosis, a chronic, progressive inflammatory disease, to be one of the main causes of CVD-related death globally. Subclinical atherosclerosis is characterized by the build-up of vSMC-like cells that cause IMT, lipid build-up, plaque development, and blood flow obstruction that can cause a heart attack or stroke. Pathological observations in human vessels confirm that atherosclerotic-prone regions of arteries that drive subclinical atherosclerosis, pathologic intimal thickening, lipid retention, and the appearance of a developed plaque regularly have early "transitional" lesions enriched with SMC-like cells called adaptive lesions(Sakamoto et al., 2018). A number of model systems have been created to produce SMCs for both *in vitro* and *in vivo* research.

1.3.1 Vascular Smooth Muscle cells (VSMC)

Hollow organs like the uterus, bladder, and digestive system organs are structurally supported by SMCs. Furthermore, they may be implicated in pathological situations such vascular remodelling during disease progression after damage, and they serve a crucial physiological role in the contractility of blood vessels under normal settings to maintain normal blood pressure. This subtype has a variety of origins and is referred to as vSMCs. Because of their diverse range of roles and different embryological origins, vSMCs are regarded as heterogeneous(Gammill & Bronner-Fraser, 2003; Hao et al., 2003; Majesky, 2007; Sinha et al., 2014).

Inside the blood artery wall, these vSMC are the predominant cell type. The primary role is to contract and control blood vessel flow. They are contained in a collagen and elastin matrix in the medial layer, where they help to regulate blood pressure and distribute blood flow by promoting vasodilation and constriction, which in turn helps to maintain vascular tone. Actin (SMA), myosin heavy chain 11 (Myh11), calponin 1 (Cnn1), Smoothelin 2 (Smtn2), and transgelin (SM22α) are among the significant phenotypic markers that they display (Owens et al., 2004). Variations in actin cytoskeletal organization, extracellular and intracellular tension, and cell contraction, migration, and survival are all regulated(Papakonstanti & Stournaras, 2008). The development and operation of the respiratory, digestive, urinary, and cardiovascular systems are significantly influenced by these cells.

It has long been recognized that vSMCs are derived from various regions of the developing embryo and aid in the creation of unique vascular tissues. The mesoderm and the neuroectoderm, or neural crest epithelial cells, are the two main sources from which they can emerge. The majority of vSMCs in the vascular tree are of mesodermal origin, such as lateral plate and paraxial mesoderm. Mesenchyme, a type of connective tissue presents during embryonic development, or mesothelium during the epithelial to mesenchymal transition are the primary sources of mesenchyme formation. The cranial neural crest, which gives rise to the aortic arch, ascending aorta, and branching carotid arteries, as well as the mesodermal background of the aortic root and annulus and descending aorta, are among the distinct embryological origins of the vSMCs that make up the tunica media of the aorta (N. Shi & Chen, 2016).

1.3.2 Induced Pluripotent Stem Cells (iPSCs)

By overexpressing foreign transcription factors, somatic cells are reprogrammed to create the unique cell type known as induced pluripotent stem cells (iPSCs) (Zachary & Morgan, 2011). Theoretically, from the three major germ layers, they can develop into any adult cell type. Thus far, it has been effectively demonstrated that iPSCs can differentiate into a wide variety of cell types, such as neuronal cells, endothelial cells, cardiomyocytes, lung and airway epithelial cells, and more (S. X. L. Huang et al., 2014). Furthermore, adult fibroblasts that transdifferentiate directly into endothelial cells, eschewing the pluripotent stem cell intermediary, allows for the creation of induced endothelial cells (iECs)(J. Li et al., 2013)(Margariti et al., 2012). Although other cell types, such as adipose stromal cells, hepatocytes, gastric epithelial cells, dental pulp stem cells, cord blood cells, and peripheral blood mononuclear cells, have also been used to generate iPSCs, dermal fibroblasts are the most common source (Koyanagi-Aoi et al., 2013)(Koyanagi-Aoi et al., 2013; Tanabe et al., 2013). Oct3/4 is a transcription factor belonging to the homeodomain that regulates the upkeep and development of pluripotent stem cells (PSCs). Partially, Oct3/4 expression is regulated by Sox2. Sox2, Nanog, and Oct3/4 make up the essential transcriptional network for pluripotency. One proto-oncogene linked to the development of cancer is c-Myc. It attracts proteins that alter chromatin, which triggers extensive transcriptional activation. Previous research has demonstrated that L-Myc, which lacks transformation activity, can substitute for c-

Myc in reprogramming (Masui et al., 2007)(Nakagawa et al., 2008). Kruppel-like factor 4 (Klf4) is a context-dependent oncoprotein or tumour suppressor that also stimulates SRY-box transcription 2 (Sox2) and is a downstream target of leukemia inhibitory factor (Nakagawa et al., 2010).The reprogramming of somatic cells into pluripotency is caused by the coordination of various reprogramming factors, while the exact pathways are still unclear (Niwa et al., 2009).
Because of partial reversal of lineage-specific methylation patterns, variable de novo methylation patterns during reprogramming, and variability in X chromosome inactivation, iPSCs show aberrant DNA methylation profiles compared to ESCs (Kim et al., 2010)(Kim et al., 2011)(K. Kim et al., 2010, 2011; Liang & Zhang, 2013). The difference between iPSCs and ESCs is no bigger than the difference between individual ESC lines, according to other analyses of human iPSCs and ESCs that have shown overlapping and non-significant differences in DNA methylation in these two cell types (Koyanagi-Aoi et al., 2013) (Liang & Zhang, 2013)(Maherali et al., 2007). Regarding their capacity to develop into mature cell types, iPSCs and ESCs appear to be comparable(Taura et al., 2009)(Taura et al., 2009; Xi et al., 2010). According to (Tokumoto et al., 2010), the situation is complicated and may be impacted by the type of donor cell, the degree of similarity between the parent and target cell types, and the iPSC derivation process.

1.3.3 Multipotent Resident Vascular Stem cell

After being exposed to particular growth factors and other biomolecules in their inductive media, mouse mesenchymal stromal stem cells (MSC) and multipotent resident vascular stem cells (mVSCs) can differentiate into a variety of cell types, including adipocytes, myocytes, chondrocytes, and osteocytes (Covas et al., 2008);(H. Huang et al., 2009);(Lin et al., 2010);(New et al., 2015a).Transforming growth factor-β (TGF-β) was found to promote SMC development (Park et al., 2013). Adipocyte genes that are involved in the synthesis of fat include fatty acid synthase (FAS)(Wakil, 1989) , lipoprotein-lipase (LPL), and fatty acid-binding protein (FABP4) (H. Shi et al., 2010). MSCs display markers that are known to be expressed by osteoblasts, the cells that form new bone *in vivo* and are in charge of laying down the matrix and mineral. These cells are cultivated in osteogenic media. Three phases have been identified for the *in vitro* development of MSCs into osteogenic offspring(Z. Huang et al., 2007). Increases in osteoblast marker gene expression are observed, particularly for fibroblast growth factor 23 (*Fgf23*), dentin

matrix protein 1 (*Dmp1*), and osteostatin (Sost) (Feng et al., 2006; Poole et al., 2005). Rat MSCs were successfully converted into endothelial cells by (Maul et al., 2011a). They also observed an increase in the expression levels of genes characteristic to endothelium, such as prominin 1 (CD133) and platelet endothelial cell adhesion molecule (PECAM1).

Mesenchymal stromal stem cell like cells (MSC-like cells) are similar to mesenchymal stromal stem cells (MSCs), which can differentiate into a variety of cell types (Covas et al., 2008);(H. Huang et al., 2009);(Lin et al., 2010);(New et al., 2015a). While MSCs are found in bone marrow, they can also be isolated from adipose tissue, umbilical cord blood, and dental pulp(Dominici et al., 2006). Both MSCs and MSC-like cells differentiate into multiple cell lineages and express markers like CD73, CD90, and CD105 (Gronthos et al., 2001). They have immunomodulatory functions, useful for treating inflammatory and autoimmune diseases (Dominici et al., 2006).Differences include their sources such as synovial fluid, dental pulp, or cultured pluripotent stem cells, and variations in differentiation potential and gene expression (Gronthos et al., 2001). MSC-like cells from pluripotent stem cells may retain pluripotency markers like OCT4 and NANOG, while those from different tissues may express specific markers like STRO-1 and CD146 (Gronthos et al., 2001).

1.3.4 Adventitial cells

The adventitia is home to a highly dynamic population of resident progenitor cells, leukocytes, adipocytes, and microvessels that work together to preserve the arterial wall and firmly react to various vascular conditions (Majesky et al., 2011). As in the formation of tertiary lymphoid organs in diseased arteries, fibrotic changes reduce compliance and promote renal damage in hypertension, and the accumulation of inflammatory cells during the development of medial dissections and aneurysms, the adventitia may be the primary site of pathological change in certain cases (Galkina et al., 2006; Hu et al., 2004; Passman et al., 2008; Psaltis et al., 2012). The adventitia and related perivascular cells in tiny vessels are crucial signalling habitats for bone marrow hematopoietic stem cells (Kramann et al., 2015)(Gräbner et al., 2009)(Guzik et al., 2007)(Tieu et al., 2009).

Antigen-1 (Sca1) stem cells from adventitial stem cells transform into osteogenic progeny and macrophage colony-forming units, two types of cells involved in vascular lesions (Psaltis et al., 2012);(Cho et al., 2013). According to studies employing lineage tracing research, a significant portion of these adventitial Sca1 cells are thought to be produced from differentiated SMCs with Myh11 genomic markings, and they play a key role in adventitial remodelling(Majesky et al., 2017). Additionally, adventitia, which is typically characterized by lymphocyte infiltrates, may contribute to the development of atherosclerosis (K. A. Campbell et al., 2012).

1.3.5 Endothelial cells

An important part of the beginning, intensification, and resolution of the inflammatory response is mediated by endothelial cells. Endothelial dysfunction and the resulting vascular remodelling it causes are linked to a number of cardiovascular disorders, including hypertension, diabetes, obesity, and atherosclerosis (Cohn, 2001)(Cohn, 2001; Xiao et al., 2014). These diseases are also associated with dysregulated inflammatory responses. Leukocyte adhesion is normally resisted by endothelial cells (ECs), which make up the innermost surface of artery walls. However, factors that cause atherosclerosis, like eating a diet high in saturated fat, smoking, having high blood pressure, high blood sugar, being obese, or having insulin resistance, can cause ECs to express adhesion molecules, which then permits leukocytes to adhere to the arterial wall (Libby et al., 2018) (Tesfamariam & Cohen, 1992). It is acknowledged that endothelial dysfunction is a major precursor to cardiovascular morbidity and death (Cohn, 2001).

1.4 Arteriosclerosis

Arteriosclerosis, also known as symmetric vascular remodelling, is the thickening of the inner and middle layers of arteries (Figure 1.2.B). A hallmark of arteriosclerosis is the formation of fibrous lesions known as neointima. This is due to the accumulation of SMC-like cells, resulting in intima-media thickness (IMT) (Bennett et al., 2016). This neointima formation causes continuous remodelling of the vessel wall, narrowing the lumen and reducing elasticity, impeding normal blood flow and leading to stroke or myocardial infarction. Stenting and age-related vascular injury are major causes of arteriosclerosis (G. A. Fishbein & Fishbein, 2009). Although the origin of neointimal cells is not fully understood, there are numerous studies on potential source(s) of these

cells. Smooth muscle cell de-differentiation has been accepted as a classical theory for decades because of its major role in intimal thickening after vascular injury (Owens, 1995). Resident vascular stem cells (Di Luca et al., 2021), circulating myeloid stem cells, and endothelial cell migration (EndMT) are also potential sources of these neointimal cells (Yuan et al., 2017).

1.4.1 Atherosclerosis

Atherosclerosis is classified as a chronic progressive inflammatory disease characterized by lipid laden vascular lesions of the arterial wall (Figure 1.2.C) and is the most common cause of morbidity affecting the current generation (Kolodgie et al., 2007)(Kolodgie et al., 2007; Sakamoto et al., 2018). Unlike other non-communicable diseases, atherosclerosis has a long asymptomatic dormant phase, with the first clinical manifestations occurring in late stages of well-advanced atherosclerosis. Necessary interventions for the prevention and reversibility of atherosclerosis require asymptomatic evidence to prescribe first-line therapy. A key feature of asymptomatic atherosclerosis is PIT. PIT is defined as the first progressive plaque responsible for the growth of advanced lesions. PIT can be divided into two categories of vascular lesion morphology: (i) diffuse intimal thickening (DIT), composed of SMC-like cells and extracellular matrix, with little or no lipid accumulation and (ii) adaptive intimal hyperplasia (AIT), commonly associated with natural aging of arteries, is composed primarily of infiltrating macrophage cells and intimal SMC-like cells, and is probably an early stage in lesion progression (Kolodgie et al., 2007) (Sakamoto et al., 2018).

Studies have shown that SMC-like cells are enriched in atherosclerotic-prone regions of the vessel in early adaptive 'transitional' lesions (Ikari et al., 1999). These atheroprone areas are susceptible to the development of PIT due to a variety of factors, including (i) disturbed blood flow resulting in endothelial dysfunction, (ii) exposure to circulating CVD risk factors, and (iii) the effect of embryological origin of neointimal cells and how the origin of these cells influences their behaviour in forming the neointima include their proliferative capacity, migratory ability, response to injury, and role in disease processes (DeBakey & Glaeser, 2000) (Cheung et al., 2012) (Bennett et al., 2016). As part of the subclinical detection and implementation of primary preventative measures for treating or delaying CVD pathogenesis, adaptive lesions have been identified in

human vessels prior to lipid retention (Sakamoto et al., 2018). It is widely accepted that SMC-like cells are responsible for most of the neointimal cells found in arteriosclerotic and atherosclerotic lesions after vascular injury (Bennett, Sinha, and Owens, 2016). (Figure1.3). This process applies to many murine arterial injury models, including balloon angioplasty, carotid artery ligation, coronary artery bypass graft (CABG), graft atherosclerosis, pulmonary hypertension, and in-stent restenosis (ISR) (Bennett, Sinha, and Owens, 2016). Early lesions have also been confirmed in a routine disease model of the mouse carotid artery after blood flow restriction by ligation. Moreover, these ligation-induced lesions can progress to advanced atherosclerotic plaques in Western-fed ApoE knockout mice (Korshunov & Berk, 2003) (Nam et al., 2009); (W. Liu et al., 2011). The ApoE knockout (KO) mouse model is extensively used in the study of neointimal cells and atherosclerosis due to its genetic modification, which involves the absence of the apolipoprotein E (ApoE) gene a key player in lipid metabolism (Zadelaar et al., 2007)(Getz & Reardon, 2012). These mice are particularly valuable because they are highly susceptible to developing atherosclerosis, even on a standard diet (Nakashima et al., 1994; Plump et al., 1992). When fed a high-fat Western diet, they rapidly develop extensive and advanced atherosclerotic lesions, more so than wild-type mice, making them ideal for studying the progression of atherosclerosis and the factors that influence it. The atherosclerotic lesions in ApoE KO mice closely resemble those found in humans, featuring lipid-laden macrophages, smooth muscle cell proliferation, and complex plaque formation (Plump et al., 1992). This similarity enhances the translational potential of findings from these models to human disease conditions. Additionally, the ApoE KO model enables researchers to delve into the underlying mechanisms of atherosclerosis, including the roles of various cell types, such as neointimal cells, in plaque formation and progression (J. L. Johnson & Newby, 2009) (Hansson Göran K., 2005). By adjusting diet, genetic background, or environmental factors, scientists can explore how these variables impact the development and progression of vascular lesions. Furthermore, ApoE KO mice serve as a crucial tool for testing potential therapeutic interventions aimed at reducing or preventing atherosclerosis (Glass & Witztum, 2001). This includes evaluating the effects of drugs, dietary supplements, or genetic modifications on the extent and composition of atherosclerotic plaques. In summary, the ApoE KO mouse model is a powerful and indispensable tool for understanding the pathophysiology of atherosclerosis and for testing potential treatments, making it highly relevant in research focused on vascular diseases and neointimal cell behaviour (Moore & Tabas, 2011).

Features associated with IMT include luminal diameter reduction, inhibition of matrix degradation, and neointimal cell accumulation of SMC-like cells and MLCs (Lan et al., 2013)(Huang, and Tan, 2013). The origin of these neointimal cells has caused much discussion and controversy within the vascular biology research community.

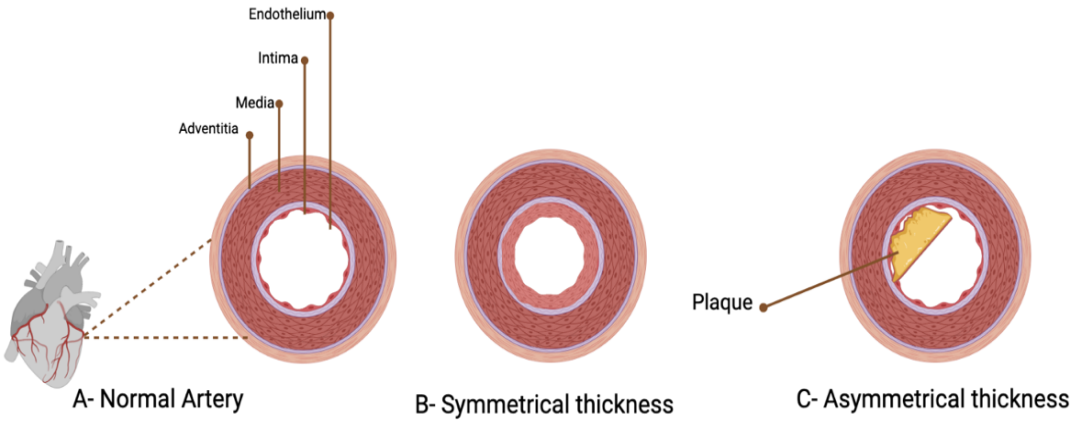

Figure 1.2. Arterial architecture in normal vessels compared with arteriosclerotic (without lipid) and atherosclerotic (with lipid) vessels with lesions. (A) Schematic of a healthy artery showing the three layers: intimal, medial and adventitial. Schematic of an arteriosclerotic (B) and atherosclerotic (C) artery showing symmetrical and asymmetrical thickening, respectively. Created with Biorender.

1.5 The neointima, the key to detecting asymptomatic atherosclerosis.

Within the layers of the arterial wall, there are three main locations that may harbour the source of neointimal cells, neointimal myogenic (SMC-like cells) and non-myogenic (non-SMCs, including MLCs) are derived from during disease progression and lesion formation - (i) the intima composed of endothelial cells, (ii) the media composed mainly of vSMCs with a small population of resident stem cells, and (iii) the adventitia composed mainly of fibroblasts with a small population of

resident vascular stem cells. Most cells found in the neointima of arteriosclerotic lesions are predominantly SMC-like cells while non-SMCs and lipid laden MLCs predominate within atherosclerotic lesions (Schiele, 2005).

The origin of both SMC-like cells and non-SMCs within lesions is widely debated. Initially, it was proposed that neointimal SMC-like cells are derived from differentiated medial vSMCs that undergo a phenotypic switch, dedifferentiate, proliferate, and migrates SMC-like cells to sites of injury. Subsequent lineage tracing studies found compelling evidence for (i) the involvement of populations of dedifferentiated resident medial vSMCs (Chappell et al., 2016a; Shankman et al., 2015), (Cherepanova et al., 2016), (ii) circulating bone marrow cells (Sata, 2003), (iii) resident stem cells (Z. Tang et al., 2012); (Tsai et al., 2012); (Shikatani et al., 2016); (Di Luca et al., 2021); (Molony et al., 2021) (iv) EC by a process known as endothelial-to-mesenchymal stem cell transition (EndoMT) (Cooley et al., 2014); (G. Wang et al., 2015). As this topic is controversial, a thorough knowledge of arterial wall structure and the cellular microenvironments in which they reside is required to elucidate possible causes (Figure 1.3).

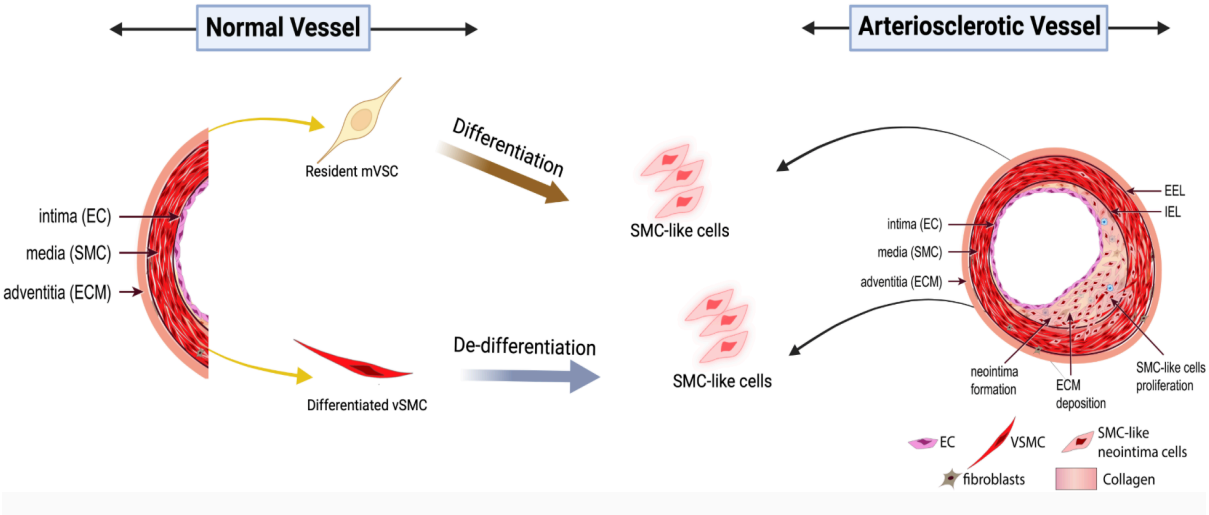

Figure1.3. Origin of neointimal vSMCs. There are two possible main sources of neointimal vSMCs (i) Dedifferentiation of vSMCs to a plastic cell that be able to undergo for differentiation, migration, and proliferation and (ii) partly differentiated resident vascular stem cells (mVSCs). Created with Biorender.

1.5.1 Origin of Neointimal Cells

Over time, the lipid-rich molecules on the arterial wall cause atherosclerotic plaques to develop, which restrict the arteries and cause myocardial infarction and stroke. Understanding the pathophysiology of atherosclerosis requires unravelling the origin and adaptability of several cell types that play crucial roles in all stages of plaque development and destabilization (Y. Li et al., 2021).

1.5.1.1 De-differentiation and reprogramed SMCs (SMC-like cells)

SMCs are typically found in the tunica media and express a variety of SMC markers, such as SMC Myh11, SM22α/transgelin, α-smooth muscle actin (SMA), Cnn1, Smtn2, and others (Alexander & Owens, 2012). Inflammatory cells invade injured endothelium and release a range of cytokines that can cause medial SMCs to migrate, proliferate, and dedifferentiate (Ross Russell, 1999). For a variety of proliferative vascular disorders *in vivo* and in sub-cultured cells *in vitro*, this process of de-differentiation and reprogramming is frequently linked to a considerable reduction in the expression of important SMC differentiation marker genes (Chamley-Campbell et al., 1979). A variety of stimuli, including Platelet-derived growth factor (PDGF), oxidized phospholipids (McDonald et al., 2006; McDonald & Owens, 2007) , transforming growth factor beta1 (TGF-β1) (Ailawadi et al., 2009; Owens et al., 2004), and retinoic acid (Spin et al., 2004, 2010, p. 300), are known to affect the SMC phenotype. These stimuli appear to work in part by altering the SMC chromatin structure (Spin et al., 2012). The transcription factor Kruppel Like Factor 4 (KLF4) controls the switching of SMC phenotypes. KLF4 factors bind to G/C-rich cis regions present in the promoters of SMC marker genes and are expressed in phenotypically-modified SMCs. KLF4 is not expressed by differentiated SMCs found in healthy blood arteries. However, after vascular injury, it is quickly caused (F. Yan et al., 2008).

Numerous studies have demonstrated that in response to damage, adult SMCs express genes or gene products typical of earlier embryonic phases, including tropoelastin, fibronectin, tenascin, F31/H19, cytokeratin 8, and extra domain-A fibronectin. Furthermore, several genes, such those specific to smooth muscle and expressed preferentially in adult cells *in vivo*, like desmin,

tropomyosin, and myosin, are down-regulated when adult cells migrate and divide in response to harmful stimuli (Frid et al., 2002). This behaviour may result in stenosis and vascular lumen obliteration, among other changes to the vascular wall. Vascular smooth muscle-like cells make up to 98% of the cells found in the restenosis lesion (Shankman et al., 2015). Numerous researchers first claimed that these neointimal SMC-like cells arose from differentiated SMCs that underwent a phenotypic shift to become de-differentiated and then started to proliferate and migrate to the site of injury in order to produce the neointima. Further convincing evidence supporting SMC switching and re-programming has been provided by lineage tracing studies that show a significant number of neointimal macrophage-like cells (Shankman et al., 2015) and neointimal SMCs (Herring et al., 2014); (Nemenoff et al., 2011) (Shankman et al., 2015) may be derived from "marked" medial differentiated SMC *in vivo* (Chappell et al., 2016a) (Cherepanova et al., 2016; Shankman et al., 2015). According to research from our group (E. Kennedy, Hakimjavadi, et al., 2014; E. Kennedy, Mooney, et al., 2014), SMCs in culture also start to exhibit neural stem markers, such as SRY-box transcription 10 (Sox10), although not to the same extent as multipotent vascular stem cells.

1.5.1.2 Bone marrow-derived Stem Cells

A few numbers of studies provide evidence in favor of the involvement of hematopoietic progenitor cells (HPCs) and circulating bone marrow-derived stem cells (BMD-SCs) in the development of vascular lesions. In the majority of these investigations, a mouse was given a bone marrow transplant before having its blood vessels cut. It was later demonstrated that a significant portion of the neointimal cells came from the donor mouse (Shimizu et al., 2001);(Sata, 2003). Atherosclerotic lesion SMCs may be derived from donor bone marrow stem cells, according to certain human investigations(Caplice et al., 2003). It has also been proposed on multiple times that these circulating cells are not differentiated into neointimal SMC-like cells, even if they are drawn to the ligation site (Hoofnagle et al., 2006).

1.5.1.3 Endothelial cells

An average adult has about 7 m^2 of endothelial cells (ECs) (Cines et al., 1998). Endothelial cells form a semipermeable monolayer in the tunica intima. All of the vessels' endothelial cells are

mesodermal in origin (Aird, 2007).Vascular endothelial cells generally quiesce circulating leukocytes, control vessel wall permeability, maintain blood fluidity, and regulate blood flow. Several endothelial-cell-dependent processes that prevent coagulation across the vascular system actively maintain blood fluidity (Bazzoni & Dejana, 2004). Endothelial cells were demonstrated to possess the capacity to change into SMC progenitor cells that exhibit myogenic markers in 1997 (DeRuiter et al., 1997). Subsequently, the progenitor cell was classified as a mesenchymal stem cell, and multiple instances of this trans-differentiation process were shown. Endothelial-to mesenchymal transition (EndMT) is the term coined to describe this process, which is characterized by the acquisition of mesenchymal markers like vimentin and fibroblast-specific protein 1 (FSP-1) and the loss of endothelial markers like CD31 and von Willebrand factor (VWF) as well as the loss of morphological features like tight junctions (P.-Y. Chen et al., 2015). Numerous studies shown that EndMT takes place during neointimal hyperplasia and that cells that have gone through this transition process are the source of SMC-like cells in the neointima (D. Chen et al., 2021)(D. Chen et al., 2021; Frid et al., 2002).

1.5.1.4 Resident vascular stem cells

Stem cells are units of organization within biological systems that are in charge of organ and tissue development as well as regeneration. These cells have the ability to differentiate into many cell lineages and self-renew (Dulak et al., 2015; Weissman, 2000). A novel theory has emerged recently, according to which resident vascular stem cells in the artery wall develop into SMC-like neointima cells. In the adventitia layer, a population of stem cell antigen 1 (Sca1)-positive cells was found. These cells may be encouraged to develop into an SMC population by passing through an intermediate myofibroblast. It was also demonstrated that these cells can help form the neointima by migrating through the media *in vivo* (Sartore et al., 2001); (Torsney et al., 2005). Further evidence from cell fate mapping research suggested that adventitial stem cells might contribute to lesion formation, but only in the event of significant vascular injury (Roostalu et al., 2018). There is evidence from recent lineage tracing and scRNA-Seq data that suggests that after severe vascular injury, a population of adventitial Sca1+ stem cells migrates into the medial layer and differentiates later into SMC-like cells to start vessel repair (J. Tang et al., 2020).

Although populations of multipotent cells have also been seen in the tunica medium, vascular stem cells are most prevalent in adventitia (Tintut et al., 2003). After being isolated from the medial layer, Sca1+ cells have demonstrated the capacity to differentiate into the SMC and EC lineages in response to the right stimuli (Sainz et al., 2006). Multipotent vascular stem cells (mVSCs) are a new population of Sca1- cells that the Song Li research group discovered in the tunica medium of rat carotid arteries in 2012 (Z. Tang et al., 2012). The carotid artery emerges from a neuroectodermal lineage, which explains why mVSCs expressed neural crest stem cell markers such Sox10, SRY-box transcription 17 (Sox17), and Nestin (Hempleman & Warburton, 2013). Additionally, this cell subset expressed the protein S100β, which binds to calcium. S100β has been demonstrated to be expressed by a variety of neural stem cell types, despite being widely utilized as a marker for mature glial cells and astrocytes (Ihrie & Alvarez-Buylla, 2008)(Ihrie & Alvarez-Buylla, 2008; Seri et al., 2004). It has also been proposed that S100β has a role in the development of neointima after ligation-induced damage (Cao et al., 2017). Furthermore, it was shown that mVSCs had significant levels of proliferation and telomerase activity, which implies stemness, and that they were negative for myogenic markers including Myh11 and Cnn1. Additionally, this study used lineage tracing to demonstrate that, after wire-induced injury, neointimal cells originated from medial and/or adventitial mVSCs rather than from the dedifferentiation of medial SMCs (Z. Tang et al., 2012).

Our lab has revealed that SMC-like cells in vascular lesions may have originated from an S100β+ resident vascular stem cell that underwent myogenic differentiation via the hedgehog signalling pathway(Molony et al., 2021). This was done via lineage tracing analysis and single cell photonic analysis. These findings provide credence to the hypothesis that mVSCs may play a role in the development of a neointimal lesion after vascular damage, if not entirely. However, more research is needed to fully understand the precise processes by which these events might take place, particularly with regard to the participation of important signalling pathways including PDGF, TGF-β1, and Notch signalling that propel mVSCs toward myogenic differentiation.

Naming conventions in scientific research are often influenced by the specific characteristics or markers used to identify and characterize cell populations(Alberts et al., 2002). In the case of vascular stem cells in mice, a specific subset of these cells expresses the S100β marker and this marker is considered crucial for their identification or functional characterization, it may be

appropriate to refer to them as "S100β mVSCs" to distinguish them from other vascular stem cell populations (Alberts et al., 2002). As we know that there are multiple populations of MVSCs, with some expressing markers such as S100 β+ (Di Luca et al., 2021) or Sca1+ (Z. Tang et al., 2012). In this study, we utilized the S100-positive mVSCs (S100 β mVSCs).

1.5.1.5 Macrophage-like cells (MLC)

The origin of macrophage-like cells is widely debated. Many studies revealed that the origin of MLC in atherosclerotic lesion is from differentiated vSMC that become dedifferentiated cells and then become MLC which it is the current theory of where roughly half of the MLC with the lesion come from (Allahverdian et al., 2014; Feil et al., 2014; Shankman et al., 2015).

A portion of the smooth muscle cells (SMCs) in advanced atherosclerotic plaques can develop into macrophage-like cells. The SMCs in the plaques are produced from preexisting SMCs in the medial layer of the vessel (Allahverdian et al., 2014; Feil et al., 2014; Shankman et al., 2015). Studies on genetic lineage tracing reveal that certain offspring of SMCs may become macrophage-like cells and cease to display SMC markers (Feil et al., 2014; Shankman et al., 2015). It is debatable and uncertain, therefore, whether these SMC-derived macrophage-like cells take on a permanent or transitory macrophage cell destiny as atherosclerosis advances(Bentzon & Majesky, 2018). Studies had been made to specifically trace SMC-derived macrophage-like cells (He et al., 2017; Y. Li et al., 2021). The both studies observed SMC-derived macrophages-like cells expressing macrophage markers CD45, CD11b, F4/80, and CD68 in the early-stage lesion. Additionally, they conducted single-cell RNA sequencing (scRNA-seq) study on cells isolated from atherosclerotic plaque and discovered that CD11b was concentrated in the macrophage population (Y. Li et al., 2021). This finding implies that CD11b reflects the macrophage or macrophage-like status of stem cells during atherosclerosis.

Data showed that macrophage-like cells produced from SMCs had a unique cell plasticity that set them apart from cells recruited from terminally differentiated monocytes(Y. Li et al., 2021). Generally speaking, macrophages were thought to accelerate the development of atherosclerosis, increase the size of lesions, and facilitate plaque rupture. There has been debate regarding the involvement of macrophage-like cells produced from smooth muscle cells in atherosclerosis. According to (Y. Li et al., 2021), they discovered that macrophage-like cells produced from SMCs may transform back into smooth muscle cells in the fibrous cap of advanced plaques, indicating

that these cells may act as a repair mechanism in atherosclerosis and play a protective function by stabilizing atherosclerotic plaques. It may be possible to discover new therapeutic targets to help cure atherosclerosis if the origin, plasticity, and potential future functions of the various cell lineages found in the plaques are better understood.

The other possible origin of MLC is from stem cells, and this is our hypothesis that we work to addresses whether murine and human S100β multipotent vascular stem cells (mVSCs) are capable of myeloid differentiation to MLCs *in vitro* in comparison with the response of murine and human vSMCs in culture.

1.6 Macrophages

1.6.1 History of Macrophages

The discovery and understanding of macrophages have evolved significantly since the late 19th century:
Ilya Metchnikoff, a Russian zoologist, made a ground-breaking discovery in the 1880s by identifying phagocytes, later known as macrophages. He described their role in phagocytosis, a process where these cells engulf and digest foreign particles, bacteria, and dying cells, which laid the foundation for the concept of innate immunity. This discovery was pivotal in understanding how the immune system defends the body against pathogens through cellular mechanisms.

Further in the early 1900s, studies significantly expanded our understanding of macrophages. Researchers discovered that these cells are present in various tissues throughout the body and play crucial roles in both innate and adaptive immunity. These investigations revealed that macrophages are not only essential for phagocytosis but also for antigen presentation, bridging the innate and adaptive immune responses. The discovery that macrophages originate from hematopoietic stem cells and differentiate into various tissue-specific forms further highlighted their versatility and importance in immune regulation and tissue homeostasis.

In the late 20th century, advances in molecular biology and immunology significantly enhanced our understanding of macrophage activation and polarization, as well as their roles in chronic inflammation and disease. Research during this period revealed the complex signalling pathways that regulate macrophage functions, including the IRF/STAT pathways, which are crucial for macrophage polarization into M1 and M2 phenotypes. M1 macrophages are associated with pro-inflammatory responses, while M2 macrophages are linked to anti-inflammatory activities and tissue repair. These insights have been pivotal in understanding how imbalances in macrophage polarization contribute to various diseases, such as diabetes, rheumatoid arthritis, and cancer

1.6.2 Macrophage: what is it? Biology and Structure

1.6.2.1 biology of macrophages

Macrophages (Mϕs) first described over a century ago by Ellie Metchnikoff (Mass & Lachmann, 2021) as we mentioned previously. After being first proposed by Van Furth as a component of the mononuclear phagocyte system, with origins in bone marrow (BM) derived monocytes (van Furth et al., 1972), tissue-resident Mϕs are now known to be derived during embryogenesis from fetal liver monocytes and/or yolk-sac Mϕs (Ginhoux & Guilliams, 2016), (Hoeffel et al., 2015), (Gomez Perdiguero et al., 2015), (Schulz et al., 2012), (Guilliams et al., 2013). However, during the neonatal window and in some tissues, like the intestine, during adulthood, BM monocytes can engraft and contribute to the tissue-resident Mϕ pool in accessible tissues, like the liver and spleen (Guilliams & Scott, 2017) , (Scott et al., 2016), (Bain et al., 2014), (Sawai et al., 2016), (Tamoutounour et al., 2013), (Beattie et al., 2016).

Macrophages play a variety of roles in both innate and adaptive immunity, making them essential parts of the immune system. As sentinel cells, macrophages are found in many bodily tissues and scout their surroundings for the presence of pathogens and cellular debris. When macrophages come across foreign particles, they utilize phagocytosis, a mechanism that allows them to engulf and eradicate pathogens or cellular debris. Furthermore, by presenting antigens to T cells, macrophages function as antigen-presenting cells, which are essential for triggering adaptive immune responses. Moreover, a variety of cytokines and chemokines secreted by macrophages

regulate inflammation and draw additional immune cells to the site of infection or injury. Because of their plasticity, macrophages can change their phenotypic in response to external stimuli (Theofilis et al., 2023).

1.6.2.2 Structure of macrophages

Macrophage morphology depends on different activity states of the cell. Cell sizes range from 10 to 30 μm in diameter and the nucleus is ovoid and about 6–12 μm in diameter (Carr, 1973). The macrophage cytoplasm contains basophilic vacuoles and granules in nature (Carr, 1973). In phase-contrast microscopy, peritoneal macrophages contain light grey diffuse cytoplasm with dark grey rod-shaped mitochondria (Carr, 1973). The periphery of the cytoplasm is finely granular and lacks structures such as the endoplasmic reticulum and attached ribosomes. Three different types of vesicles are displayed in the cytoplasm in the form of pinocytotic vesicles with organelles of various sizes containing particulate matter (North & Mackaness, 1963). Ribosomes can be seen attached to the outer portion of the nuclear envelope, which is continuous with the endoplasmic reticulum (North & Mackaness, 1963). The cytoplasmic dense granules are secondary lysosomes primarily derived from endocytic vacuoles. In inflammatory macrophages, narrow cytoplasmic processes are observed that remain tightly entangled with neighbouring epithelioid cells. Some observations may even point to granuloma giant cells as a result of pre-established macrophage fusion (Shibata et al., 1991).

1.6.3 Subtypes of macrophages

Macrophages are known to influence the development of cancers, chronic inflammatory diseases like arteriosclerosis, and infectious diseases because they can present antigens to T cells and act as effectors for cell-mediated immunity (Hirayama et al., 2017). Furthermore, phagocytosis is essential to that procedure. All vertebrate tissues contain macrophages, and various stimuli have distinct effects on the phenotypes of these cells(Hirayama et al., 2017). Based on their functions, Mills et al. classified macrophages into two subtypes: M1 (classically activated macrophages) and (alternatively activated macrophages) (Mills et al., 2000). however, the M1 and M2 nomenclature is overly simplistic in explaining the wide range of distinct polarization phenotypes observed in tissue macrophages, which are triggered by a variety of environmental stimuli, including

prostaglandins, cytokines, fatty acids, and molecules derived from pathogens, such as lipopolysaccharides (LPSs).

M1 macrophages are pro-inflammatory and antimicrobial, whereas M2 macrophages have an anti-inflammatory function (Porta et al., 2015; Weisser et al., 2013) (Figure 1.4).

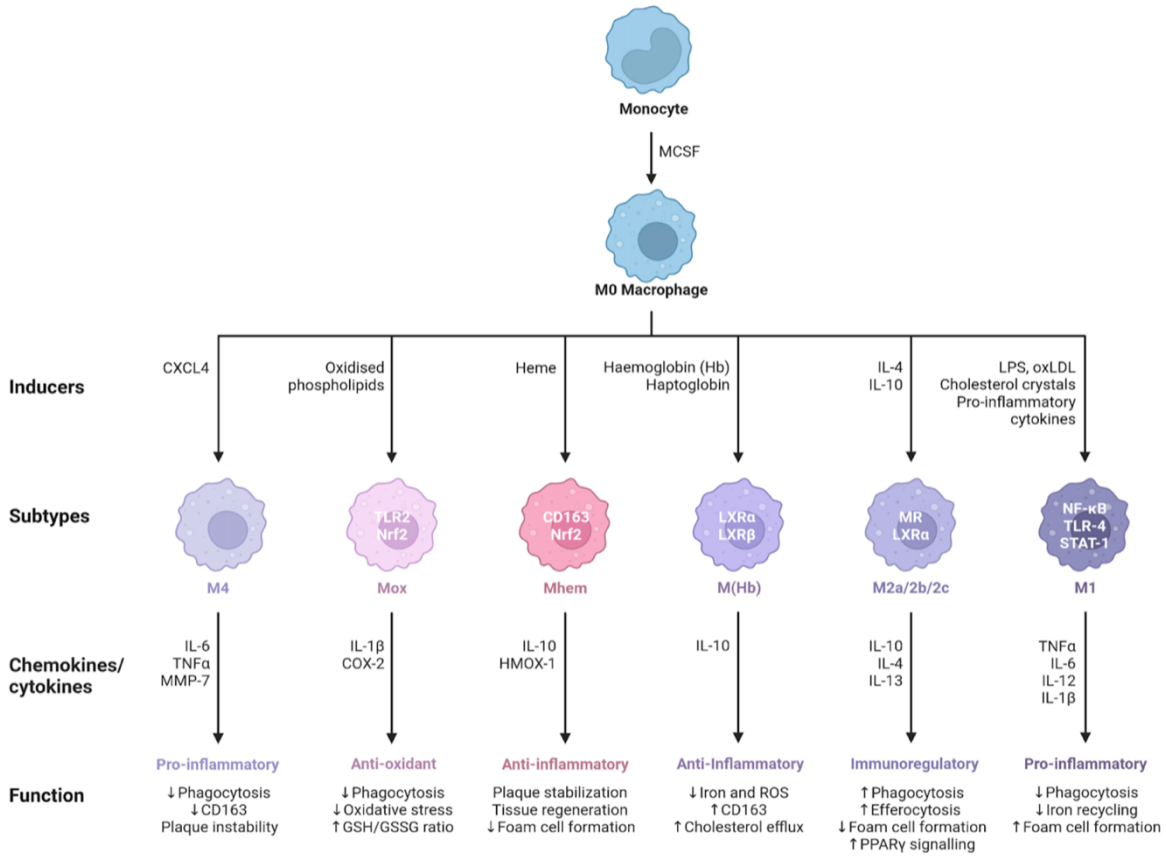

Figure 1.4 Macrophage Subtypes in Atherosclerosis. Monocytes are differentiated to M0 macrophages via monocyte colony stimulating factor (MCSF). Depending on the tissue microenvironment the M0 macrophage is then polarized to a particular subtype. The primary subtypes are pro-inflammatory M1 and anti-inflammatory M2 macrophages. In addition, multiple other subtypes have been identified including M(Hb), Mhem, Mox and M4. All of these subtypes produce various chemokines and cytokines and have different functions within the atherosclerotic plaque (Habib & Finn, 2014)(this template was adapted from the original submission. edits were made to enhance scientific accuracy).

To establish foetomaternal tolerance and shield the fetus from the maternal immune microenvironment, the number and proportion of M1/M2 macrophages at the maternal-fetal interface vary with the stages of gestation. More macrophages polarize into alternatively activated (M2-like) macrophages in order to maintain foetomaternal tolerance, suggesting that the immunosuppressive characteristics of M2 macrophages are required for a healthy pregnancy. At the maternal-fetal interface, there are more classically activated (M1) macrophages in aberrant pregnancies. Apoptotic cell phagocytosis, spiral artery remodelling, and trophoblast invasion are just a few of the normal pregnancy processes that depend on the balance of polarization between M1 and M2 macrophages. On the other hand, improper trophoblast invasion and insufficient uterine vessel remodelling were linked to the dysregulated polarization of macrophages, which ultimately resulted in spontaneous abortion, preeclampsia, and preterm birth (Guenther et al., 2012) (Schonkeren et al., 2011) (Gonzalez et al., 2011). (Yao et al., 2019)summarized the current understanding of the mechanisms underlying macrophage polarization.

1.6.3.1 The polarization of macrophages

Maintaining homeostasis and repairing tissue depend on macrophage polarization (Patel et al., 2017). The process by which macrophages develop unique functional phenotypes in response to particular signals and stimuli from their surroundings is known as "macrophage polarization" (Mantovani et al., 2004) (Canton, 2014) (Sica & Mantovani, 2012) (Chistiakov, Bobryshev, et al., 2015). It is possible to polarize macrophages into two different types: M1 (classically activated) and M2 (alternatively activated). The subcategories of M2 macrophages are M2a, M2b, M2c, and M2d. The cell surface markers, released cytokines, and biological roles of these macrophages vary. However, research has shown that rather than being simple schema, the induction routes and regulated biological processes are complex interlacing network systems (Atri et al., 2018). M1/M2 polarity results from the metabolism of arginine through two opposing pathways: the iNOS pathway generates citrulline and NO from arginine, while the arginase pathway generates ornithine and urea from arginine, producing M1-like macrophages (Lampiasi et al., 2016).

Once Th1 cytokines (like IFN-γ and TNF-α) and lipopolysaccharide (LPS) activate macrophages, they polarize into M1 macrophages, which are identified by TLR-2, TLR-4, CD80, CD86, iNOS, and MHC-II surface phenotypes. Numerous cytokines and chemokines, such as TNF-α, IL-1α, IL-

1β, IL-6, IL-12, CXCL9, and CXCL10, are released by these cells and provide positive feedback to unpolarized macrophages. In other words, more unpolarized macrophages are drawn to the M1 state by these factors. It has been demonstrated that important transcription factors like NF-kB, STAT1, STAT5, IRF3, and IRF5 control the expression of M1 genes. It appears that the two main pathways leading to M1 macrophage polarization and subsequent microbicidal and tumoricidal effects are STAT1 and NF-κB (Martinez & Gordon, 2014; P. J. Murray, 2017; Porta et al., 2015; N. Wang et al., 2014; Weisser et al., 2013).

M2 polarization is a reaction to cytokine downstream signals, including TGF-β, IL-4, IL-13, IL-10, and IL-33(Porta et al., 2015) (N. Wang et al., 2014). Interestingly, Th2 cytokines are produced by IL-33 and IL-25, which amplify M2 macrophage activation. Only IL-4 and IL-13 directly induce M2 macrophage activation (O'Shea & Paul, 2010). The expression of surface markers such as mannitol receptor, CD206, CD163, CD209, FIZZ1, and Ym1/2 can also be used to identify M2 macrophages. A number of cytokines and chemokines, including TGF-β, IL-10, CCL1, CCL17, CCL18, CCL22, and CCL24, are up-regulated (N. Wang et al., 2014) (Gordon & Martinez, 2010). These chemokines also draw unpolarized macrophages to acquire the M2 state (Mulder et al., 2014). It has been demonstrated that important transcription factors like STAT6, IRF4, JMJD3, PPARδ, and PPARγ control the expression of M2 genes. As of right now, M2 macrophage activation has been linked to the STAT6 pathway. Macrophages play a role in angiogenesis, immunomodulation, tissue repair, and infection prevention (Mantovani et al., 2013; Porta et al., 2015). Figure 1.5 depicted the primary distinctions between M1 and M2 macrophages.

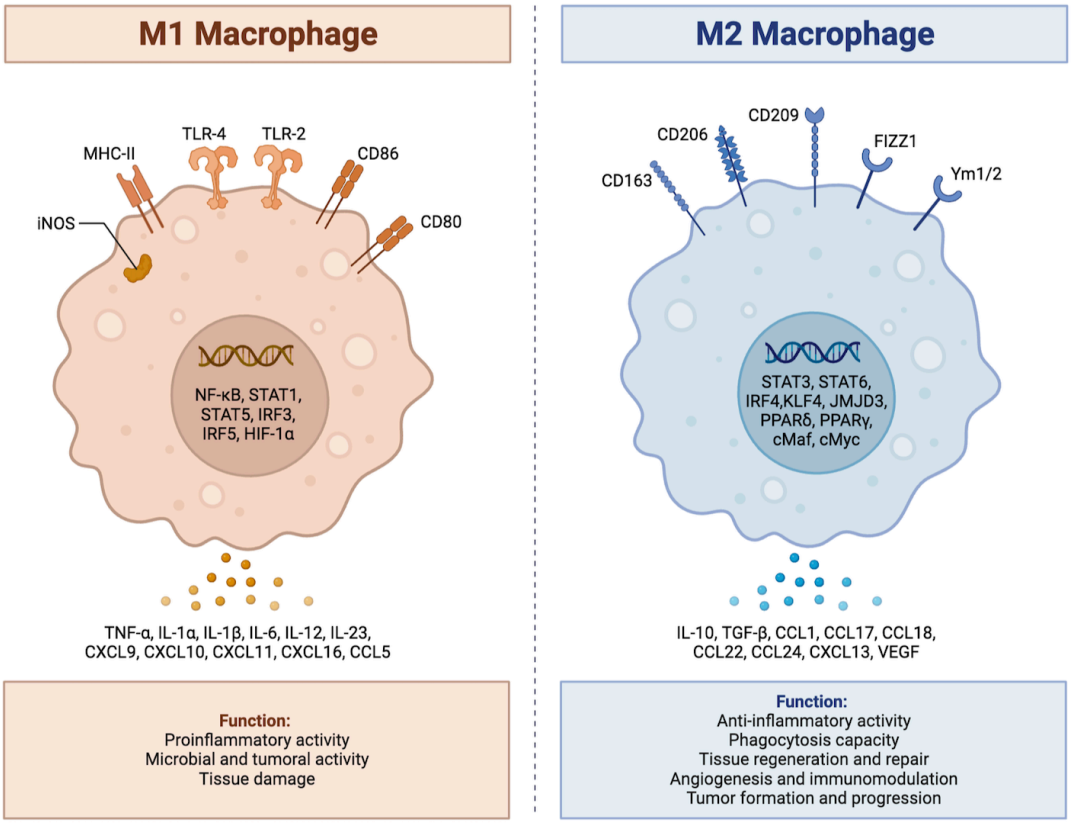

Figure 1.5 macrophages polarization: M1 and M2 subtypes. Created with Biorender.

1.6.4 Macrophages origin and function

The Greek terms makros and phagein are the source of the term macrophage, which literally translates to "big eater." Mϕs have multiple functions in addition to their specialized role in phagocytosis. On the other hand, Mϕs play a variety of roles in tissue development, homeostasis, and repair, as well as in the innate immune response and the start of inflammation. There is a lot of evidence to suggest that origin may not be the primary determinant of function. There is a lot of evidence to suggest that function may not be determined solely by origin. When grafted into neonatal Csf2rb2-/-mice, all Mϕs progenitors were demonstrated to be able to produce functional lung Alveolar Mϕs (AMs) (van de Laar et al., 2016). Similarly, in the liver, the transcriptional profile of monocyte-derived Kupffer cells (KCs) was highly homologous to that of their embryonic

counterparts (Scott et al., 2016). Therefore, it appears that the differentiated Mϕ's fate and functions are determined by the local environment that the progenitor enters (Guilliams & Scott, 2017). Crucially, Mϕs exhibit distinct epigenetic landscapes in each tissue, which support specialized transcriptional profiles (Scott et al., 2016) , (van de Laar et al., 2016), (Gautier et al., 2012). This implies that each tissue-resident Mϕs population will have certain functions that are particular to the tissue in which they reside. For example, muscle-cell Mϕs in the intestine control gastrointestinal motility (Muller et al., 2014), splenic red pulp macrophages are specialized in iron acquisition and metabolism (Kohyama et al., 2009), (Haldar et al., 2014). that Mϕs in the bone, known as osteoclasts, are specialized in bone resorption (Takayanagi et al., 2002), and that microglia in the brain perform synaptic "pruning," which is essential for the growth and preservation of the central nervous system (Parkhurst et al., 2013). We refer to these extra organ-beneficial functions as "accessory" functions (Okabe & Medzhitov, 2016).

1.6.4.1Macrophages and Immunity (How do macrophages function against pathogens?)

An array of microorganisms resides within the human body(Hirayama et al., 2017). The host immune system keeps microbes from invading despite constant exposure to a variety of microorganisms. The innate and adaptive immune systems make up the human immune system. By identifying and eliminating bacteria, myeloid cells like dendritic cells, neutrophils, and macrophages are essential to the innate immune system. Additionally, antigen-specific T and B cells work with the adaptive immune system to eliminate pathogens through the production of antigen-specific antibodies or cytotoxic reactions. The first line of defense is the innate immune system, which responds quickly.

The adaptive immune system is triggered, nevertheless, in cases where this system is unable to eradicate the infections entirely. When an infection is still in its early stages, the innate immune system eliminates and blocks infections. Humans are born with innate immunity, which is essential to the continuation of life. When pathogens and stresses enter the body, innate immunity detects them and eliminates them by triggering an inflammatory response(Hirayama et al., 2017). When receptors on innate immune cells identify particular molecular patterns originating from pathogens or stresses, an inflammatory response is initiated. Microorganisms provide pathogen-associated molecular patterns (PAMPs), which are recognized by pattern recognition receptors (PRRs) on

many epithelial cells and innate immune cells. On the other hand, regardless of the existence of a pathogenic infection, damage-associated molecular patterns (DAMPs) trigger and activate an immune response in response to trauma, ischemia, or tissue damage (Schenten & Medzhitov, 2011). Germline-encoded PRRs known as toll-like receptors (TLRs) are essential for host cell recognition and defense against microbial pathogens.

The identification of the TLR family in the fruit fly Drosophila provided a means of advancing the understanding of innate immunity cells' recognition mechanisms against microbiological components (Lemaitre et al., 1996). TLRs identify a variety of substances originating from viruses or bacteria as ligands. The TLR4-MD2 complex recognizes LPS, which is a component of the cell wall of Gram-negative bacteria, while heterodimeric TLR2/TLR1 and TLR2/TLR6 recognize bacterial lipopeptides and peptide glycans. Additionally, TLR3, TLR7, TLR8, and TLR9 all of which develop in the phagosome are capable of recognizing nucleic acids, such as viral RNA or bacterial genomic DNA. The signals that TLRs identify set off a chain reaction that induces the expression of genes by activating transcription factors like NF-κB and adapter molecules like myeloid differentiation primary response 88 (MyD88) and Toll/interleukin-1 receptor (TIR)-domain-containing adapter-inducing interferon-β (TRIF) (Kawai & Akira, 2011).

Different types of PRRs, such as NOD-like receptors (NLRs), the HIN-200 receptor family, and RIG-1-like receptors (RLRs), are present in the cytoplasm in addition to the PRRs on the cell membrane. These include molecules that serve as stress sensors against cytoplasmic pathogens. Along with ASC and caspase-1, a number of NLRs, including NALP1 and NALP3, form the inflammasome and mediate the maturation of pro-interleukin (IL)-1β into IL-1β that is ready for release. Caspases-1 are thought to be involved in the exclusion of pathogenic substances and the escalation of inflammation through the induction of pyroptosis, a highly inflammatory type of programmed cell death (Martinon et al., 2009). When RLRs detect viral double-stranded RNA, they use the interferon-β promoter stimulator to initiate a downstream signal cascade (IPS-1). Consequently, the production of inflammatory cytokines and type I interferons triggers an antiviral immune response (Bruns & Horvath, 2014). As was already mentioned, PRRs differ from one another in how they identify pathogens and mount an immune response against them.

The inflammasome forms a multiprotein complex in the cytoplasm that is several hundred kDa in size, according to recent studies. Inflammasome-related molecules polymerize the complex after

it is secreted outside of the cell. Larger complexation is thus stimulated extracellularly. Extensive complexation was found to exacerbate inflammation by triggering the release of pro-inflammatory cytokines (Baroja-Mazo et al., 2014; Franklin et al., 2014). To further cause inflammation, activated macrophages phagocytose the inflammasome complex.

1.6.4.2 Mechanisms of Phagocytosis

Phagocytosis is a cellular process for ingesting and eliminating particles larger than 0.5 μm in diameter, including microorganisms, foreign substances, and apoptotic cells (Levin et al., 2016). Cells presents in many cell types and is therefore an essential process for tissue homeostasis (Rabinovitch, 1995). However, only specialized cells called professional phagocytes perform phagocytosis with high efficiency. Macrophages, neutrophils, monocytes, dendritic cells, and osteoblasts are among these specialized cells(Rabinovitch, 1995).These professional phagocytes express a number of phagocytic receptors that activate signalling pathways leading to phagocytosis(Rabinovitch, 1995). This process consists of several stages: i) detection of ingested particles, ii) activation of internalization, iii) formation of a specialized vacuole called phagosome, and iv) maturation of the phagosome to turn it into a phagolysosome (Uribe-Querol & Rosales, 2020) (Figure 1.6).

The cells that play an important role in phagocytosis, serve as an intermediary between particular bacterial surface antigens and cellular receptors. After this bridge, the bacteria are encircled by membrane protrusions that then absorb them into the phagosome, which is created when cell membranes fuse together (Ueno & Wilson, 2012). Numerous signalling cascades can be triggered during this process due to the diversity of phagocytic receptors. These receptors can be categorized according to the types of ligands they recognize, which include opsonins, apoptotic bodies, and foreign molecules identified by distinctive molecular patterns. They vary in their degree of ligand specificity. Multiple PRRs on phagocytes bind selectively to distinct PAMPs. For example, certain polysaccharides on the surface of fungi are phagocytosed by Dectin-1 and the mannose receptor (Herre et al., 2004)(Ezekowitz et al., 1990; Herre et al., 2004).

Furthermore, a number of scavenger receptors trigger phagocytosis in response to PAMP recognition. These receptors include the macrophage receptor with collagenous structure

(MARCO) and scavenger receptor A (SR-A), both of which attach to the surface molecules of both Gram-positive and Gram-negative bacteria (Peiser et al., 2000; Thomas et al., 2000; van der Laan et al., 1999). Opsonins are a class of soluble molecules that can be adsorbed onto foreign surfaces to act as adaptors, binding and activating powerful phagocytic receptors. Specifically bound to microbial surface antigens, immunoglobulin G (IgG) recognizes the fragment crystallizable (Fc) region of phagocytes by interacting with their fragment crystallizable γ receptors (FcηRs) (C. L. Anderson et al., 1990; Nimmerjahn & Ravetch, 2008).

The complement system's C3b and iC3b molecules have the ability to attach to external particles. Apart from eliminating extraneous particles, phagocytosis plays a crucial role in the organism's cell turnover process because billions of cells undergo apoptosis every day and need to be eliminated. Depending on whether the cells are apoptotic or not, the phagocytosis mechanism varies. Increased phosphatidylserine (PS) surface exposure is thought to be the most well-characterized signature of apoptotic cells (Fadok et al., 1992). PS is primarily found in the inner leaflet of the plasma membrane in non-apoptotic cells. On the outside leaflet of the plasma membrane, PS concentration rises 300-fold after the apoptosis pathway is activated (Borisenko et al., 2003). Furthermore, soluble proteins that bind to exposed PS and function as linkers, akin to opsonins, include milk-fat globular protein (MFG)-E8, growth arrest-specific protein (Gas)6, and protein S (H. A. Anderson et al., 2003; Hanayama et al., 2002).

Microbes and apoptotic cells are immediately exposed to both oxygen-dependent and -independent attacks after being absorbed into the phagosome via one of several methods of receptor stimulation. NADPH-oxidase and phospholipase A2 both produce reactive oxygen species (ROS) and free fatty acids shortly after being absorbed into the phagosome. To some extent, these molecules exhibit a sterilizing effect against bacteria (Akaki et al., 1997; Roos, 1991). Subsequently, lysosomes like azurophilic granules, different hydrolases, and myeloperoxidase (MPO), a fundamental sterilization protein, fuse into the phagosome and break down microbial or apoptotic cells. The phagosome's pH is then lowered by the proton ATPase pump, which initiates either an oxygen-independent sterilization system using lysosomal enzymes and basic sterilization proteins (Hiemstra, 2006; Spitznagel, 1990) or a potent oxygen-dependent sterilization system, primarily

through halogenation (Klebanoff, 1968). Interestingly, macrophages do not contain MPO; instead, they contain Fe2+ ions that bind to chelators, like adenosine, to replace MPO.

Dendritic cells and macrophages are examples of antigen-presenting cells (APCs). They activate acquired immunity through helper T cell activation and present peptide antigens derived from digested bacteria on the major histocompatibility complex class II. Dendritic cells present antigens in the lymph node, whereas macrophages present antigens within tissues. The most potent APCs are dendritic cells, which are the only ones that can stimulate naïve T cells to become effector T cells (Guilliams et al., 2014).

Additional ligands released by pathogen degradation are recognized by receptors in the cytosol or on the phagolysosomal membrane. For instance, TLR9 is activated and the inflammatory response is increased when bacterial DNA is released into the cytosol. Moreover, the NLRP3 inflammasome is stimulated by the breakdown of S. aureus peptidoglycan in phagosomes; however, the exact mechanism by which this occurs is still unknown. According to a recent study, macrophages are able to detect microbial viability and effectively protect the host when bacterial components are released into the cytosol (Underhill & Goodridge, 2012).

The cell surface expresses toll-like receptors (TLR)-2, -4, and -5, which are able to identify bacterial components. Viral DNA and RNA are recognized by TLR-3, -7, and -9, which are expressed in the endosome. Following stimulation, each activates NF-κB or interferon regulatory transcription factor (IRF)-3 to produce inflammatory cytokines such as interleukin (IL)-6 or tumour necrosis factor (TNF)-α. Caspase-1 is produced and activated by NOD-like receptors (NLRs), including NLRP-1 and -3. These NLRs also mediate the conversion of pro-IL-1β to mature IL-1β. Pyroptosis and inflammation are brought on by mature IL-1β. When multiple receptors recognize different antigens, phagocytosis is triggered. The figure displays representative receptors. By using phagocytosis, antigen-loaded harmful cells are broken down and rendered sterile (Hirayama et al., 2017).

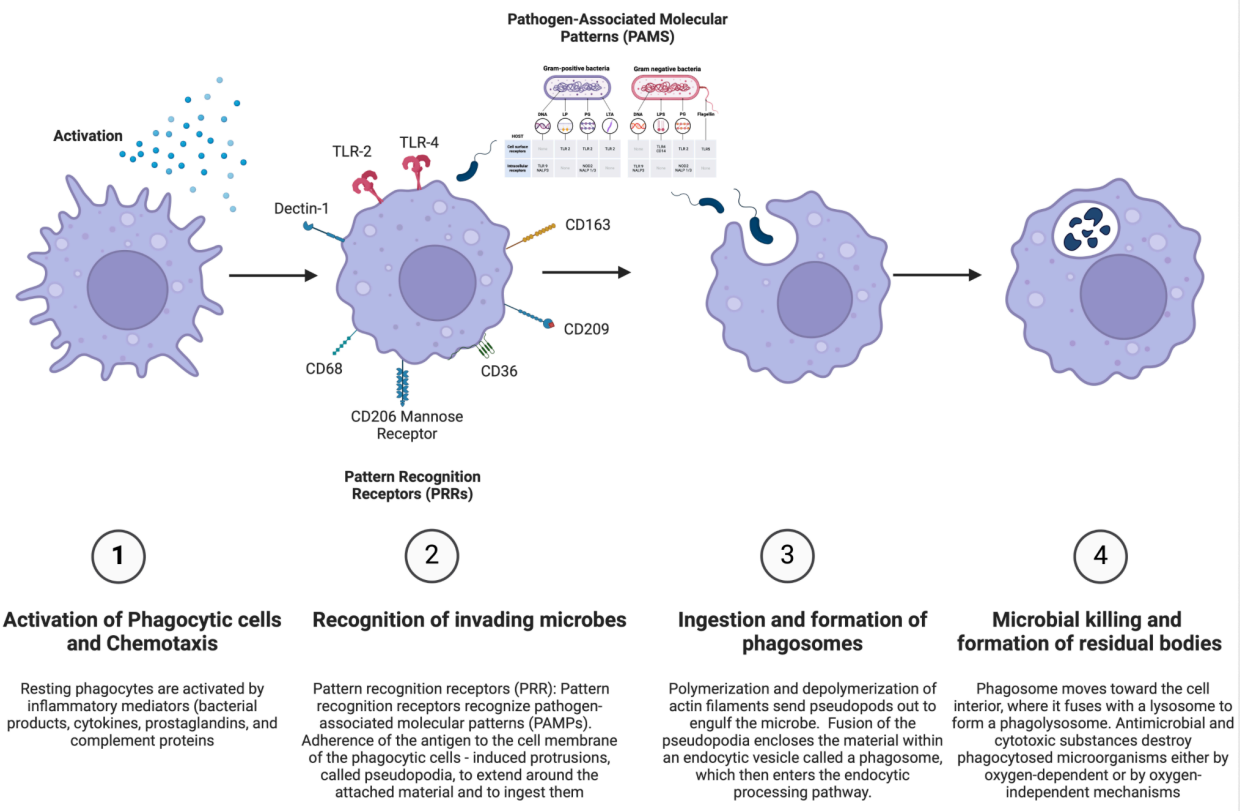

Figure 1.6 Overview of phagocytosis mechanisms by macrophages. The process of phagocytosis involves several phases: i) detection of the particle to be ingested, ii) activation of the internalization process, iii) formation of a specialised vacuole called phagosome, and iv) maturation of the phagosome to transform it into a phagolysosome. Created with Biorender.

1.6.4.3 Lipid metabolism

Macrophages and reverse cholesterol transport:

Macrophages have become important players in lipid metabolism due to the same mechanisms that have evolved to allow them to protect the body from infection, such as phagocytosis of pathogens. Macrophages have developed ways to remove cholesterol from cells because they are good at absorbing lipoproteins from dying cells. Foam cells are produced by macrophages when excess cholesterol is not removed from them. These foam cells play a role in the formation and breaking down of atherosclerotic plaques (Moore et al., 2013).

Because of the same mechanisms that have allowed them to protect the body from infection, such as phagocytosis of pathogens, macrophages have emerged as key players in lipid metabolism. Because macrophages are adept at absorbing lipoproteins from dying cells, they have devised methods for removing cholesterol from cells. When macrophages do not get rid of extra cholesterol, they produce foam cells. The development and degradation of atherosclerotic plaques are influenced by these foam cells (Moore et al., 2013). When cellular cholesterol builds up, it triggers the activation of multiple transcription factors (TFs) , such as the retinoid X receptor (Rxr), the liver X receptor α and β (Lxra, Lxrb), and the peroxisome proliferator-activated receptor (Ppar) family, which includes Ppara and Pparg. (Duffy & Rader, 2009), (Klappacher & Glass, 2002). The ATP-binding cassette subfamily A member 1 (ABCA1) and ABCG1 are upregulated in expression by Lxr and Rxr when they form heterodimers (M. A. Kennedy et al., 2005), (N. Wang et al., 2004), and (Hara & Yokoyama, 1991).

Although the exact role of ABCG1 *in vivo* is still up for debate (M. A. Kennedy et al., 2005), (Tarling & Edwards, 2011), (Nakamura et al., 2004), these transporters control the efflux of free cholesterol to lipid-poor ApoA-I and other poorly lipidated apolipoproteins to eventually form mature HDLs (Hutchins & Heinecke, 2015). As an alternative, passive efflux of free cholesterol may also happen through facilitated diffusion (SR-BI-mediated pathway) or simple diffusion (aqueous diffusion pathway) (Phillips, 2014) (Figure 1.7).

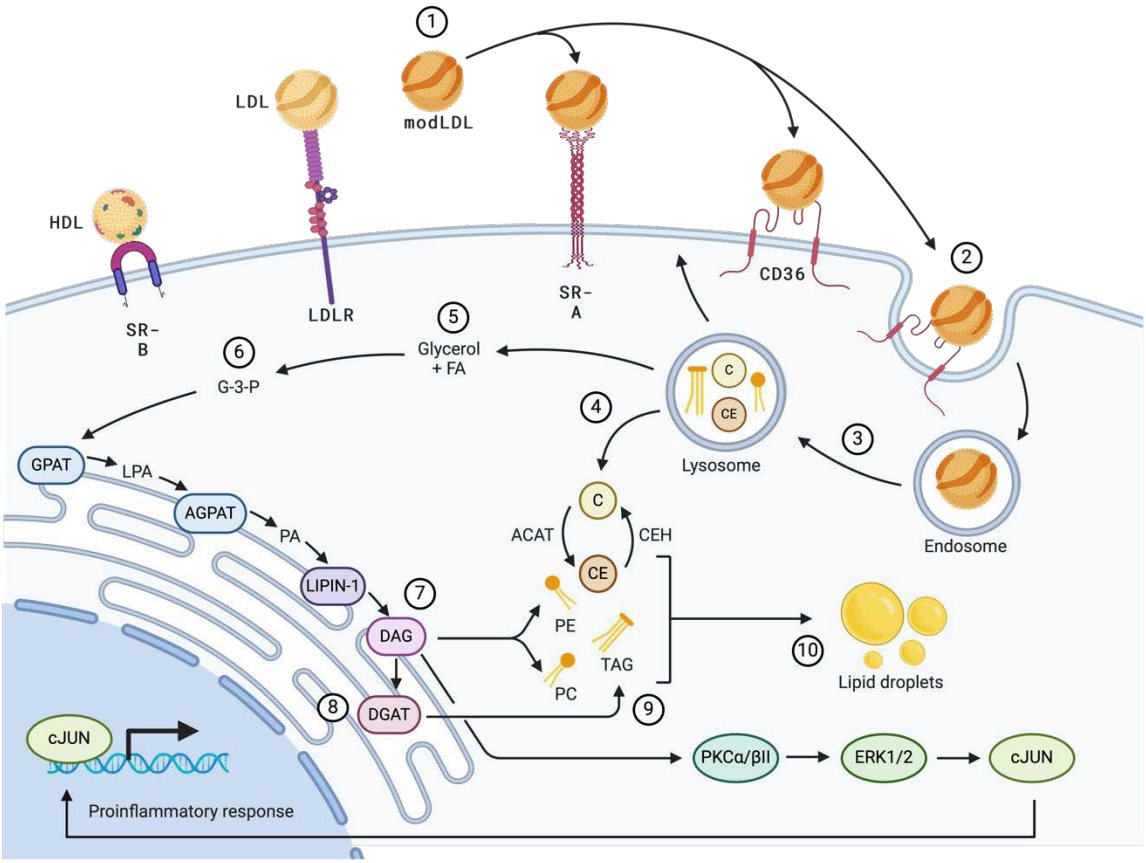

Figure 1.7: Uptake of LDL into Macrophages. Macrophages take up LDL, VLDL and oxidised lipoproteins via macropinocytosis, phagocytosis and scavenger receptor-mediated pathways including LOX-1, SR-A1, CD36and SR-B1. Free cholesterol and fatty acids are generated following degradation of ingested lipids in the lysosome. Such cholesterol can be utilised to form lipid rafts. Accumulation of cellular cholesterol leads to activation of several transcription factors, including PPARγ, LXRs and RXRs which subsequently regulate expression of their target genes including transporters such as ABCA1 and ABCG1 which regulate the efflux of free cholesterol and scavenger receptors. Alternatively, passive efflux of free cholesterol can also occur. Created with Biorender.

1.6.4 Macrophages and Progression of atherosclerosis

Since atherosclerosis is the main pathological cause of CVD (X.-H. Yu et al., 2019), a thorough investigation of the pathophysiology of atherosclerosis is imperative. Numerous cells, including macrophages, vascular smooth muscle cells, and endothelial cells, are involved in the development of atherosclerosis. Specifically, macrophages play a pivotal role in the progression of the entire pathological process of atherosclerosis, from the early stage of foam cell formation to the late stage of atherosclerotic plaque rupture (W. Chen et al., 2022) (Figure 1.8). Research has indicated that the impact of macrophages on atherosclerotic plaques is influenced not only by the quantity of macrophages infiltrated but also by the degree of their polarization and the proportion of various phenotypes (X. Liu et al., 2021)(Canfrán-Duque et al., 2023; X. Liu et al., 2021).

Large and medium arteries are the main types of arteries affected by atherosclerosis, a chronic inflammatory disease (Tabas & Bornfeldt, 2016) (Shapouri-Moghaddam et al., 2018) (Soehnlein & Libby, 2021)(Grover & Mackman, 2020; Soehnlein & Libby, 2021). Damaged endothelial cells allow low-density lipoprotein cholesterol (LDL-C) to enter the intima, where it is changed into oxidized LDL-C, due to the influence of major risk factors. Oxidized low-density lipoprotein (LDL-C) stimulates endothelial cells to express chemokines and adhesion factors, which draws in monocytes from the circulation. These monocytes then undergo macrophage differentiation in a local milieu enriched in growth factors and proinflammatory cytokines. Macrophages rapidly recognize and consume oxidized low-density lipoprotein (LDL-C) via scavenger receptors on their surface, converting into foam cells that form the initial atherosclerotic lesions (Khatana et al., 2020). Stable or unstable plaques develop as the disease worsens due to the buildup of foam cells, local necrosis, and the creation of a fibrous cap (Libby, 2021). Due to alterations in hemodynamics, stress, and inflammatory reactions, plaque instability leads to plaque rupture, bleeding, and thrombosis in the advanced stages of atherosclerosis. Foam cell production and accumulation are therefore critical phases in the pathogenesis of atherosclerosis (Poznyak et al., 2020).

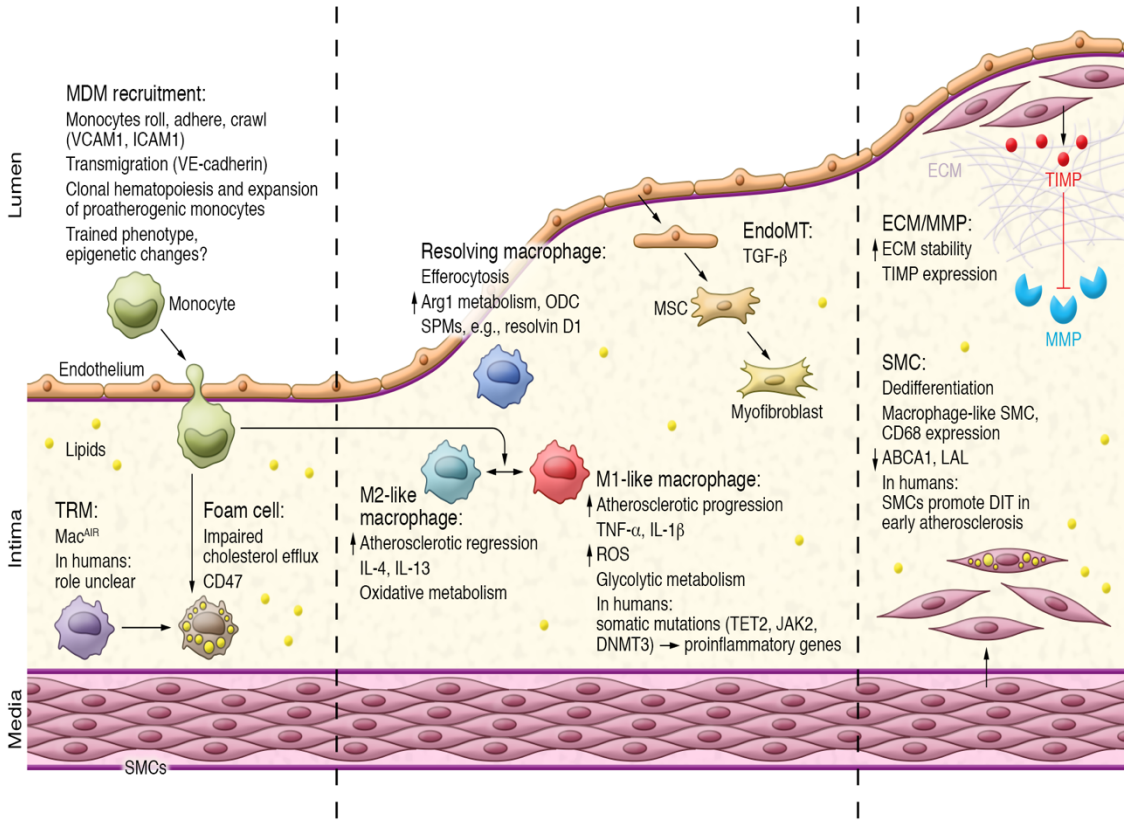

Figure 1.8 Overview of macrophage function during each stage of atherosclerosis. Early stages of cholesterol-rich atherosclerosis. In the intima, MDM is recruited through endothelial interactions and differentiation to engulf excess lipids along with TRM to become foam cells. Certain macrophages adopt a proinflammatory M1-like phenotype that promotes inflammation and necrotic core formation during disease. In addition, endothelial cells can undergo EndoMT and vSMCs dedifferentiate into macrophage-like SMCs to become foam cells. growing plaque. To accommodate plaque size growth, ECM remodelling occurs via MMPs, and when ECM decreases, SMC fibre caps. When diluted, plaques tend to rupture. During disease regression and when cholesterol metabolism and excretion are efficient, macrophages play a pro-degradative role M2-like phenotype. Along with SPM, increased M2-like macrophages promote resolution of inflammation and plaque regression. Figure is adapted from the original submission (Susser & Rayner, 2022).

1.6.5 The origin of macrophages within arteriosclerotic lesions

The role of macrophages in inflammation and disease has been thoroughly investigated from their initial description in the late 19th century; nevertheless, due to their plasticity and tissue-specific roles, much is still unknown (Susser & Rayner, 2022). Macrophages are unique that they occur in virtually all tissues and have varying effects including (i) physiological roles essential for tissue homeostasis, (ii) phagocytosis of cell debris and microorganisms, (iii) tissue repair and assembly, (iv) regulation of immune response by cytokine production (Rasheed & Rayner, 2021). Recent advances in lineage tracing technology have revealed that there are two main populations of macrophages:

1- Tissue-Resident Macrophages (TRM)

TRM seeded early in fetal development, it has the capacity to self-renew and adapt to roles and characteristics and it can be identified through a common expression mouse tissue-type-independent signatures (e.g., CD64 and MerTK), additionally, TRM can be further tagged by tissue-specific gene expression signature (e.g F4/80+Clec4F^{+} Kupffer cells in liver, TRAP^{+}CD61^{+} osteoclasts in bone (N. C. Williams & O'Neill, 2018);(Takayanagi et al., 2002).

2- Monocyte-Derived Macrophages (MDM)

Bone marrow derived monocytes as the name suggests are derived from differentiation of bone marrow cells. Monocytes leave the circulation and enter tissues. Both TRM and MDM act similarly to phagocytes and can induce and promote immune responses at the same time. MDM are mainly derived from hematopoietic stem cells in the bone marrow and spleen which differentiate into monocytes and then macrophages in response to a specific signal. Steady state MDM are present in small amounts in tissues and replenished. Recruitment and differentiation of monocytes by growth factors and others macrophage colony-stimulating factor (Gomez et al., 2018)(Gomez et al., 2018; Rahman et al., 2017). A subset of classic monocytes is ready to be recruited to the subendothelial space at the first signs of inflammation or damage. These monocytes are characterized by high expression of Ly6C (mouse) or CD14 (human) depending on the stimulus with proinflammatory (also known as M1/classically activated) or pro-resolving (also known as M2/alternatively) activated. Although these phenotypes have been thoroughly

investigated in cell culture, MDMs are more likely to exhibit more transitory forms *in vivo* due to the diverse stimuli they experience (Moore et al., 2018). Through the activation of Toll-like receptor 4 (TLR4), pathogen-associated molecular patterns such lipopolysaccharide produced by infection with gram-negative bacteria or other receptors, such as those stimulated by IFN-, polarize M1 macrophages *in vitro*. They exhibit an ability to kill bacteria, produce reactive oxygen species (ROS), have a preference for glycolytic metabolism, and release a number of inflammatory cytokines like TNF- and IL-1, inducible nitric oxide synthase (iNOS) as a result of polarization (L. Shi et al., 2019)(L. Shi et al., 2019; Yunna et al., 2020). Upon stimulation with IL-4 or IL-13, alternatively activated M2 macrophages polarize, leading to an increase in phagocytic capacity, a preference for oxidative metabolism, and the release of pro-resolving molecules like IL-10 and TGF- that support angiogenesis, tissue repair, and immunoregulation (Rahman et al., 2017).

A deeper comprehension of macrophages in all diseases, including atherosclerosis, has been made possible by our comprehension of the distinct characteristics of TRMs and MDMs. Reparative M2-like macrophages are more prevalent in regressing and stable plaques during repair, whereas proinflammatory or M1-like macrophages are typically observed in plaques that are progressing and have active inflammation (Libby, 2003; Moore et al., 2013; E. P. K. Yu et al., 2017). Although macrophages are the cause of inflammation within a plaque, they also undergo phenotypic shifts in response to tissue demands and are necessary for the stabilization and resolution processes that follow plaque regression in mice (Susser & Rayner, 2022).

3- Stem cell (SC)

Since the pioneering research by S. Yamanaka's laboratory (Takahashi & Yamanaka, 2006) that described transcriptional factors able to convert mature somatic cells into pluripotent cells, iPSCs started to be widely used to generate a wide variety of specialized cell types. One of the actively developed directions is the differentiation of iPSCs into innate immune cells, particularly, into macrophages. Among the different pathways of iPSC differentiation, lineage specification into macrophages is a recently developed and rapidly growing technique. Until recently, peripheral blood monocyte-derived macrophages (MDM) were the major source of human macrophages (Luque-Martin et al., 2021). Recently, approaches to generate macrophages (iMphs) from induced

or embryonic pluripotent stem cells have been developed and shown to have several advantages over the MDM model (Buchrieser et al., 2017; Lee et al., 2018; Takata et al., 2017; Tasnim et al., 2019). The technique's benefits include the capacity to produce genetically modified cells, scalability, standardization, and easy access to PSCs (Klatt et al., 2019; Yeung et al., 2017; H. Zhang et al., 2017) , which , taken collectively , greatly increases the model's potential uses (Lyadova et al., 2021).

4- Vascular smooth muscle cells (vSMCs)

In atherosclerosis, vSMCs are thought to migrate from the media to the intima, where they also take up lipoproteins. The coexistence of macrophages and vSMCs in the intima raises many questions about whether and how these cells communicate and influence each other (Allahverdian et al., 2014). While the accumulation of large numbers of SMC-like cells in the human intima is evidence that atherosclerosis is predominantly SMC- rather than a macrophage-mediated disease, many studies have purported that differentiation of vSMCs into macrophages is also prevalent (Rong et al., 2003). This idea has been difficult to test because the expression of vSMC and macrophage markers in tissue sections only provides a snapshot that is blind to lesion dynamics and cell ontogeny (Feil et al., 2014) (Swirski & Nahrendorf, 2014). However, the development of advanced lineage tracing techniques has since presented additional compelling evidence that purports that vSMC transdifferentiate into macrophages within atherosclerotic lesions. While SMC-like cells in atherosclerotic plaques are purported to be derived from pre-existing vSMCs in the medial layer of vessel, a subset of these cells in the advanced atherosclerotic plaques may differentiate into macrophage-like cells or foam cells (Shankman et al., 2015). Moreover, a dual genetic lineage approach to specifically trace lineage conversion of SMC-derived macrophage-like cells revealed that a subset of these cells re-adopted the SMC lineage in the fibrous cap, contributing to fibroblasts and pericytes in the plaque (Y. Li et al., 2021).

To summarize , origins of macrophages within arteriosclerotic lesions that are important in atherosclerotic disease progression and regression according to several researchers and studies are :Tissue-Resident Macrophages (TRMs) which are seeded early in fetal development of atherosclerotic plaques (N. C. Williams & O'Neill, 2018);(Takayanagi et al., 2002), Monocyte-Derived Macrophages (MDMs) are derived from the differentiation of monocytes when they exit

the circulation into tissue (Gomez et al., 2018; Rahman et al., 2017), macrophages generated from induced embryonic pluripotent stem cells (Lyadova et al., 2021) and macrophage-like cells that derived from vSMCs in the medial layer of vessel in the advanced atherosclerotic plaques (Shankman et al., 2015) (Figure 1.9).

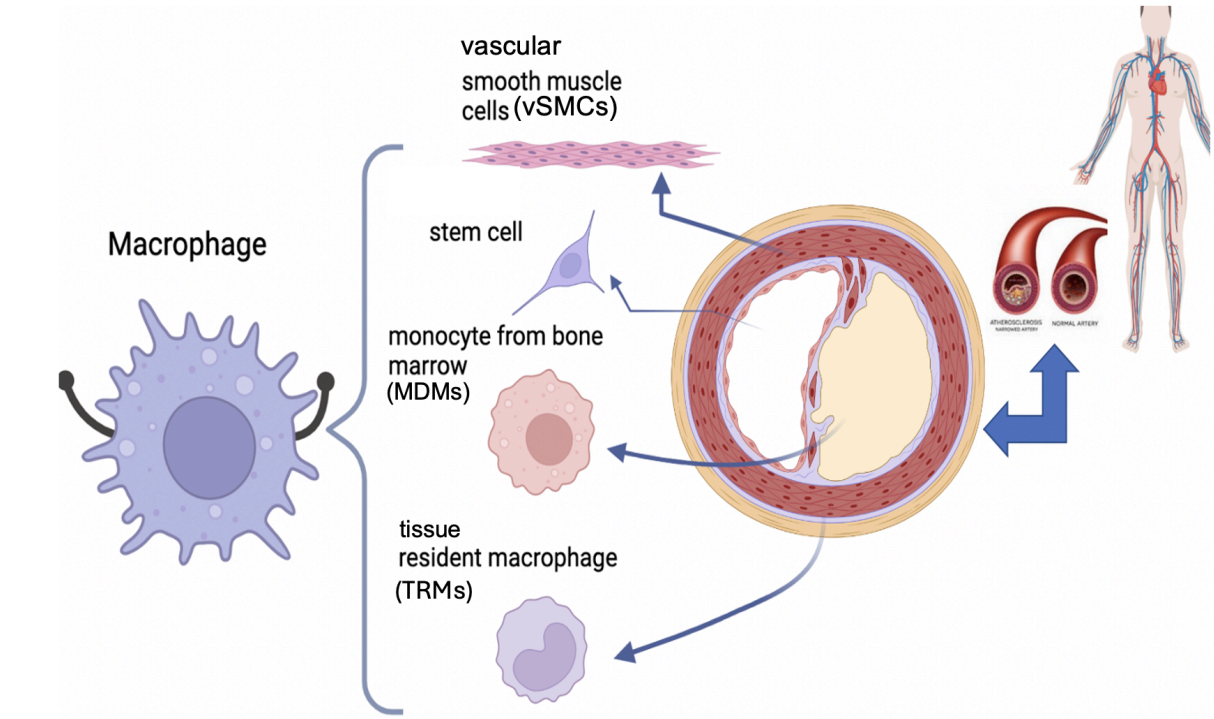

Figure 1.9 The origin of macrophages within arteriosclerotic lesions. Many studies indicate the origin of macrophage-like cell in the arteriosclerosis lesions which are vSMC, SC, MDM and TRM. Created with Biorender.

1.6.6 The Role of bone marrow derived monocytes and macrophages in atherosclerotic lesions.

The endothelial layer lining the lumen of blood vessels is the primary physical barrier between blood and tissue. Healthy endothelium regulates vascular tone and cell adhesion and maintains vascular homeostasis through anticoagulant, antithrombotic and anti-inflammatory effects (Auffray et al., 2007). During atherosclerosis, these homeostatic properties are lost. It is estimated that less than 1% of all patrolling monocytes migrate to the subendothelial space in the resting unstimulated endothelium (Auffray et al., 2007)(Figure 1.10). However, when activated, such as in hypercholesterolemia or impaired blood flow, monocytes are recruited. This accumulation of MDM cells is a highly regulated process in which monocytes roll, adhere and crawl through interactions with endothelial cells (EC) and then migrate from the vascular lumen to the intima.

Release of inflammatory cytokines such as TNF-α and IL-1β from TRMs induces rapid expression of EC adhesion molecules such as E and P-selectin, intercellular adhesion molecule 1 (ICAM1) and vascular cell adhesion molecule 1 (VCAM1) (Bennett et al., 2016) (C. Shi & Pamer, 2011). This expression of adhesion molecules and presentation of adhesion chemokines by monocytes (i.e., CCL2, CCL5) allows them to roll on the vascular EC monolayer, overcoming the force of blood flow (C. Shi & Pamer, 2011; H. Xu et al., 2008; Zarbock et al., 2008). Rolling depends on the interaction of selectins and monocyte P-selectin glycoprotein ligand 1 (PSGL1), VCAM1, monocyte-expressed very late antigen 4 (VLA4), and CD44, which allows monocytes to switch from rolling to firm attachment (Bennett et al., 2016) (C. Shi & Pamer, 2011; H. Xu et al., 2008; Zarbock et al., 2008). C-C and C-X-C chemokines such as CCL2 and IL-8 also contribute to firm adhesion of monocytes (Luscinskas et al., 2000). Circulation and attachment are followed by crawling, a chemotactic phase in which monocytes spread laterally to find the best migration site. Intraluminal crawling depends on monocyte factors, lymphocyte function-associated antigen 1 (LFA1) and macrophage-1 antigen (Mac1), which interact with endothelial ICAM1 and ICAM2 (Schenkel et al., 2004). The final stage of monocyte migration can occur at either intercellular or paracellular junctions in the endothelium. EY lacks proper tension joints; instead, they have vascular endothelial cadherin (VE-cadherin), which is a gatekeeper for migration. Cellular signals from adherent monocytes dissociate adherens junctions through VE-cadherin phosphorylation, allowing macrophages to enter the subendothelial intima (Allingham et al., 2007).

The multifaceted mechanisms that activate the expression of adhesion and transmigration signals in ECs during atherosclerosis have been discussed elsewhere (Zhou et al., 2014), but are triggered when lipoproteins trapped in the subendothelial space are engulfed by TRMs, leading to the secretion of TNF-α on luminal ECs by inducing chemokines and adhesion molecules. Furthermore, since atherosclerosis occurs mainly in arterial branches and areas of disturbed/non-laminar flow, the low shear stress environment enables the expression of adhesion molecules and induces EC permeability through developmental regulators TGF-β, BMP and Wnt, among others (Souilhol et al., 2020). This notion is also supported by recent evidence that neuronal guidance cues (eg semaphorins, netrins and ephrins), which normally function as neuronal guidance signals during development, play an important role in the interaction of ECs with monocytes in the atherosclerotic environment (Fiorelli et al., 2021) (Bruikman et al., 2020) (van Gils et al., 2013) (van Gils et al., 2012). It is likely that the interplay between lipoprotein retention and low shear stress over decades works together to exacerbate plaque formation: as the lesion grows, blood flow patterns are disrupted, activating EC permeability programmes and allowing more excess lipid to pass through; while TRMs are activated in response to excess cholesterol, they express more adhesion molecules and further increase permeability and immune cell recruitment.

Retention of LDL-derived lipids from the intimal circulation is the primary step in the development of atherosclerotic damage. Under homeostatic conditions, TRMs deal with lipids in the extracellular space via intracellular metabolic pathways (such as autophagy), storage (via lipid droplet formation), or efflux (via transfer of free cholesterol to available HDL particles). However, during the progression of atherosclerosis, cholesterol control is lacking. Captured LDL is easily modified by aggregation (agLDL) and/or oxidation (ox-LDL) and is therefore easily recognized by scavenger cells and TLRs of the innate immune system. In addition, TRMs cleave large LDL aggregates via lysosomal exocytosis, leading to cholesterol crystal formation and subsequent inflammasome activation (Haka et al., 2009). TRMs attempt to remove excess lipids, but this process quickly becomes overwhelmed, causing macrophages to become “foam cells” (X.-H. Yu et al., 2013).

Cholesterol efflux in HDL and/or its apolipoprotein A1 (apoA1) depends on the activity of the ATP-binding cassette transporters ABCG1 and ABCA1 (Chistiakov et al., 2016). When efflux

receptors are unavailable (eg low or impaired HDL) (Ouimet et al., 2019) (Gofman & Lindgren, 1950) or when lipid droplet metabolism is impaired (eg, reduced autophagy) (Ouimet & Marcel, 2012), ER stress is triggered and/or foam cells undergo programmed apoptosis (collapse)or necrotic cell death (rupture). Initially, apoptosis, along with efficient efferocytosis of other macrophages, prevents plaque growth. In the late stage of atherosclerosis, when apoptosis is overwhelmed or inhibited, foam cells can undergo necroptosis through a cascade of receptor-interacting serine/threonine protein kinase 1 (RIPK1), RIPK3, and mixed-lineage kinase domain-like pseudokinase (MLKL), leading to rupture of the cell membrane and release of its inflammatory contents (Doran et al., 2020) (D'Arcy, 2019). The released content then acts as an inflammatory signal to recruit MDMs. In addition, foam cells have high levels of CD47 (a strong "don't eat me" signal) and reduced expression of MerTK (an important efferocyte receptor), rendering efferocytosis ineffective (Decker et al., 2021). In addition, other forms of cell death may contribute to the development of the lesion. Pyroptosis is a caspase-1-mediated inflammatory cell death that results in a pore-induced intracellular trap that releases the cytosolic contents of the cell (Kovacs & Miao, 2017) (Y.-J. Xu et al., 2018). Ferroptosis, a recently described form of inflammatory cell death caused by iron-dependent lipid peroxidation, has recently been shown to be critical in the development of atherosclerosis (Ouyang et al., 2021) (H.-F. Yan et al., 2021) (Y. Wang et al., 2021). The combined inefficiency of efferocytosis and increased cell death, especially in necrotic forms of cell death, results in the formation of a necrotic nucleus, dead and dying macrophages, cellular debris and modified lipids (Moore & Tabas, 2011) (Tabas & Bornfeldt, 2016). The presence of a necrotic core indicates an advanced and unstable lesion.

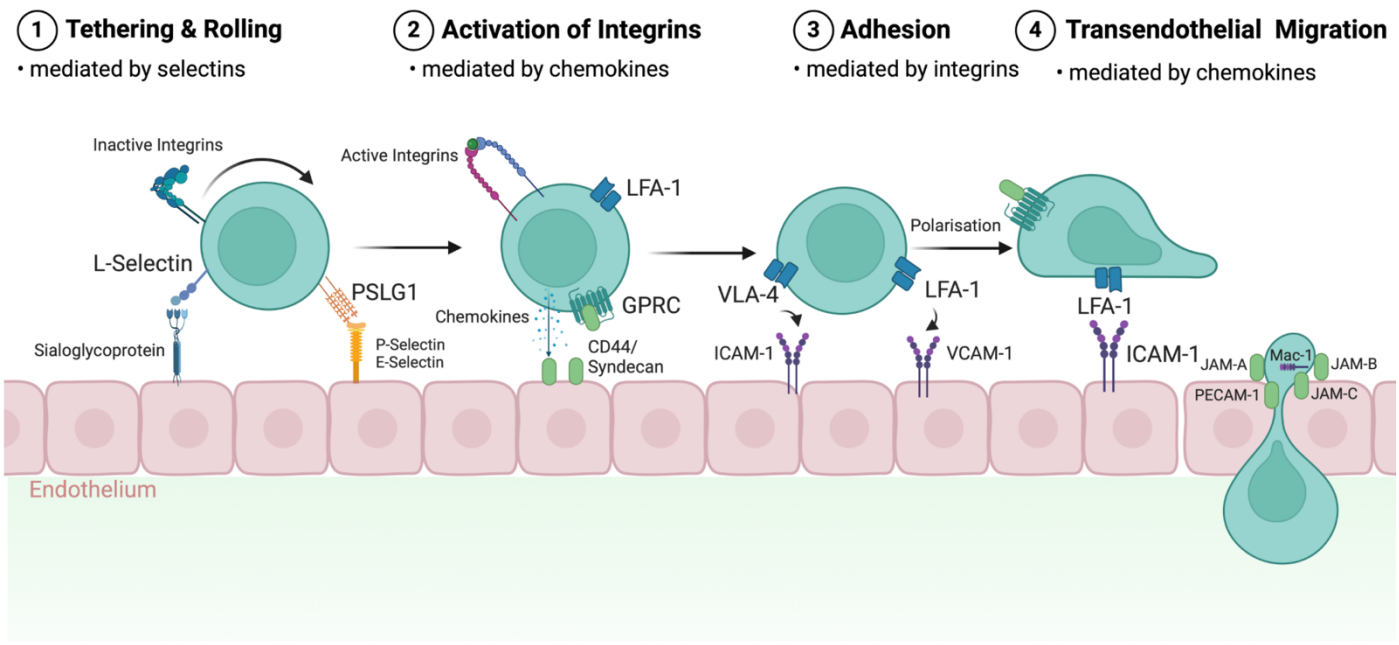

Figure 1.10 Overview of monocyte-endothelial cell interaction and transmigration. Monocyte migration to inflammatory sites is a multistep process with many molecules involved. First, selectins mediate the initial tethering and rolling of monocytes along the cytokine-activated endothelial cells. Then, the monocyte interacts with chemokines that are bound to transmembrane heparan sulphate proteoglycans (CD44 and sydecan) expressed in the endothelium. The activation of GPCR leads to the activation of integrins and the consequent monocyte arrest mediated by the interaction of LFA1 and VLA4 with ICAM1 and VCAM, respectively. Once a monocyte establishes firm adhesion to the vascular endothelium, it undergoes a morphological change known as polarization, in which chemokine receptors and activated integrins redistribute to the leading edge. After polarization, monocytes migrate toward interendothelial junctions and then transmigrate into the underlying tissues. The members of the JAM family expressed by endothelial cells (JAM-A, JAM-B, JAM-C) interact with the activated integrins of monocytes (LFA1, VLA4, Mac1) and allow the transmigration through tight junctions. Lastly, PECAM-1 (CD31) and CD99 hemophilic engagement and endothelial retraction lead to monocyte extravasation. PSGL: P-selectin glycoprotein ligand-1; GPCR: G-protein-coupled receptors; LFA1: lymphocyte function-associated antigen 1; VLA4: very late antigen 4; ICAM1: intercellular adhesion molecule 1 (ICAM1/CD54); VCAM: vascular cell-adhesion molecule 1; Mac1: macrophage receptor 1; PECAM: platelet/endothelial cell-adhesion molecule 1. Created with Biorender.

1.6.7 The Role of intimal macrophages and macrophage-like cells (MLCs) in atherosclerotic lesions.

AS mentioned previously, vSMCs form the medial layer of intact arteries and are fully differentiated but quiescent, with contractile function characterized by high levels of αSMA and smooth muscle myosin heavy chain (SM-MHC, coded MYH11) (Bennett et al., 2016). In the early stages of atherosclerosis, medial SMCs differentiate and migrate into the intimal space in a process of DIT (Allahverdian et al., 2018) (J. H. Campbell & Campbell, 2012; Chistiakov, Orekhov, et al., 2015) (Nakashima et al., 2008). The early process of DIT is unique to human plaques, but intimal thickening can be induced experimentally in animals (Nakashima et al., 2008), (Gomez & Owens, 2012). Intimal SMCs lose contractile function, in part due to decreased expression of αSMA and SM-MHC, and acquire phenotypes reminiscent of fibroblasts, osteoblasts, and macrophages (Sorokin et al., 2020). Several years ago, studies *in vitro* (Andreeva et al., 1997) (Babaev et al., 1993) (Babaev et al., 1990) and mouse (Gomez & Owens, 2012), (Rong et al., 2003), (Owens et al., 2004) showed that in a proatherogenic environment, SMCs downregulate the contractile markers Sm22α (encoding SM22α or transgelin) and Acta2, Cd68 and Cd11b (Sorokin et al., 2020). Loss of these key functional differentiation markers of SMCs occurs at least in part through epigenetic silencing of contractile gene promoters and activation of stemness-related genes, resulting in undifferentiated SMCs (Gomez et al., 2015; M. Liu et al., 2021). Emerging evidence suggests that both murine and human transitional SMCs also exhibit impaired signalling in the retinoic acid pathway, which can be therapeutically manipulated to reduce atherosclerosis (Pan et al., 2020). Taken together, these observations led to the understanding that plaque foam cells, historically considered to be of TRM or MDM origin, are at least partially transdifferentiated SMCs (Pryma et al., 2019) (Allahverdian et al., 2014).

In humans, more than 50% of foam cells in human middle coronary atherosclerosis have been suggested to be of SMC origin (Allahverdian et al., 2014). This population of macrophage-like SMCs tends to become foam cells due to lower expression of ABCA1 and lysosomal acid lipase (LAL), both of which are important for efficient cholesterol efflux (Dubland et al., 2021). In addition, SM22α is required for the efficient nuclear translocation of LXRα, a key anti-inflammatory transcription factor that promotes cholesterol efflux, further contributing to the foam cell phenotype of these cells (Zhang et al., 2021). Transdifferentiated SMCs have also been shown

to expand in a clonal manner reminiscent of cancer (Zhang et al., 2021) (Benditt & Benditt, 1973) (Y. Wang et al., 2020). As in cancer, clonal expansion provides several survival advantages, such as adaptation to toxic environments and suppression of efferocytosis by CD47 (the “don't eat me” signal) (DiRenzo et al., 2017).

Although intimal macrophages have been intensively studied for nearly a century, we are only now beginning to understand the diversity of intimal macrophages and macrophage-like cells. Advances in understanding plaque development and its macrophage content have been made possible by advances in lineage-tracing technology, which marks cells *in vivo* along their differentiation pathway, making them easily identifiable by fluorescent or other genetic markers. This tracking technique, combined with the power of single-cell RNA sequencing, enabled unprecedented, detailed mapping of every cell in a tissue or sample. This technique has been used to map entire systems such as the hematopoietic system, lungs, kidneys, and heart (Wagner & Klein, 2020). Through this, it has been revealed that the interior of the plaque is more complex than previously thought. Prominent examples include the finding that, as described in the section above, SMCs adopt a macrophage-like phenotype and express CD68 during progression of atherosclerosis (Sorokin et al., 2020), (Rong et al., 2003), (M. Liu et al., 2021), (Gomez et al., 2015), (Pryma et al., 2019), (Allahverdian et al., 2014). Fate mapping and high-resolution transcriptomics also enabled aortic intimal macrophages, also known as MacAIR cells, a unique subtype of macrophages that accumulate in the aortic arch at birth and are maintained through CSF1-dependent local proliferation, largely replaced by recruited MDMs (J. W. Williams et al., 2020). These MacAIR cells were originally classified as dendritic cells, which were thought to be the earliest phagocytes in the aortic arch of mice. The role of local proliferation and MDM replacement from the circulation in maintaining this distinct cell pool is still debated (J. W. Williams et al., 2020). This study surprisingly found that MacAIR cells express high levels of Il1b transcript but almost undetectable Nlrp3, a component of the inflammasome complex required for IL-1β activation. Therefore, in contrast to the previously hypothesized murine atherosclerotic plaques, which originate from macrophages, there are different subtypes that preferentially take up excess lipid or produce powerful anti-inflammatory cytokines. Many of these observations were previously made using other techniques, but the combination of lineage tracing and high-resolution

transcriptomics allowed these cells to be characterized in more detail (Wagner & Klein, 2020) , (Williams et al., 2020), (Robbins et al., 2013).

Another macrophage association that plays a direct role in the progression of atherosclerosis is the interaction of macrophages with the extracellular matrix (ECM), which consists of biologically active proteins such as collagens (I, III, IV and V), elastin, glycoproteins (fibronectin), thrombospondin, vitronectin, osteopontin and proteoglycans, which provide tensile strength and elasticity to the arterial wall (Katsuda & Kaji, 2003). In the early stages of atherosclerosis, the ECM acts as a mesh to trap cholesterol in the arterial wall. The proteoglycans of the subendothelial space directly interact with apoB of the LDL particle due to its strong positive charge and the negative charge of the proteoglycans - the so-called response-retention hypothesis (Williams & Tabas, 1995). ECM components of the subendothelial space are mainly secreted by modulated SMCs, while matrix metalloproteinases (MMPs), enzymes that break down ECM and other proteins, are mainly released by macrophages. The ratio of ECM to MMP is tightly regulated and sensitive to an inflammatory stimulus such as TGF-β, which promotes collagen and elastin synthesis. In addition, tissue inhibitors of metalloproteinases (TIMPs) are secreted by the same cells as endogenous inhibitors, allowing rapid regulation of MMP-mediated ECM remodeling (Katsuda & Kaji, 2003). ECs or other cells produce TGF-β; it increases collagen production, while proinflammatory TNF-α and IFN-γ secreted by inflammatory cells decrease collagen synthesis (Katsuda & Kaji, 2003), (Chistiakov et al., 2013). While MMPs are elevated due to macrophages within the lesion, this is associated with reduced plaque stability through both structural reduction and the release of inflammatory cytokines, which are also trapped in the ECM. When there are fewer MMPs, the plaque is more stable throughout the ECM, which helps form a strong fibrous cap (Chistiakov et al., 2013). As such, the communication and interaction between macrophages and SMCs dictates the state of the ECM and thus the structural stability of the plaque.

During the progression of atherosclerosis, macrophages also interact with other cells of the innate and adaptive immune system. These pathways and interactions have been discussed extensively in other reviews (Moore et al., 2013),(Hansson & Hermansson, 2011), (Schaftenaar et al., 2016), but the adaptive immune system is increasingly recognized for its clinical contribution and protection against atherosclerosis. As antigen-presenting cells, macrophages and dendritic cells present ox-

LDL as a foreign body in their major histocompatibility complex to activate T lymphocytes, which further stimulate B-cell activation (Moriya, 2019)(Sage et al., 2019)(Moriya, 2019; Sage et al., 2019; Sage & Mallat, 2014). M1 macrophages and Th1 cells promote atherosclerosis by producing inflammatory cytokines and chemokines, while M2 macrophages, Tregs, and B-1 cells suppress inflammation, reduce plaque size, and promote plaque persistence (Herrero-Fernandez et al., 2019),(Winkels et al., 2018). IgM autoantibodies, which can be produced endogenously and react with the oxidized phospholipid found in oxLDL, have been used to treat advanced stages of atherosclerosis (Chang et al., 1999) (Palinski et al., 1996) (Cherepanova et al., 2020) (Que et al., 2018). Cherepanova et al. generated a novel IgM autoantibody, 10C12, targeting similar oxidized phospholipids and showed that administration of this autoantibody to $Igm^{-/-}$ $ApoE^{-/-}$ mice fed a low-fat diet increased lipid accumulation in the aorta by 40% (Cherepanova et al., 2020). Using a similar concept, Zhang et al. developed a novel human single-chain variable fragment antibody against oxLDL oxidation epitope ASA6, which reduced the area of atherosclerotic lesions in $ApoE^{-/-}$ mice by regulating fatty acid metabolism and preventing M1 macrophage polarization (Zhang et al., 2021). In addition, conjugation of ASA6 to MRI/near infrared II (NIR-II) bifunctional nanoparticles provided a dual therapeutic and diagnostic tool that enabled non-invasive imaging of atherosclerotic lesions—which was previously very difficult (Zhang et al., 2021).

Although the accumulation of macrophages and their interaction with other cells in the vessel wall directly causes atherosclerosis, they are also important for plaque stabilization and regression. The regression process of atherosclerosis requires new monocytes from the circulation in response to CCR2, and without these MDMs, regression does not occur (Rahman et al., 2017). In contrast, MDMs that cannot become inflammatory macrophages (eg, by removing TRAM downstream of TLR4 activation or removing the proinflammatory neuronal leader netrin-1) can be pushed to a soluble phenotype to promote atherosclerotic regression (Geng et al., 2021) (Schlegel et al., 2021). Both clinically and experimentally, the primary mechanism by which pre-existing atherosclerotic lesions begin to regress and heal is through the reduction of circulating plasma lipid levels. In mouse models, this usually involves removal of excess lipids from foam cells by increasing cholesterol efflux through ABCA1 via the apoA1/HDL reverse cholesterol transport pathway (Fisher, 2016). When cholesterol efflux is activated under conditions of high HDL, plaque

macrophages acquire an M2-like phenotype, releasing proinflammatory cytokines such as IL-10 and TGF-β, which promote tissue repair and angiogenesis (Forrester & Griendling, 2017). The soluble phenotype also promotes phagocytosis of debris and efferocytosis of apoptotic cells, helping to reduce the necrotic core. Indeed, efferocytosis and lysis of apoptotic cells promote macrophage proliferation, increasing the number of macrophages available for efferocytosis and further promoting the regression process (Gerlach et al., 2021). To achieve an effective efferocyte response during the inflammatory response, macrophages change their metabolic profile to promote oxidative metabolism and activation of phagolysosomes to lyse engulfed apoptotic cells. Without full efferocyte capacity, or if the metabolic requirements of efferocytosis are not met, atherosclerosis cannot be reversed (Yurdagul, 2021). During resolution of inflammation, macrophages produce polyamines such as putrescine, spermidine, and spermine, which support proliferation and other processes during tissue repair. In an atherosclerotic environment, pro-soluble macrophages require arginine, a precursor of polyamines, for sustained efferocytosis of dead cells and regression of atherosclerosis. Loss of expression of arginase 1 (Arg1) and ornithine decarboxylase (Odc) in macrophages impairs atherosclerosis regression in mice due to lack of MerTK expression and ineffective efferocytosis (A et al., 2021; Yurdagul et al., 2020). On the other hand, changes in the metabolic environment can also alter the pro-inflammatory and anti-inflammatory responses of macrophages during the progression of atherosclerosis. Desmosterol, a precursor of the cholesterol biosynthetic pathway, has been found to reduce ROS and NLRP3 inflammasome activation in mice, and inhibition of desmosterol signalling promotes atherosclerosis (Muse et al., 2018; Spann et al., 2012; X. Zhang et al., 2021). Another product of the cholesterol biosynthetic pathway, mevalonate, can trigger epigenetic reprogramming and macrophage inflammatory activation through trained immunity, and blocking mevalone production with statins reduces this inflammatory activation (Bekkering et al., 2018). Together, these studies suggest that MDMs are likely to be flexible to acquire a pro- or atherosclerotic phenotype, depending on the inflammatory signals they receive, the metabolic environment, and the expression of the machinery required to induce a progression or regression response. Macrophage foam cells, such as transdifferentiated SMCs, have not been fully investigated for the regression of atherosclerosis; however, in mice and humans, transdifferentiated SMC foam cells express low levels of ABCA1 compared to macrophages, suggesting that approaches that promote cholesterol efflux for regression of existing plaques would be deficient in SMC foam cell-rich

lesions (Wang et al., 2019). On the other hand, SMCs from both the medial and intimal layers contribute to plaque stability by forming a fibrous cap through the secretion of ECM proteins (Sorokin et al., 2020). Therefore, controlling the phenotype of SMCs in the lesion is crucial to ensure the removal of excess cholesterol and promote plaque stability, and both processes are important therapeutic goals. And just as the interaction between macrophages and T cells is necessary for the progression of inflammatory atherosclerosis, the interaction of T cells, especially Tregs, with macrophages is important for the activation of M2 macrophage differentiation programs in plaque regression (Sharma et al., 2020). Therefore, macrophages cannot be considered only as agents of inflammation and disease in the vessel wall, but are also responsible for disease reversal and stabilization, which are very important therapeutically. Specific pro-resolution mediators (SPM) have recently become a new therapeutic target to promote healing and resolution of inflammation. SPMs are a subclass of lipid mediators derived from arachidonate, eicosapentaenoic acid, docosahexaenoic acid, or n-3-docosapentaenoic acid, which are metabolized to lipoxins, resolvins, protecins, and maresins (Serhan, 2014). Comparison of stable and unstable regions of human atherosclerotic lesions reveals an imbalance between pro-resolving SPM and pro-inflammatory lipids; especially in areas of plaque instability, the ratio of leukotriene B4 (LTB4) to resolvin D1 (RvD1) is higher. In $Ldlr^{-/-}$ mice with advanced lesions, administration of RvD1 restored the RvD1/LTB4 ratio, reduced the necrotic core, and increased fibrous cap formation, which increased plaque stability. Interestingly, this increase in fibrous cap thickness was not due to a change in total SMC or macrophage concentration; instead, it is thought that SPMs specifically promoted the detachment of inflammatory cells from plaques and changed their phenotype to a pro-dissolving program (Fredman et al., 2016). SPMs act directly through their cell surface receptors to promote phagocytic clearance and efferocytosis by macrophages, which then increases SPM biosynthesis and synergistically promotes atherosclerotic regression. In advanced atherosclerosis, RvD1 can also promote the removal of necrotic cells by defeating the “don't eat me” signal CD47 through ER-mediated phagocytosis (Decker et al., 2021). New roles for SPM continue to emerge as we begin to study this class of lipid mediators, and RvD1, in particular is emerging as a very promising new therapeutic target.

1.7Aims and Objectives

While macrophages, MLCs, vSMCs and SMC-like cells are major contributors to plaque growth, the contribution of resident mVSCs to the appearance of SMC-like cells and MLCs remains controversial. In both humans and mice, the relative contribution of SMC-like cells and MLCs, the timing of their appearance, and their relative proximity to each other and deposited lipids in the artery wall are all key determinants of the initiation and progression of atherosclerosis. These cells proliferate locally within the atherosclerotic plaque and while they are natural targets for novel therapies, current approaches are limited. A clearer understanding of these steps and the interactions between lipid and mVSCs and their myogenic SMC-like progeny that accumulate within atherosclerotic lesions and influence foam cell development and regression are likely to provide fertile ground in the years ahead for development of novel treatments that will reduce ischemic vascular disease beyond what is possible with currently available treatments.

Therefore, the central question that this thesis work addresses is whether murine and human S100β mVSCs are capable of myeloid differentiation to MLCs when exposed to cholesterol, oxidized LDL (ox-LDL) and myeloid differentiation media *in vitro* in comparison with the response of murine and human vSMCs in culture to the same treatments.

1.7.1 Aims

- Determine whether resident mouse S100β mVSC undergo myeloid differentiation in response to cholesterol and\or ox-LDL

- Determine whether human induced pluripotent stem cell (hiPSC)-derived S100β vascular stem cells (SNEPS) undergo myeloid differentiation in response to cholesterol and\or ox-LDL.

The overall strategy to address these objectives is outlined in Figure 1.11, Both mouse and human S100β mVSCs in culture were treated in the presence of myeloid inductive stimuli (ox-LDL, cholesterol, myeloid differentiation media) before morphological changes, lipid uptake and expression of myeloid differentiation markers (CD68, MacII, F4/80, CD11b) was assessed by phase contrast microscopy, Oil Red O uptake, immunocytochemistry, flow cytometry and RT-qPCR. Mouse J7441 macrophages and THP-1 derived macrophages (following PMA treatment) were utilized as positive controls.

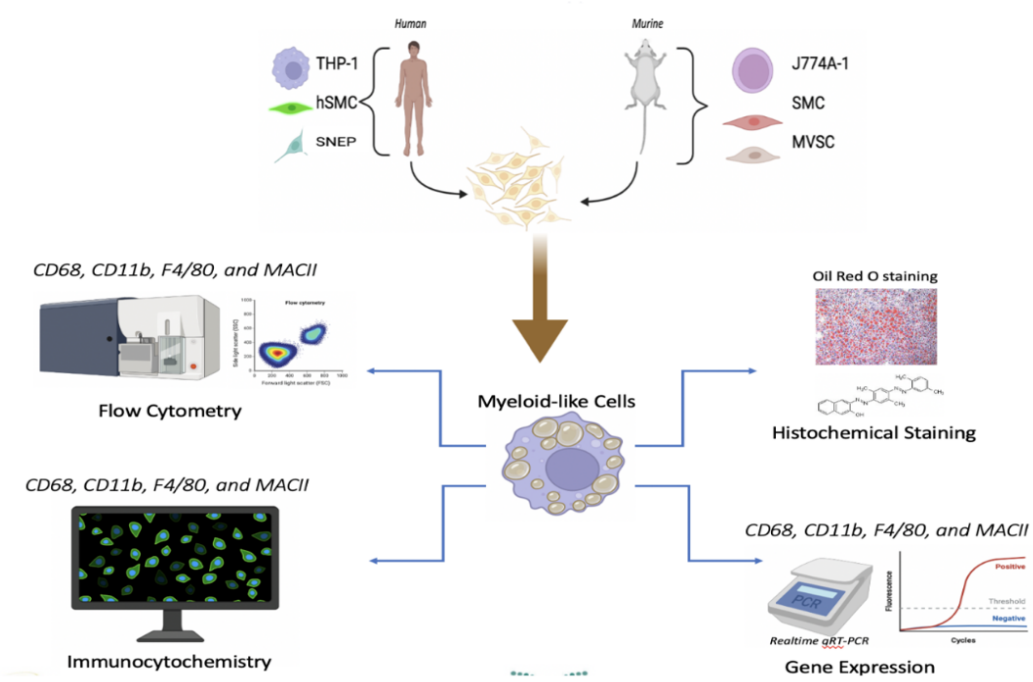

Figure 1.11 Experimental strategy. Schematic to illustrate strategy to address whether mVSCs and vSMCs undergo myeloid differentiation *in vitro*. Created with Biorender.

Chapter 2

Materials & Methods

2.1 Biological materials

2.1.1 Commercial cell lines & tissue-derived cells

Table 2.1: Commercial cell lines & tissue-derived cells

Cells	Morphology	Cell origin	Description	Supplier' name
Mouse Aortic Smooth Muscle Cells (MOVAS)	Spindle	Mouse	Primary vascular aortic smooth muscle cells isolated by collagenase	ATTC (CRL-2797TM)
Mouse Vascular Stem Cells (mVSC)	spindle	NE	mVSCs derived from the thoracic aortic medial layer by enzymatic dispersion	_
J774A-1	Spherical Macrophage	Mouse	cell line isolated in 1968 from the ascites of an adult, female mouse with reticulum cell sarcoma	ATTC TIB-67 ™
THP-1	Spherical monocytes	Human	a monocyte isolated from peripheral blood from an acute monocytic leukemia patient	ATCC, Cat: ATCC-TIB-202
hiPSCs	Embryoid body	Human skin tissue	White British male 65-69, disease status: normal	HipSci
hiPSc -derived SNEPs	spindle	hiPSC	HiPSC derived Spontaneous NE progenitor cells (SNEPS) are derived from induced pluripotent stem cells generated using a non-chemical stimulus	_
hSMC	hill and valley	SNEP	SNEP-derived vSMCs (SNEP-SMCs) are derived from hiPSC derived SNEP	_

2.1.2 Growth Medium

Table 2.2: growth medium

Cell Line	Medium	Supplier	Components
MOVAS	RPMI 1640 With L-glutamine and sodium bicarbonate, liquid, sterile	ATCC cat: CRL-2797 ™	94% RPMI 5% FBS 1% P/S
mVSC	MM1	-	92,96% DMEM. 2% Chick Embryo Extract (CEE). 1% FBS embryonic qualified (ATCC). 1% P/S 1X B-27 Supplement serum free(50X). 1X CTSTM (Cell Therapy Systems) N-2. 0.02 µg/mL Recombinant Mouse FGF basic Protein (100 µg/mL). 50 nM 1:20 diluted 2-Mercaptoethanol. 1:10 diluted Retinoic Acid (RA).

J774A-1	Dulbecco's Modified Eagle's Medium (DMEM)	ATCC cat:30-2002	94% DMEM 5% FBS 1% P/S
THP-1	RPMI 1640 With L-glutamine and sodium bicarbonate, liquid, sterile	ATCC cat:30-2001	89% RPMI 10% heat-inactivated FBS 1% P/S 1:20 diluted 2-Mercaptoethanol
SNEP	Gibco™ Essential 8™ Flex Medium Kit	Gibco™ cat: A2858501	98.5% Essential 8™ Flex Medium 1% E8 SUPPLEMENT 0.5% P/S
hSMC	Dulbecco's Modified Eagle's Medium (DMEM)	ATCC cat:30-2002	94% DMEM 5% FBS 1% P/S (10ng/ml) PDGF-BB (2ng/ml) TGF-β1
Smooth Muscle cells differentiation media	MEF		94% DMEM F12 5% FBS 0.5% P/S 0.5% L-Glutamine 1:20 diluted 2-Mercaptoethanol

2.1.3 PCR Primers and Antibodies:

Table 2.3: primers from integrated DNA technologies (IDT)

PRIMER	SEQUENCE
m *Mac-2*	F-5'>AGGAGAGGGAATGATGTTGCC<3' R-5'>GGTTTGCCACTCTCAAAGGG<3'
m Cd68	F-ACTTCGGGCCATGTTTCTCT R-GCTGGTAGGTTGATTGTCGT
m *F4/80*	F-CTTTGGCTATGGGCTTCCAGTCC R-GCAAGGAGGACAGAGTTTATCGTG
m *GABDH*	F-5'-GCCTCCAAGGAGTAAGAAAC-3' R-5'-CTGGGATGGAAATTGTGAGG-3'
m *S100β*	F-5'-ATCAACAACGAGCTCTCTCAC-3' R-5'-CATCTTCGTCCAGCGTCT-3'
m *Cnn1*	F-5-GCTTGTCTGCTGAAGTAAAGAAC-3 R-5'-TCCATGAAGTTGTTCCCGATG-3'
h *CD68*	F-5'-GAACCCCAACAAAACCAAG3' R-5'-GATGAGAGGCAGCAAGATG-3')
h *GAPDH*	F-5'-AACAGCCTCAAGATCAGCAA-3' R-5'-CAGTCTGGGTGGCAGTGAT03')
EMR1	F-5'-CCAAGGGGGATAAGATGAAG3' R-5'CACCAAGGAGATGATTAATGCC-3'
h *MAC-2*	F-5'CCATCTTCTGGACAGCCAAGTG R-5'-TATCAGCATGCGAGGCACCACT
h *CNN1*	F-5'-GTGCTACAGGGTCCAACATAG-3' R-5'-CAGTCGCTGCAAACCAAAC-3'
h *S100β*	F-5'-GGAGTCAGGTCTCAGTGATAAAG-3' R-5'-TGCGAGTTCTGATGGAGTTG-3'

2.1.4 Antibodies:

Table 2.4: antibodies

Antibody	Supplier
Rabbit monoclonal [EP798Y] to calponin 1 (CNN 1)	Abcam Cat: ab46794
Rabbit anti-Galectin 3 (MAC ll)	Abcam Cat: ab76245
Rabbit monoclonal [EP1576Y] to S100 beta (S100*β)*	Abcam Cat: ab52642
AF anti-CD68	Abcam Cat: ab222914
AF546 Goat-Rabbit secondary antibody	Invitrogen Cat: A11008
CD68 Monoclonal Antibody, PE	eBioscience Cat: 12-0689-42
CD11b Monoclonal Antibody, PE-Cyanine7	eBioscience Cat:25-0112-81
F4/80 Monoclonal Antibody, APC	eBioscience Cat:17-4801-82

2.1.5 Macrophage Markers during myeloid differentiation

- **CD68**

CD68 is a heavily glycosylated type I transmembrane glycoprotein, that is highly associated with endosomal/lysosomal compartment (Holness & Simmons, 1993). A high rate expression of CD68 on the surface had been detected with murine macrophages (Kurushima et al., 2000) and cultured monocyte THP-1 cells (Ramprasad et al., 1996).For usage in flow cytometric analysis and immunocytochemistry, we bought CD68 Monoclonal Antibody (eBioY1/82A (Y1/82A)), PE, from eBioscience™ Catalog # 12-0689-42, we used 5 µL (0.5 µg) per test as recommended by the supplier. As mentioned in section 2.2.3.5.1 for flow cytometery, and section 2.2.3.2 for immunocytochemistry.

- **CD11b**

CD11b, a transmembrane glycoprotein, serves as a cell surface marker that aids in identifying and characterizing specific immune cell populations, particularly macrophages (H.-A. Kim et al., 2017). We bought CD11b Monoclonal Antibody, Cyanine7 from eBioscience™ Catalog # 25-0112-81, used 5 µL (0.5 µg) per test as recommended by the supplier. As mentioned in section 2.2.3.5.1 for flow cytometery, and section 2.2.3.2 for immunocytochemistry.

- **F4/80**

A surface marker , It has been suggested that mouse tissue macrophage populations can be identified by high expression of F4/80 (Schulz et al., 2012). also known as EMR1 in human (Baud et al., 1995). We bought F4/80 Monoclonal Antibody, APC from eBioscience™ Catalog # 17-4801-82, used 5 µL (0.5 µg) per test as recommended by the supplier. As mentioned in section 2.2.3.5.1 for flow cytometery.

- **MAC II**

MacII, also known as Galectin 3, MAC-2 has a high expression levels in myeloid cells in human and mice tissues (Hohsfield et al., 2022). (H.-A. Kim et al., 2017). We bought

Rabbit anti-Galectin 3 (MAC ll) from Abcam, Catalog # ab76245. Section 2.2.3.2 for immunocytochemistry.

2.1.6 Chemical and Biological agents

Table 2.5: Chemical and biological agents

SUPPLIER	PRODUCTS
Sigma	• Cholesterol, cat: C4951-30mg • Bovine Serum Albumin (BSA) cat: A4503 • Glycine cat: G8898 • L-Glutamine cat: G7513 • Penicillin-Streptomycin(P/S) cat: P4333
Peprotech	• Animal-Free Recombinant Human TGF-β1, cat: 100-21C • Recombinant Human PDGF-BB, cat:100-14B
Sigma Aldrich	• Oil red O stain commission, cat: O0625-25G • FORMALDEHYDE MOLECULAR BIOLOGY REAGENT, cat: F8775-500ML • Retinoic acid (100nM) cat: R2656 • Triton X-100, cat: T8787 • Trypsin, cat: T4174), • TWEEN. 20, cat: P1379 • Fluoromount™ Aqueous Mounting Medium, Cat: F4680 • 2-Propanol, cat: I9516 • 2-mercaptoethanol, cat:M-7154
Saralab	Chick Embryo Extract (CE-650-J)
R&D System	Recombinant Mouse FGF basic Protein (3139-FB-025)
Bioline	• SensiFAST SYBR No-ROX One-Step Kit (500 rxns), cat: BIO-72005 • SensiMix SYPER No ROX kit, cat: QT650-05

My bio	ReliaPrep RNA Cell Miniprep System 250 PREPS, cat: Z6012
Generon	Human Plasma low density lipoprotein (ox-LDL) Oxidized, purified, cat: LDLO13-N-1 x 1
Invivogen	Phorbol 12-Myristate 13-Acetate (PMA) 5mg, cat: tlrl-pma
Stem cell	• StemSpan Myeloid Exp Supplement II 100X, cat: 2694 • Vitronectin, cat**:** 100-0763
Fisher scientific	• MP Biomedicals™ Cryopres™ Dimethyl Sulfoxide (>99.9% USP DMSO for cryopreservation) 50mL, cat: 16379855 • HANKS balanced salt solution, cat:88284 • DPBS X1, CAT: 10708144
Invitrogen	DAPI (4',6-Diamidino-2 Phenylindole, Dihydrochloride) Cat: D1306
ATCC	• DMEM F12, cat: 30-2006 • F-12K, cat: 30-2004 • Fetal bovine serum, cat: 30-2020 • Dulbecco's Modified Eagle's Medium (DMEM), cat: 30-2002 • RPMI-1640 Medium, cat: 30-2001
Merk group	Gelatin Solution Bioreagent, 2% in H_2O, cat: G1393-100 ml
Gibco	• N-2 Supplement, cat: A1370701 • B-27. Supplement, serum free, cat:17504044) • 2-Mercaptoethanol (50 mM), cat: 31350010) • TrypLE™, cat: 12563029 • Essential™ 8 medium kit, cat: A1517001 • Poly-D-lysine, cat: A38904-01 • Knock-out serum, cat:10828028
Abcam	Chromatin Extraction Kit, cat: ab223876.

2.1.7 Plasticware

Table 2.6: plasticware

Supplier	Product
Thermo scientific	• Nunc serological pipettes, 5 ml, individually wrapped, cat:170355N • Nunc serological pipettes, 10 ml, individually wrapped, cat:170356N • Nunc serological pipettes, 25 ml, individually wrapped, cat:170357N • Nunc 15ml conical sterile polypropylene centrifuge tubes, bulk, cat:339650 • Nunc 50ml conical sterile polypropylene centrifuge tubes, bulk, cat:339652 • Filter Nalgene Mach V membrane 0.2µm cat: 10229090 • Cover Glass, cat: 12440S
Fisher scientific	• Nunc easy flask T25, sterilized, filter cap, cat: 10232771 • Nunc easy flask T75, sterilized, filter cap, cat: 10364131 • Nunc easy flask T175, sterilized, filter cap, cat: 10246131 • Plastic, sterile, syringe 20 ml, cat:15889152

2.2 Methods:

2.2.1 Cell Culture and Maintenance

All cell culture techniques were performed aseptically in the Bioscience Air 2000 M.AC. Laminar flow cabinet. Cells were seeded onto Nunc EasyFlask 75 cm^2 or 25 cm^2 Nunclon Delta Surface Culture Wear and maintained in a Hera cell water-jacketed cell incubator at 37°C in a 5% CO_2 humidified atmosphere. Cells were visualized and imaged at various magnifications using an Olympus CK30 phase-contrast microscope. All cell lines were cultured in the same manner. Briefly, for subculturing, medium was aspirated from 70-80% confluent cells, washed with Dulbecco's Phosphate Buffered Saline (DPBS), and then removed. Cell dissociation was initiated using 1X trypsin solution. After dissociation, old medium was added to dilute the effect of trypsin. Fresh medium was added to new culture vessels (i.e., flasks or plates), the appropriate inoculum density was added to each flask (as per supplier's recommendations), and the flasks were placed at 37 °C 5% CO_2 (Harman, 2023).

2.2.1.1 Mouse Aortic Smooth Muscle Cells (MOVAS)

The slow growth of primary vSMC cultures makes them unusable for more than a few passages because of senescence and phenotypic changes that happen late in the culture (Afroze et al., 2003). In addition, using primary cells requires a lot of work, money, and time. Additionally, complementary *in vitro* studies of animal models of cardiovascular illness, where transgenic alterations and/or their effects have been limited to vSMC *in vivo*, would be made possible by an immortalized mouse vSMC line (Ju et al., 2001; You et al., 2003). For these reasons, (Afroze et al., 2003) developed and characterized a novel mouse vSMC cell line (MOVAS) that has as same features as vSMC *in vitro*.

These cells are immortalized smooth muscle cells cultured *in vitro* (Ju et al., 2001)(Ju et al., 2001; You et al., 2003). This indicates that they either originated from de-differentiated smooth muscle cells (SMCs) or stem cells (figure 2.1). De-differentiated MOVAS cells show much lower expression of muscle differentiation markers compared to freshly differentiated vascular smooth muscle cells (vSMCs) (Deng et al., 2017). The cells undergo changes in culture due to either de-differentiation or the presence of a small percentage of stem cells, after digestion and expansion, become SMC-like cells (Luca et al., 2018). While SMC-like cells and de-differentiated cells have different origins, they are functionally similar(Luca et al., 2018). Studies have demonstrated that *in vitro*, SMCs that transitioned to myeloid cells were de-differentiated SMCs (F. Zhang et al., 2021) (Maiseyeu et al., 2022). *In vivo* experiments also suggest that both differentiated vSMCs and de-differentiated SMCs can undergo myeloid differentiation, as evidenced by genomic markers specific to SMCs (Luca et al., 2018)(Luca et al., 2018; F. Zhang et al., 2021). Consequently, all *in vitro* experiments conducted for this study utilized de-differentiated SMCs (MOVAS).

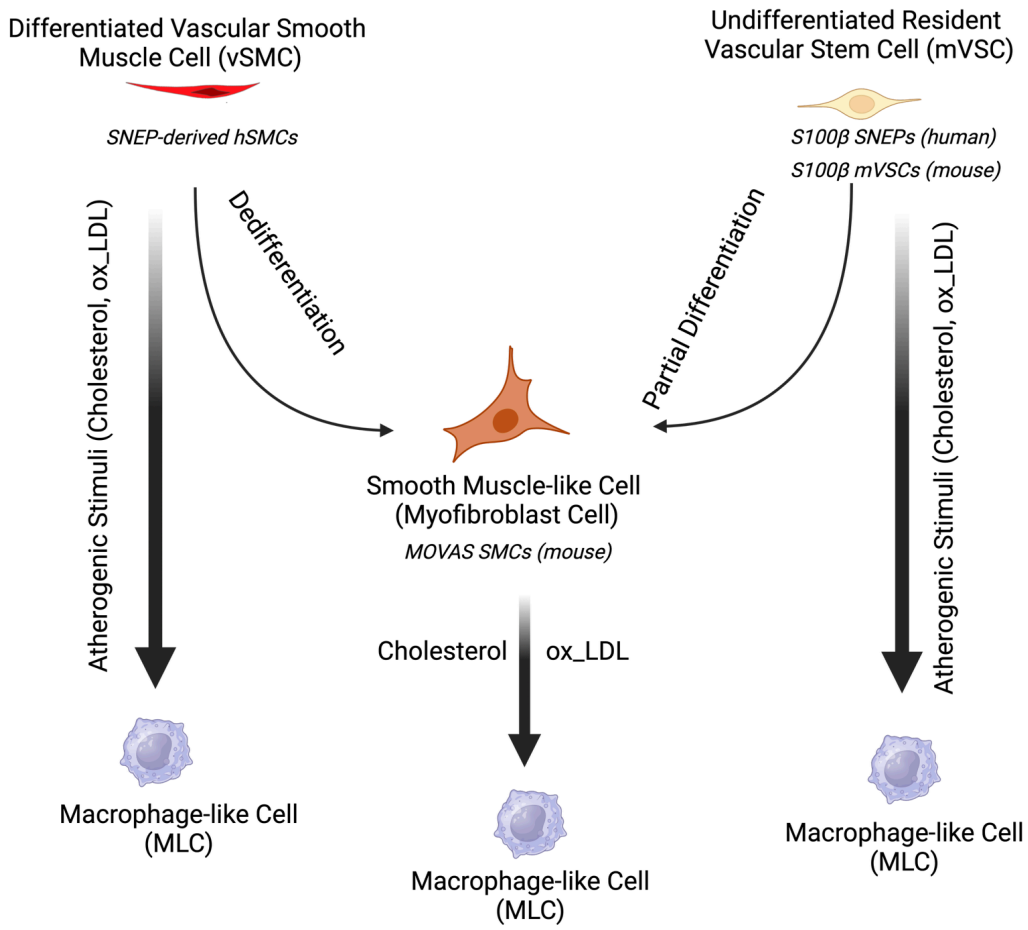

Figure 2.1. Overview of vascular smooth muscle cells (vSMCs), de-differentiated SMCs and resident multipotent vascular stem cells (mVSCs) used in this study. Differentiated SMCs were generated from human iPSC-derived S100β cells, undifferentiated S100β stem cells were derived from aortic tissue (mVSCs) and from hiPSCs. SMC-like cells (MOVAS SMCs-like) were either dedifferentiated SMCs or adult stem cell derived progeny. Created with Biorender.

We purchased mouse aortic smooth muscle cells isolated by collagenase (MOVAS, ATCC® CRL-2797™) commercially from ATCC and cultured in RPMI supplemented with 10% ATCC FBS and 1% penicillin and streptomycin. Experiments were continued until cells reached passage 30. SMC differentiation marker (Cnn1) was validated using immunocytochemistry (ICC) and by RT-qPCR to investigate the expression of SMC differentiation (Gusti, 2023).

2.2.1.2 Isolation and culture of mouse vascular stem cell (mVSCs) by explant or sequential seeding after enzymatic dispersion.

A protocol for isolating mVSCs from the medial layer of the aortic arch and thoracic aorta were performed, as previously described but with some minor modifications (Tang et al., 2012). Isolated aortic mVSCs were cultured in maintenance media MM1 for S100β neuroectodermal cells, as described by Tang and his colleagues (Tang et al., 2012).

2.2.1.2.1 Adventitial layer removal

The use of animals in this research was in compliance with EU legislation (Directive 2010/63/EU) to protect animals used in research and adhered to the 3Rs'. Mouse strains C57BL and Thy1 mice were anesthetized with an overdose of sodium pentobarbital (0.1mg/g) and confirmed dead. The chest was cut open in front to expose its internal organs. These were removed and the posterior part of the ribcage was removed. The aorta was carefully excised using forceps and scissors and carefully removed. Aortic tissues were placed in cold PBS and adipose tissue was removed using two forceps. A 2 mL syringe and needle were used to wash the luminal area of the vessel to remove all traces of blood. The endothelium was removed by repeated rubbing of the vessel wall. The outer adventitial layer was then enzymatically removed by incubation with 2.5 mg/ml collagenase solution for 10-20 minutes at 37°C. Once the adventitia became loose, it was carefully removed with forceps as intact layer under a dissecting microscope (Figure 2.2). The remaining medial layer of the aorta was then cut into individual pieces ~ 1mm and placed on a 6 well plate precoated with CELLstart™ dilution (Table 2.7) and left to facilitate explant culture with minimal disturbance at 37° C, 5% CO_2 for 1 week. (Figure 2.3). The aortic pieces were then removed with a forceps and the explanted cells sub-cultured and expanded in MM1 media (Di Luca, 2019).

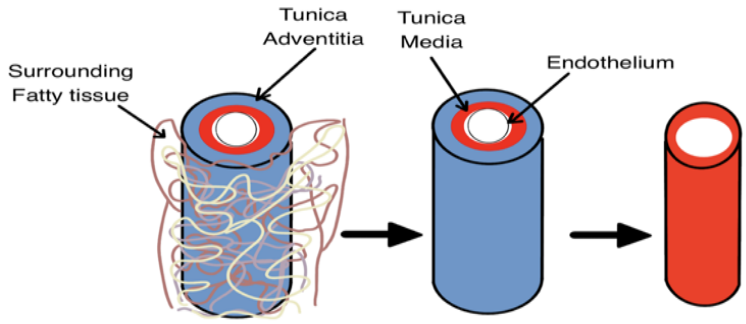

Figure 2.2. Removal of the adventitial layer following enzymatic treatment (Di Luca, 2019).

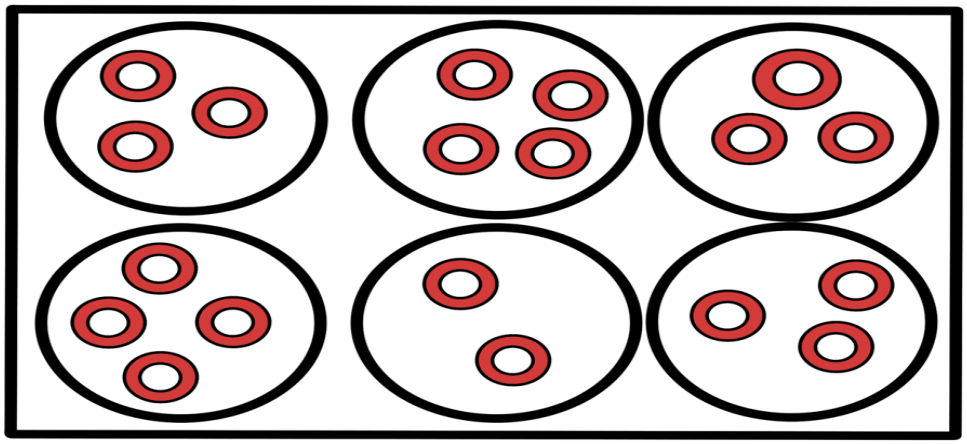

Figure 2.3. Tissue pieces on a CellStart pre-coated 6-well plate (Di Luca, 2019).

Table 2.7: CellStart Dilution for a 6-well plate

Stock Solutions	Final Concentrations	Volumes 5ml (750 µl/well)
Dulbecco's Phosphate Buffered Saline with calcium and magnesium	1x	4410 µl
CTSTM CELLstart™ Substrate	1:50	90 µl

The final solution was filtered using a 0.2 µm syringe end filter under sterile conditions.

2.2.1.2.2 Enzymatic Dispersion

The aorta was cut into small pieces of tissue with a sterile blade and placed in 0. 25 mg /ml type III elastase at 37 °C. Tissues were vortexed approximately every 15 minutes for 2 hours until the tissue was completely digested. Dispersed cells were centrifuged and washed twice with warm NE-MM before sequential seeding of a CELLstart™ pre-coated 6-well plate with 2 ml of NE-MM (Figure 2.4) Cells were incubated at 37 °C, 5% CO_2 for 1 week with minimal disturbance (Tang et al., 2012).

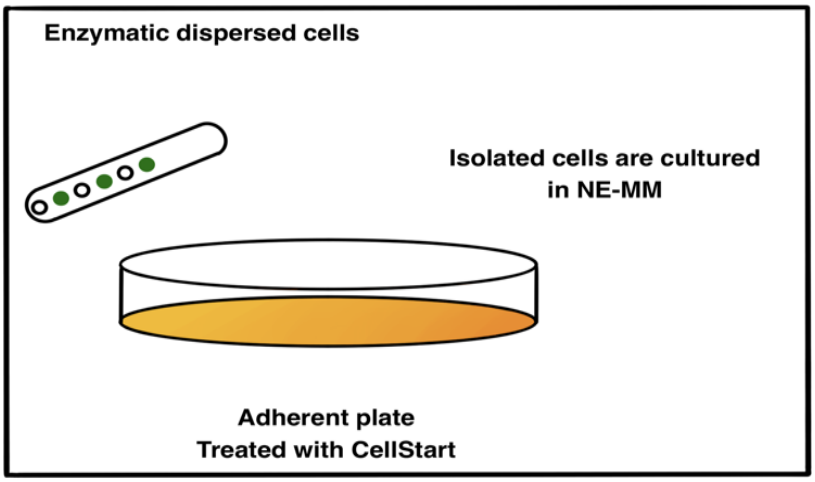

Figure 2.4. Schematic illustration of the sequential seeding step on a CellStart™ pre-coated 6-well plate after cell enzymatic dissociation (Di Luca, 2019).

2.2.1.2.3 Generation of multipotent vascular stem cells (mVSCs)

The dispersed cells were centrifuged, washed twice with warm MM1 and seeded into one well of a non-adherent 6-well plate containing 2 ml of MM1 (first seeding) for 48 hours. Suspension cells were transferred to pre-coated CELLstart™ 6-well wells (second seeding) plate in 2 mL of fresh MM1 media (Figure 2.5). Cells were incubated at 37° C, 5% CO_2 for 1 week with minimal disturbance. Cells were washed with Hank's Balanced Salt Solution (HBSS) and sub-cultured in 0.5.x Select TrypLE. After P1, no CELLstart™ precoated vessels were needed. Cells were maintained in adherent cell culture grade plates/flasks. Cells were healthy and proliferating when seeded at a cell density of 1 x 10^4 cells/cm^2 or higher and fed every 3 to 4 days. Cells were grown in MM1 to passage 20 and their phenotype routinely confirmed by flow cytometry expression and ICC for expression of the mVSC marker S100β (Di Luca, 2019).

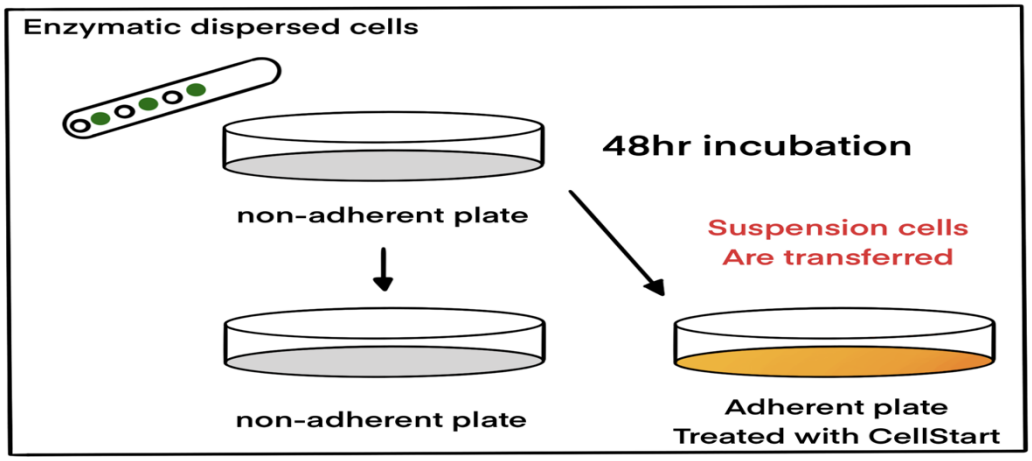

Figure 2.5. Schematic illustration of the seeding steps of the modified enzymatic dispersion protocol (Di Luca, 2019).

2.2.1.3 Human induced pluripotent stem cells (HiPSCs)

Human induced pluripotent stem cells (hiPSCs) were cultured as per the suppleir's instructions. Before seeding cells, the surface of the culture wear was pre-coated using Vitronectin (10µg/ml) and incubated at room temperature for 1 hour. Cells were grown and maintained in feeder-free conditions in xeno-free, serum-free, complete Essential 8™ medium (E8) media (ingredients proprietary to manufactures formulation), replacing 95% of the medium daily. Cells were sub-cultured by washing once with sterile PBS, incubated with EDTA (0.5mM) for 4-8 at room temperature while being observed under phase-contrast microscopy until colonies displayed bright halos around the edges and small holes appeared throughout. The EDTA was aspirated, and the recommended volume of E8 was added to the well. The dislodged cell colonies were then gently washed from the culture-wear by pipetting the medium around the well using a 5ml or 10ml stripette until the desired cell aggregates were achieved. The resulting cell solution was then seeded into as many wells as were required. ROCK inhibitor (10mM) was added to optimise colony growth after subculturing. The culture wear was then agitated gently within the tissue culture incubator, ensuring even distribution of cells across the culture wear was achieved. Cells were frozen down in freezing media that contains knock-out serum solution with 10% DMSO (Burtenshaw, 2020).

2.2.1.3.1Generation of HiPSCs-derived NE progenitors (SNEP)

HiPSCs were cultured as described above until reaching 70% confluency. Cells were then split at a ratio of 1:10 and left at 37°C, 5 %CO_2 for 24 hours. Following 24-hour incubation, cells were incubated in E8 and left for 4-5 days. After this time period hiPSC colonies began to lose their typical defined boarders followed by cell migration from the colonies. In order to promote proliferation of the migrated cells dense hiPSC colonies were manually removed using a sterile glass picker. The remaining cells were sub-cultured at 60% confluency using EDTA solution (1:1000) for 4-8 minutes at room temperature while observed under phase-contrast microscopy until cells displayed bright halos. When this was achieved the EDTA solution was aspirated, and the recommended volume of E8 medium was added to the well. The dislodged cell colonies were then gently washed from the culture-wear by pipetting the medium around the well three times until a single cell suspension was obtained. Cells were then centrifuged at 300 x g for 3mins; the

supernatant was removed, and the required amount of E8 media was added. Cells were then titrated into single cells using a 1ml syringe and 0.22μm gauge needle. Cells were frozen down in knock-out serum solution with 10% DMSO. The vile was frozen slowly in a Mr. Frosty and placed in the -80°C overnight and transferred to liquid nitrogen the following day. The cells were used between passages 2-15 (Burtenshaw, 2020).

2.2.1.3.2 Human iPSC derived smooth muscle cells (hSMC)

Following SNEP progenitor differentiation, cells were treated with 1X TrypLE for 3–5 min at 37 °C in a 5% CO_2 incubator. Cell culture plates were gently tapped and checked periodically under a phase-contrast microscope to ensure that all cells had been dissociated into single cells. TrypLE was terminated by the addition of 10 volumes of DMEM to dilute one volume of TrypLE used. Cells were then collected and centrifuged the cell for 3 minutes at 200g at room temperature. The supernatant was aspirated and discarded. The remaining cells were re-suspended in DMEM supplemented 10% FBS (Sigma) 1% Penicillin Streptomycin, PDGF-BB (10ng/ml) and TGF-β1 (2ng/ml). Cells were then plated onto gelatin-coated (0.1% wt/vol) plates at a seeding density of 20,000 cells per cm^2. Cells were maintained at 37°C in a 5% CO_2 incubator. After one day of PDGF-BB and TGF-β1 treatment, 50–70% of the cells attached to the plate. The media was discarded to remove floating cells and replaced with a fresh medium. After day 12 of PDGF-BB and TGF-β1 treatment, all cells appeared spindle-shaped. Complete medium was then changed to DMEM 10% FBS, 1% Penicillin streptomycin for expansion. Cells were frozen down using 90% (volume/volume) FBS + 10% (vol/vol) DMSO (Figure 2.6) (Burtenshaw, 2020).

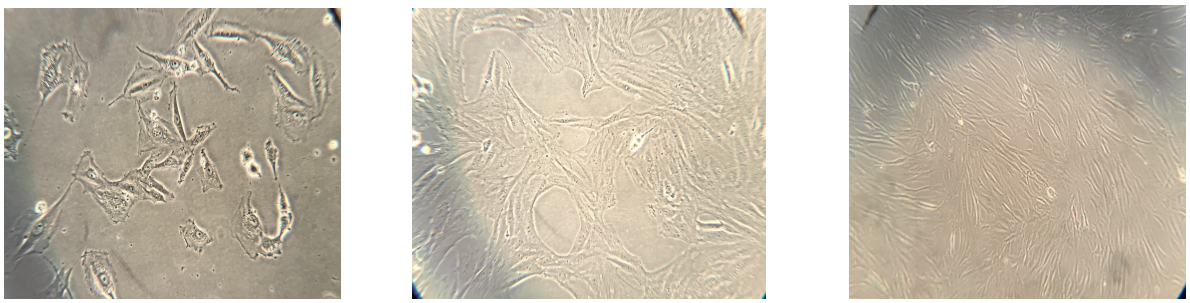

Figure 2.6. Morphological changes in cells following treatment with myogenic inductive stimuli. Representative phase-contrast images of S100β SNEPs were treated with PDGF-BB, 10 ng/ml and TGF-β1, 2 ng/ml in DMEM for 12 days to generate hSMC. Media supplemented with PDGF-BB, TGF-β1 was replaced every 3 days.

2.2.1.4 THP-1 Human Monocytic Leukaemia Cells

THP 1 Human Monocytic Leukaemia Cells were purchased from ATCC, Cat: ATCC-TIB-202 and cultured in RPMI-1640 supplemented with 10% ATCC FBS heat inactivated, 1% penicillin/streptomycin and 0.05 mM 2-mercaptoethanol as recommended by the supplier's. Experiments were performed in cells up to passage 10. Cells were thawed and dispersed by gentle agitation and grown in RPMI-1640 media supplemented with 0.05 mM 2-Mercaptoethanol in a 5% CO_2 humidified atmosphere at 37 °C. Upon taking up the cells from liquid nitrogen, cells were not spun down, but cultured in 10 mL prewarmed supplemented growth media in a T75 flask suitable for suspension cells. For subculturing , cells were spun down at 100 x g for 5 min (Tsuchiya et al., 1982).

PMA-Induced Differentiation of THP-1 Monocyte into Macrophages

The biology and function of monocytes and macrophages are extensively studied using THP-1 cells (Tsuchiya et al., 1982). In terms of cell morphology, macrophage surface markers, and cytokine production, PMA is frequently utilized to promote differentiation into cells that resemble

human MDMs (Tsuchiya et al., 1982). THP-1 cells were differentiated *in vitro* into macrophages by the administration of 185 ng/mL PMA1;100 for 3, 7 and 10 days in flask suitable for adherent cells (Figure 2.7). The treatment induced the typical hallmarks of macrophages, represented by cell adhesion, spread morphology, increased granularity and irregular nucleus shape MDMs (Meijer et al., 2015).

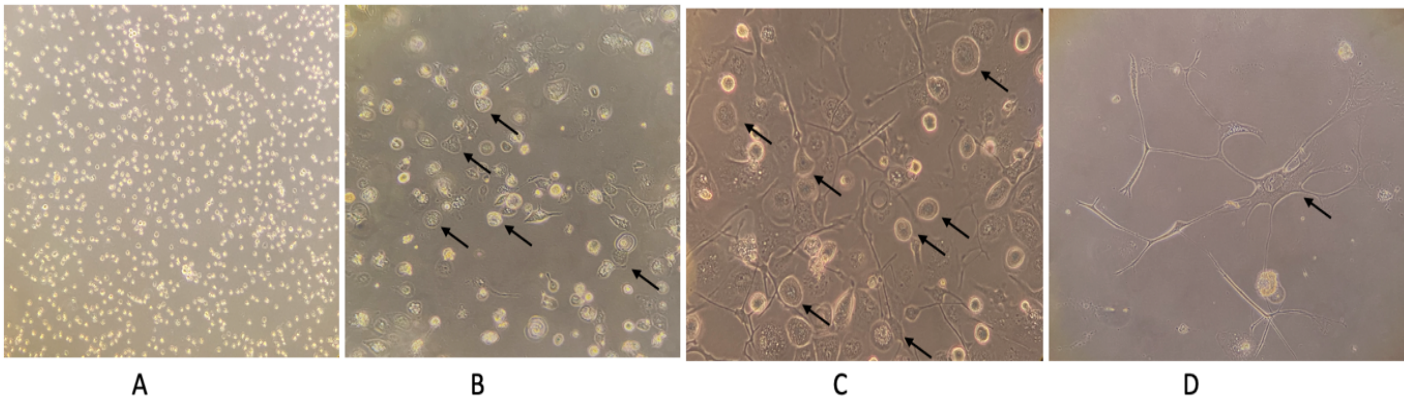

Figure 2.7. Morphological changes in THP-1 monocytes before and after PMA to induce myeloid differentiation. Representative phase-contrast images following myeloid differentiation of THP-1 cells before and after treatment with PMA. (A) THP-1 monocytes cells in culture. (B) Differentiated THP-1 to macrophages following PMA treatment after 3 d, (C) day 7 and (D) day 10 to demonstrate change in morphology as cells become rounded and bigger, pointed with black arrows.

2.2.2 Cryopreservation

To generate cryostocks, trypsin or tryple was diluted in DPBS at 300 x g for 5 min, before cells were dispersed and pelleted, resuspended in 90% complete medium, 10% DMSO, and transferred to cryovials. The cryovials were then appropriately labeled and placed in a Mr Frosty™ freezer box and stored for 24 hours in the -80 freezer. The cryovials were then removed and stored in liquid nitrogen for long periods. For resuscitation, cells were thawed very quickly at 37°C and transferred to prewarmed complete medium in centrifuge tubes. Cells were then pelleted at 300×

x for 5 min, medium removed and resuspended in pre-warmed fresh medium. Cells were then seeded (Figure 2.8) (Hakimjavadi, et al., 2014).

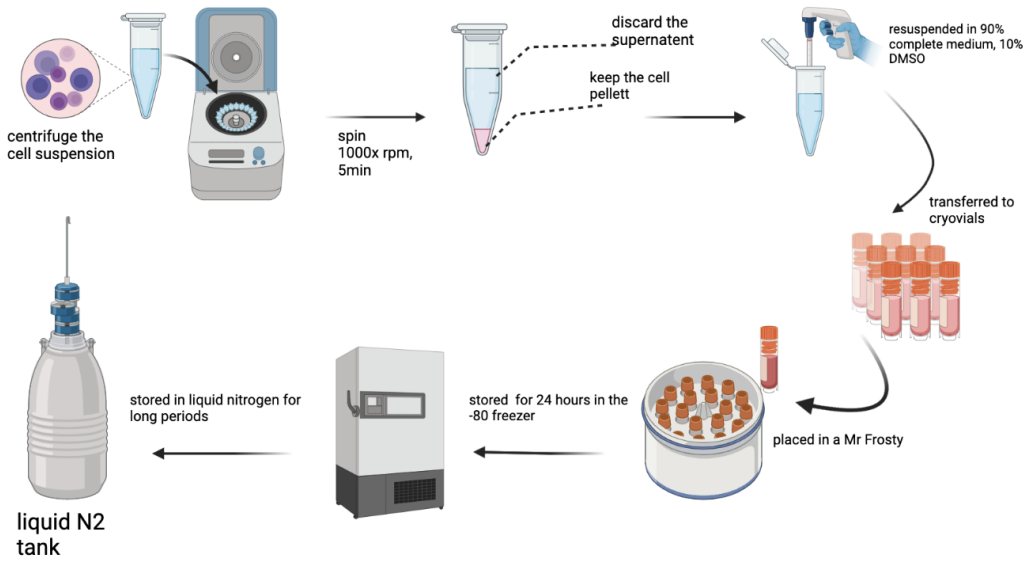

Figure 2.8. Schematic of Cryopreservation Protocol. Created with Biorender.

2.3 Cell Characterisation

2.3.1 Coverslip Preparation

A Petri dish was filled with coverslips by using sterile forceps gently placed in UV light in a laminar flow hood for 1 hour to ensure a sterile condition. Coverslips were removed and washed 3 times with sterile H_2O. Coverslips were then air dried for 1 hour again under UV light in a laminar flow hood before use (Gusti, 2023).

2.3.2 Immunocytochemistry (ICC)

Cells were seeded at low density (~5,000 cells/well) onto sterile coverslips in 6-well plates. Once the cells reached the desired confluency, the cell culture medium was aspirated, and the cells were washed with PBS. The protocol for ICC was as follows (Figure 2.9). Cells were fixed by incubation with 3.7% formaldehyde for 15 minutes at room temperature (RT). Cells were washed three times with PBST (PBS containing 1% Tween-20). For intracellular staining, cells were permeabilized by incubation with 0.025% Triton X-100 for 15 min at RT. Cells were washed 3 times with PBST. Wells were blocked with PBS containing 5% BSA, 1% Tween-20, and 0.3 M glycine for 1 hour at room temperature. Samples were incubated overnight at 4°C with primary antibodies or (conjugated antibodies) diluted to appropriate concentrations in antibody dilution buffer (5 µl in 300 µl). Cells were washed three times with PBST. Samples were incubated with secondary antibody (diluted in antibody dilution buffer for 1 hour and protected from light). Cells were washed 3 times with PBST. Cell nuclei were stained by incubating cells with DAPI (diluted to 2 µg/ml) for 15 min at room temperature. Cells were washed 3 times with PBST. Coverslips were then placed on glass slides using mounting medium and stored at 4°C to dry for 24 h. Images were acquired using an Olympus CK30 microscope with Cell F software. Four different magnifications were used: 10X, 20X, 60X and 100X. A secondary antibody control was used to define the background negative threshold prior to imaging and to limit the exposure rate to eliminate false positives. At least five images (minimum n = 3) from an Olympus CK30 microscope per experimental group were analysed with ImageJ software. The antibodies were checked for nonspecific binding in positive cell line of macrophages J774A-1, de-differentiated MOVAS and S100β mVSC cells by using Secondary antibody (AF546 2AB) only. AF546 Goat-Rabbit secondary antibody was tested the for immune activity to determine the fluorescent level in the mentioned cell lines (Figure 2.10). This test to control the positive staining of the primary antibody to approve that no staining of the secondary antibody alone (Burtenshaw, 2020).

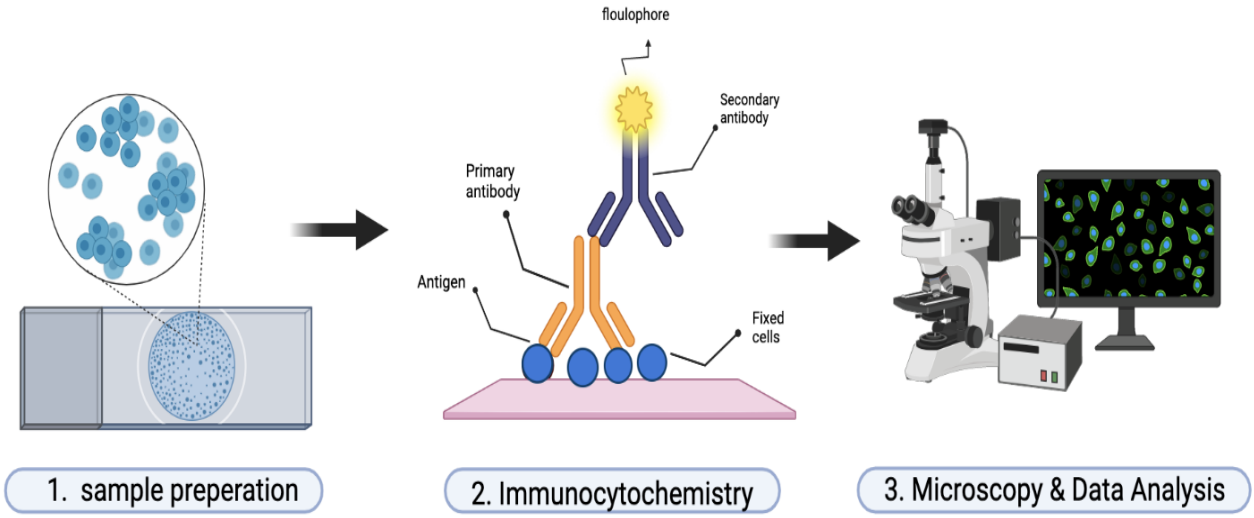

Figure 2.9 Schematic of immunocytochemistry (ICC) Protocol. Visualization of the occurrence or the location of a specific protein/antigen interactions by ICC. (1) Target cells are seeded on to a coverslip for interrogation. To minimize non-specific binding, the cells were then blocked using bovine serum albumin (BSA) (2) The fixed cells are then incubated using antigen-specific primary antibodies of interest. Following nocturnal incubation, the cells are then exposed to a conjugated fluorescent secondary antibody. (3) Fluorophore is exposed to light resulting in detectable excitation. Fluorophore excitation is visualized by fluorescent microscope. Created with Biorender.

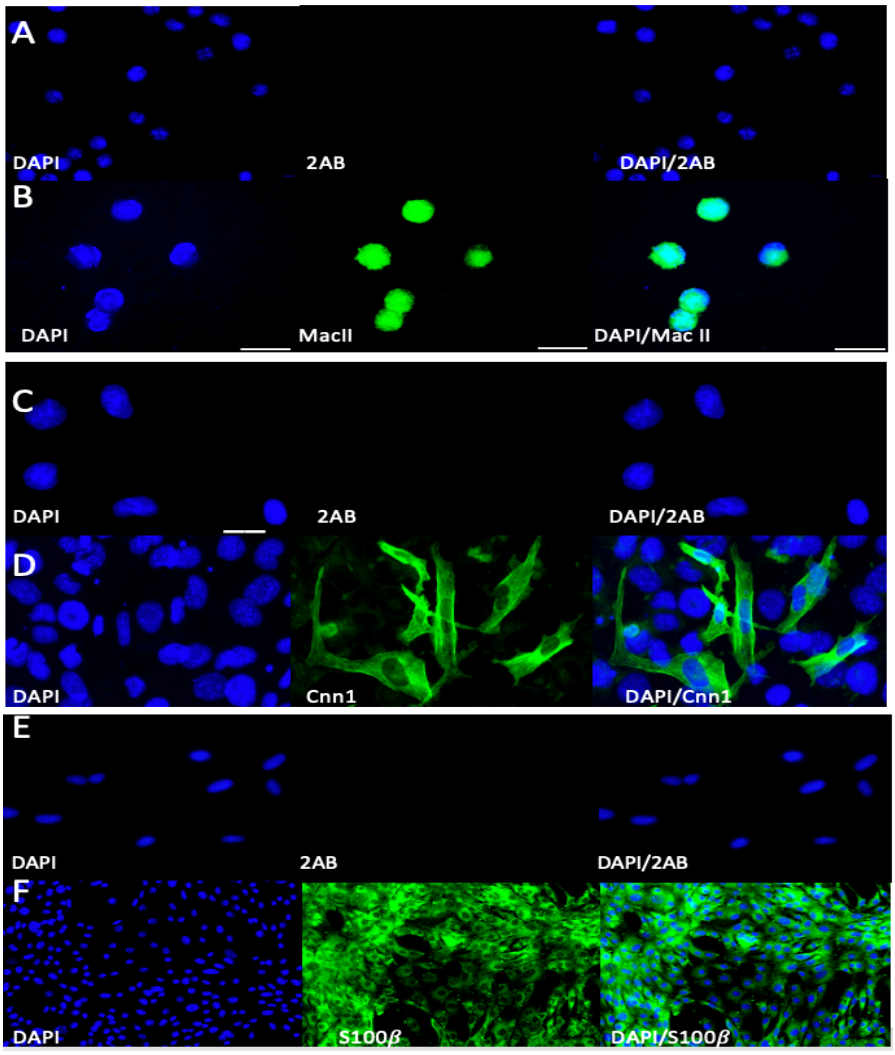

Figure 2.10 Confirmation of macrophage marker, MacII in J774A-1 cells(A+B), SMC marker, Cnn1 in SMC cells (C+D) and S100β in stem cells(E+F) using ICC. (A, C, E) An IgG control (secondary antibody probing without primary antibody staining) was used to account for background fluorescence or off-target binding of secondary IgGs in J774A-1, MOVAS SMCs and mVSC respectively. Immunocytochemical analysis of the expression of macrophage markers Mac II in J774A-1 (B), SMC marker Cnn1 in MOVAS (D) and stem cell marker S100β in mVSC (F).

2.3.3. Polymerase Chain Reaction (PCR)

2.3.3.1 RNA Isolation

RNA was extricated from cells utilizing the Promega Reliaprep RNA Miniprep™ as per manufacturers guidelines (Figure 2.11). Briefly, cells were pelleted by centrifugation at 1500 rpm for 5 minutes and resuspended in 1:100 1-thioglycerol: BL buffer (TG+BL) lysis buffer depending on the number of cells. Isopropanol was added and sample vortexed and exchanged to a clean Reliaprep Minicolumn in a collection tube and centrifuged at 13,000 x g for 30 seconds. An RNA wash solution which contains ethanol was added to the tube and centrifuged once more at 13,000 x g for 30 seconds. DNase I protein and MnC were added to the column and incubated for 15min to remove DNA. The column was washed and centrifuged at 13, 500 x g for 15 seconds. After 3 more wash steps, nuclease-free water was added to the column before centrifugation to elute the decontaminated RNA. Quantitation of nucleic acid concentration and quality was assessed by Nanodrop ND- 1000 Spectrophotometer (Thermo Scientific).

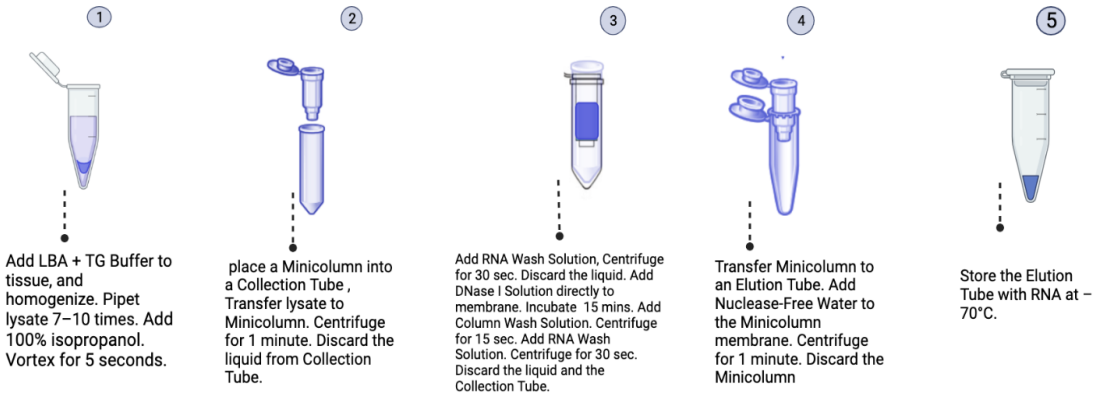

Figure 2.11 Steps for RNA Isolation from cells. Created with Biorender according to the protocol from manufacturer.

2.3.3.2 Real time Polymerase Chain Reaction RT-PCR

RNA was isolated as described in section (2.2.3.3.1) before RT- qPCR was performed by realtime PCR (Figure 2.12), using the SensiFAST™ SYBR No-ROX Kit with the Rotor-GeneRG-3000™ light cycler from Corbett Research using primers listed in (Table 2.3). The gene-specific primer (*MacII*) for this PCR were adopted from (Gupta et al., 2014); The gene-specific primers

(*Cd68+F4/80*) were adopted from (Khazen et al., 2005). Total RNA (2-10 ng) was then reverse transcribed and PCR amplified in a one-step reaction containing RT mix, SYBR green mix, and Rnase inhibiter at 45 °C for 10 mins , polymerase activated at 95 °C for 2 mins followed by 40 cycles of 95 °C for 5 seconds for denaturation , 55 °C for 10 seconds for annealing and 72 °C for 5 seconds for extension with acquire at the end of the step (Figure 2.13A).

Samples were run in triplicate with a no reverse transcriptase (-RT) control. Gene expression was normalized to the expression of housekeeping genes GAPDH. Ratios of gene expression were calculated using the efficiency-corrected ΔCt method. The ratio of the control was calculated so the value of the control compared to itself is always 1 as the ratio is 1:1. Results were plotted using PRISM software (Figure 2.13C). Melting curve analysis was performed on all runs to confirm that amplification of one amplicon per primer occurred at the validated melting temperature (Figure 2.13B).

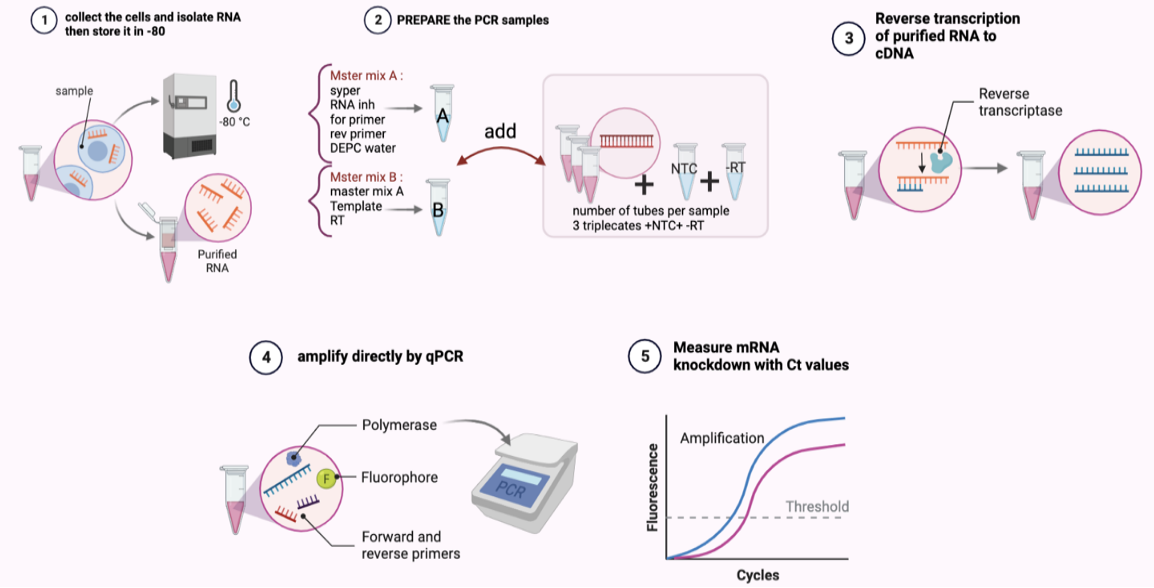

Figure 2.12. Schematic of RT-qPCR Protocol. Created with Biorender according to the protocol from manufacturer.

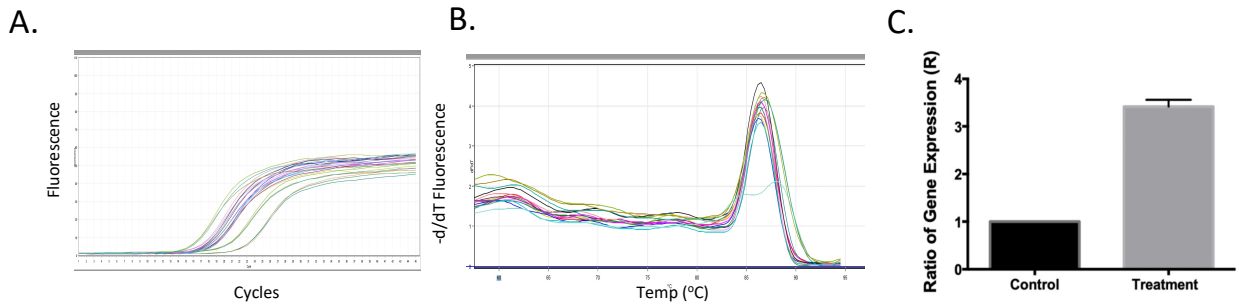

Figure 2.13. (A) Target gene amplification using IDT primers. Shown as fluorescence versus cycle number (40 cycles). To determine the Ct value, a threshold baseline value was set at the point of exponential growth of the amplification curve. (B) Melting curve analysis was performed for each run as an internal validation to ensure amplification of a single amplicon per run. (C) Gene expression was normalized using the housekeeping genes GAPDH. Gene expression ratios were calculated using the efficiency-corrected delta Ct method. Results were plotted using the Graphpad PRISM software.

2.3.3.4. Oil Red O Stain Preparation

In the fume hood Oil red O powder (300mg) was added to 100ml of 99% isopropanol. A 30ml of the Oil Red O stock was added to 20ml of deionized water. The solution was sterile filtered using a 0.2µM filter. Cells at 60-80% confluency were cultured in the absence or presence of three different myeloid inductive stimuli (ox-LDL, cholesterol and myeloid differentiation media) with replacement of medium every 2-3 days, before the cells were fixed with 3.7% formaldehyde at RT for 15 mins, washed twice with HBSS at 4^0C. A 2ml solution of 60% isopropanol was then added to cells for 2 minutes. The cells were washed briefly again in PBS and the working concentration solution of Oil Red O was added, ensuring the cells were fully covered with the stain. The samples were left at room temperature for more than 1 hour. After the incubation, the cells were washed five times in deionized water ensuring that most of the stain had been removed. The cells were then assessed and imaged using an Olympus CK30 microscope under phase Contrast and IMAGE J software **(**Figure 2.14) (Gusti, 2023).

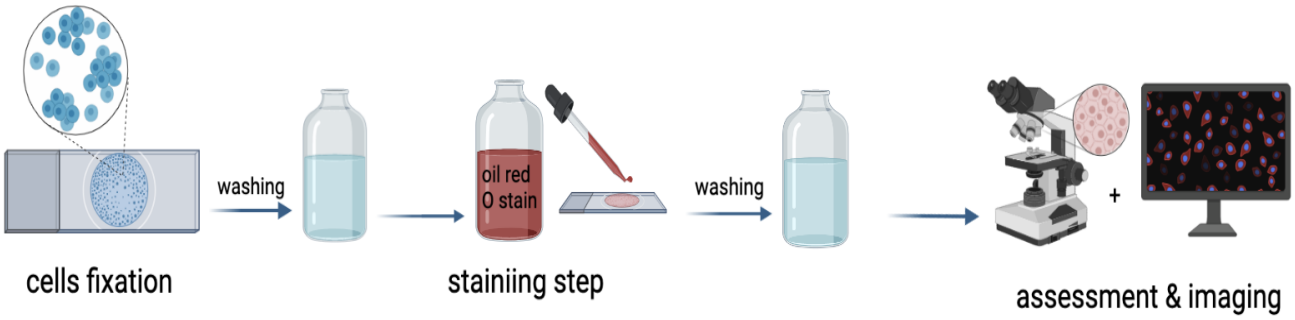

Figure 2.14 Schematic of representation of histochemical staining of lipid with Oil Red O stain. Created with Biorender.

2.3.3.5 Flow Cytometry

Flow cytometry was used to screen a series of cell lines for different markers representing their phenotypes. The macrophage markers were CD68-PE conjugated, CD11B-PE-Cynine 7 conjugated and F4/80-APC conjugated. Briefly, 10,000 cells were used per sample. After the cells were pelleted at 2,000 RPM, 5 µl of primary antibody diluted in 100 µl PBS and added to each tube, incubated for 30-50 mins in 37°C, before the cells were washed with PBS twice to insure removal of free antibody. Cells were selected from debris based on their forward and side scatter properties. Single cells were defined as having an aspect ratio of approximately 1. Antibody expression was displayed on a bivariant plot e.g. FITC vs SSC. Multiple histogram overlays were created using the analysis software tool to demonstrate the difference between control vs treated samples (Burtenshaw, 2020).

For Gating and Markers analysis, the samples were analysed by the Amnis™ CellStream™ flow cytometer. Cells were selected from the debris based on their forward and side scatter properties. Single cells were defined with an aspect ratio of approximately 1 (Figure 2.15A). Antibody expression was displayed on a bivariate graph. CD68 vs. SSC (Figure.2.15B). Several histogram overlays were generated using the analysis software tool to show the differences between stained and unstained samples (Figure 2.15C) (Burtenshaw, 2020).

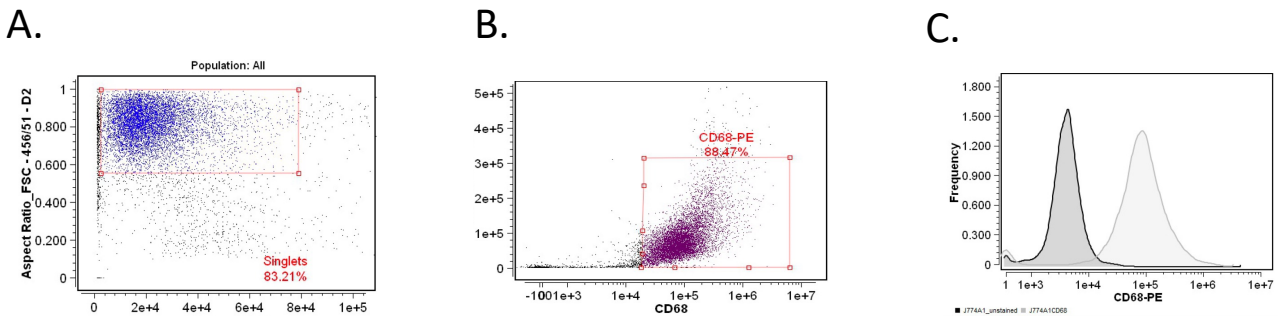

Figure 2.15 Gating strategy for flow cytometry. Single cells were defined as having an aspect ratio of approximately 1 (A). Antibody expression was displayed on a bivariant plot e.g., CD68 vs SSC. (B) Multiple histogram overlays were created using the analysis software tool to demonstrate the difference between unstained vs stained samples (C).

2.4 Myeloid Inductive Stimuli

2.4.1 Oxidized low density lipoprotein (ox-LDL)

Low-density lipoprotein is the main carrier of cholesterol to cells (Trinick & Duly, 2013). The accumulation of oxidized low-density lipoproteins (ox-LDL) in the endothelial layer of the aorta causes the appearance of atherosclerosis(Trinick & Duly, 2013).

Cells were treated with 50 µg/ml from stock concentration of ox-LDL from Generon (catalogue number LDLO13-N-1) of 5.8 mg/ml for 7 days with changing media every 2-3.

2.4.2 Cholesterol

Cholesterol is an important molecule that has a key role in regulating cell differentiation and function (Parhami et al., 2002). In this study, cells were treated with a final concentration of 10 µg/ml water soluble cholesterol (Sigma catalogue number = C4951-30) for 7 days with changing media every 2-3 days.

2.4.3 Myeloid Differentiation Media

Cells were treated with StemSpan™ Myeloid Expansion Supplement II (100 X) supplement from STEMCELL in serum-free culture for expansion of human monocytes according to the manufacturer's guidelines. It contains a combination of recombinant cytokines formulated to promote the expansion and differentiation of human myeloid progenitor cells, generating many $CD14^+$ monocytes from $CD34^+$ cells.

2.5 Data Analysis and Management

Results are expressed as mean ± SEM. Experimental points were performed in triplicate in at least three independent runs. Data were normalized and analysed using GraphPad 8 Prism™ (GraphPad software, La Jalla, California, USA). For normal distribution of data, a t-test or two-way ANOVA without parametric pairing was performed followed by Tukey's correction to compare two and three groups, respectively. For nonparametric data, Mann-Whitney or Clustal-Wallis tests with Dunn's multiple comparison test (one-way ANOVA nonparametric test) were performed to compare two and three groups, respectively. The corresponding statistical tests are listed in each Figure and values of $p \leq 0.05$ were considered significant. PCR data were analysed, and fold changes were calculated using the comparative CT method ($\Delta\Delta CT$) using Microsoft Office Excel 2011. Morphometric, immunocytochemical, and immunohistochemical images were analysed using ImageJ, an image analysis software (Schneider et al., 2012). The volume change was calculated using morphometry, which is the area of the arterial layer measured by the software. For immunocytochemistry and immunohistochemistry, software was used to calculate the percentage of DAPI-stained cells that were positive for specific markers.

Chapter 3

The effects of myeloid induction stimuli on myeloid differentiation of mouse vascular smooth muscle cells (vSMCs) and resident S100β stem cells (mVSCs)

3.1 Introduction:

Atherosclerotic lesions are characterized by the deposition of cholesterol within the arterial wall concurrent with the accumulation of intimal smooth muscle cell (SMC)-like cells and non- SMCs (Sanchez & Veith, 1998);(Ylä-Herttuala et al., 1989). A crucial hallmark of subclinical atherosclerosis is PIT defined as the initial progressive plaque responsible for the rise of advanced lesions (Virmani et al., 2000). Adaptive intimal thickening (AIT) composed primarily of infiltrating macrophage like cells (MLC) and intimal SMC-like cells is considered an important transitional non-atherosclerotic plaque that likely represents the earliest phase of lesion progression (Velican & Velican, 1981). The source of the MLC and SMC-like cells contributing to AIT is a topic of much controversy. The two major sources that are the focus of this chapter include the de-differentiation of medial SMCs (Chappell et al., 2016b) and the partial differentiation of resident S100 calcium-binding protein β (S100β) mVSCs (Z. Tang et al., 2012).

The pathogenesis and pathophysiology of atherosclerosis is complex (Milioti et al., 2008);(Milutinović et al., 2020). Lipid-laden macrophages have been widely recognized to be the primary cell type found within atherosclerotic lesions (Insull, 2009). However, this has been recently challenged (Bennett et al., 2016), as a number of studies have identified de-differentiated SMCs to be the major source of MLCs in atherosclerotic plaques (Allahverdian et al., 2014);(Feil et al., 2014);(Shankman et al., 2015); (Wang et al., 2019). The purported plasticity of SMC suggests that they are able to convert into a MLC phenotype upon cholesterol-loading (Rong et al., 2003);(Vengrenyuk et al., 2015). This results in SMC losing expression of classical SMC differentiation markers, while triggering expression of classical macrophage markers in these cells (Vengrenyuk et al. 2015; Shankman et al. 2015; Feil et al. 2014). Moreover, MLCs of SMC origin have been shown to have decreased ABCA1 expression, which may exacerbate atherosclerosis (Allahverdian et al. 2014); (Choi et al., 2009).

Several previous studies have suggested that differentiated SMCs are capable of dedifferentiation and redifferentiation into several discrete phenotypes within the vessel wall following injury and during disease progression (Espinosa-Diez et al, 2021). De-differentiated SMCs are considered prone to further differentiate into alternative phenotypes such as osteogenic-like, macrophage-like

(myeloid) and MSC-like cells that have inherent tri-lineage multipotency capacity including adipogenic, osteogenic and chondrogenic differentiation.

Several *in vitro* studies have shown that SMCs can undergo phenotypic transition to osteoblasts in a calcified environment, determined by an increased expression of the osteocyte markers, including sclerostin *(Sost)* (Zhu et al., 2011). While no studies have reported SMC differentiation into adipogenic-like cells, several studies have shown that adipocytes can differentiate into SMC-like cells (Wang et al., 2010). In the case of vasculogenic differentiation, SMCs have been shown to differentiate into endothelial-like cells and express endothelial markers, such as platelet endothelial cell adhesion molecule 1 (PECAM1) (Hong et al., 2017). When vascular SMCs were treated with oxidised low-density lipoprotein (LDL), cells gradually dedifferentiated into macrophage-like cells, with an increase in the macrophage marker, Cluster of differentiation 68 (Cd68) (Yuan et al., 2022). Differentiation of SMCs to MSC-like cells has been reported and these mesenchymal stem cell (MSC)-like cells have the capacity to differentiate into osteogenic, adipogenic and chondrogenic-like cells if they acquire the tri-lineage multipotent capacity of classical MSCs (Pan et al., 2020).

However, the SMC differentiation towards non-SMC cells *in vitro* and *in vivo* has been questioned. Tang et al., provided data *in vitro* using cell culture and lineage tracing experiments indicating that differentiated mature vascular SMCs are incapable of proliferation either *in vivo* in response to injury or *in vitro* in cell culture. Instead, there exists a small population (<10%) of undifferentiated MSCs in the media that proliferate to completely reconstitute medial cells in response to vascular injury. This has been supported by a publication from our lab which concluded that SMCs in culture are derived from a non-SMC but from an S100 calcium-binding protein β (S100β) parent population following flow restriction (Di Luca et al., 2021). *In vivo*, it has been reported that Tamoxifen can remain in tissues and induce fluorescent tag expression in cells for up to four weeks after the last injection has taken place (Reinert et al., 2012). This could result in stem cells following myogenic or non-myogenic differentiation being tagged as of SMC origin.

Several *in vitro* studies have also shown that undifferentiated S100β stem cells can undergo transition to osteogenic, adipogenic and vasculogenic progeny either directly or indirectly through

an MSC-like intermediate (Tang et al., 2012). MSCs have the capacity to develop into several cell types, i.e., adipocytes, myocytes, chondrocytes, and osteocytes (Covas et al., 2008);(H. Huang et al., 2009);(Lin et al., 2010);(Liao et al., 2012). Model cell culture systems have been indispensable in identifying and characterizing the steps in the commitment and differentiation programs. Myogenic differentiation is stimulated by the presence of transforming growth factor beta (TGF-β) (Park et al., 2013), neurogenic differentiation by the presence of forskolin and valproic acid (New et al., 2015), and osteogenic cell differentiation by the presence of β-glycerol phosphate, ascorbic acid, dexamethasone (Tirkkonen et al., 2013) and dihydroxyvitamin D_3 (Logovskaya et al., 2013). Bone marrow-derived MSCs may differentiate into multiple cell types that are involved in cardiovascular pathologies, including vascular calcification (Liao et al., 2012). Sera et al., successfully generated adipocytes from mouse hematopoietic stem cells *in vivo* and were stained positively with *Fabp4* (Sera et al., 2009). When cultured in osteogenic media, MSCs express markers known to be expressed by bone forming osteoblasts, which are the cells responsible for laying down the matrix and mineral during new bone formation *in vivo* (Huang *et al*., 2007). Osteocyte marker gene expression increases following osteogenic differentiation, especially *Sost* (Feng et al., 2006); (Poole et al., 2005). Maul *et al* successfully differentiated rat MSCs to endothelial cells and found an increase in expression levels of *Pecam1* (Maul et al., 2011b).

The slow growth and senescence of primary vSMC cultures make them unusable after a few passages (Afroze et al., 2003). Using primary cells is also resource-intensive. To facilitate complementary *in vitro* studies of cardiovascular models with transgenic alterations, an immortalized mouse SMC line (MOVAS) was developed (Afroze et al., 2003; Ju et al., 2001; You et al., 2003). These immortalized cells, cultured *in vitro*, likely originated from de-differentiated SMCs or stem cells, showing lower expression of muscle differentiation markers compared to freshly differentiated vSMCs (Deng et al., 2017). In culture, they may de-differentiate or originate from stem cells, becoming SMC-like cells (Luca et al., 2018). Functionally similar, SMC-like and de-differentiated cells can undergo myeloid differentiation both *in vitro* and *in vivo*, as shown by genomic markers specific to SMCs (F. Zhang et al., 2021; Maiseyeu et al., 2022). All in vitro experiments for this study utilized de-differentiated SMCs (MOVAS).

Therefore, the major aim of this Chapter was to determine whether mouse S100β mVSCs and mouse SMCs (MOVAS) can undergo myeloid differentiation into MLCs *in vitro*.

Objectives:

The main aims of this chapter are to: -

1. Characterize the phenotype of J774A-1 macrophages, mouse MOVAS SMCs and mouse S100β mVSCs in culture.
2. Compare the morphology and the uptake of lipids in mouse MOVAS SMCs and mouse S100β mVSCs following treatment with myeloid differentiation inductive stimuli *in vitro*.
3. Determine the mRNA levels of macrophage genes in mouse MOVAS SMCs and mouse S100β mVSCs following treatment with myeloid differentiation inductive stimuli *in vitro*.
4. Determine the protein levels of macrophage markers in mouse MOVAS SMCs and mouse S100β mVSCs following treatment with myeloid differentiation inductive stimuli *in vitro*.

3.2 Methods

In order to investigate the multipotency of mouse S100β mVSCs and ability of MOVAS SMCs to dedifferentiate into MLCs, mVSCs were isolated from the aortic arch region using enzymatic dispersion and sequential plating of cells following removal of the adventitia and endothelium, as described in 2.2.1.2. mVSC were grown and expanded in maintenance media type 1 (MM1). A de-differentiated SMCs cell line (MOVAS), which is immortalised, were purchased commercially. ICC was then carried out (Section 2.2.3.2). in order to characterise the mVSC population by probing for the calcium-binding protein S100β. ICC was also used to investigate the expression of SMC differentiation markers, such as Cnn1 with MOVAS. Marker validation is the primary reason for examining S100β mVSCs for S100β expression is to confirm their identity as S100β-positive vascular stem cells (VSCs). S100β is a specific marker that helps in defining this particular

population of stem cells. Verifying the presence of S100β ensures that the cells under study are indeed the S100β mVSCs, thus validating the cell type being analyzed (Rothermundt et al., 2003). Cnn1is a smooth muscle cell-specific marker , by assessing Cnn1 expression, we can determine the extent to which these cells exhibit smooth muscle cell-like, which is essential for understanding in vascular biology (Gimona et al., 2002).

Cultured MOVAS and mVSCs were seeded in wells of a 6-well plate at 5 x 10^3 cells/well and incubated at 37°C for 24 h. Media was then replaced with MM1 (stem cell maintenance media) for mVSC and complete RPMI media for MOVAS, both media were supplemented with three different stimuli which are cholesterol 10 µg/ml, oxidized low density lipoprotein (ox-LDL) 50 µg/ml and 10 µl/ml of myeloid differentiation media. Cells were incubated at 37°C for 7 d with media replacement every 3-4 days. Following 7 d incubation, phase-contrast images of mVSCs and MOVAS pre-and post-treatment were analysed and revealed morphological changes following treatments.

To determine whether mVSCs and/or SMCs change their phenotype in response to myeloid differentiation inductive stimuli, cultured cells were imaged before and after treatment to compare their morphology prior to harvesting. Oil red O was performed as described in chapter 2 Section 2.2.3.4. Oil Red O is a lipid-soluble dye used for staining and up taking lipids in tissue sections and cultured cells. This staining technique is particularly useful for identifying lipid droplets within cells and tissues, providing a visual representation of lipid accumulation (Koopman et al., 2001). The expression level of *Cd68-PE* and *Mac II* and *F4/80* genes was measured using quantitative real-time polymerase chain reaction (RT-qPCR) as described in Chapter 2, Section 2.2.3.3.1.and 2.2.3.3.2. RT-qPCR is a widely used technique to quantify mRNA levels of specific genes, thereby providing critical insights into gene transcription activity. By measuring mRNA levels, we can infer the expression patterns and activity of particular genes under various conditions. This method is essential for understanding the molecular mechanisms regulating gene expression (Higuchi et al., 1993). Additionally, RT-PCR allows for the comparison of gene expression levels between different cell types (compared MOVAS SMCs and S100β mVSCs to J774A-1).This comparative analysis is vital for identifying differential gene regulation and understanding how gene expression varies across different cellular contexts, which can provide insights into cellular function and disease mechanisms (Raymond et al., 1999). The protein expression levels of MLC markers were

determined by immunocytochemistry (ICC), as described in Section 2.2.3.2, targeting specific macrophage-like markers namely Cd68 and MacII and by flow cytochemistry as described in Section 2.2.3.5. ICC is employed to visualize the presence and localization of specific proteins within cells using labelled antibodies. This technique enables us to see where proteins are situated within the cellular context, which is crucial for understanding their function and interaction with other cellular components (Thelin et al., 2006). In summary, examining J774A.1 cells for MacII and CD68 expression , and MOVAS SMCs and S100β mVSCs for S100β, Cnn1 and MacII and CD68 before and after the myeloid stimuli using ICC is crucial for validating cell identity, characterizing functional properties, comparing marker expression under different conditions such as myeloid differentiation , and providing visual confirmation of marker localization. These aspects are fundamental for advancing the understanding of macrophage biology and their roles in various physiological and pathological processes.

Flow cytometry is a powerful technique used to analyze the physical and chemical characteristics of cells, including the expression of specific markers. It provides a quantitative assessment of protein levels across large populations of cells, which is essential for precise measurement and comparison between different cell types (Herzenberg et al., 2006). Flow cytometry also allows for detailed profiling of cell populations by distinguishing different subpopulations based on the expression of surface and intracellular markers. This detailed analysis helps in understanding cellular heterogeneity and the specific characteristics of various cell subsets (Shapiro et al., 2005).

Data for all experiments in this section was generated over at least three biological replicates. Normality tests were used to determine if data followed a parametric distribution pattern. Variation across samples was analysed by calculating p-values. The type of test used to calculate this was governed by the outcome of the normality test. Statistical significance was assigned to p-values <0.05.

3.3 Results

3.3.1 Mouse S100β mVSCs and mouse MOVAS SMCs express key lineage specific phenotypic markers.

Female Bl/tgtgt Thy1 YFP mice were anesthetized and culled as described in Material and Methods Section 2.2.1.2. After isolation of mVSC, Suspension cells were then transferred to an adherent 6-well plate and cultured in MM1. ICC was carried out on this cell population and on MOVAS cells as described in Material and Methods Section 2.2.3.2 to confirm the presence of lineage specific protein markers. Cultured MOVAS SMCs were relatively positive for SMC differentiation marker expression Cnn1 (Figure 3.1C) and negative with the stemness marker S100β (Figure 3.1D). S100β mVSCs were found to be positive for S100β expression (Figure 3.1A) but negative for Cnn1 expression (Figure 3.1B). Examining S100β mVSCs for Cnn1 expression and MOVAS SMCs for S100β expression provides strong evidence for the stemness of S100β mVSCs, as they should not express the smooth muscle cell (SMC) marker Cnn1. Conversely, confirming that MOVAS SMCs express the specific SMC marker Cnn1, but not the stem cell marker S100β, validates their identity as smooth muscle cells. This distinction supports the use of S100β mVSCs as a model for stem cells and MOVAS SMCs as a model for smooth muscle cells in our study.

Collectively, the ICC data on S100β mVSCs and MOVAS SMCs indicated that these cells exhibit the expected expression of specific phenotypic markers for S100β mVSCs and MOVAS SMCs *in vitro.*

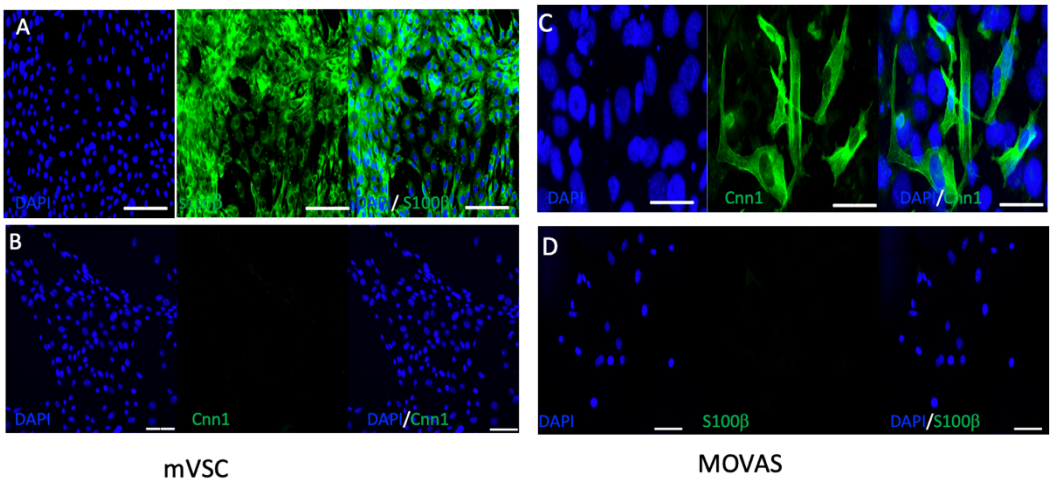

Figure 3.1. Characterization of mVSC and MOVAS SMCs by ICC. Representative images of fluorescent staining of DAPI nuclei and immunocytochemical of the SMC marker Cnn1 and the stem cell marker S100β in mVSC and MOVAS, respectively. Analysis of the expression of S100β in mVSCs (A) and MOVAS (D) and Cnn1 in mVSCs (B) and MOVAS SMCs (C) using anti-S100β and anti- Cnn1 primary antibodies. Cells were probed with an appropriate secondary antibody and stained with DAPI for nuclei visualization. Magnification at x 20 for mVSCs and x60 for MOVAS, scale Bar indicates 50 µm mVSC and 25 µm MOVAS SMCs. all images are taken with Olympus DP-50 fluorescence microscope. All images are representative of n > 5 images Per experimental group from 3 independent cultures

3.3.2 J774A-1 macrophage expresses key myeloid phenotypic markers and lipid uptake.

Examining J774A.1 cells with macrophage markers Mac-2 and CD68 by ICC is essential for validating the identity of these cells as macrophages(Iqbal et al., 2014). Mac-2 (also known as Galectin-3) and CD68 are well-established markers of macrophages, Confirming the expression of these markers ensures that the cells being studied are indeed macrophages, which is crucial for the validity of subsequent experiments involving these cells (Reinartz et al., 2016). Mac-2 and CD68 play significant roles in macrophage biology, Mac-2 is involved in cell adhesion, migration, and immune response modulation, while CD68 is a glycoprotein associated with lysosomal/endosomal compartments and is involved in phagocytic activity(Reinartz et al., 2016).By examining these markers, we can gain insights into the functional properties of J774A.1 cells. This is important for understanding how these cells behave in different experimental conditions (Reinartz et al., 2016).

ICC was carried out on a population of J774A-1 macrophages as described in Section 2.2.3.2, to confirm the presence of macrophage protein markers MacII and Cd68. An IgG control (secondary antibody probing without primary antibody staining) was used to account for background fluorescence or off-target binding of secondary IgGs figure (3.2A).

Cultured J774A-1 macrophages were positive for macrophage protein markers MacII and Cd68 (Figure 3.2 B and C)). Cultured J774A-1 macrophages were stained positively for Oil Red O (Figure 3.2D).

Collectively, the ICC and histochemical staining data on J774A-1 macrophage indicated that these cells exhibit the expected expression of myeloid macrophage-specific phenotypic markers *in vitro.* This cell line will be used as a positive control.

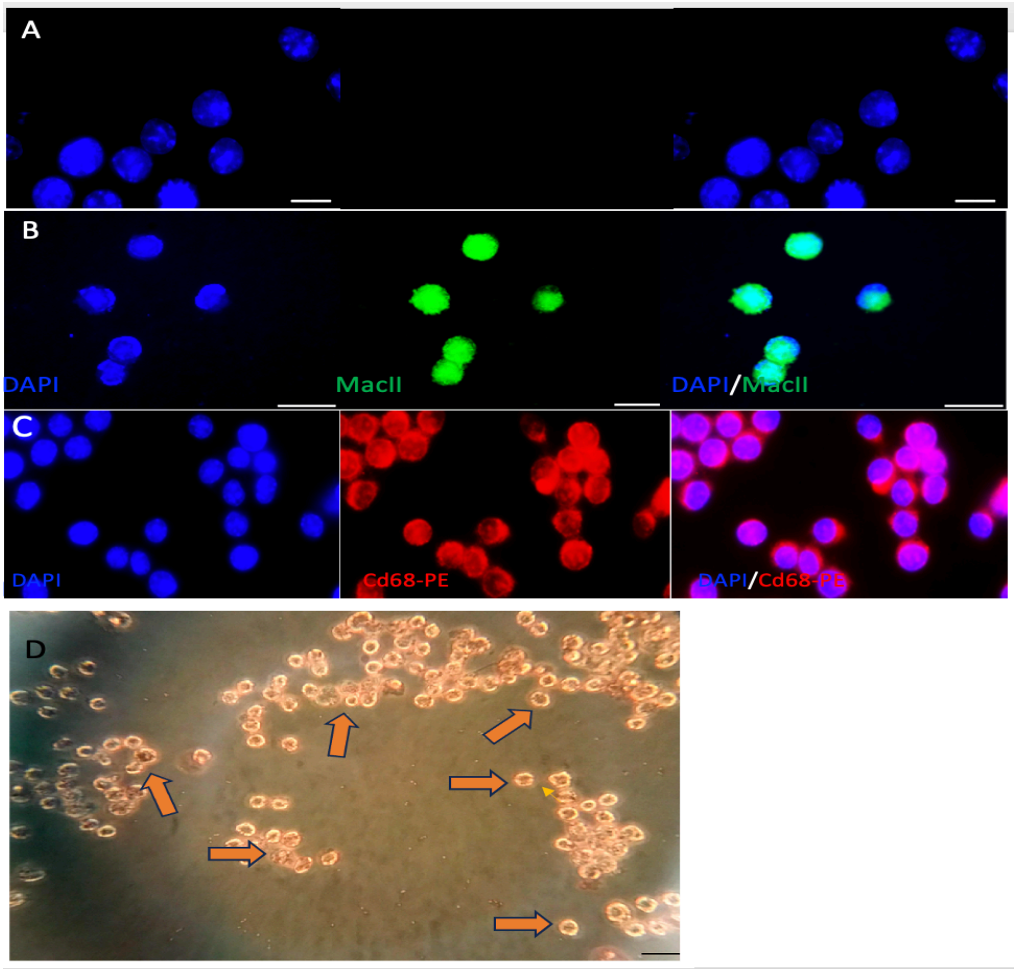

Figure 3.2 Characterization of J774A-1 macrophages. Representative images of fluorescent staining of DAPI nuclei and immunocytochemical analysis of the expression of macrophage markers, MacII and Cd68, respectively. (A) Cells stained with secondary antibody IgG without primary antibody was used to determine level of background/off-target fluorescence. (B) MacII (Green) and (C) Cd68-PE (Red) in J774A-1. (D) J774A-1 stained immunohistochemically with Oil Red O, positive stained cells pointed with arrows. All images were taken with Olympus DP-50 fluorescence microscope, image (A+B) at x60 magnification and (C and D) images at x20 magnification but were cropped to match other image. Cd68-PE conjugate and Alexa Fluor 488 secondary antibody was used with MacII for visualization of primary antibody binding. All images are representative of n > 5 images Per experimental group from 3 independent cultures - scale bar representative of 20 µm (A, B) 50 µm(C), and 25 µm for (D).

3.3.3 Morphological changes and lipid uptake of mouse S100β mVSCs and MOVAS SMCs following treatment with myeloid differentiation inductive stimuli.

MOVAS and mVSCs cells were cultured as described in “Strategy” section 3.2. Oil red O staining was performed as described in chapter 2 section 2.2.3.4.

There was no notable change in the morphology of MOVAS SMCs grown in media supplemented with ox-LDL as the cells did not transition from elongated cells displaying a ‘hill and valley’ phenotype, typical of SMCs, to a more rounded phenotype, typical of macrophages (Figure 3.3 panel 1).In contrast, there was a notable change in the morphology of S100β mVSCs as cells became more rounded when treated with each inductive stimulus (Figure 3.3 panel 2 B, C, D).

MOVAS SMCs grown in media supplemented with myeloid inductive stimuli (cholesterol, ox-LDL and myeloid differentiation media) were not stained positively for Oil Red O (Figure 3.4 panel 1 B, C, D). Unlike MOVAS SMCs, S100β mVSCs grown in media supplemented with myeloid inductive stimuli were stained positively for Oil Red O (Figure 3.4 panel 2 B, C, D).

Collectively, there were no significant changes either in morphology, or uptaking lipid in MOVAS SMC. While in S100β mVSCs, there was a notable change in morphology as well as lipid up take.

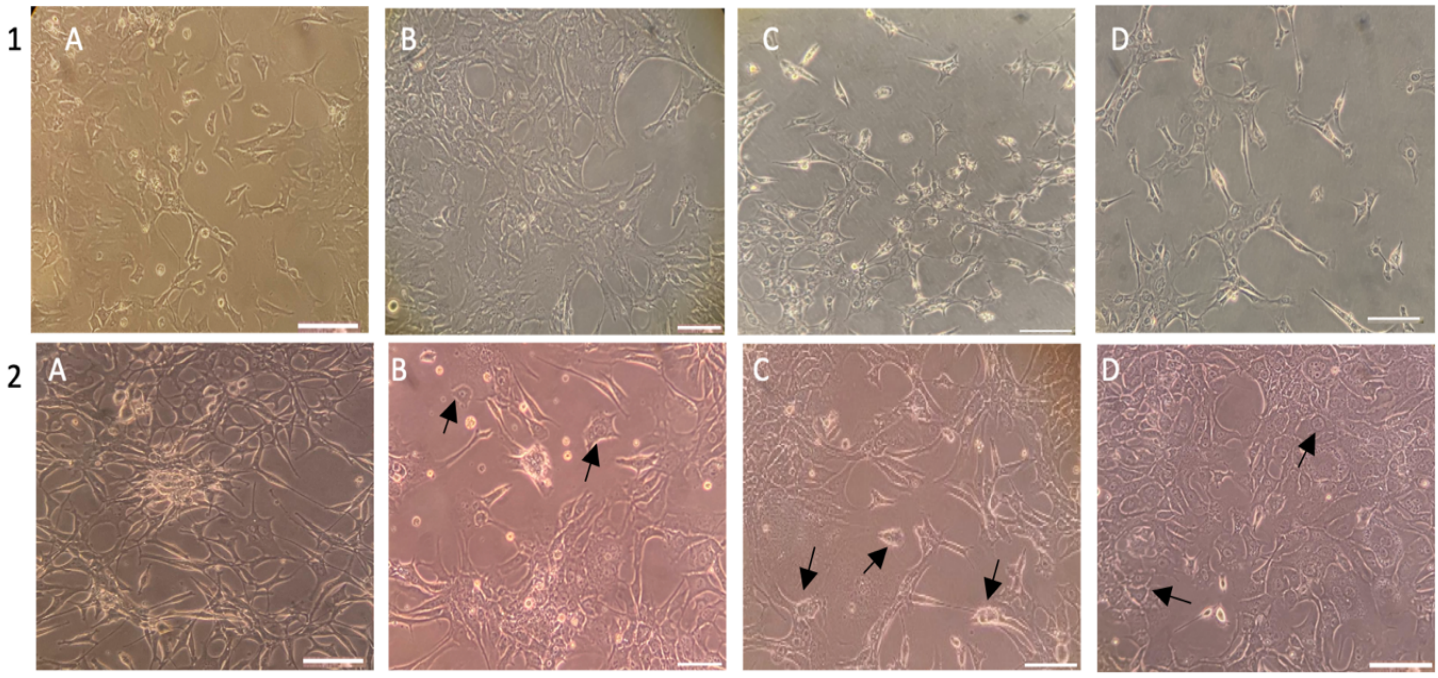

Figure 3.3. Morphological changes in cells following treatment with myeloid inductive stimuli. Representative phase-contrast images of (1) MOVAS SMC and (2) S100β mVSC before and after treatment with myeloid differentiation inductive stimuli. The cell morphology of (A) Control (untreated cells) (B) cholesterol (C) ox-LDL and (D) myeloid differentiation media, respectively, on cell morphology after day 7 in culture. All images are representative of n >5 images per experimental group from three independent cultures— magnification at x20, scale bar representative of 50µm. Arrows indicate more rounded MLCs.

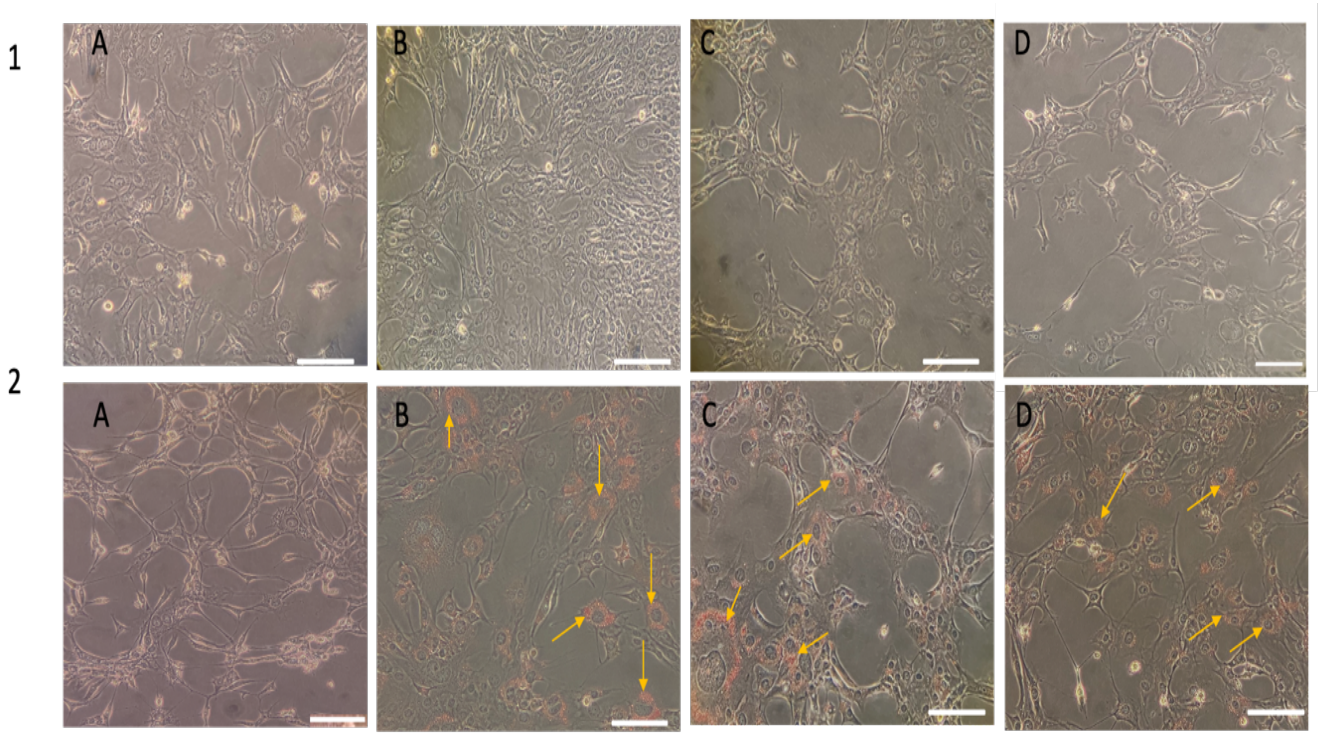

Figure 3.4. Lipid uptake in cells in cells following treatment with myeloid inductive stimuli. Representative phase-contrast images of Oil Red O staining of lipid uptake in (1) MOVAS SMCs and (2) S100β mVSC before and after treatment with myeloid differentiation indictive stimuli. Oil Red O staining of (A) Control (untreated cells) and cells grown in media supplemented with cholesterol (B) ox-LDL (C) and myeloid differentiation media (D), respectively. Images are taken after day 7 of treatment. All images are representative of n >5 images per experimental group from three independent cultures— magnification at x20, scale bar representative of 50µm. Arrows indicate positive cells.

3.3.4 The mRNA expression levels of myeloid genes (*Cd68, MacII* and *F4/80) in* MOVAS SMCs and mouse S100β mVSCs in response to myeloid differentiation inductive stimuli *in vitro*.

MOVAS and mVSCs cells were cultured as described in "Strategy" section 3.2. The expression level of *Cd68, Mac II* and *F4/80* genes were measured using RT-qPCR as described in Chapter 2, section 2.2.3.3.1.and 2.2.3.3.2.

The expression level of key myeloid genes (*Cd68, Mac II* and *F4/80)* was significantly higher in J774A-1 macrophages, when compared to MOVAS SMCs at baseline (Figure 3.5A). While there was a tendency for increased expression levels of *Cd68* and *Mac II* genes in MOVAS treated with ox-LDL and myeloid differentiation media compared to cells at baseline, it did not reach the level of significance (Figure 3.5A). There was a slight decrease in the expression levels of *Cd68* and *Mac II* genes in cells treated with cholesterol compared to cells at baseline, but it also did not reach the level of significance (Figure 3.5A). In parallel, there was a slight increase in the expression levels of *F4/80* gene expression in cells treated with cholesterol, ox-LDL and myeloid differentiation media compared to cells at baseline, but it did not reach the level of significance (Figure 3.5A).

The expression level of key myeloid genes (*Cd68, Mac II* and *F4/80)* was significantly higher in J774A-1 macrophages, when compared to S100β mVSCs at baseline (Figure 3.5B). There was a slight increase in the expression levels of *Cd68* and *F4/80* genes in S100β mVSCs treated with ox-LDL and myeloid differentiation media compared to cells at baseline, but it did not reach a level of significance (Figure 3.5B). Again, there was a slight decrease in the expression levels of the *MacII* gene in cells treated with cholesterol compared to cells at baseline but did not reach a level of significance (Figure 3.5B).

Collectively, the expression level of key myeloid genes (*Cd68, Mac II* and *F4/80*) in S100β mVSCs and MOVAS SMCs treated with cholesterol 10 µg/ml, oxidized low density lipoprotein (ox-LDL) 50 µg/ml and 10 µl/ml myeloid differentiation media for 7 days were insufficient to confirm myeloid differentiation of either of these cells towards macrophages.

When comparing MOVAS SMCs to S100β mVSCs, the expression level of the key myeloid gene (*Cd68)* was significantly higher in S100β mVSCs treated with cholesterol and myeloid differentiation media compared to MOVAS SMCs (Figure 3.6A). While there was a slight increase in the expression level of *Cd68* S100β mVSCs treated with ox-LDL compared to MOVAS SMCs but did not reach the level of significance. The expression level of the myeloid gene of *Cd11b* (Figure 3.6 B) did not reach the level of significance in S100β mVSCs compared to MOVAS SMCs, but there was a tendency for increased expression levels in S100β mVSCs treated with cholesterol. There was no significant change in the expression level of the myeloid gene (*F4/80)* in the three treatments between MOVAS SMCs and S100β mVSCs (Figure 3.6 C).

Collectively, S100β mVSCs treated with cholesterol and myeloid differentiation media have a significant expression level of the myeloid gene (*Cd68*) compared to MOVAS SMCs. Whether the comparison in the expression level of key myeloid genes (*Mac II* and *F4/80)* in S100β mVSCs and MOVAS SMCs treated with cholesterol 10 µg/ml, oxidized low-density lipoprotein (ox-LDL) 50 µg/ml and 10 µl/ml myeloid differentiation media for 7 days has an increase but did not reach the level of significance to state in order to differentiate the cells into macrophages like-cell.

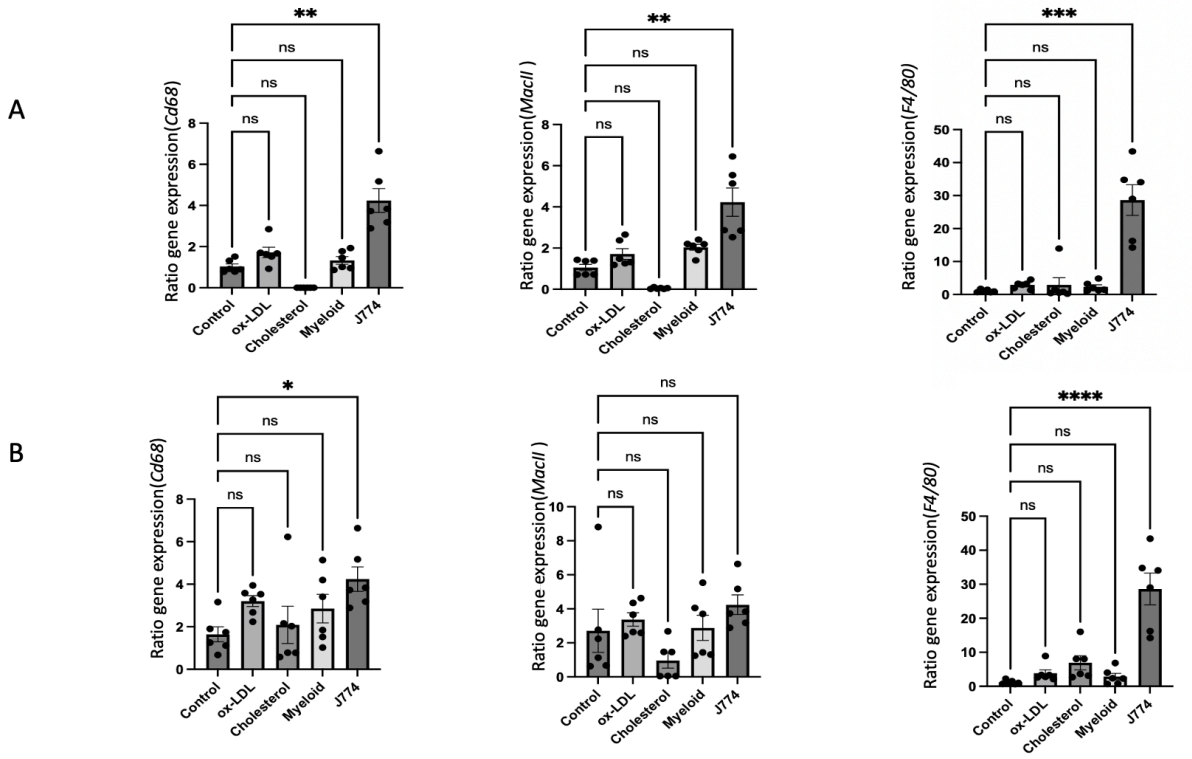

Figure 3.5 The expression of myeloid genes *Cd68, MacII* and *F4/80* in (A) MOVAS SMCs and (B) S100β mVSCs following treatment with myeloid differentiation inductive stimuli. *Cd68, MacII* and *F4/80* mRNA levels were measured in MOVAS SMCs and S100β mVSCs after 7 days treatment and compared to J774A-1. Total RNA was isolated from cells and measured by realtime RT-qPCR with *Gapdh* as an internal control. Data are expressed as the ratio of gene expression (R) and represent the mean SEM of 2 experiments performed in triplicate. * $p<0.05$ *** $p<0.001$ **** $p<0.0001$ **** $p<0.0001$ vs control.

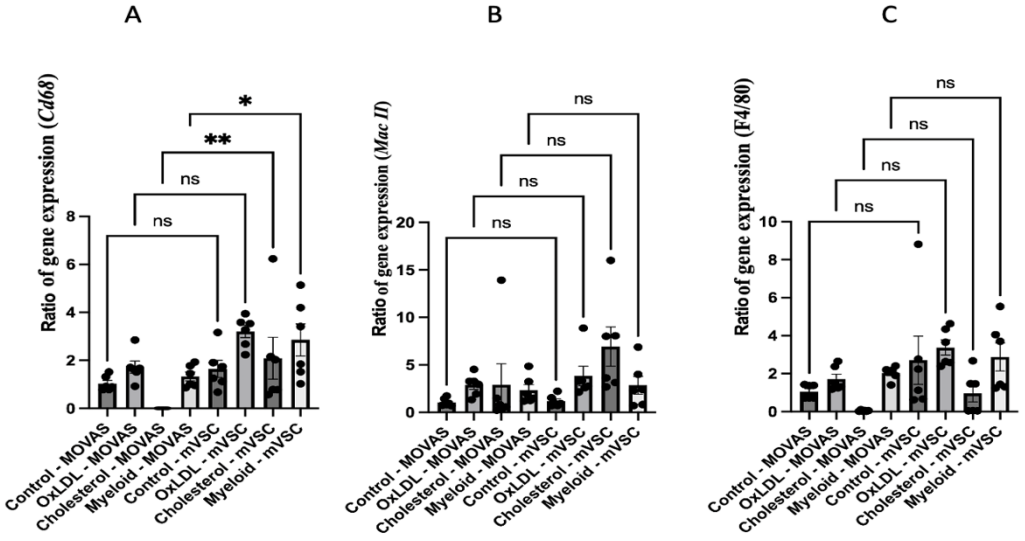

Figure 3.6 Comparison of the expression of myeloid genes (A) *Cd68, (B) MacII* and (C) *F4/80* between MOVAS SMCs and S100β mVSCs following treatment with myeloid differentiation inductive stimuli. *Cd68, MacII* and *F4/80* mRNA levels were measured in MOVAS SMCs and S100β mVSCs after 7 days treatment, Total RNA was isolated from cells and measured by realtime RT-qPCR with *Gapdh* as an internal control. Data are expressed as the ratio of gene expression (R) and represent the mean SEM of 2 experiments performed in triplicate. * p<0.05 *** p<0.001 **** p<0.0001 **** p<0.0001 vs control.

3.3.5 The protein expression levels of myeloid markers (Cd68, MacII and F4/80*) in* MOVAS SMCs and mouse S100β mVSCs in response to myeloid differentiation inductive stimuli *in vitro*.

To determine the protein levels of myeloid markers, MOVAS and mVSCs cells were cultured as described in "Strategy" section 3.2. Myeloid markers were detected in cells by either immunocytochemical analysis (ICC) or immunophenotyped by flow cytometry.

ICC was carried out to confirm the presence of macrophage protein markers, MacII and Cd68 as described in Section 2.2.3.2. For flow cytometry, 10,000 cells were used per sample as described in Section 2.2.3.5.

ICC analysis revealed that J774A-1 macrophages were predominantly positive for MacII as a control (Figure 3.7E + 3.7F, 3.9E + 3.9F). MacII was primarily expressed on the cell membrane of these treated cells. MOVAS SMC did not express MacII at baseline (Figure 3.7 A). There was a significant increase in the number of MacII positive cells in MOVAS SMCs following treatment of cells with media supplemented with all three myeloid differentiation inductive stimuli (cholesterol, ox-LDL and myeloid differentiation media) when compared to the control cells at baseline (Figure 3.7 C-D).

In a similar fashion, ICC analysis revealed that J774A-1 macrophages were also predominantly positive for Cd68 (Figure 3.8E +3.8F, 3.10E+3.10F). The number of Cd68 positive cells increased marginally but significantly in MOVAS SMCs following treatment of cells with media supplemented with myeloid differentiation media, when compared to the control cells at baseline (Figure 3.8 A and D). In contrast, the number of Cd68 positive cells did not increase significantly when supplemented with cholesterol or ox-LDL, compared to the control cells at baseline (Figure 3.8 B, C and F).

In parallel, ICC analysis revealed a significant increase in the number of MacII and Cd68 positive cells in S100β mVSCs following treatment of cells with media supplemented with all three myeloid differentiation inductive stimuli (cholesterol, ox-LDL and myeloid differentiation media) when compared to the control cells at baseline (Figure 3.9 A-D and 3.10 A-D). The fraction of

cells expressing MacII and Cd68 were as high as 89% and 82%, respectively, (Figure 3.9 F and 3.10 F). The data suggested that cholesterol, ox-LDL and myeloid differentiation media promoted myeloid differentiation of S100β mVSCs into macrophage-like cells after 7-day treatment. Collectively, S100β mVSCs have a higher fraction rate (over 80%) of cells expressing MacII and Cd68-PE compared to MOVAS-SMCs (Figure 3.11).

Flow cytometric analysis of Cd68, Cd11b and F4/80 expression in J774A-1 macrophages was used as a control. The level of Cd68, Cd11b and F4/80 was significantly higher in J774A-1 macrophages compared to MOVAS SMCs at baseline *in vitro* (Figure 3.12A, B). In MOVAS SMCs, there was a significant increase in the expression levels of Cd68 in cells treated with ox-LDL compared to cells at baseline (Figure 3.12B). In contrast, the level of expression of Cd68 in cells treated with cholesterol or myeloid differentiation media did not change significantly (Figure 3.12B). There was no change in the expression of Cd11b in cells treated with cholesterol, ox-LDL or myeloid differentiation media compared to cells at baseline (Figure 3.13B) whereas the expression of F4/80 increased significantly with cholesterol and myeloid differentiation media, respectively, but not ox-LDL, when compared to cells at baseline (Figure 3.14B).

The level of Cd68, Cd11b and F4/80 was also significantly higher in J774A-1 macrophages compared to S100β mVSCs at baseline *in vitro* (Figure 3.15B, 3.16B, 3.17B). Flow cytometric analysis of S100β mVSCs revealed that there was a significant increase in the expression of Cd68 in cells treated with ox-LDL and myeloid differentiation media, but not cholesterol, when compared to cells at baseline (Figure 3.15 A, B). There was also a significant increase in the expression of Cd11b in cells treated with ox-LDL, but not cholesterol or myeloid differentiation media, when compared to cells at baseline (Figure 3.16 A, B). There was a significant increase in the expression of F4/80 in cells treated with cholesterol, ox-LDL and myeloid differentiation media (Figure 3.17B).

Collectively, ox-LDL treatment was the most efficient at increasing the expression of all three myeloid markers in S100β mVSCs whereas ox-LDL only promoted Cd68 expression in MOVAS SMCs.

The level of Cd68, Cd11b and F4/80 was significantly higher in J774A-1 macrophages compared to S100β mVSCs and MOVAS SMCs at baseline *in vitro* (Figure 3.18).

The comparison between S100β mVSCs and MOVAS SMCs grown in their inductive medium supplemented with cholesterol, ox-LDL, and myeloid differentiation media revealed that there was an increase in the expression of Cd68 and Cd11b in S100β mVSCs supplemented with ox-LDL compared to MOVAS SMCs supplemented with ox-LDL (Figure 3.19). In parallel, there was an increase in the expression of F4/80 in S100β mVSCs supplemented with cholesterol compared to MOVAS SMCs supplemented with cholesterol (Figure 3.19).

Collectively, by ICC data, it has shown the predominant positively for J774A-1 macrophages with MacII and Cd68 markers. MOVAS SMC did not express macrophage markers significantly when compared to J774A-1. On the contrary, S100β mVSCs had showed an extreme increase with MacII and Cd68 markers when compared to J774A-1 *in vitro.*

Flow cytometric analysis revealed the level of Cd68, Cd11b and F4/80 was significantly higher in J774A-1 macrophages compared to MOVAS SMCs and S100β mVSCs at baseline. The cholesterol and ox-LDL supplements had a notable increase in S100β mVSCs more than MOVAS SMC in Cd68, Cd11b and F4/80 expression *in vitro.*

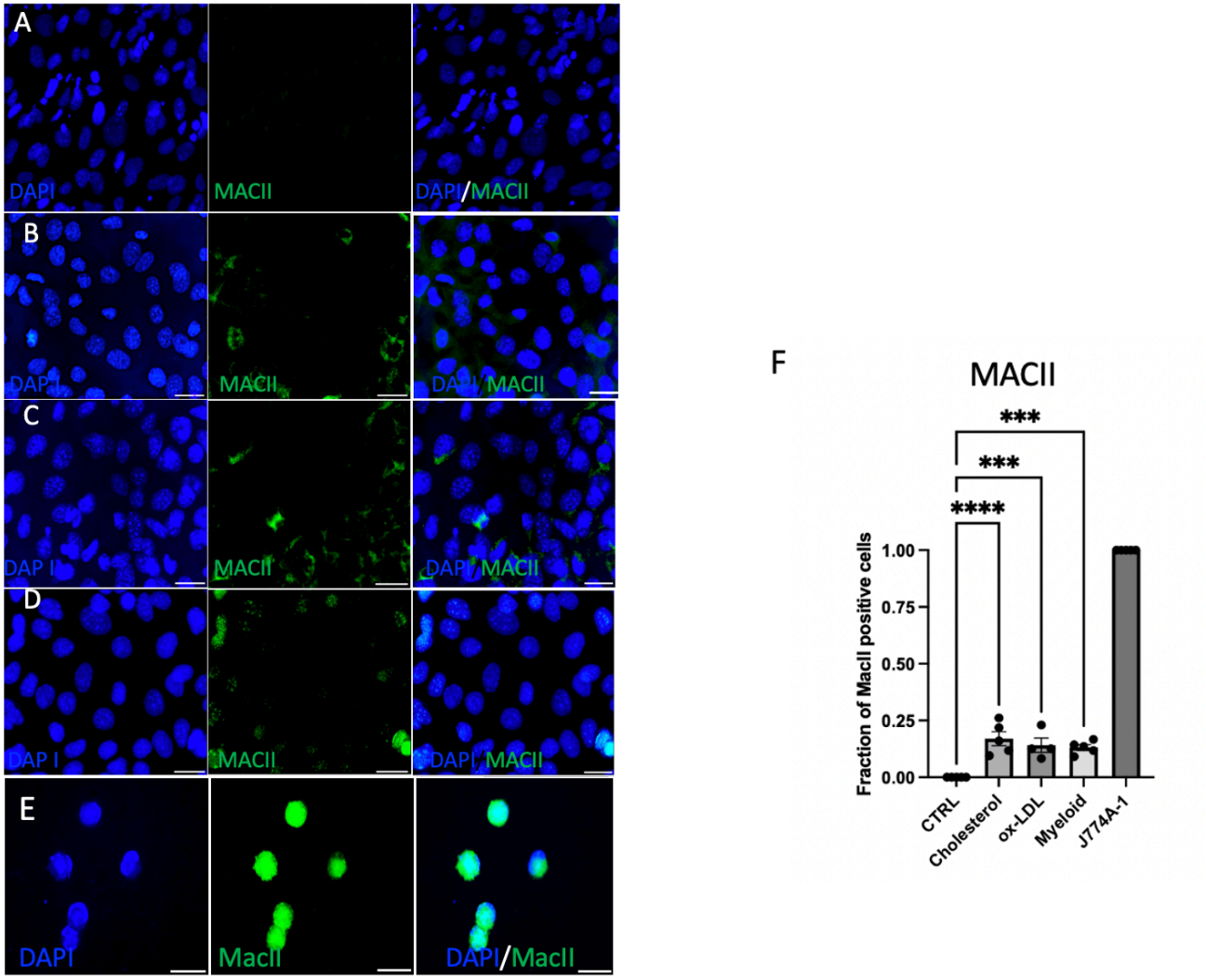

Figure 3.7 Myeloid differentiation of Mouse Aortic Smooth Muscle Cells (MOVAS SMCs) into macrophage-like cells (MLCs). Representative images of fluorescent staining of DAPI nuclei and immunocytochemical analysis of the expression of the macrophage marker MacII (green) in MOVAS SMCs. (A) CONTROL (CTRL - No treatment) and (B) cholesterol (C) oxidized low-density lipoprotein (ox-LDL), (D) myeloid differentiation media, compared to J774A-1 macrophages (E). (F)Fraction of positive cells. All images are taken with Olympus DP-50 fluorescence microscope, image (A) at x20 magnification but were cropped to match other images, and (B, C, D and E) images at x60 magnification. Alexa Fluor 488 secondary antibody used with MacII for visualization of primary antibody binding. All images are representative of n > 5 images per experimental group from 3 independent cultures - scale bar representative of 50 µm for A and 20 µm for B, C, D and E. *** $p<0.001$ **** $p<0.0001$ vs CTRL.

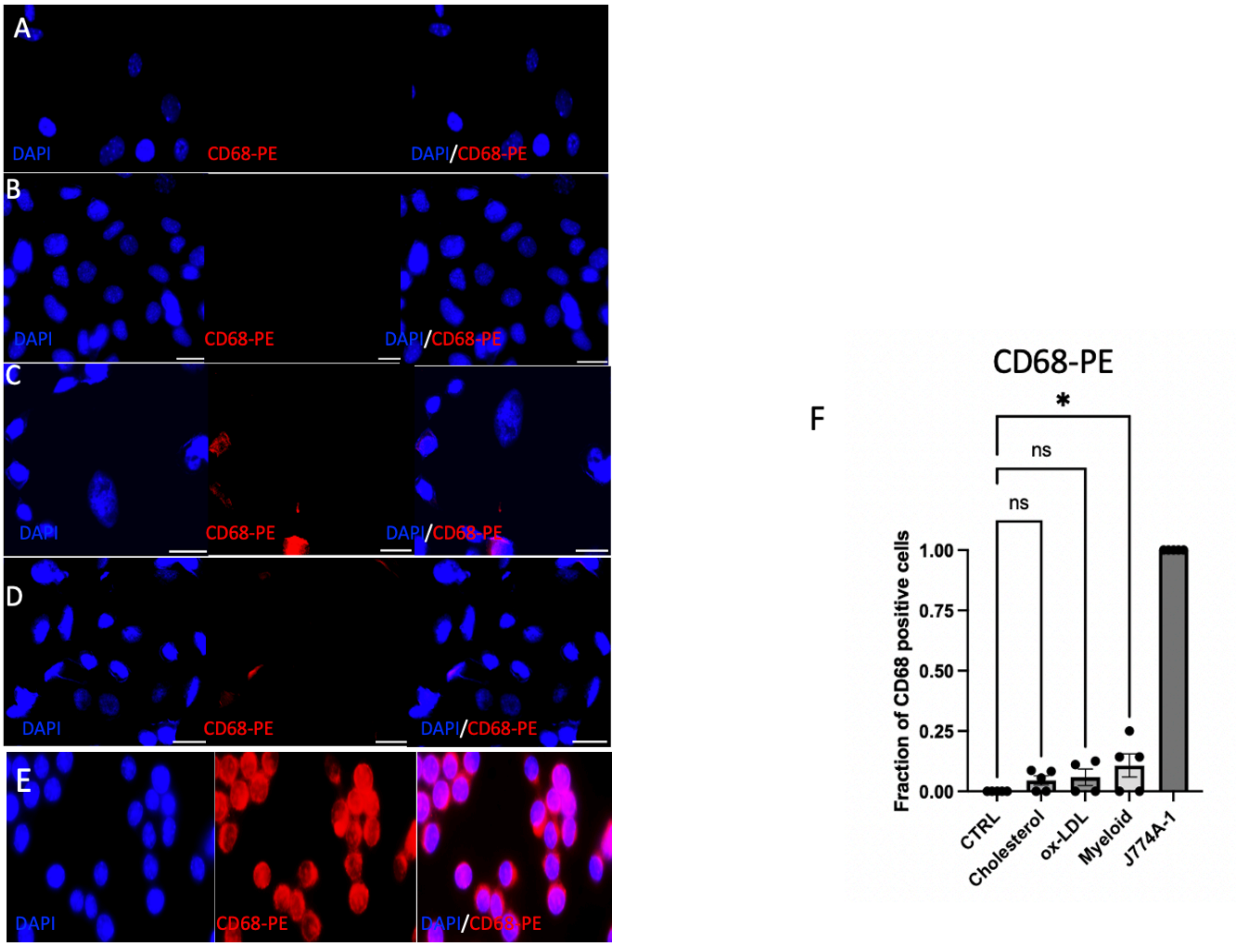

Figure 3.8 Myeloid differentiation of Mouse Aortic Smooth Muscle Cells (MOVAS) into macrophage-like cells (MLCs). Representative images of fluorescent staining of DAPI nuclei and immunocytochemical analysis of the expression of the macrophage marker, Cd68-PE (red) in MOVAS. (A) CONTROL (CTRL - No treatment) and (B) cholesterol (C) oxidized low-density lipoprotein (ox-LDL) and (D) myeloid differentiation media, compared to J774A-1 macrophages(E). Fraction of positive cells (F). All images are taken with Olympus DP-50 fluorescence microscope, image (A+E) at x20 magnification but were cropped to match other images, and (B, C, D and E) images at x60 magnification. All images are representative of n > 5 images per experimental group from 3 independent cultures - scale bar representative of 20 µm for B, C and D, and 50 µm for A+E. * $p<0.05$ vs CTRL

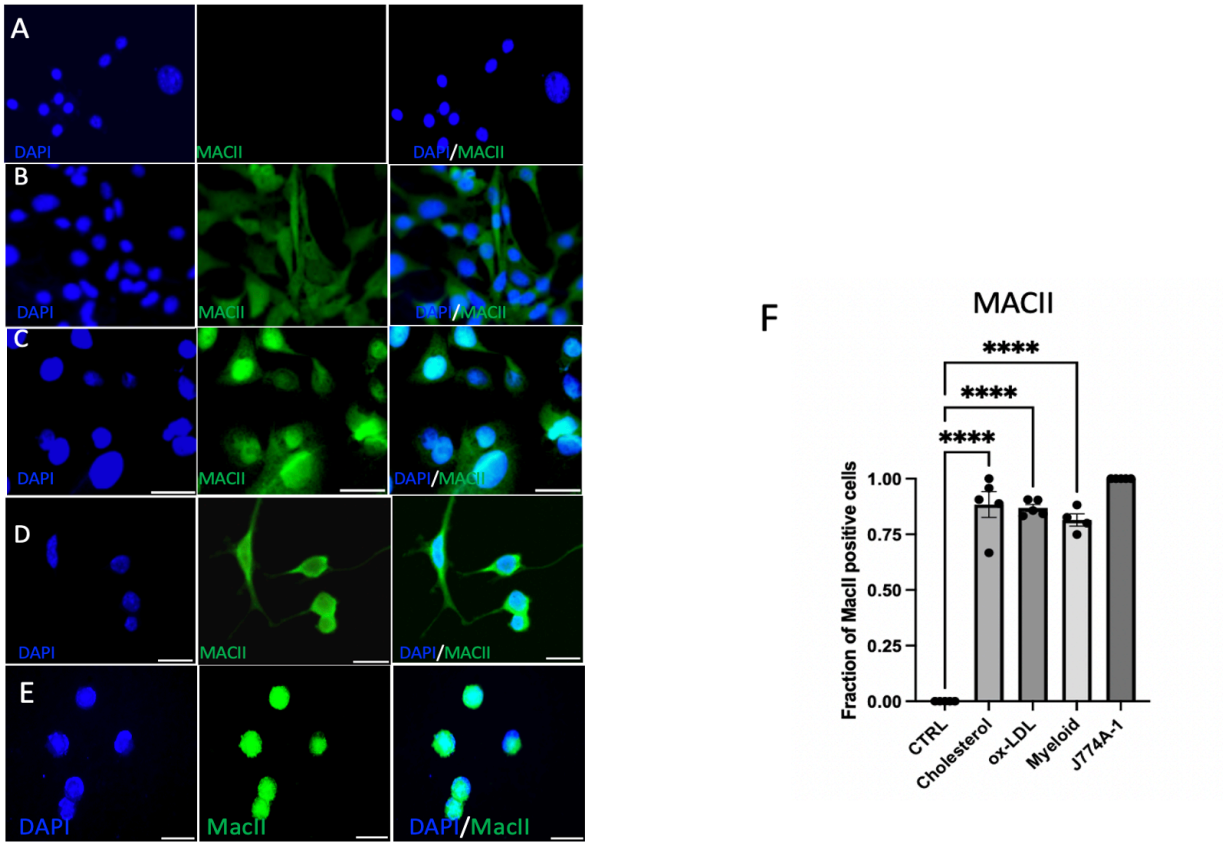

Figure 3.9 Myeloid differentiation of S100β mVSCs into macrophage-like cells (MLCs). Representative images of fluorescent staining of DAPI nuclei and immunocytochemical analysis of the expression of the macrophage marker, MacII (green) in S100β mVSCs. (A) CONTROL (CTRL - No treatment) and (B) cholesterol (C) oxidized low-density lipoprotein (ox-LDL) and (D) myeloid differentiation media, compared to J774A-1 macrophages (E). (F)Fraction of positive cells. All images are taken with Olympus DP-50 fluorescence microscope, image (A+B) at x20 magnification but were cropped to match other images, and (C, D and E) images at x60 magnification. Alexa Fluor 488 secondary antibody used with MacII for visualization of primary antibody binding. All images are representative of n > 5 images per experimental group from 3 independent cultures - scale bar representative of 50 µm for A, B and 20 µm for C, D and E. **** $p<0.0001$ vs CTRL.

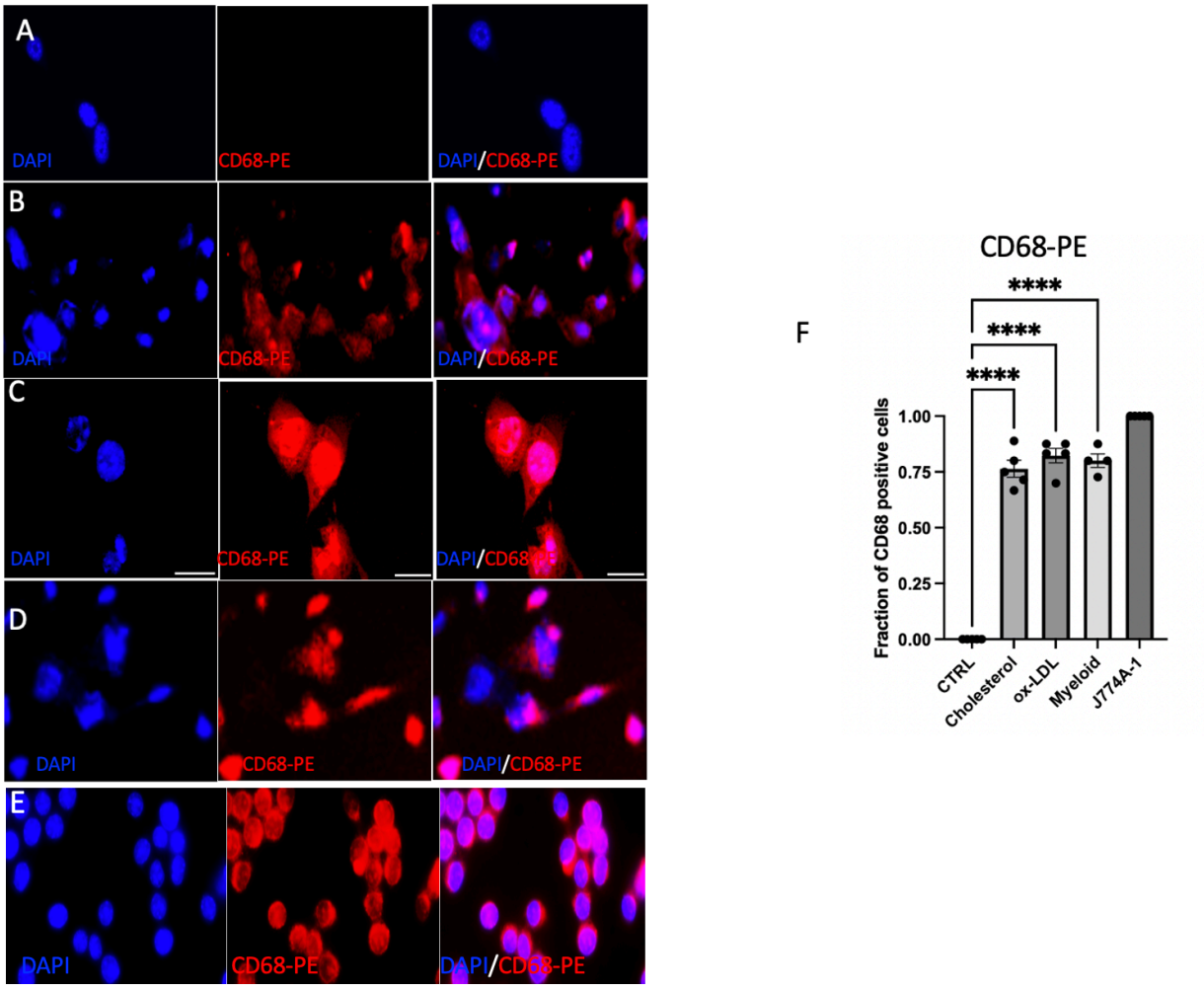

Figure 3.10 Myeloid differentiation of S100β multipotent vascular stem cells (mVSCs) into macrophage-like cells (MLCs). Representative images of fluorescent staining of DAPI nuclei and immunocytochemical analysis of the expression of macrophage marker Cd68-PE (Red) in mVSCs. (A) Control (CTRL - No treatment) and (B) cholesterol (C) oxidized low-density lipoprotein (ox-LDL) and (D) myeloid differentiation media, compared to J774A-1 macrophages (E). (F)Fraction of positive cells. All images are taken with Olympus DP-50 fluorescence microscope, images (A+B+D+E) at x20 magnification but were cropped to match other images, and (C) image at x60 magnification. Cd68-PE conjugated for visualization of primary antibody binding. All images are representative of n > 5 images per experimental group from 3 independent cultures - scale bar representative of 20 µm for C and 50 µm for A, B, D and E. **** $p<0.0001$ vs CTRL.

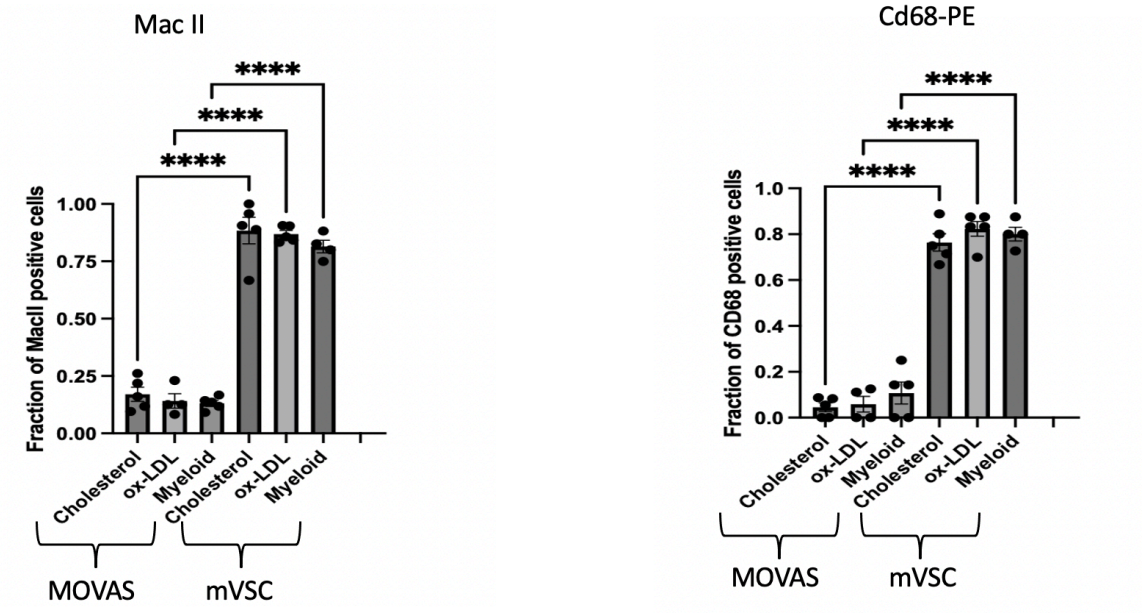

Figure 3.11. Comparison of the number of MACII and CD68-PE positive cells in MOVAS SMCs and S100β mVSC following treatment with myeloid inductive stimuli. All images are representative of n > 5 images per experimental group from 3 independent cultures. **** $p<0.0001$ vs MOVAS

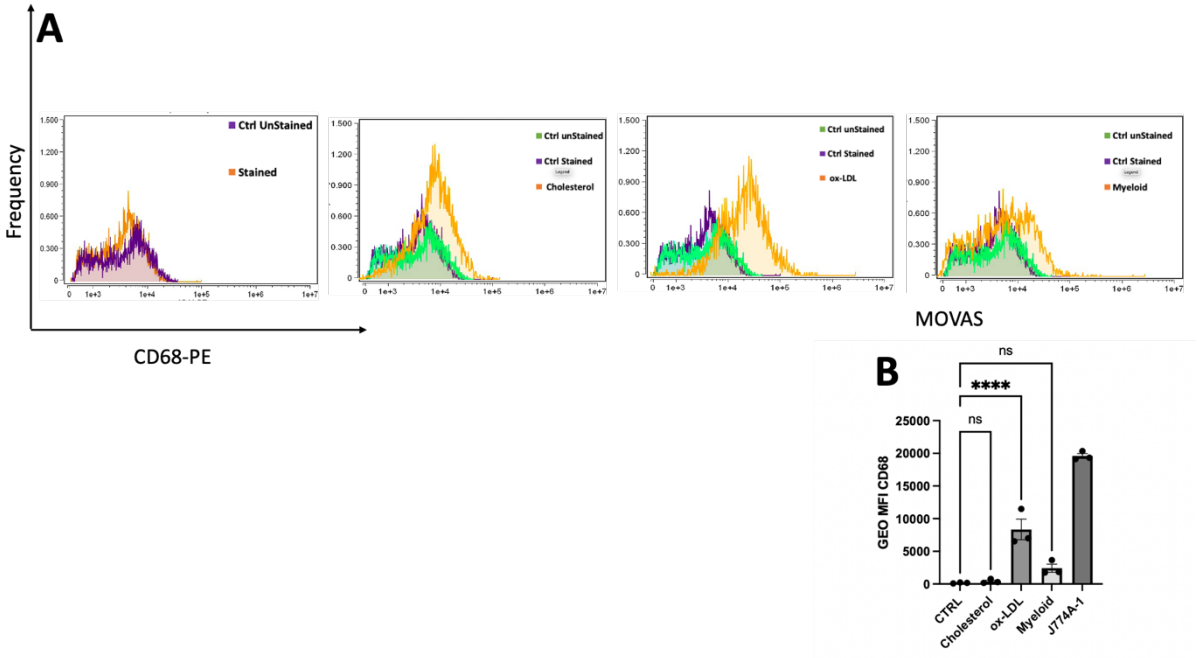

Figure 3.12 Flow cytometric analysis of Cd68 expression in MOVAS SMCs before and after treatment with myeloid inductive stimuli. Representative histogram plots for Cd68 staining of MOVAS SMCs with a Cd68-PE conjugated antibody in (A) CONTROL (CTRL - No treatment) and following treatment with media supplemented with cholesterol, oxidized low-density lipoprotein (ox-LDL) and myeloid differentiation media, and (B) geometric mean fluorescent intensity (GEO MFI) of Cd68 positive cells. J774A-1 macrophages were used as a positive control. Cd68 expression was analysed and compared by overlaying the histograms of unstained/stained control versus stained treated cells. Flow cytometry was performed using the Amnis™ Cellstream Flow Cytometer. Cell debris were excluded from the analysis based on scatter signals. Data are from the average of three independent experiments. Data are ± SEM **** $p<0.0001$ vs CTRL.

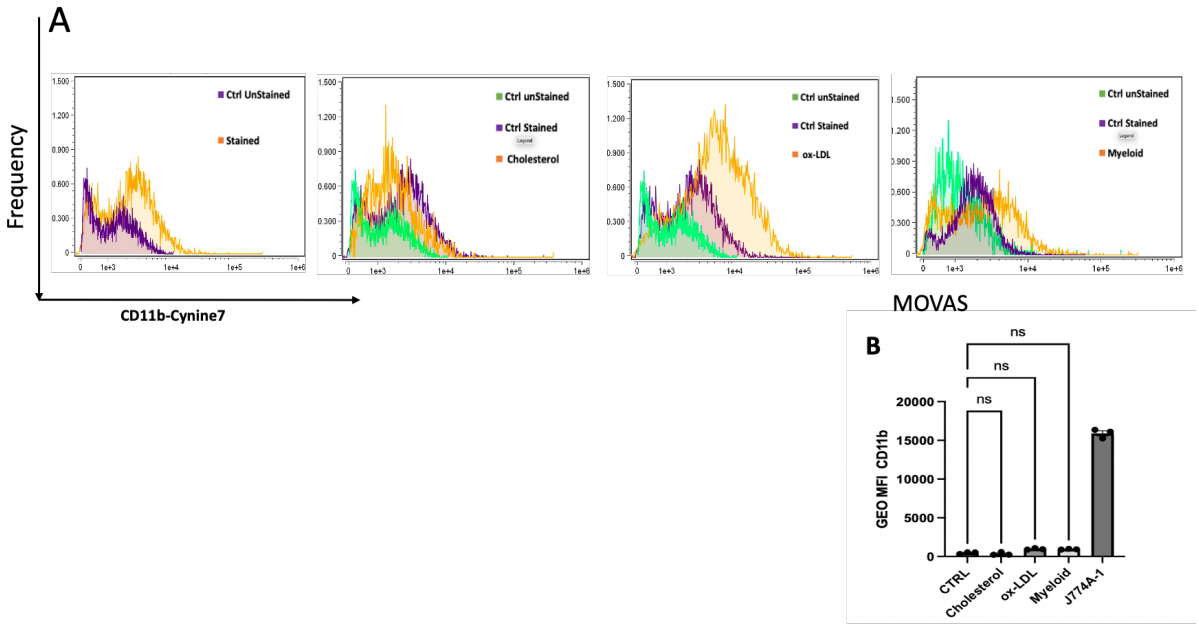

Figure 3.13 Flow cytometric analysis of Cd11b expression in MOVAS SMCs before and after treatment with myeloid inductive stimuli. Representative histogram plots for Cd11b staining of MOVAS SMCs with a Cd11b-Cynine7 conjugated antibody in (A) CONTROL (CTRL - No treatment) and following treatment with media supplemented with cholesterol, oxidized low-density lipoprotein (ox-LDL) and myeloid differentiation medium, and (B) geometric mean fluorescent intensity (GEO MFI) of Cd11b positive cells. J774A-1 macrophages were used as a positive control. Cd11b expression was analysed and compared by overlaying the histograms of unstained/stained control versus stained treated cells. Flow cytometry was performed using the Amnis™ Cellstream Flow Cytometer. Cell debris were excluded from the analysis based on scatter signals. Data are from the average of three independent experiments. Data are ±SEM *** $p<0.001$ vs CTRL.

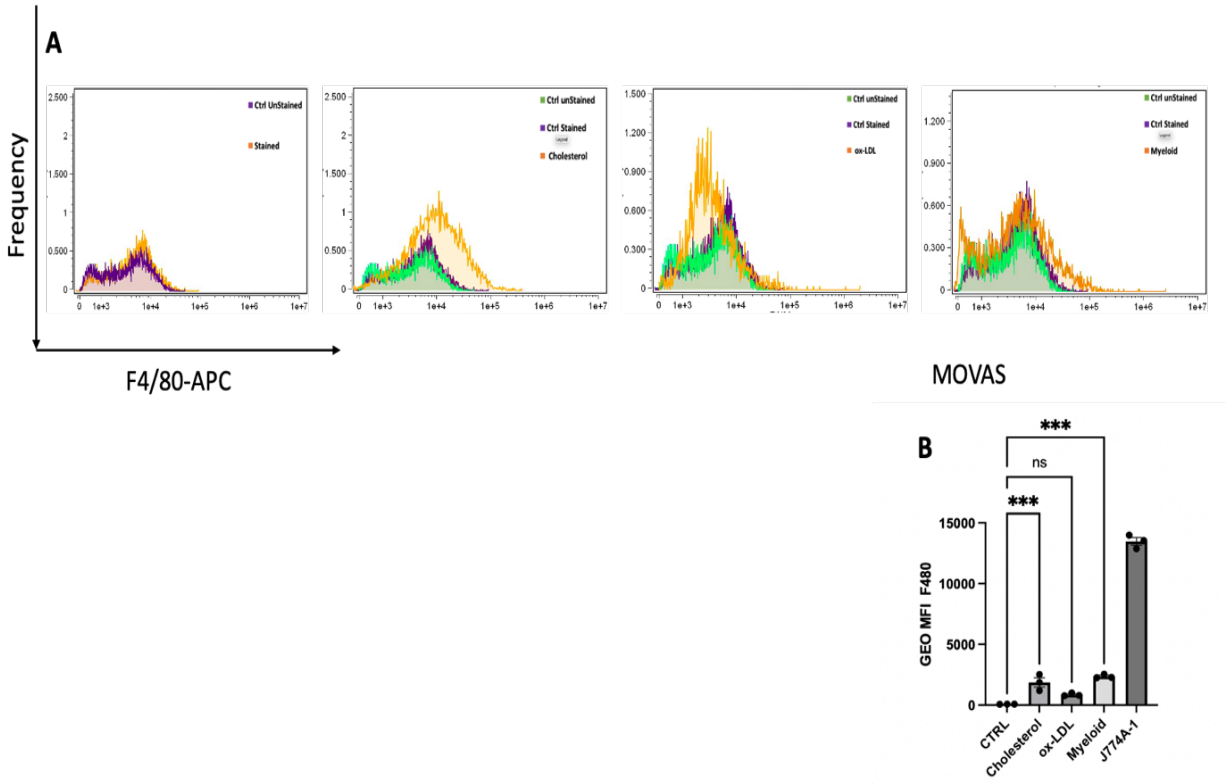

Figure 3.14 Flow cytometric analysis of F4/80 expression in MOVAS SMCs before and after treatment with myeloid inductive stimuli. Representative histogram plots for Cd11b staining of MOVAS SMCs with a F4/80-APC conjugated antibody in (A) CONTROL (CTRL - No treatment) and following treatment with media supplemented with cholesterol, oxidized low-density lipoprotein (ox-LDL) and myeloid differentiation media, and (B) geometric mean fluorescent intensity (GEO MFI) of F4/80 positive cells. J774A-1 macrophages were used as a positive control. F4/80-APC expression was analysed and compared by overlaying the histograms of unstained/stained control versus stained treated cells. Flow cytometry was performed using the Amnis™ Cellstream Flow Cytometer. Cell debris were excluded from the analysis based on scatter signals. Data are from the average of three independent experiments. Data are ±SEM *** $p<0.001$ vs CTRL.

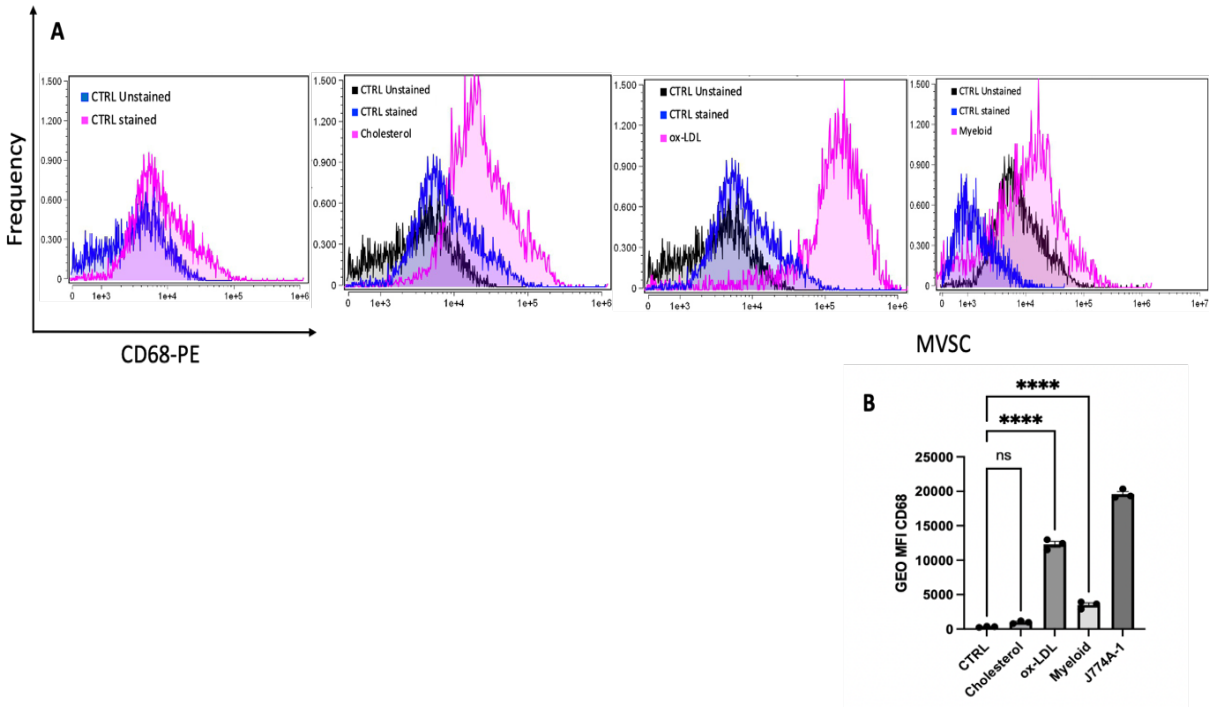

Figure 3.15 Flow cytometric analysis of Cd68 expression in S100β mVSCs before and after treatment with myeloid inductive stimuli. Representative histogram plots for Cd68 staining of S100β mVSCs with a Cd68-PE conjugated antibody in (A) CONTROL (CTRL - No treatment) and following treatment with media supplemented with cholesterol, oxidized low-density lipoprotein (ox-LDL) and myeloid differentiation media, and (B) geometric mean fluorescent intensity (GEO MFI) of Cd68 positive cells. J774A-1 macrophages were used as a positive control. Cd68 expression was analysed and compared by overlaying the histograms of unstained/stained control versus stained treated cells. Flow cytometry was performed using the Amnis™ Cellstream Flow Cytometer. Cell debris were excluded from the analysis based on scatter signals. Data are from the average of three independent experiments. Data are ± SEM **** $p<0.0001$ vs CTRL.

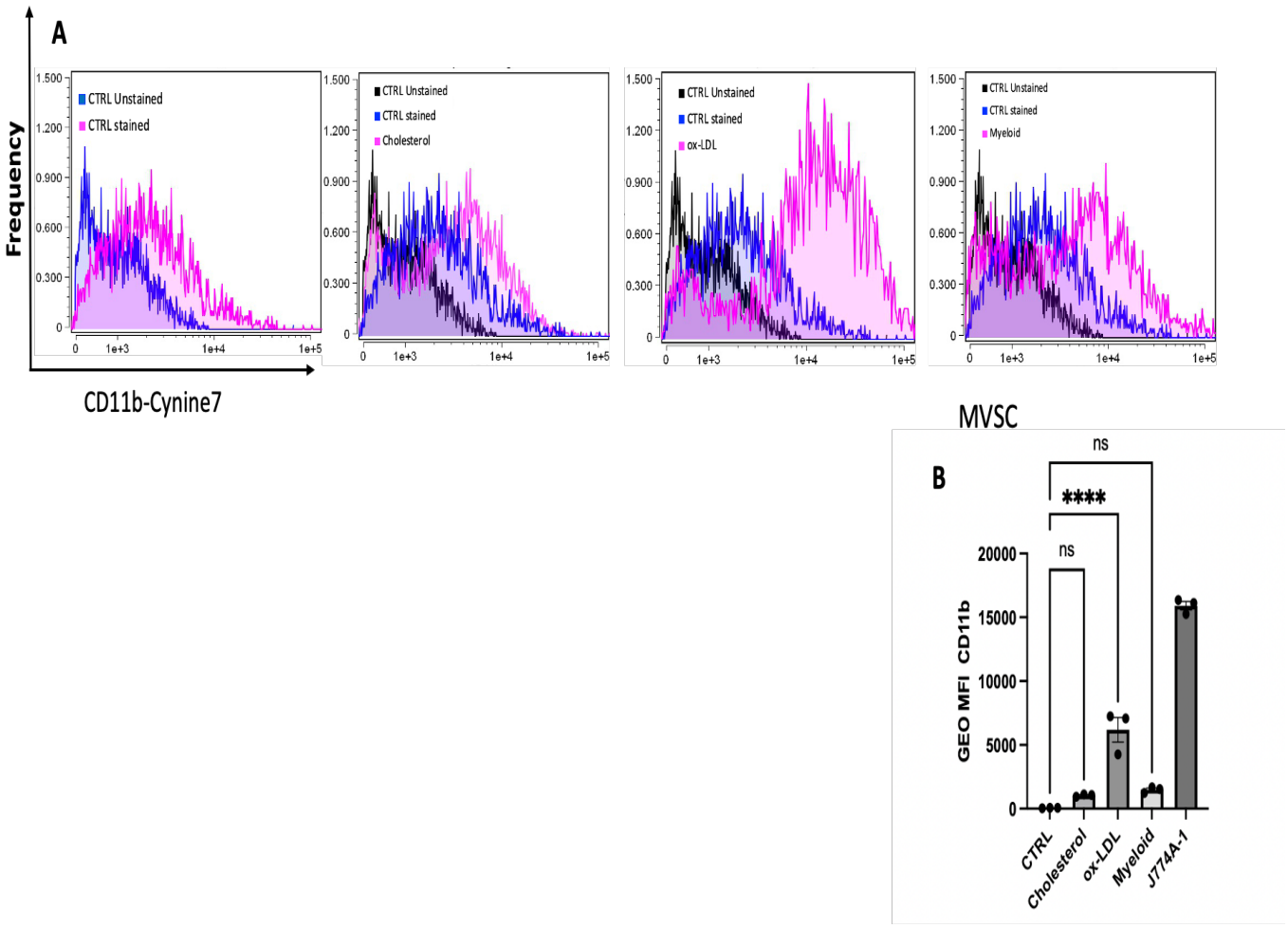

Figure 3.16 Flow cytometric analysis of Cd11b expression in S100β mVSCs before and after treatment with myeloid inductive stimuli. Representative histogram plots for Cd11b staining of S100β mVSCs with a Cd11b-Cynine7 conjugated antibody in (A) CONTROL (CTRL - No treatment) and following treatment with media supplemented with cholesterol, oxidized low-density lipoprotein (ox-LDL) and myeloid differentiation media, and (B) geometric mean fluorescent intensity (GEO MFI) of Cd11b positive cells. J774A-1 macrophages were used as a positive control. Cd11b expression was analysed and compared by overlaying the histograms of unstained/stained control versus stained treated cells. Flow cytometry was performed using the Amnis™ Cellstream Flow Cytometer. Cell debris were excluded from the analysis based on scatter signals. Data are from the average of three independent experiments. Data are ±SEM **** $p<0.0001$ vs CTRL.

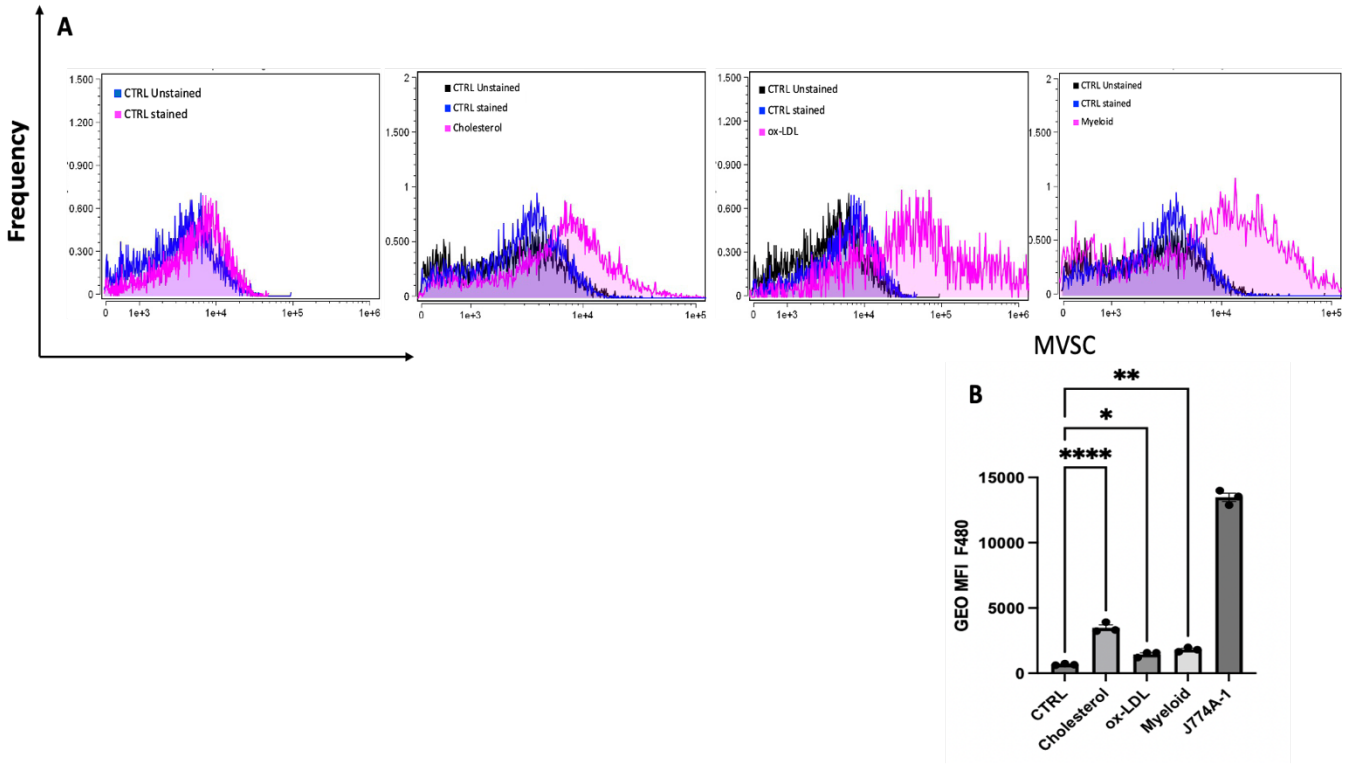

Figure 3.17 Flow cytometric analysis of F4/80 expression in S100β mVSCs before and after treatment with myeloid inductive stimuli. Representative histogram plots for F4/80 staining of S100β mVSCs with a F4/80-APC conjugated antibody in (A) CONTROL (CTRL - No treatment) and following treatment with media supplemented with cholesterol, oxidized low-density lipoprotein (ox-LDL) and myeloid differentiation media, and (B) geometric mean fluorescent intensity (GEO MFI) of F4/80 positive cells. J774A-1 macrophages were used as a positive control. F4/80 expression was analysed and compared by overlaying the histograms of unstained/stained control versus stained treated cells. Flow cytometry was performed using the Amnis™ Cellstream Flow Cytometer. Cell debris were excluded from the analysis based on scatter signals. Data are from the average of three independent experiments. Data are ±SEM * $p<0.05$ ** $p<0.01$ **** $p<0.0001$ vs CTRL.

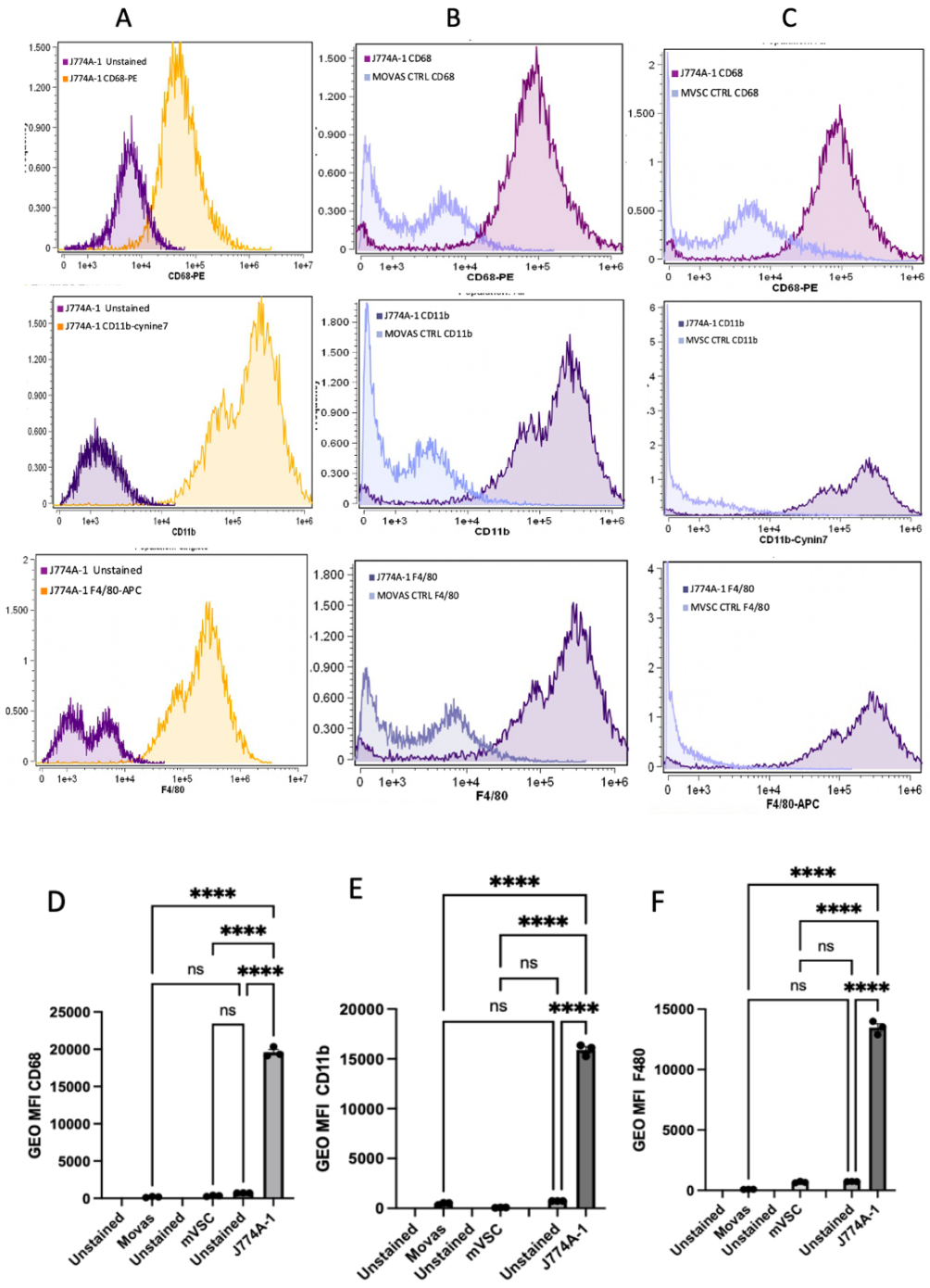

Figure 3.18 Immunophenotyping of mouse macrophage cell line, J774A.1 compared to MOVAS SMCs and mouse S100β mVSCs by Amnis™ Cellstream Flow Cytometry. Cells were immunophenotyped using three macrophage markers: CD68, CD11b, and F4/80. The cells These markers were specifically labelled with fluorescent dyes, namely PE, Cynin7, and APC, respectively. Each histogram illustrates the fluorescent intensity, indicative of the expression level

of the corresponding antigen in (A) J774A-1 compared to (B) MOVAS and (C) MVSC, across a population of 10,000 cells per sample preparation. To assess and compare the antigen expression, the histogram derived from the unstained sample was superimposed with the histogram obtained from the sample stained with the conjugated antibody. These histograms pertain to one of three independent experiments conducted. (D-F) Bar charts representation of expression level of the CD68-PE, CD11b-Cynine7 and F4/80-APC geometric mean fluorescent intensity (GEO MFI) of all stained samples from the average of three independent experiments against CD68-PE, CD11b-Cynine7 and F4/80-APC stained J774A-1 mouse macrophage cell line using GraphPad Prism V9. Data are ±SEM **** p<0.0001.

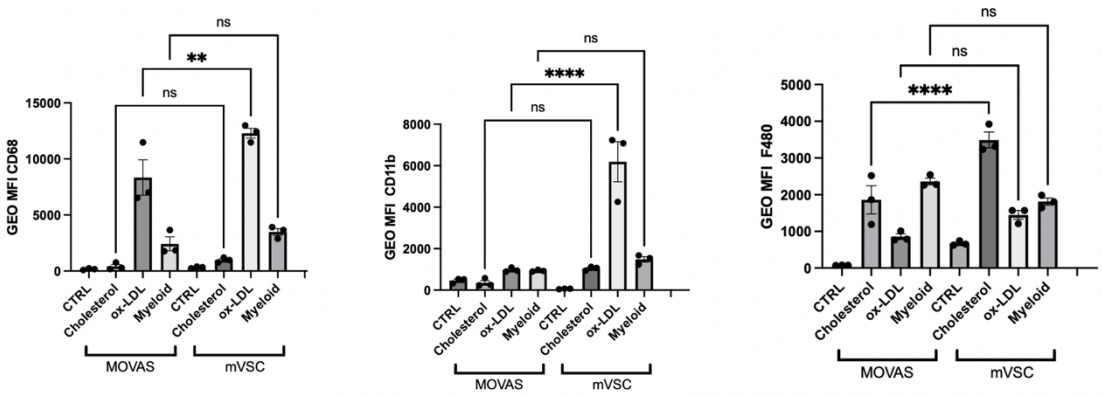

Figure 3.19 Comparison of the expression of Cd68, Cd11b and F4/80 in MOVAS-SMC vs S100β mVSCs before and after treatment with myeloid inductive stimuli. Geometric mean fluorescent intensity (GEO MFI) of myeloid positive cells following growth in their maintenance medium supplemented for 7 days to differentiate them into macrophage-like cells, the expression level of the Cd68-PE, Cd11b-Cynine7 and F4/80-APC was analysed and compared by overlaying the histograms of unstained/stained control versus stained treated cells. Flow cytometry was performed using the Amnis™ Cellstream Flow Cytometer. Cell debris was excluded from the analysis based on scatter signals. Data are the mean ± SEM from the average of three independent experiments * p<0.05 ** p<0.01 *** p<0.001 **** p<0.0001 vs MOVAS.

3.4 Summary

MOVAS SMCs

- MOVAS SMCs exhibited myogenic expression of Cnn1, a SMC differentiation marker, *in vitro.*
- There was no significant change in the morphology, lipid uptake of Oil Red O, or mRNA levels of myeloid genes *Cd68, Mac II* and *F4/80* of MOVAS SMCs following treatment of cells with cholesterol, ox-LDL or myeloid differentiation media *in vitro*.
- Myeloid differentiation media promoted Cd68 and MacII protein expression in MOVAS SMCs while flow cytometric analysis revealed increases in Cd68 with ox-LDL and F4/80 with cholesterol and myogenic differentiation media, respectively.

S100β mVSCs

- S100β mVSCs exhibited stem cell expression of S100β, a neuroectoderm differentiation marker, *in vitro.*
- There was a notable change in the morphology and lipid uptake of Oil Red O but no significant increase in myeloid genes *Cd68, Mac II* and *F4/80* of S100β mVSCs following treatment of cells with cholesterol, ox-LDL or myeloid differentiation media *in vitro*.
- S100β mVSCs treated with cholesterol, ox-LDL or myeloid differentiation media increased their expression of myeloid differentiation markers, Cd68 and MacII expression *in vitro* while flow cytometric analysis of myeloid differentiation marker expression revealed that only ox-LDL promoted a significant increase in all 3 myeloid markers.

3.5 Discussion

The major focus of this Chapter was to determine whether de-differentiated vascular SMCs and/or S100β mVSCs in culture could undergo myeloid differentiation following treatment of cells with three myeloid differentiation inductive stimuli (cholesterol, ox-LDL and myeloid differentiation media). Collectively, the data suggests that both cell types sporadically respond to myeloid inductive stimuli but only S100β mVSCs responded to ox-LDL by increasing their expression of all phenotypic markers of myeloid differentiation when compared to de-differentiated MOVAS SMCs. By using cultured S100β mVSCs, MOVAS SMCs and cultured J774A-1 macrophages as a positive technical control, MOVAS SMCs and S100β mVSCs demonstrate similar sporadic phenotypic characteristics but only S100β mVSCs differentiated into MLCs when loaded with ox-LDL by increasing Cd68, Cd11b and F4/80 expression.

The accumulation of neointimal cells, primarily SMC-like cells within lesions, leading to intimal thickening and subclinical atherosclerosis is known as a hallmark of arterial pathology in cardiovascular disease (CVD) (Benditt & Benditt, 1973). This accumulation leads to the development of early adaptive lesions (Velican & Velican, 1981) and an essential marker of subclinical disease yet the fundamental aspects of vascular cell accumulation, proliferation and the phenotypic changes within the vessel wall remain unresolved (Benditt & Benditt, 1973). The purported involvement of reprogrammed de-differentiated SMC-like cells in vascular lesions through a process of phenotypic modulation or switching has been at the forefront of our understanding of arteriosclerotic lesion formation for many years (Albarrán-Juárez et al., 2016); Chappell et al., 2016; (Herring et al., 2014); (Nemenoff et al., 2011). Although the field has made tremendous progress in characterizing the phenotypic changes in vascular SMCs, our understanding of phenotypic transition dynamics of other cells including endothelial cells and resident vascular stem cells and their respective contribution in subclinical atherosclerosis remains limited. Lineage tracing and single-cell RNA transcriptomics studies (scRNA-seq) studies, or a combination of both have provided compelling evidence of SMC phenotypic and functional diversity (Dobnikar et al., 2018); Wirka et al., 2019). A rare number of medial Sca1 positive SMCs are thought to de-differentiate and populate atherosclerotic lesions by their selective expansion and investment concomitant with profound and diverse modifications of their original phenotype and

function (Dobnikar et al., 2018). However, recent lineage tracing studies from our research group have recently provided further compelling evidence that adventitial and/or medial S100β mVSCs and their progeny significantly contribute to lesion formation in murine models of arteriosclerotic disease (Di Luca et al., 2021, Molony et al., 2021, Liu et al., 2022). These S100β cells may become activated, clonally proliferate and differentiate down vascular and non-vascular lineages that subsequently dictate, in part, lesion formation.

The accumulation of SMC-like and non-SMCs [MLCs, endothelial cells (ECs), osteoblasts (OBs), adipocytes (APs), mesenchymal stem cells (MSCs)] play an important role during vascular disease progression and lesion formation (Bonacina et al., 2023). Normal arterial vessels and lesions following injury or during arteriosclerotic (carotid ligation/wire-induced injury etc) and atherosclerosis (apolipoprotein E deficient mouse model (ApoE) or low-density lipoprotein receptor (LDL-R) deficient mice fed a high fat diet) are heterogeneous with a variety of cellular phenotypes found in the adventitial, medial and intimal layers (Potente et al., 2017; Van Kuijk et al., 2019). Recent evidence suggests that most of the major cell types in atherosclerotic plaques, e.g. macrophages, endothelial cells, T-cells, and SMC-like cells are heterogeneous and/or plastic to some extent. Although macrophages, endothelial cells, T cells, and SMCs are the most discussed cells relating to disease progression, recent research in the field has highlighted the role of S100β resident vascular stem cells (DiLuca et al., 2021), (Molony et al., 2021), (W. Liu et al., 2020). They may originate from a resident progenitor stem cell, which can give rise to various cell types like (myo)fibroblasts, SMC-like cells or non-SMCs (El Agha et al., 2017).

For decades, it had been assumed that differentiated medial SMCs undergo phenotypic modulation and switching to become de-differentiated SMCs that are plastic and contribute to the accumulation of both SMC-like cells and non-SMCs, within vascular lesions. Initial results from SMC lineage tracing system studies revealed that >95% of SMC-derived cells in atherosclerotic lesions from brachiocephalic arteries of SMC-*EYFP*+/+ *ApoE*−/− mice using Cre-LoxP (cyclization recombinase)-(locus of x-over, P1) were not detectable as being of SMC origin following Acta2 or Myh11 immunostaining (Gomez et al., 2013). Moreover, a sizable proportion of *Myh11* marked non-SMC cells were enriched for the stable SMC epigenetic mark, H3K4me2 on the *Myh11* locus using a proximity ligation assay (PLA) *in vitro*. The authors concluded that non-SMC phenotypes that include myeloid cells (MLCs), mesenchymal-like cells, fibroblasts, -,

adipogenic - and osteogenic-like cells are derived from *Myh11* marked differentiated SMCs. These data suggest that a substantial proportion of the marked non-SMCs within lesions that are enriched for H3K4me2 at the *Myh11* locus are derived from a parent differentiated SMC (Gomez et al., 2013). The central de-differentiated SMC type is classified as a mesenchymal-like phenotype. These cells subsequently seem to differentiate into fibroblast-like, macrophage- like, osteogenic-like, and adipocyte-like cells, which require the transcription factor Krüppel- like factor 4 (KLF4) and contribute differentially to vascular disease (Yap et al., 2021). Using an *in vivo* fate mapping approach, with either a constitutive or an inducible *Myh11*-driven cyclization recombinase (Cre) mouse model, it has been demonstrated that SMCs are also able to adapt toward an adipocyte-like phenotype (Long et al., 2014). Single-cell RNA sequencing (scRNA-Seq) studies have reported that a fibroblast-like SMC phenotype is also observed following vascular injury, such as during atherosclerotic progression or aortic aneurysm formation. This phenotype is also referred to as myofibroblasts-like SMCs or fibromyositis (Buam et al., 2011). Recent scRNA-seq data also suggests that a Sca1 cell population within the medial layer of the vessel wall is a heterogeneous population that consists of endothelial cells, perivascular adipocytes, and platelet-derived growth factor receptor alpha or beta (PDGFRα) (PDGFRβ) stromal cells. An intersectional genetics strategy pinpointed the Sca1/PDGFRα cell population as the main source of *de novo* SMC and non-SMC-like cells during healing of severe transversal arterial injury (J. Tang et al., 2020). These Sca1-derived SMCs possessed more propensity to expand compared with pre-existing SMCs, imparting them an important fraction of SMCs regeneration. Genetic Sca1 cell ablation supports their involvement in vessel repair and recovery (Tang et al., 2020).

De-differentiated SMCs reportedly acquire a macrophage-like phenotype (MLC) when exposed to cholesterol or ox-LDL *in vitro* (Vengrenyuk et al., 2015); (Rong et al., 2003), and when fed a western high fat diet in atherosclerotic models in mice *in vivo* (Shankman et al., 2015), (Wang et al., 2019). However, the propensity of S100β mVSCs to differentiate to MLCs when compared to MOVAS SMCs has not been addressed. Enzymatic dispersion was used to isolate a population of resident stem cells from the medial layer of a mouse aortic arch. The aortic arch was chosen as this is a high risk area for arteriosclerotic lesion formation (Redheuil et al., 2010). The aortic arch has its embryological origin in the neuroectoderm and so many of the cells present in this area still express markers related to that origin (Bacakova et al., 2018). These cells are referred to as multipotent vascular stem cells (mVSCs) and express neural stem cell markers, S100β, Sox10,

Sox17 and Nestin (Tang et al., 2012). Using ICC, mVSCs expressed S100β and are negative for Cnn1, a SMC intermediate differentiation marker. Despite having a medial and/or adventitial origin, these cells are not derived from medial SMCs as they do not enrich for the stable SMC epigenetic mark, H3K4me2 at the *Myh11* locus and do not express SMC differentiation genes (DiLuca et al., 2021). On the other hand, MOVAS SMCs express Cnn1 and are negative for S100β. Clearly, both cell lines exhibit the expected expression profile of specific phenotypic markers for S100β mVSCs and MOVAS *in vitro,* respectively.

It was therefore decided to examine the ability of S100β mVSCs and MOVAS SMCs to undergo myeloid differentiation *in vitro*. There was no clear change in the morphology or reproducible expression of myeloid markers in MOVAS SMCs following any of the supplements that drive myeloid specification compared to their phenotypic characteristics when grown in maintenance medium. This could be due to the immortalized state of these cells. Nevertheless, a recent study has reported that MOVAS SMCs express functional SREBP-2/miR-33a, ABCA1, and ABCG1, can transdifferentiate into MLCs, an effect that can be reversed when treated with the cholesterol acceptors apoAI and HDL (Esobi et al., 2021). While myeloid differentiation media promoted Cd68 and MacII protein expression in MOVAS SMCs and flow cytometric analysis revealed increases in Cd68 with ox-LDL and F4/80 with cholesterol and myogenic differentiation media, respectively, the expression of biomarkers of myeloid differentiation into MLCs was sporadic.

While previous studies have demonstrated the ability of mVSCs in general to undergo lineage specification (Tange et al., 2012), this study is one of the first to demonstrate the ability of aortic arch-derived S100β mVSCs to undergo myeloid lineage-specification, particularly in response to ox-LDL. There was a clear change of the morphology of S100β mVSCs following myeloid specification in comparison to their morphology when grown in their maintenance medium, with several cells adopting a more rounded macrophage phenotype. These initial data indicate that these S100β mVSCs may undergo myeloid differentiation. Using Oil Red O staining, the uptake of lipids was examined. While there was no visible uptake of lipids in MOVAS SMCs supplemented with cholesterol, ox-LDL, and myeloid differentiation media, there was clearly visible uptake of lipids in S100β mVSCs supplemented with these myeloid differentiation inductive stimuli, a hallmark of both adipocytes and macrophages (Xu er al., 2010).

Notably, there was no change in the level of myeloid-specific genes *Cd68*, *MacII* and *F4/80* in S100β mVSCs and MOVAS SMCs grown in their maintenance medium supplemented with inductive stimuli for 7 days, when compared to baseline. These genes are highly expressed in J774A-1 macrophages. This lack of transcriptional activity could be due to the duration of the treatment which may not have been the ideal temporal window to measure myeloid-specific gene expression.(Rong et al., 2003) managed to demonstrate an increase in the expression of macrophage-related genes *Cd68, Mac-2,* and *ABCA1* mRNA in mouse SMC supplemented with cholesterol after a 72 hours treatment (Rong et al., 2003). Moreover, these studies were performed on freshly isolated mouse aortic SMCs from thoracic aortas of 8-week-old C57BL/6 mice by using cells with a passage number ≤5. Furthermore, the phenotype of these cells was only confirmed using alpha actin (ACTA2), a non-specific SMC differentiation marker. Previous studies had suggested that the proliferation rate of RFP^- cells gradually outgrew RFP^+ cells in primary cultures of aortic medial cells from *Myh11-Cre/Rosa-loxP-RFP* mice cultured over 2 weeks *in vitro* suggesting that non-SMCs (RFP^- cells), such as S100β/$Sox10^+$ cells may outgrow SMCs (RFP^+ cells) and predominate these cultures when the cholesterol loading is performed. This may account for previous studies demonstrating a trans differentiation of aortic SMCs to MLCs.

The discrepancy between protein and mRNA data can be attributed to two main factors. First, protein degradation can lead to a reduction in protein levels that do not correspond to changes in mRNA levels due to transcriptional activity. This means that even if mRNA levels increase, the corresponding protein might be degraded, preventing its accumulation and thus not reflecting the transcriptional changes. Second, mRNA itself can be unstable and degraded before it is translated into protein. Therefore, an observed increase in mRNA might be misleading, as the mRNA could be degraded before being translated into protein. Similarly, variations in protein levels might not always be a result of translation efficiency but could be influenced by the protein's degradation dynamics. (Belle et al., 2006; Y. Liu et al., 2016; Vogel & Marcotte, 2012).

The correlations between the rates of the processes creating and degrading the participating molecules determine the abundances of proteins and mRNA (Vogel & Marcotte, 2012). Single-cell techniques for measuring mRNA and protein levels have developed significantly in recent years, enabling comprehensive high-throughput investigation of several genes. The results of these tests differ from those of population-wide studies. Bacterial protein and mRNA abundances appear

to be completely uncorrelated, according to a recent large-scale investigation of single Escherichia coli cells (Taniguchi et al., 2010); however, neither the measurements nor their independent verification have been completed. However, mRNA concentrations account for roughly 54–77% of the variation in average protein levels, and the population average of the signals from numerous single-cell observations yields correlations that are equivalent to bulk measurements on cell populations. The different lifetimes of the molecules bacterial mRNAs have a short half-life and are produced in small numbers per cell, which causes their concentrations in single cells to fluctuate significantly more than those of the longer-lived corresponding proteins can be used to explain the lack of correlation between RNA and protein concentration in single cells.

These variations vanish when averaging across populations, and there is a correlation between the amounts of mRNA and protein (Vogel & Marcotte, 2012). The lack of correlation can be attributed in part to translation regulation: although this is not true at the mRNA level, concentrations of proteins within the same complex are less noisy when comparing different classes of genes across yeast cells (Fraser et al., 2004; Gandhi et al., 2011).

Collectively, several previous studies *in vitro* offer a solid foundation for understanding why protein levels might not always correlate with mRNA data, emphasizing the complexities of post-transcriptional and post-translational regulation. (Belle et al., 2006) explained that protein degradation rates can significantly impact protein abundance, causing protein levels to not always reflect changes in mRNA levels. (Vogel & Marcotte, 2012) Highlighted how mRNA stability and degradation play crucial roles in determining protein levels, which can lead to discrepancies between mRNA and protein data. (Y. Liu et al., 2016) discussed how post-transcriptional and translational controls, including mRNA degradation, contribute to the differences observed between mRNA and protein levels.

Moreover, it was evident that the cells morphologically changed their shape, with some cells rounding up as they become more MLCs. While it was not addressed directly in the thesis, this could reflect the level of apoptosis in response to the stimuli, as we used three stimuli (cholesterol, oxLDL, myeloid differentiation media) so it might result in different levels of apoptosis. But the change in shape could reflect a change in cell death, and this could be responsible for some of the discrepancies.

Studies have shown that cholesterol accumulation in macrophages can lead to endoplasmic reticulum (ER) stress, which in turn can trigger apoptosis. This process can form shape changing for the cells and disrupts normal cellular functions , including protein synthesis, folding, and degradation, resulting in a mismatch between mRNA levels and corresponding protein expression (Calaluce et al., 2010; Marcel et al., 2009). Cholesterol has been shown to induce apoptosis and cell rounding through pathways involving reactive oxygen species (ROS) and mitochondrial-mediated processes. Specifically, cholesterol can upregulate apoptosis-related proteins such as cleaved caspase-3 and Bax while downregulating anti-apoptotic proteins like Bcl-xL. This leads to DNA/RNA fragmentation and cell death (K. Li et al., 2020).

Another study has been demonstrated the link between cholesterol-induced cellular stress and cell death when the accumulation of oxidized LDL in cells occurs. This process leads to (ER) stress and apoptosis (Wu et al., 2021).

Several previous studies *in vitro* (Matsumoto et al., 2000; Rong et al., 2003) and *in vivo* (Feil et al.,2014; Allahverdian et al.,2014) highlighted the contribution and trans differentiation of medial SMC to myeloid-like cells. However, data in this chapter suggest that S100β mVSCs are fully capable of differentiation into macrophage-like cells (MLCs) and acquiring the myeloid markers at protein levels. The next chapter will investigate whether a similar profile occurs in human aortic and S100β stem cells.

Chapter 4

The effects of myeloid induction stimuli on myeloid differentiation of human vascular smooth muscle cells (hSMCs) and hiPSC-derived S100β stem cells (SNEPs)

4.1 Introduction:

The appearance of infiltrating macrophage like cells (MLC) and intimal SMC-like cells is considered an important transitional state for non-atherosclerotic plaque that likely represents the earliest phase of lesion progression that is known as adaptive intimal thickening (AIT) ((Velican & Velican, 1981). The source of the MLC and SMC-like cells contributing to AIT is a topic of much controversy. The two major sources that are the focus of this chapter include the de-differentiation of medial SMCs (Chappell et al., 2016) and the partial differentiation of resident S100 calcium-binding protein β (S100β) multipotent vascular stem cell mVSCs (Tang et al., 2012).

The previous chapter of results highlighted the ability of S100β mVSCs to differentiation into myeloid-like cells. The overall outcome of that transition was more compelling than the de-differentiation of MOVAS SMC into myeloid-like cells as S100β mVSCs exhibited macrophage markers, in response to ox-LDL. This could be due to the phenotypic state of MOVAS SMCs which were purchased commercially and are known to be immortalized. However, the question arises as to whether SMCs generated from an hiPSC progenitors respond in a similar manner to the same myeloid induction factors.

Therefore, the major aim of this Chapter was to validate the mouse data from the previous chapter and determine whether hiPSC-derived NE progenitor cells (S100β SNEPs) and hiPSC-derived smooth muscle cells (hSMC) can undergo myeloid differentiation into macrophages like cells (MLCs).

Objectives:

The main aims of this chapter are to:

1. Generate human macrophages from THP-1 monocytes following treatment with PMA and characterise their myeloid phenotype.

2. Generate and characterise hiPSC-derived smooth muscle cells (hSMC) and human hiPSC-derived S100β NE progenitor cells (SNEPs) in culture.
3. Compare the morphology and the uptake of lipids in hSMCs and S100β SNEPs following treatment with myeloid differentiation inductive stimuli (cholesterol, ox-LDL and myeloid differentiation media) *in vitro*.
4. Determine the mRNA levels of macrophage genes (*CD68, MACII* and *EMR1*) in human hSMCs and S100β SNEPs following treatment with myeloid differentiation inductive stimuli (cholesterol, ox-LDL and myeloid differentiation media) *in vitro*.
5. Determine the protein levels of macrophage markers in human hSMCs and S100β SNEPs by flow cytometry following treatment with myeloid differentiation inductive stimuli (cholesterol, ox-LDL and myeloid differentiation media) *in vitro*.

4.2 Methods:

To differentiate THP-1 monocytes into THP-1 macrophages, THP-1 cells were cultured and seeded in a 6-well plate at 5 x 10^3 cells/well at 37°C for 24 h in complete RPMI media. The media was then replaced with media supplemented with PMA1:100 (185nM for 72 hours) and incubated at 37°C. Following 3 d incubation, phase-contrast images of THP-1 pre-and post-treatment were taken to reveal morphological changes following treatments (as described in section 2.2.1.4). Macrophage markers MACll, CD68 were monitored by the ICC to confirm the differentiation of THP-1 cells into macrophages. As we mentioned in the previous result section, CD68 is a well-established marker for macrophages, commonly used to identify and confirm the differentiation of monocyte-derived cells into macrophages (Reinartz et al., 2016). By examining CD68 expression in THP-1 macrophage cells, we can validate that the differentiation process has successfully yielded macrophages (Holness & Simmons, 1993). MacII (galectin-3) is another important marker of macrophages, Examining MacII expression alongside CD68 provides additional validation that THP-1 cells have differentiated into functional macrophages (F.-T. Liu & Rabinovich, 2005). Examining both CD68 and MacII provides robust validation of the THP-1 cells' differentiation status. This dual-marker approach ensures that the observed characteristics are due to macrophage differentiation and not other factors (Jago et al., 2014). before cells were immunophenotyped by flow cytometry using CD68, CD11b, F4/80 to assess myeloid differentiation.

Human hiPSC-derived SNEPs were generated as described in section 2.2.1.3. Human hiPSCs were cultured according to an established protocol. (Figure 4.1A, 4.1B).

In order to generate embryologically defined myogenic (SMC) subtypes, hiPSC-derived S100β SNEPs were cultured in DMEM supplemented with 10% FBS, 1% PS, TGF-β1 (2ng/ml), and PDGF (10ng/ml) for 12 days Following the myogenic differentiation protocol as mentioned in section 2.2.3.1.2 (Figure 4.2A-C).

Characterising hiPSC-derived SNEPs by ICC (Section 2.2.3.2) to examine the calcium-binding protein S100β expression as it known as stem cells marker, to confirm the successful differentiation and identity of these cells (Mi et al., 2009). Investigating CNN1 in S100β hiPSC-derived SNEP helps determine whether these cells possess characteristics beyond stemness differentiation, potentially indicating a mixed lineage or transitional cell states (Benyamin et al., 2012). ICC was also used to investigate the expression of SMC differentiation markers CNN1 in hiPSC-derived smooth muscle cells (hSMC) to confirm that these cells have differentiated correctly into smooth muscle lineage (Owens, 1995). S100β expression was also examined with hSMCs, to determine whether there is any unintended stemness differentiation occurring alongside the intended smooth muscle differentiation. This ensures the purity and specificity of the differentiation protocol used to derive hSMCs from hiPSCs (Takahashi & Yamanaka, 2006). Comparing Lineage Commitment By examining both S100β and CNN1 in hiPSC-derived SNEP and hSMC, we can compare the lineage commitment and differentiation efficiency of the cells. This comparative analysis can reveal insights into the differentiation pathways under different culture conditions (Takahashi & Yamanaka, 2006). Cross-Validation of Differentiation Markers Using both S100β and CNN1 provides a robust validation of the differentiation status of hiPSC-derived cells. S100β ensures the identification of stemness characteristics, while CNN1 confirms smooth muscle identity. This dual marker approach enhances the reliability of experimental results (Murry & Keller, 2008).

In order to investigate the multipotency of human S100β SNEPs and the ability of hSMC to de-differentiate into MLCs, cultured hSMCs and S100β SNEPs were seeded on a 6-well plate at $5x10^3$ cells/well and incubated at 37°C for 24 h. Media was then replaced with E8 media (SNEP

maintenance media) and complete DMEM+TGF-β1 (2ng/ml) and PDGF (10ng/ml) media for hSMC and both media were supplemented with three different stimuli which are cholesterol 10 µg/ml, oxidized low density lipoprotein (ox-LDL) 50 µg/ml and 10 µl/ml of myeloid differentiation media. Cells were incubated at 37°C for 7 d with media replacement every 3-4 days. Following 7 d incubation, phase-contrast images of S100β SNEPs and hSMC pre-and post-treatment were analysed to reveal morphological changes following treatments.

To determine whether S100β SNEPs and/or hSMCs change their phenotype in response to myeloid differentiation inductive stimuli, cultured cells were imaged before and after treatment to compare their morphology prior to harvesting. Oil red O staining was performed as described in Chapter 2 section 2.2.3.4. Oil Red O is a lipid-soluble dye used for staining and up taking lipids in tissue sections and cultured cells. This staining technique is particularly useful for identifying lipid droplets within cells and tissues, providing a visual representation of lipid accumulation (Koopman et al., 2001). The expression level of *CD68* and *Mac II* and *EMR1* genes was measured using quantitative real-time polymerase chain reaction (RT-qPCR) as described in Chapter 2, section 2.2.3.3.1.and 2.2.3.3.2. RT-qPCR is a widely used technique to quantify mRNA levels of specific genes, thereby providing critical insights into gene transcription activity. By measuring mRNA levels, we can infer the expression patterns and activity of particular genes under various conditions. This method is essential for understanding the molecular mechanisms regulating gene expression (Higuchi et al., 1993). Additionally, RT-PCR allows for the comparison of gene expression levels between different cell types (compared hSMCs and S100β SNEPs to THP-1 macrophages).This comparative analysis is vital for identifying differential gene regulation and understanding how gene expression varies across different cellular contexts, which can provide insights into cellular function and disease mechanisms (Raymond et al., 1999). The protein expression levels of MLC markers were determined by immunocytochemistry (ICC) as described in section 2.2.3.2, targeting specific macrophage markers namely CD68 and MACII and by flow cytochemistry as described in section 2.2.3.5. ICC is employed to visualize the presence and localization of specific proteins within cells using labelled antibodies. This technique enables us to see where proteins are situated within the cellular context, which is crucial for understanding their function and interaction with other cellular components (Thelin et al., 2006). In summary, examining THP-1 macrophage cells for MACII and CD68 expression , and hSMCs , S100β

SNEPs for S100β, CNN1 and MACII and CD68 before and after the myeloid stimuli using ICC is crucial for validating cell identity, characterizing functional properties, comparing marker expression under different conditions such as myeloid differentiation , and providing visual confirmation of marker localization. These aspects are fundamental for advancing the understanding of macrophage biology and their roles in various physiological and pathological processes.

Flow cytometry is a powerful technique used to analyze the physical and chemical characteristics of cells, including the expression of specific markers. It provides a quantitative assessment of protein levels across large populations of cells, which is essential for precise measurement and comparison between different cell types (Herzenberg et al., 2006). Flow cytometry also allows for detailed profiling of cell populations by distinguishing different subpopulations based on the expression of surface and intracellular markers. This detailed analysis helps in understanding cellular heterogeneity and the specific characteristics of various cell subsets (Shapiro et al., 2005).

Data for all experiments in this section were generated over at least three biological replicates. Normality tests were used to determine if data followed a parametric distribution pattern. Variation across samples was analysed by calculating p-values. The type of test used to calculate this was governed by the outcome of the normality test. Statistical significance was assigned to p-values <0.05.

4.3 Results

4.3.1 Human hiPSC-derived S100β SNEP and hiPSC-derived smooth muscle cells (hSMC) morphology and express key phenotypic markers.

HiPSC-derived SNEPs were generated (as described in section 2.2.1.3.1) before phase-contrast microscopy was performed to monitor the migration of peripheral HiPSC cells and the loss of distinct colony borders (Figure 4.1 A). Expansion of SNEPs was achieved by day 10 (Figure 4.1 B). SNEPs generated from HiPSCs were cultured in Essential 8™ complete medium. Images generated from (Burtenshaw, 2020).
HiPSC-derived smooth muscle cells (hSMC) were generated (as described in section 2.2.1.3.2) before phase-contrast microscopy was performed, Cell culture plates were gently tapped to ensure that all cells had been dissociated into single cells (Figure 4.2 A). images were taken to monitor the morphology changing (Figure 4.2 B), differentiation from SNEPs to spindle-shaped hSMC achieved after 12 days of cultured in DMEM+TGF-β1 and PDGF supplemented media (figure 4.2 C).

The expression of NE marker S100β for SNEP and SMC differentiation marker CNN1 for hSMC were determined by ICC, as described in Chapter 2, section 2.2.3.2.

The expression of NE marker S100β was positively detected in SNEPs (Figure 4.1C) but cells were negative for the expression of smooth muscle cell marker CNN1 (Figure 4.1D). Positive expression of CNN1 detected in hSMC (Figure 4.2D) and no expreission detection of NE marker S100β (Figure 4.2E).

Collectively, the ICC data on S100β SNEP and hSMCs indicated that these cells exhibit the expected expression of specific phenotypic markers for NE progenitors (S100β) and SMC markers (CNN1), respectively *in vitro.*

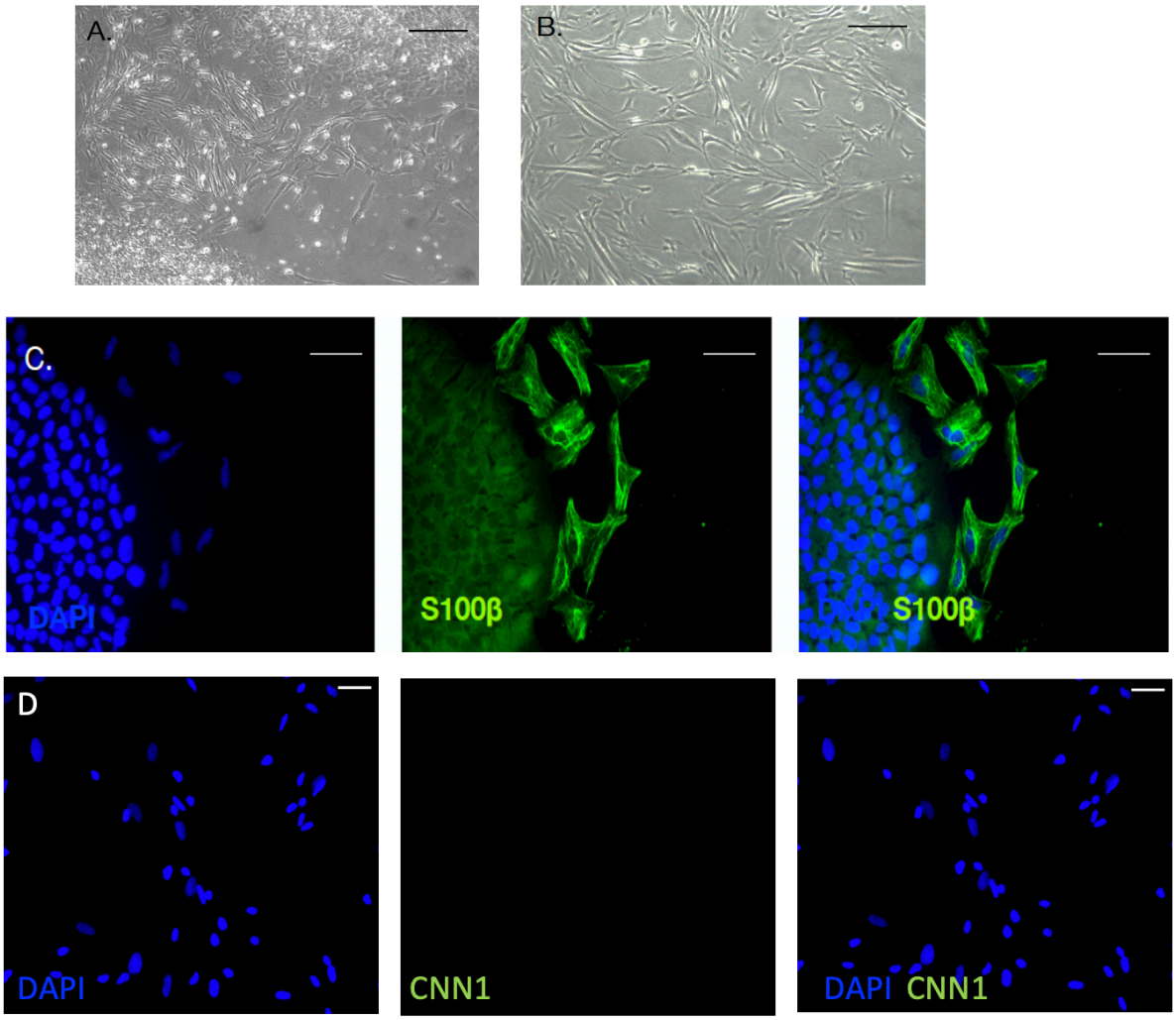

Figure 4.1 Characterisation of hiPSC-derived SNEPs by ICC. (A+B) Representative phase-contrast images following induction of NE differentiation after 7 d. Images A+B at x10, x20 magnification, Scale bar representative of 20µm and 50µm respectively. (C+D) Representative images of fluorescence staining of DAPI nuclei and immunocytochemical analysis of NE marker S100β (C) to confirm their stem cell phenotype and analysis of smooth muscle cell marker CNN1 (D). All images were taken using Olympus DP-50 fluorescent microscope, images C, D at x20 magnification. Alexa Fluor 488 secondary antibody used for visualisation of primary antibody binding. All images are representative of n >6 images per experimental group from three independent cultures—scale bar representative of 50µm.

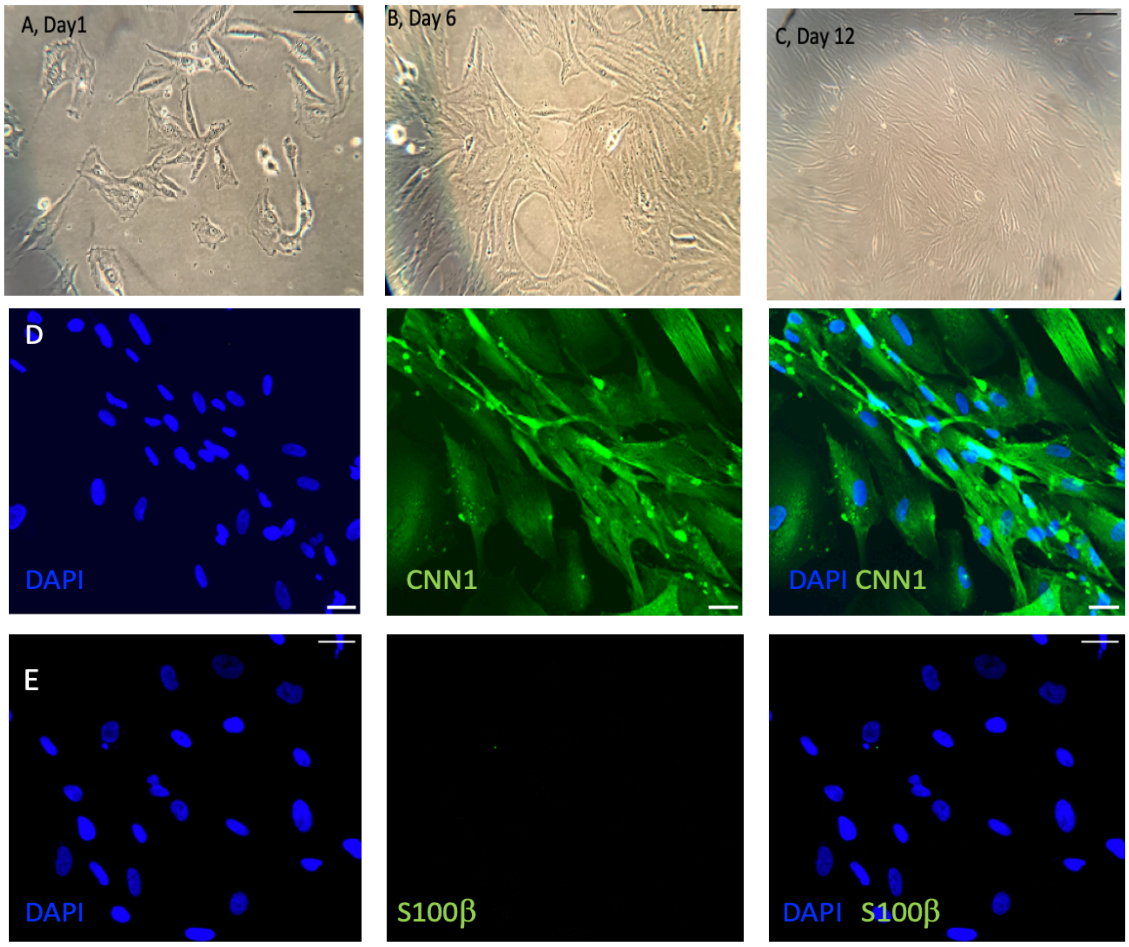

Figure 4.2 Characterisation of hiPSC-derived smooth muscle cells (hSMC) by ICC. (A, B &C) Representative phase-contrast images of S100β SNEPs A+B at x60 magnification and C at x20 magnification, Scale bar representative of 20µm for (A+B) and 50µm for (C). Cells were treated with PDGF-BB, 10 ng/ml and TGF-β1, 2 ng/ml in DMEM for 12 days. Media supplemented with PDGF-BB, TGF-β1 was replaced every 3 days. (D+E) Representative images of fluorescence staining of DAPI nuclei and immunocytochemical analysis of smooth muscle cell marker CNN1(D), And analysis of the expression of S100β (E). All images were taken using Olympus DP-50 fluorescent microscope, images (D+E) at x60 magnification. Alexa Fluor 488 secondary antibody used for visualization of primary antibody binding. Scale bar representative of 20µm for (A+D+E) and 50µm for (B+C). All images are representative of n >5 images per experimental group from three independent cultures.

4.3.2 THP-1 macrophages express key myeloid phenotypic markers.

Cultured THP-1 monocytes were treated with 185 ng/mL PMA to drive myeloid differentiation of these cells into macrophages *in vitro* (Tsuchiya et al., 1982). THP-1 cells are a leukemic cell line derived from a patient with acute monocytic leukemia and are routinely used as a model for monocyte-macrophage differentiation in numerous studies(Tsuchiya et al., 1982). In general, THP-1 cells exhibit a large, round, single-cell morphology and are routinely grown in suspension(Tsuchiya et al., 1982). PMA is one of the most common reagents used to induce THP-1 differentiation into macrophage-like cells (Meijer et al., 2015). PMA treatment induced a significant change in the morphology of these cells whereby the cultures became heterogeneous, adherent with a high number of big cells, increased density, and a notable cell elongation (Meijer et al., 2015) (Figure 4.3 B and D). There was little Oil Red O lipid uptake in cultured THP-1 monocytes (Figure 4.3C), whereas THP-1-derived macrophages stained positively for Oil Red O following PMA treatment (Figure 4.3D).

In parallel cultures, THP-1 cells were immunophenotyped before and after PMA treatment. ICC was carried out (as described in Chapter 2, section 2.2.3.2) on a population of THP-1 monocytes and PMA-induced macrophages to confirm the presence of macrophage markers MacII and CD68 in these cells. THP-1 monocytes were sparsely positive for CD68 and MACII, respectively when compared to PMA induced THP-1 macrophages, which were clearly positive for the macrophage protein markers (Figure 4.4).

Collectively, the ICC data on PMA-induced THP-1 macrophages indicated that these cells exhibit the expected expression of myeloid macrophage-specific phenotypic markers *in vitro.* In addition, the histochemical Oil Red O staining data showed the ability for THP-1 macrophages to take up lipids. This cell line will be used as a positive control.

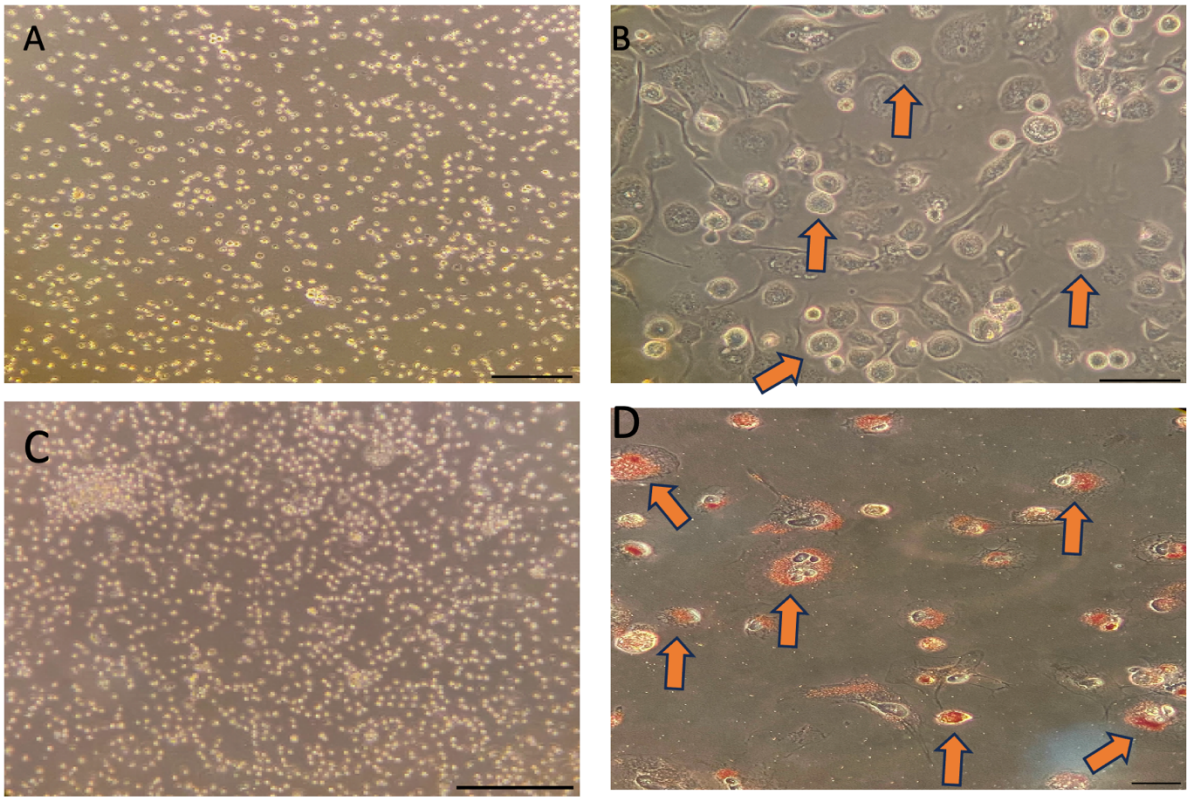

Figure 4.3 Morphological changes and Oil Red O lipid uptake in THP-1 monocytes before and after PMA induced myeloid differentiation. Representative phase-contrast images following myeloid differentiation of THP-1 cells before and after 72 hours treatment with 185 ng/mL PMA. (A) Undifferentiated THP-1 cells in culture. At x20, Scale bar = 50 µm. (B) Differentiated THP-1 macrophages following PMA treatment (changing in morphology rounded and bigger, pointed with yellow arrows). At x60 and Scale bar = 15 µm. (C+D) Representative images of Oil Red O lipid uptake in THP-1 monocytes before and after treatment with PMA (pointed with arrows). Magnification at x20 and x60, scale bar 50 µm and 20 µm respectively.

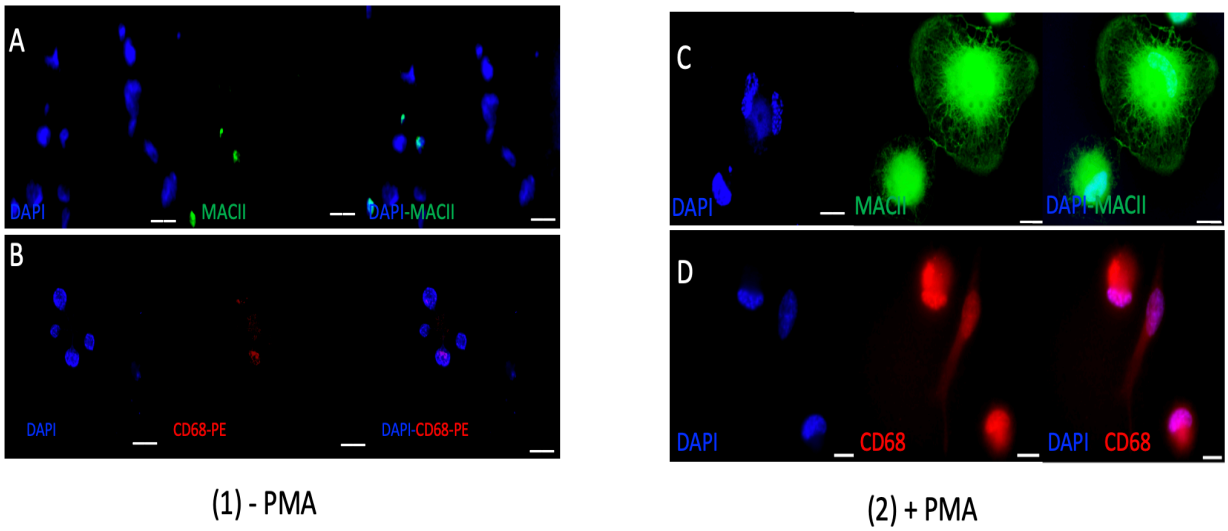

Figure 4.4 Phenotypic changes in THP-1 monocytes before and after PMA-induced myeloid differentiation by ICC. Representative images of fluorescent staining of DAPI nuclei and immunocytochemical Analysis of the expression of macrophage markers MACII (green) (A+C) and CD68-PE (red) (B+D) in THP-1. (1) THP-1 monocyte (no PMA), (2) Cells were treated with PMA1:100 (185nM), for three days. all images are taken with Olympus DP-50 fluorescence microscope, images at x60 magnification. CD68-PE conjugate and Alexa Fluor 488 secondary antibody used with MACII for Visualization of primary antibody binding. All images are representative of n > 5 images Per experimental group from 3 independent cultures - scale bar representative of 50 µm for (A+B) and 20 µm for (C+D).

4.3.3 Morphological changes and lipid uptake of hiPSC-derived smooth muscle cells (hSMC) and hiPSC-derived NE progenitor cells (S100β SNEPs) following treatment with myeloid differentiation inductive stimuli.

Cultured hSMCs and S100β SNEPs as described in "strategy" section 4.2. Oil red O staining was performed as described in chapter 2 section 2.2.3.4.

There was no significant change in the morphology of hSMCs grown in media supplemented with myeloid inductive stimuli as the cells did not transition from elongated cells displaying a 'hill and valley' phenotype, typical of SMCs, to a more rounded phenotype, typical of macrophages. (Figure 4.5 (1) B, C and D). Similarly, there was no notable change in the morphology of S100β SNEPs when treated with cholesterol 10 μg/ml (Figure 4.6B panel 1), but there is a notable change in the morphology when S100β SNEP when treated with oxidise low density lipoprotein (ox-LDL) 50 μg/ml and 10 μl/ml of myeloid differentiation media (Figure 4.6C and D panel 1).

While there was no significant change in morphology of hSMCs grown in media supplemented with myeloid inductive stimuli (cholesterol, ox-LDL and myeloid differentiation media), there was some uptake of lipid when treated with cholesterol and ox-LDL (Figure 4.5 (2) F and G) but not myeloid differentiation media (Figure 4.5 (2) H) when stained with Oil Red O. In contrast, when S100β SNEPs were grown in media supplemented with myeloid inductive stimuli, a significant number of cells stained positively for Oil Red O following each treatment (Figure 4.6 F, G and H panel 2).

Collectively, there were no significant changes in morphology for both hSMCs and S100β SNEPs. But Staining with Oil red O, lipid uptake was detected in hSMCs that only treated with cholesterol and ox-LDL, while majority of S100β SNEPs cells were highly took up lipids following the three treatments of myeloid inductive stimuli.

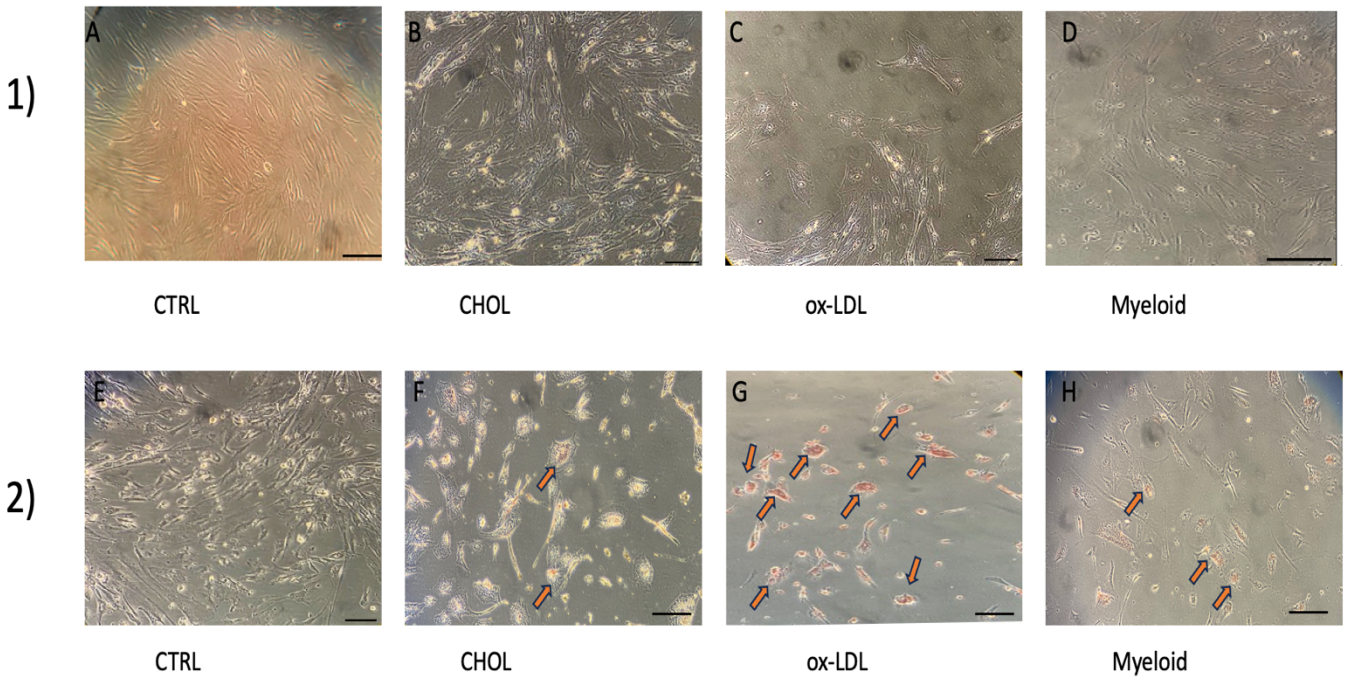

Figure 4.5 Lipid uptake in hSMCs before and after treatment with myeloid inductive stimuli. Representative phase-contrast images of Oil Red O staining of lipid uptake in hiPSC-derived hSMCs before and after treatment with cholesterol, ox-LDL and myeloid differentiation media. Panel (1) for morphology changing and panel (2) for Lipid uptake. A hSMC control, B, C and D cells grown in three types of supplemented differentiation medium, E hSMC control, F, G and H cells grown in three types of supplemented differentiation medium media respectively after day 7. Images at x20 magnification. All images are representative of n >5 images per experimental group from three independent cultures—scale bar representative of 50µm. Arrows are representative of positive cells.

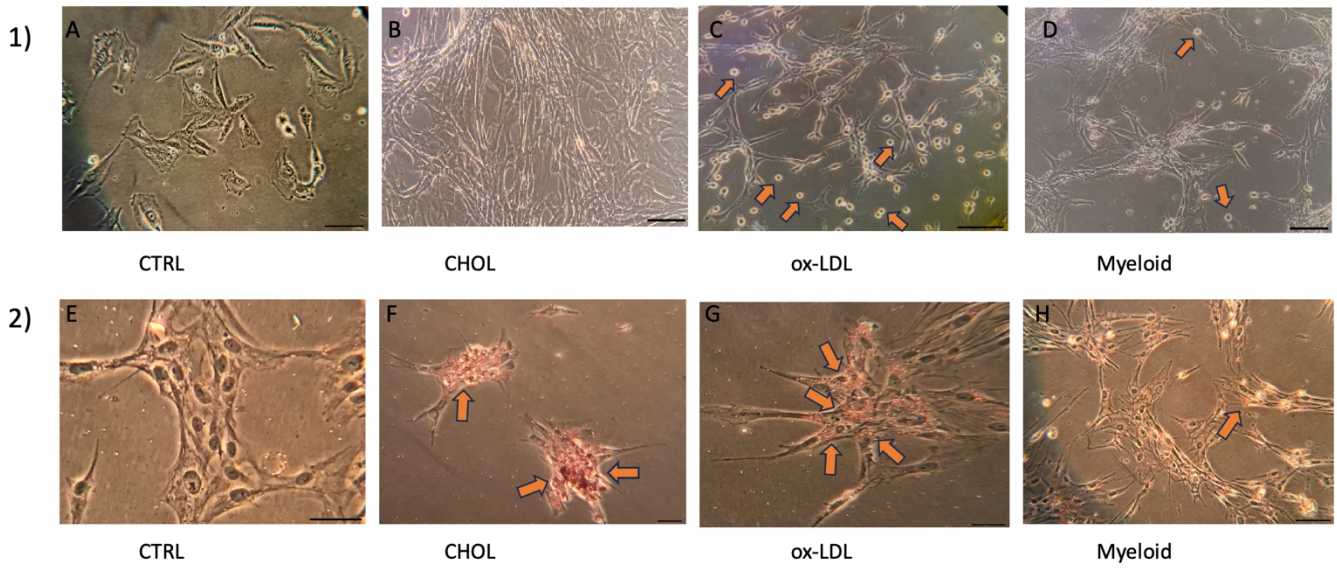

Figure 4.6 Lipid uptake in S100β SNEPS before and after treatment with myeloid inductive stimuli. Representative phase-contrast images of Oil Red O staining of lipid uptake in control hiPSC derived S100β SNEPs and following treatment with cholesterol, ox-LDL and myeloid differentiation media. Panel (1) for morphology changes and panel (2) for lipid uptake. A-D S100β SNEP control cells and S100β SNEP cells treated with three myeloid inductive stimuli respectively. (E-H) S100β SNEP control cells and S100β SNEPs grown in three types of supplemented differentiation medium respectively, all images were taken after day 7 of treatment. (B, C, D and H) at x20 magnification and (A, E, F and G) at x60 magnification. Images are representative of n >5 images per experimental group from three independent cultures—scale bar representative of 50µm (B, C, D and H) and 25 µm (A, E, F and G). arrows in panel (1) are representative of morphology changes and arrows in panel (2) are representative of positive cells.

4.3.4 The mRNA expression levels of myeloid genes (CD68, MacII and EMR1) in hiPSC-derived smooth muscle cells (hSMC) and hiPSC-derived NE progenitor cells (S100β SNEPs) in response to myeloid differentiation inductive stimuli *in vitro*.

Cultured hSMCs and S100β SNEPs as described in "strategy" section 4.2. The expression level of *CD68, MACII* and *EMR1* genes were measured using RT-qPCR as described in Chapter 2, section 2.2.3.3.1.and 2.2.3.3.2.

The expression level of key myeloid genes (*CD68, MACII* and *EMR1)* were significantly higher in THP-1 macrophages, when compared to hSMCs at baseline (Figure 4.7 A). There was a slight increase in the expression level of *CD68* gene in cells treated with myeloid differentiation media, when compared to cells at baseline (Figure 4.7A). While there was a tendency for increased expression levels of *CD68* and *MACII* genes in hSMC treated with ox-LDL and myeloid differentiation media compared to cells at baseline, it did not reach the level of significance (Figure 4.7A). There was no change in the expression level of *EMR1* gene in hSMCs treated with cholesterol, ox-LDL and myeloid differentiation media, when compared to hSMCs at baseline (Figure 4.7 A).

The expression level of key myeloid genes (*CD68, MAC II* and *EMR1*) were significantly higher in THP-1 macrophages, when compared to S100β SNEPs at baseline (Figure 4.7 B). There was an increase in the expression level *CD68* gene in cells treated with myeloid differentiation media compared to cells at baseline (Figure 4.7 B). While there was a tendency for increased expression levels of *CD68* gene in S100β SNEPs treated with ox-LDL and cholesterol, it did not reach the level of significance. There was a slight increase in the expression level of *MAC II* gene in cells treated with cholesterol and ox-LDL compared to cells at baseline (Figure 4.7 B). While there was a tendency for increased expression levels of *MAC II* gene in S100β SNEPs treated with myeloid differentiation media it did not reach the level of significance. (Figure 4.7.B). There was a decrease in the expression level of key myeloid gene *EMR1* when S100β SNEPs were treated with myeloid differentiation media and cholesterol compared to cells at baseline, it did not reach the level of significance (Figure 4.7 B).

A comparison between the expression of *CD68* in hSMCs and S100β SNEPs revealed a significantly higher level in S100β SNEPs treated with myeloid differentiation media compared to hSMCs (Figure 4.8). The expression level of the key myeloid genes *MAC II* and *EMR1* was higher

in S100β SNEPs treated with ox-LDL. While there was a tendency for increased expression levels of *CD68, Mac II* and *EMR1* genes in S100β SNEPs treated with cholesterol when compared to hSMCs, it did not reach the level of significance.

Collectively, the expression level of key myeloid genes (*CD68, Mac II* and *EMR1*) in S100β SNEPs treated with cholesterol 10 μg/ml, oxidized low density lipoprotein (ox-LDL) 50 μg/ml and 10 μl/ml myeloid differentiation media for 7 days showed a greater capacity for myeloid differentiation of cells towards macrophages when compared to hSMCs.

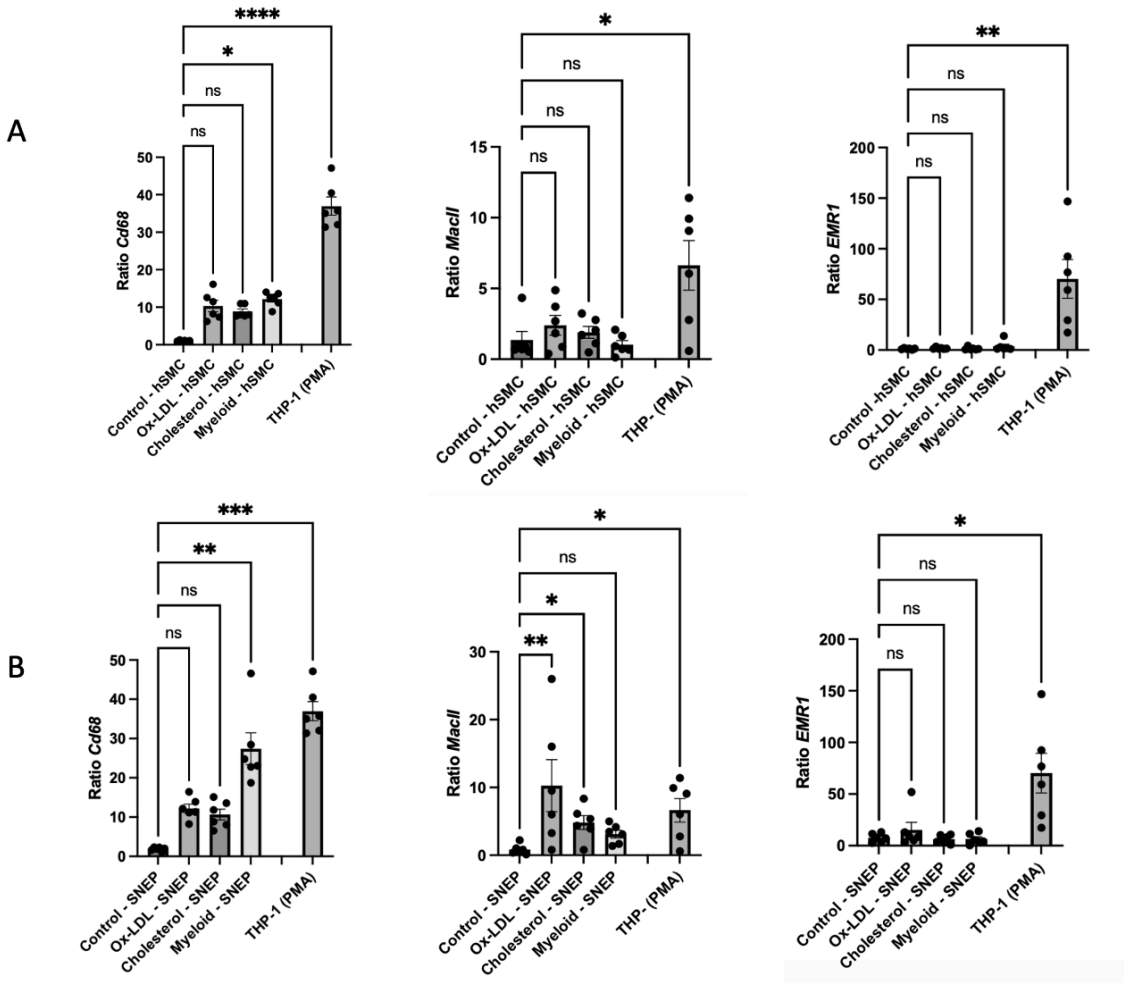

Figure 4.7 The expression of myeloid genes *CD68, MACII* and *EMR1* in (A) hSMCs and (B) S100β SNEPs before and after treatment with myeloid inductive stimuli. *CD68, MacII* and *EMR1* mRNA levels were measured in hSMCs and SNEP after 7 days treatment and compared to levels in THP-1 macrophages. Total RNA was isolated from cells and measured by realtime RT-qPCR with *GAPDH* as an internal control. Data are expressed as the ratio of gene expression (R) and represent the mean SEM of 2 experiments performed in triplicate. * $p<0.05$ *** $p<0.001$ **** $p<0.0001$ **** $p<0.0001$ vs Control

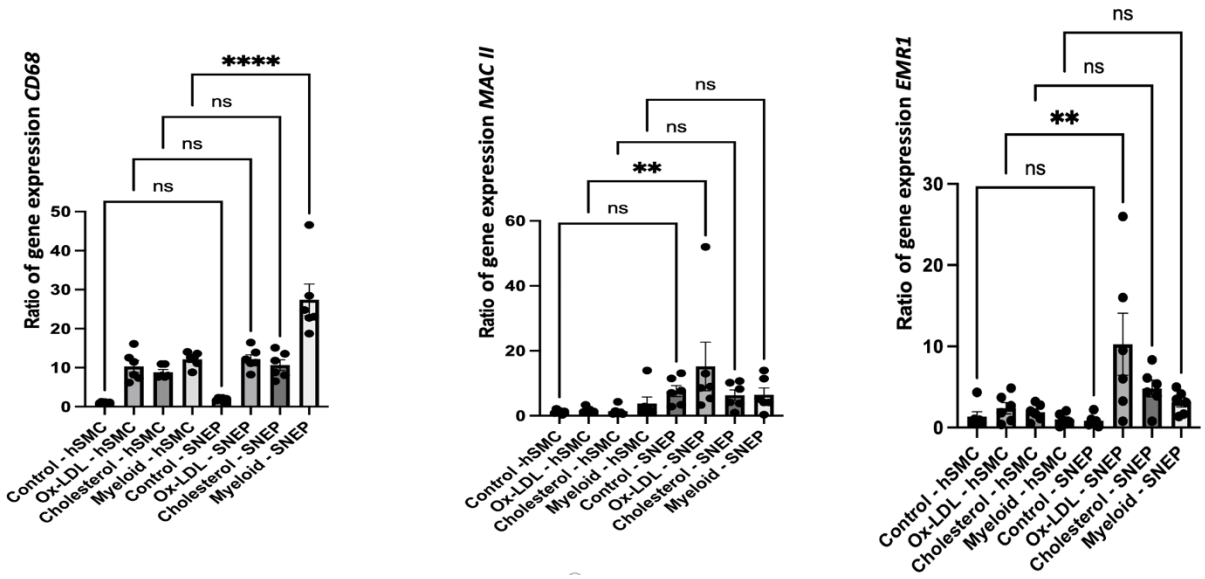

Figure 4.8 Comparison of the expression of myeloid genes (A)*CD68, (B) MACII* and (C) *EMR1* between hSMCs and S100β SNEPs before and after treatment with myeloid inductive stimuli. *CD68, MACII* and *EMR1* mRNA levels were measured in hSMCs and S100β SNEPs after 7 days treatment, Total RNA was isolated from cells and measured by realtime RT-qPCR with *GAPDH* as an internal control. Data are expressed as the ratio of gene expression (R) and represent the mean SEM of 2 experiments performed in triplicate. * $p<0.05$ *** $p<0.001$ **** $p<0.0001$ **** $p<0.0001$ vs Control.

4.3.5 The protein expression levels of myeloid markers (CD68, MACII and F4/80)) in hiPSC-derived smooth muscle cells (hSMC) and hiPSC-derived NE progenitor cells (S100β SNEPs) in response to myeloid differentiation inductive stimuli *in vitro*

Cultured hSMCs and S100β SNEPs were seeded on a 6-well plate at 5 x 10^3 cells/well and incubated at 37°C for 24 h. Media was then replaced with E8 (SNEP cell maintenance media) and complete DMEM (supplemented with TGF-β1 (2ng/ml) and PDGF (10ng/ml) media for hSMCs, both supplemented with three different myeloid inductive stimuli (cholesterol 10 µg/ml, oxidized low density lipoprotein (ox-LDL) 50 µg/ml and 10 µl/ml of myeloid differentiation media). Cells were incubated at 37°C for 7 d with media replacement every 3-4 days. Myeloid markers were detected in cells by either immunocytochemical analysis (ICC) or immunophenotyping using flow cytometry.

ICC was carried out to confirm the presence of macrophage protein markers, MACII and CD68 as described in section 2.2.3.2.

ICC analysis revealed that THP-1 macrophages were predominantly positive for MACII as a control (Figure 4.9E, 4.9F and 4.11E ,4.11F). MACII was primarily expressed on the cell membrane of these treated cells. In contrast, hSMCs did not express MACII at baseline (Figure 4.9 A). There was a significant increase in the number of MACII positive cells in hSMCs following treatment of cells with media supplemented with cholesterol and ox-LDL, but not myeloid differentiation media, when compared to the control cells at baseline (Figure 4.9 B-C and F).

In a similar fashion, ICC analysis revealed that THP-1 macrophages were also predominantly positive for CD68 (Figure 4.10E, F and 4.12E, F). There was a significant increase in the number of CD68 positive cells when supplemented with cholesterol and ox-LDL but not with myeloid differentiation media, when compared to the control cells at baseline (Figure 4.10 B, C, D & F).

In parallel, ICC analysis revealed a significant increase in the number of MACII and CD68 positive cells in S100β SNEPs following treatment of cells with media supplemented with all three myeloid differentiation inductive stimuli (cholesterol, ox-LDL and myeloid differentiation media)(Figure 4.11B,C,D and 4.12B,C,D) when compared to the control cells at baseline (Figure 4.11A and

Figure 4.12A). The fraction of cells expressing MACII and CD68 were as high as 90% and 94%, respectively, (Figure 4.11 F and Figure 4.12 F).

A comparison of the data between hSMCs and S100β SNEPs suggested that cholesterol, ox-LDL and myeloid differentiation media promoted myeloid differentiation of S100β SNEPs into macrophage-like cells to a greater extent after 7-day treatment.

Collectively, S100β SNEPs have a higher fraction rate (over 90%) of cells expressing MACII and CD68 when compared to hSMCs (Figure 4.13).

Myeloid markers CD68, CD11b and F4/80 were also detected in cells by immunophenotyping using flow cytometry. Flow cytometric analysis of expression in THP-1 macrophages was used as a positive control for human macrophages. The level of CD68, CD11b and F4/80 was significantly higher in THP-1 macrophages when compared to both hSMCs and hiPSC derived S100β SNEPs at baseline *in vitro* (Figure 4.14).

The level of CD68, CD11b and F4/80 was significantly higher in THP-1 macrophages compared to treated and untreated hSMCs (Figure 4.15-17). There was a significant increase in the expression levels of CD68 in cells treated with cholesterol and myeloid differentiation media compared to cells at baseline (Figure 4.15 B). In contrast, the level of expression of CD68 in cells treated with ox-LDL did not change significantly (Figure 4.15B). There was no significant change in the expression of CD11b (Figure 4.16 B) or F4/80 (Figure 4.17 B) in cells treated with cholesterol, ox-LDL or myeloid differentiation media compared to cells at baseline when compared to cells at baseline.

The level of CD68, CD11b and F4/80 was also significantly higher in THP-1 macrophages compared to treated and untreated S100β SNEPs at baseline *in vitro* (Figure 4.18 B, 4.19 B, 34.20 B).

Flow cytometric analysis of S100β SNEPs revealed that there was a significant increase in the expression of CD68 in cells treated with cholesterol, ox-LDL and myeloid differentiation media when compared to cells at baseline (Figure 4.18 A, B). There was also a significant increase in the expression of CD11b in cells treated with cholesterol and ox-LDL, but not myeloid differentiation media, when compared to cells at baseline ((Figure 4.19 A, B). There was a significant increase in

the expression of F4/80 in cells treated with cholesterol, ox-LDL but not with myeloid differentiation media (Figure 4.20 A, B).

Collectively, cholesterol and ox-LDL treatment were the most efficient at increasing the expression of all three myeloid markers in SNEPs whereas cholesterol and myeloid differentiation media only promoted CD68 expression in hSMCs.

A comparison of the data between hSMCs and S100β SNEPs suggested that cholesterol, ox-LDL and myeloid differentiation media promoted myeloid differentiation of S100β SNEPs into macrophage-like cells to a greater extent after 7-day treatment (Figure 4.21).

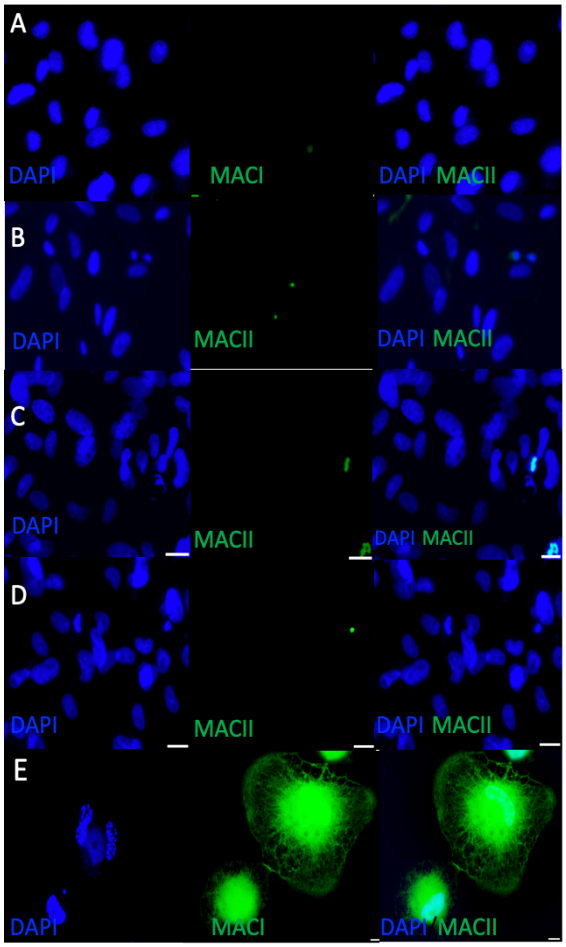

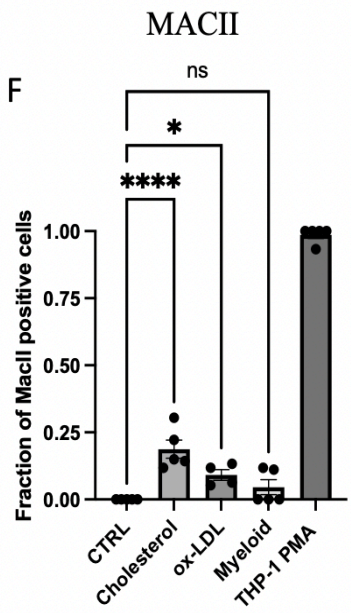

Figure 4.9. Characterization of hiPSC-derived hSMCs transition into macrophage-like cells before and after treatment with myeloid inductive stimuli. Representative images of fluorescent staining of DAPI nuclei and immunocytochemical analysis of the expression of macrophage markers MACII (green) in hSMC. (A) hSMC control, (B - D) hSMC cells treated with cholesterol, oxidized low-density lipoprotein (ox-LDL) and myeloid differentiation medium respectively, compared to THP-1 PMA(E). (F) Percentage of MACII positive cells. All images are taken with Olympus DP-50 fluorescence microscope, images (A+B) at x20 magnification but were cropped to match other images, and (C, D and E) images at x60 magnification. Alexa Fluor 488 secondary antibody used with MACII for visualization of primary antibody binding. All images are representative of n > 5 images per experimental group from 3 independent cultures - scale bar representative 50 µm (A, B), 20 µm (C, D and E). Data are ± SEM * $p<0.05$ *** $p<0.001$ **** $p<0.0001$ **** $p<0.0001$ vs CTRL.

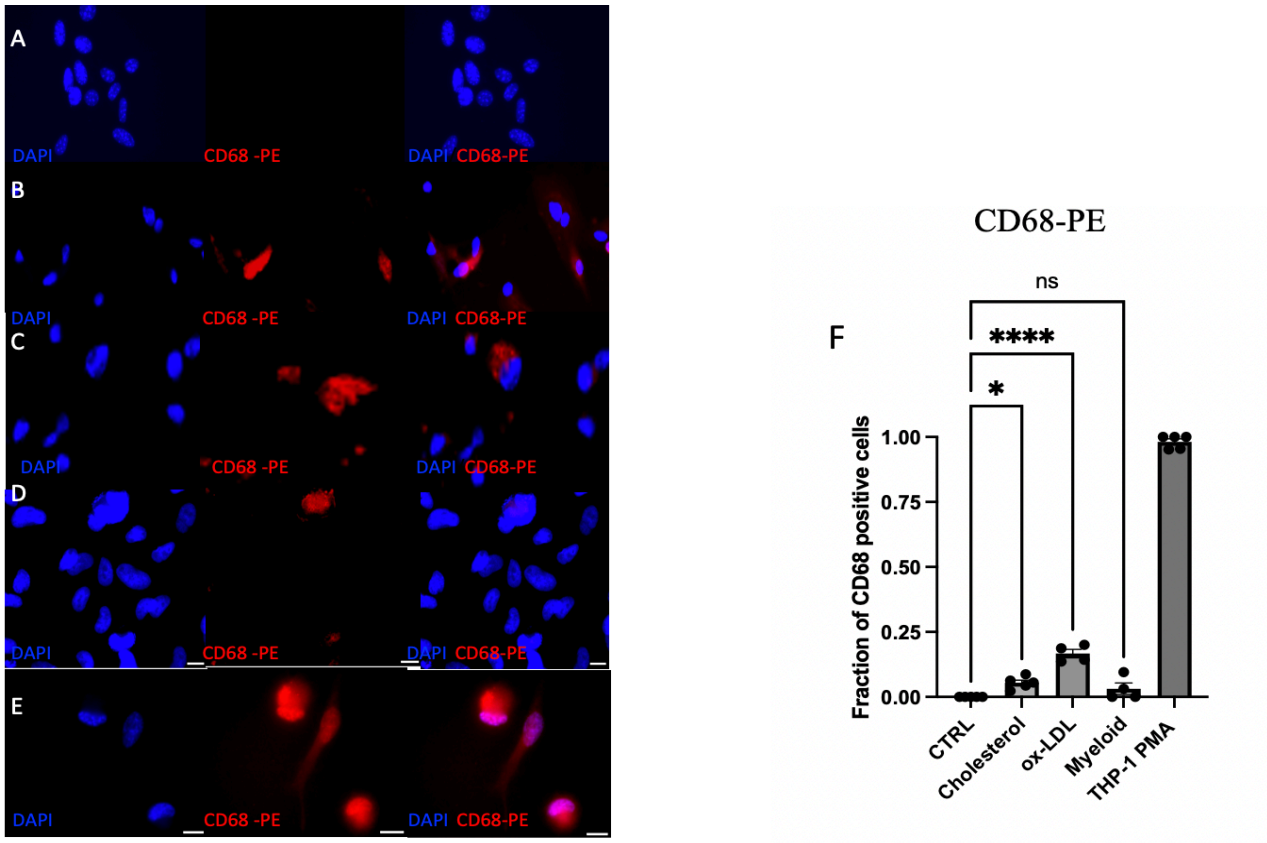

Figure 4.10. Characterization of hiPSC-derived hSMC transition into macrophage-like cells before and after treatment with myeloid inductive stimuli. Representative images of fluorescent staining of DAPI nuclei and immunocytochemical analysis of the expression of macrophage markers CD68 (red) in hSMC. (A) hSMC control, (B-D) hSMC cells treated with cholesterol, oxidized low-density lipoprotein (ox-LDL) and myeloid differentiation medium respectively, compared to THP-1 PMA(E). (F) Percentage of CD68 positive cells. All images are taken with Olympus DP-50 fluorescence microscope, images (A+B+C) at x20 magnification but were cropped to match other images, and (D+E) images at x60 magnification. All images are representative of n > 5 images per experimental group from 3 independent cultures - scale bar representative 50 µm (A, B, C), 20 µm (D+E). Data are ± SEM * $p<0.05$ *** $p<0.001$ **** $p<0.0001$ **** $p<0.0001$ vs CTRL.

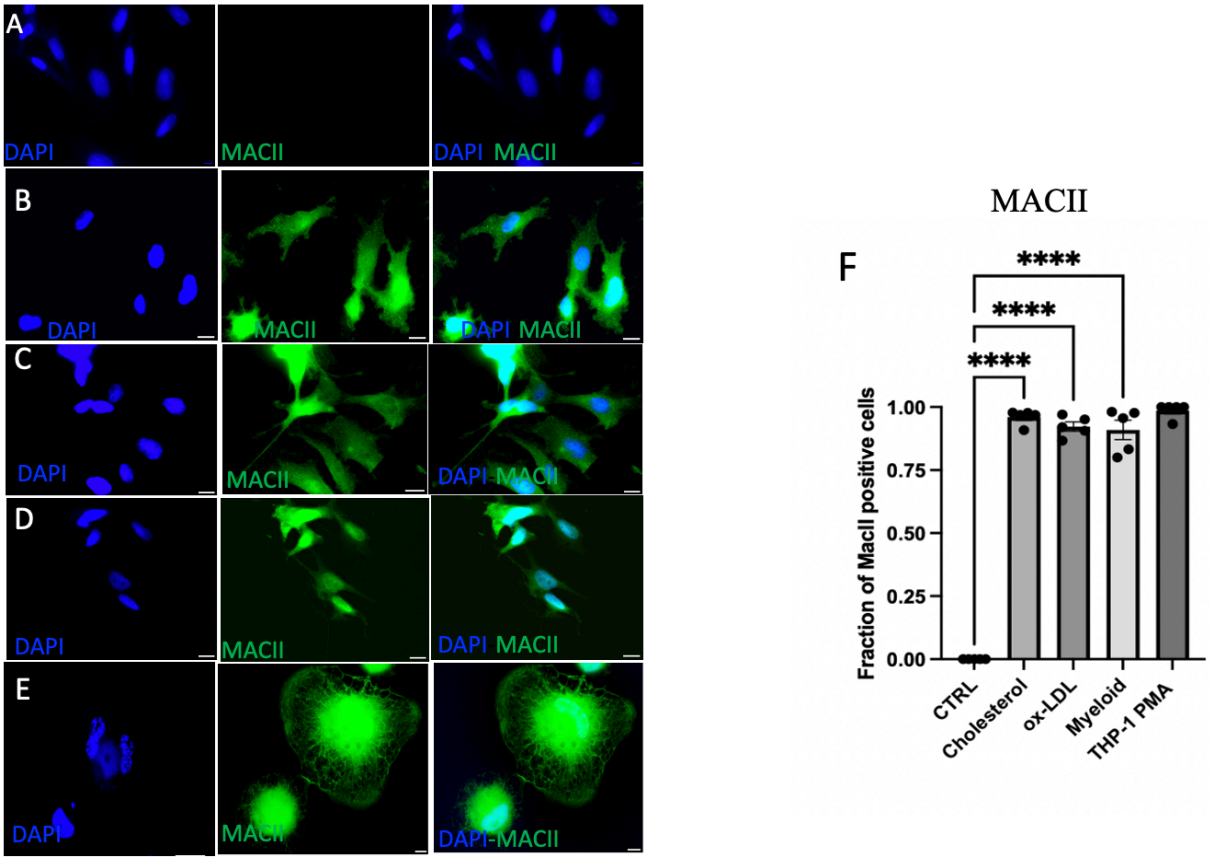

Figure 4.11. Characterization of hiPSC-derived S100β SNEP transition into macrophage-like cells before and after treatment with myeloid inductive stimuli. Representative images of fluorescent staining of DAPI nuclei and immunocytochemical analysis of the expression of macrophage markers MACII (green) in S100β SNEPs. (A) S100β SNEP control, (B-D) hSMC cells treated with cholesterol, oxidized low-density lipoprotein (ox-LDL) and myeloid differentiation medium respectively, compared to THP-1 PMA(E). (F) Percentage of MACII positive cells. All images are taken with Olympus DP-50 fluorescence microscope, image (A) at x20 magnification but were cropped to match other images, and (B+C+D+E) images at x60 magnification. Alexa Fluor 488 secondary antibody used with MACII for visualization of primary antibody binding. All images are representative of n > 5 images per experimental group from 3 independent cultures - scale bar representative of 50 µm for A, 25 µm for B, C, D and 20 µm for E. Data are ± SEM * $p<0.05$ *** $p<0.001$ **** $p<0.0001$ **** $p<0.0001$ vs CTRL.

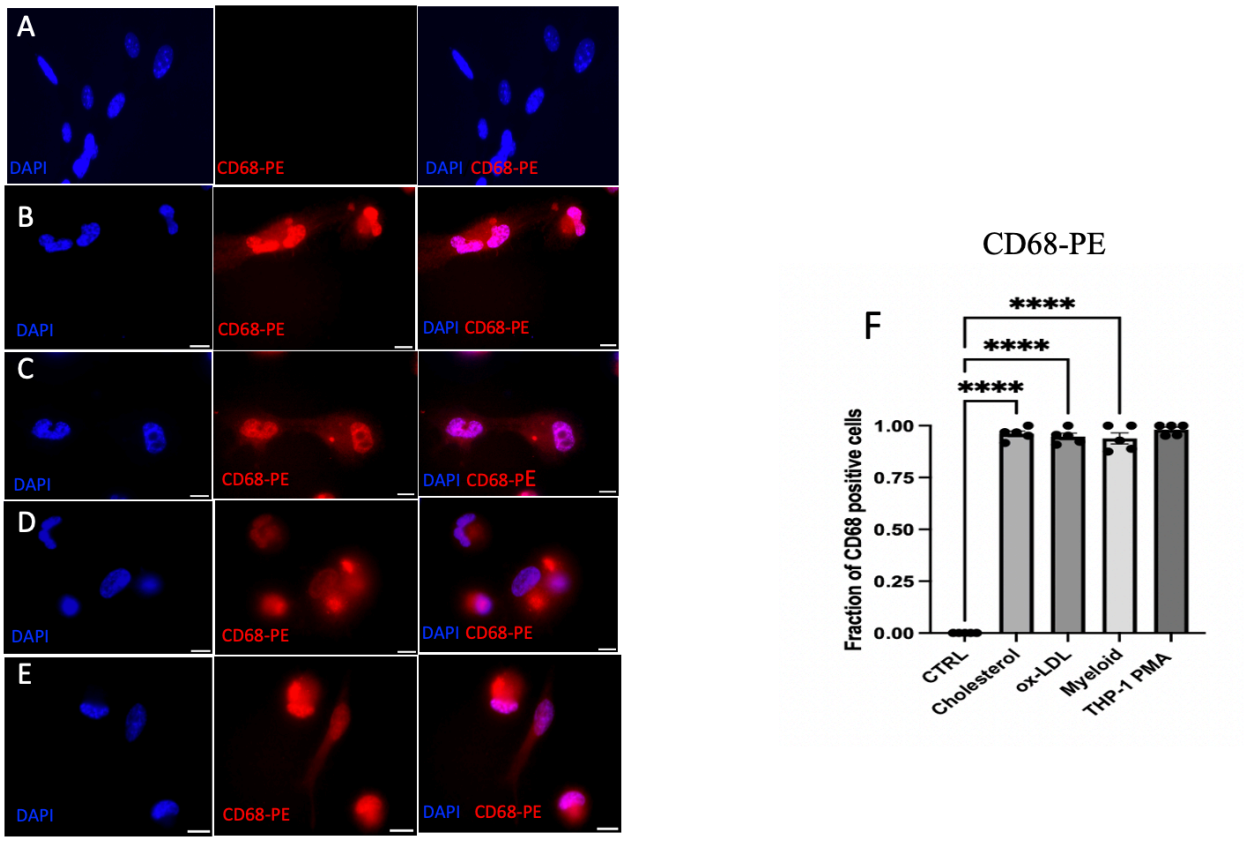

Figure 4.12 Characterization of hiPSC-derived S100β SNEP transition into macrophage-like cells before and after treatment with myeloid inductive stimuli. Representative images of fluorescent staining of DAPI nuclei and immunocytochemical analysis of the expression of macrophage markers CD68 (red) in S100β SNEPs. (A) S100β SNEP control, (B-D) cells treated with cholesterol, oxidized low-density lipoprotein (ox-LDL) and myeloid differentiation medium respectively, compared to THP-1 PMA(E). (F) Percentage of CD68 positive cells. All images are taken with Olympus DP-50 fluorescence microscope, image (A) at x20 magnification but were cropped to match other images, and (B+C+D+E) images at x60 magnification. All images are representative of n > 5 images per experimental group from 3 independent cultures - scale bar representative 50 µm(A), 20 µm for (B- E). Data are ± SEM * p<0.05 *** p<0.001 **** p<0.0001 **** p<0.0001 **** p<0.0001 vs CTRL.

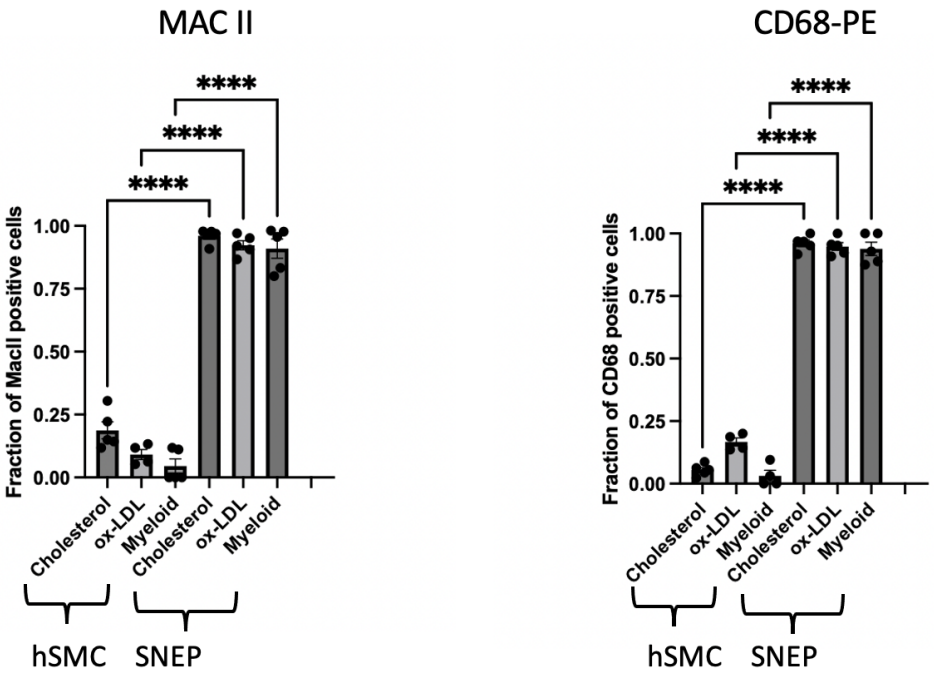

Figure 4.13 Comparison of the number of MACII and CD68 positive cells between hSMC and SNEP before and after treatment with myeloid inductive stimuli. Cells were treated with cholesterol, oxidized low-density lipoprotein (ox-LDL) and myeloid differentiation medium respectively before the percentage of CD68 and MACII positive cells were evaluated. All images are taken with Olympus DP-50 fluorescence microscope. All images are representative of n > 5 images per experimental group from 3 independent cultures. Data are the mean Data are ± SEM * $p<0.05$ *** $p<0.001$ **** $p<0.0001$ **** $p<0.0001$.

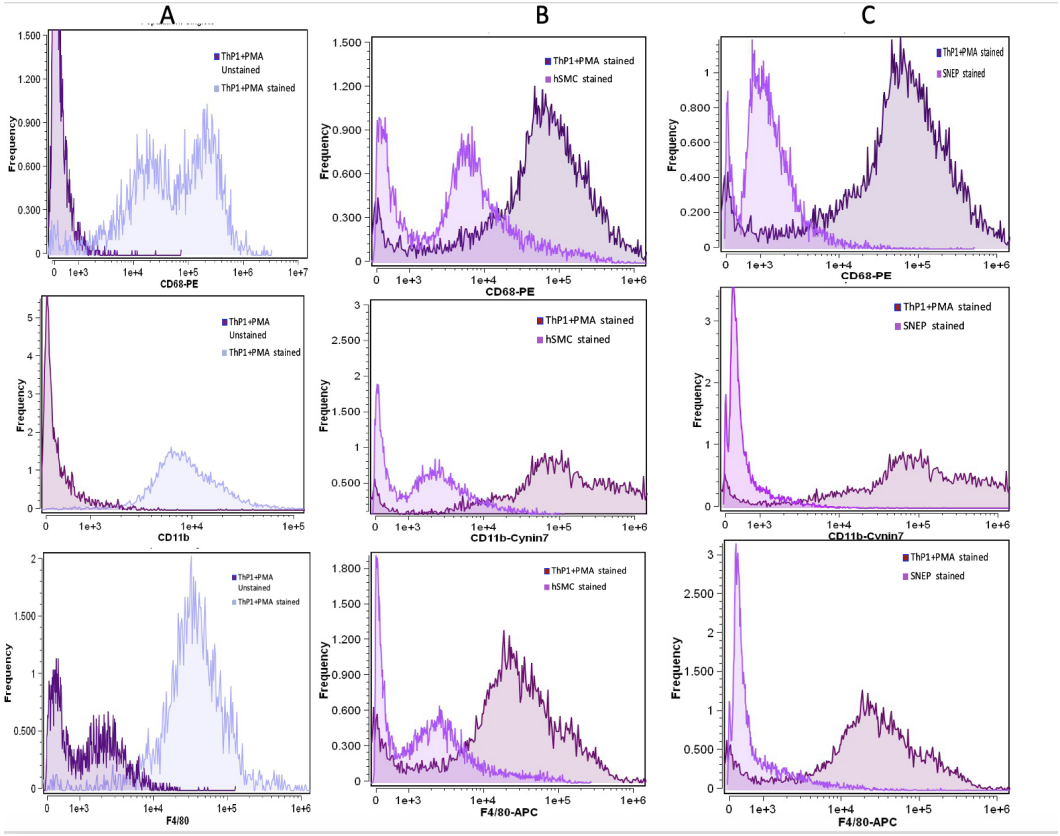
A
B
C
ThP1+PMA Unstained
ThP1+PMA stained
hSMC stained
SNEP stained
Frequency
CD68-PE
CD11b
CD11b-Cynin7
F4/80
F4/80-APC

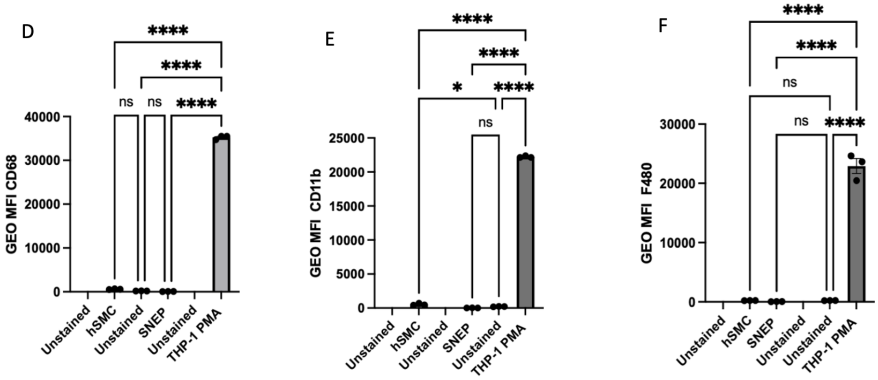
D
E
F
GEO MFI CD68
GEO MFI CD11b
GEO MFI F480
ns
****
*
Unstained
hSMC
SNEP
THP-1 PMA

Figure 4.14 Immunophenotyping human PMA-induced THP-1 macrophages compared to hiPSC derived hSMCs and hiPSC-derived S100β NE progenitor cells (S100β SNEPs) by Amnis™ Cellstream Flow Cytometry. Cells were immunophenotyped using three macrophage markers: CD68, CD11b, and F4/80. These markers were specifically conjugated with fluorescent dyes, PE, Cynin7, and APC, respectively. Each histogram illustrates the fluorescent intensity, indicative of the expression level of the corresponding antigen in (A) THP-1 compared to (B) hSMCs and (C) S100β SNEPs, across a population of 10,000 cells per sample preparation. To assess and compare antigen expression, the histogram derived from the unstained sample was superimposed with the histogram obtained from the sample stained with the conjugated antibody. The data are representative of three independent experiments. Bar charts represent the expression level of the CD68-PE, CD11b-Cynine7 and F4/80-APC by analysing the geometric mean fluorescent intensity (GEO MFI) from an average of three independent experiments. Data are ±SEM * $p<0.05$ *** $p<0.001$ **** $p<0.0001$ **** $p<0.0001$.

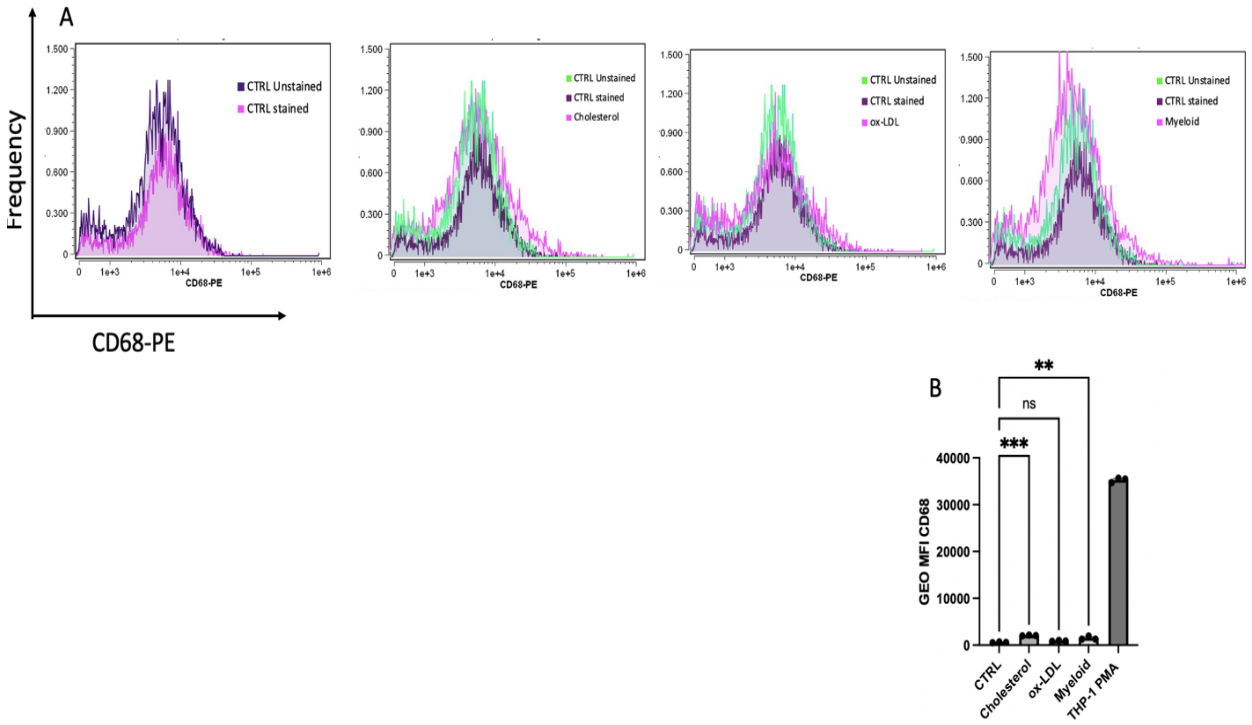

Figure 4.15 Flow cytometric analysis of CD68 expression in hSMCs before and after treatment with myeloid inductive stimuli. Representative histogram plots for CD68 staining of hSMCs with a CD68-PE conjugated antibody in (A) CONTROL (CTRL - No treatment) and following treatment with media supplemented with cholesterol, oxidized low-density lipoprotein (ox-LDL) and myeloid differentiation media, and (B) geometric mean fluorescent intensity (GEO MFI) of CD68 positive cells. THP-1 PMA macrophages were used as a positive control. CD68 expression was analysed and compared by overlaying the histograms of unstained/stained control versus stained treated cells. Flow cytometry was performed using the Amnis™ Cellstream Flow Cytometer. Cell debris were excluded from the analysis based on scatter signals. Data are from the average of three independent experiments. Data are ± SEM * $p<0.05$ *** $p<0.001$ **** $p<0.0001$ **** $p<0.0001$ vs CTRL.

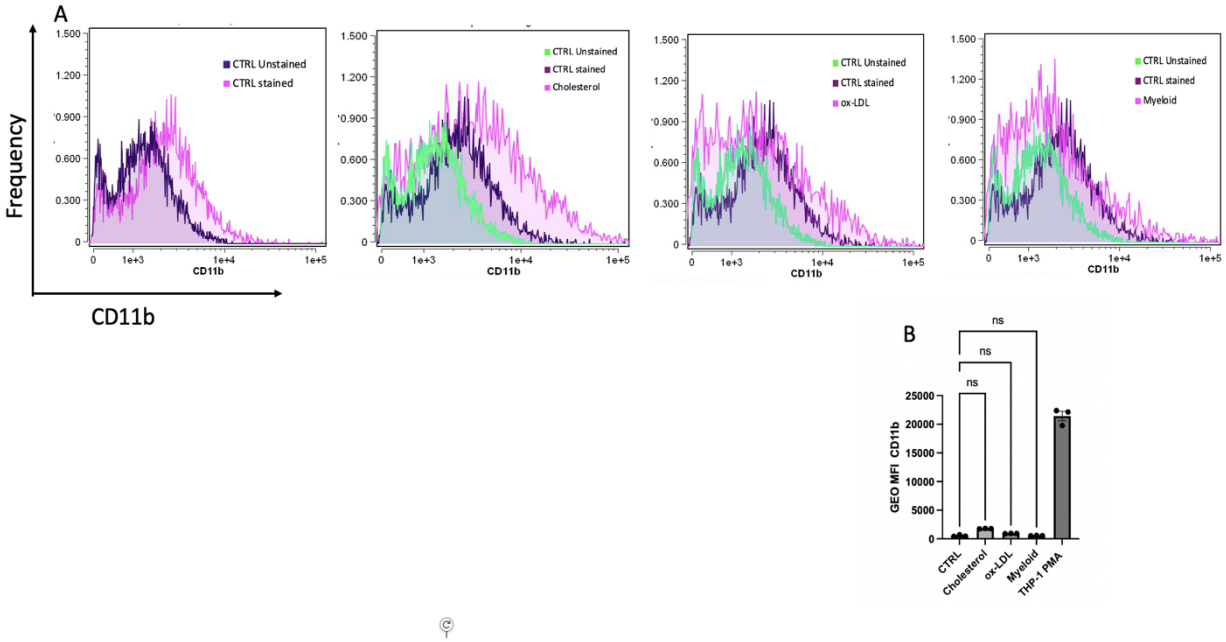

Figure 4.16 Flow cytometric analysis of CD11b expression in hSMCs before and after treatment with myeloid inductive stimuli. Representative histogram plots for CD11b staining of hSMCs with a CD11b-Cynine conjugated antibody in (A) CONTROL (CTRL - No treatment) and following treatment with media supplemented with cholesterol, oxidized low-density lipoprotein (ox-LDL) and myeloid differentiation media, and (B) geometric mean fluorescent intensity (GEO MFI) of CD11b positive cells. THP-1 PMA macrophages were used as a positive control. CD11b expression was analysed and compared by overlaying the histograms of unstained/stained control versus stained treated cells. Flow cytometry was performed using the Amnis™ Cellstream Flow Cytometer. Cell debris were excluded from the analysis based on scatter signals. Data are from the average of three independent experiments. Data are ± SEM * $p<0.05$ *** $p<0.001$ **** $p<0.0001$ **** $p<0.0001$ vs CTRL.

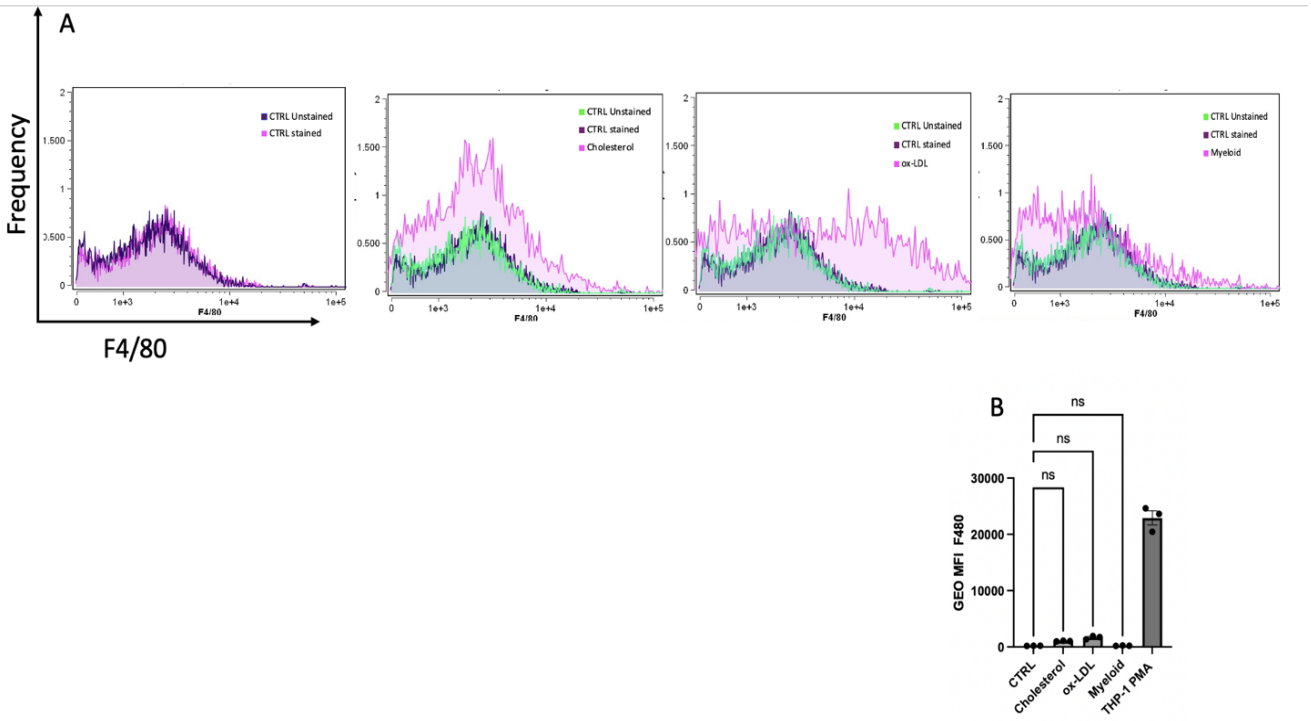

Figure 4.17 Flow cytometric analysis of F4/80 expression in hSMCs before and after treatment with myeloid inductive stimuli. Representative histogram plots for F4/80 staining of hSMCs with a F4/80 -APC conjugated antibody in (A) CONTROL (CTRL - No treatment) and following treatment with media supplemented with cholesterol, oxidized low-density lipoprotein (ox-LDL) and myeloid differentiation media, and (B) geometric mean fluorescent intensity (GEO MFI) of F4/80 positive cells. THP-1 PMA macrophages were used as a positive control. F4/80 expression was analysed and compared by overlaying the histograms of unstained/stained control versus stained treated cells. Flow cytometry was performed using the Amnis™ Cellstream Flow Cytometer. Cell debris were excluded from the analysis based on scatter signals. Data are from the average of three independent experiments. Data are ± SEM **** $p<0.0001$ vs CTRL.

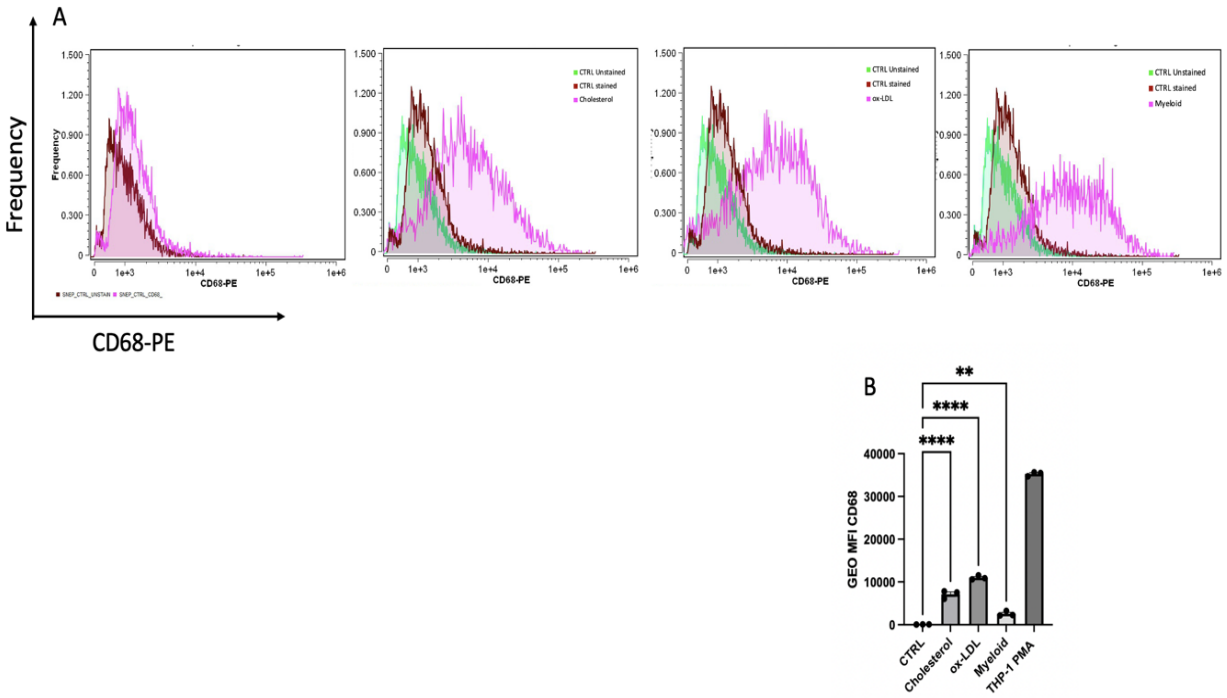

Figure 4.18 Flow cytometric analysis of CD68 expression in S100β SNEPs before and after treatment with myeloid inductive stimuli. Representative histogram plots for CD68 staining of SNEPs with a CD68-PE conjugated antibody in (A) CONTROL (CTRL - No treatment) and following treatment with media supplemented with cholesterol, oxidized low-density lipoprotein (ox-LDL) and myeloid differentiation media, and (B) geometric mean fluorescent intensity (GEO MFI) of CD68 positive cells. THP-1 PMA macrophages were used as a positive control. CD68 expression was analysed and compared by overlaying the histograms of unstained/stained control versus stained treated cells. Flow cytometry was performed using the Amnis™ Cellstream Flow Cytometer. Cell debris were excluded from the analysis based on scatter signals. Data are from the average of three independent experiments. Data are ± SEM **** $p<0.0001$ vs CTRL.

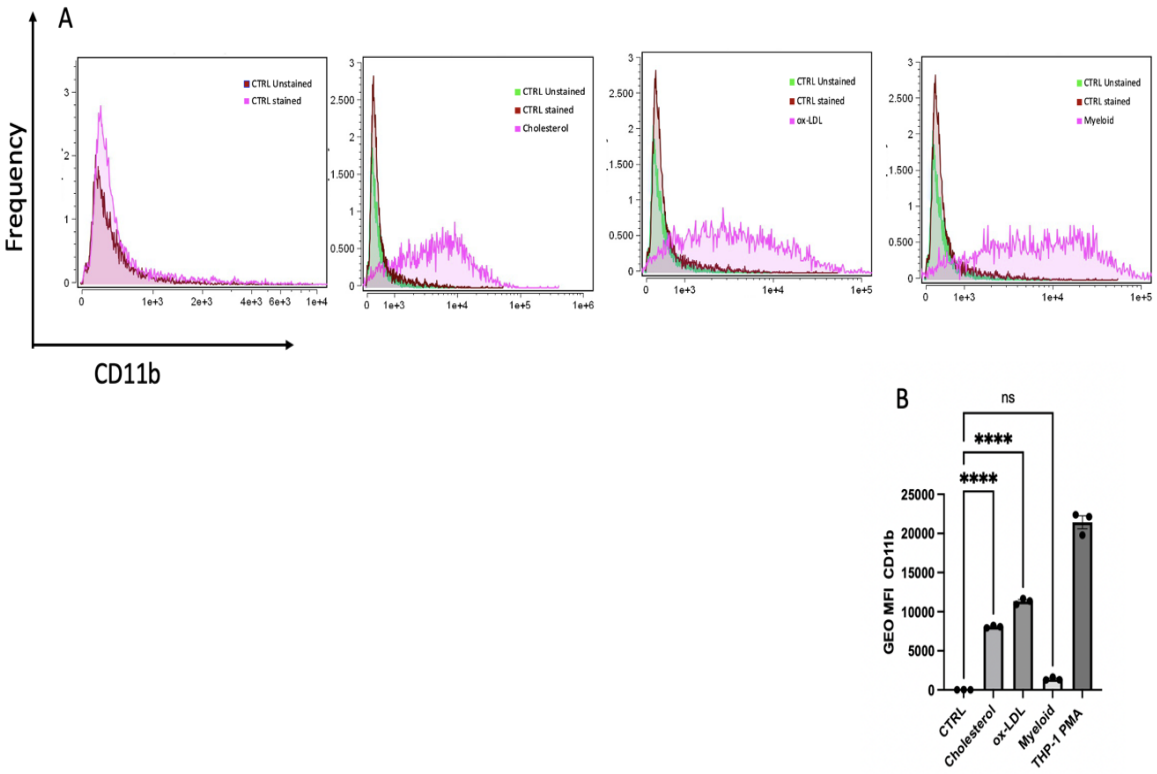

Figure 4.19 Flow cytometric analysis of CD11b expression in S100β SNEPs before and after treatment with myeloid inductive stimuli. Representative histogram plots for CD11b staining of SNEPs with a CD11b-Cynine conjugated antibody in (A) CONTROL (CTRL - No treatment) and following treatment with media supplemented with cholesterol, oxidized low-density lipoprotein (ox-LDL) and myeloid differentiation media, and (B) geometric mean fluorescent intensity (GEO MFI) of CD11b positive cells. THP-1 PMA macrophages were used as a positive control. CD11b expression was analysed and compared by overlaying the histograms of unstained/stained control versus stained treated cells. Flow cytometry was performed using the Amnis™ Cellstream Flow Cytometer. Cell debris were excluded from the analysis based on scatter signals. Data are from the average of three independent experiments. Data are ± SEM **** $p<0.0001$ vs CTRL.

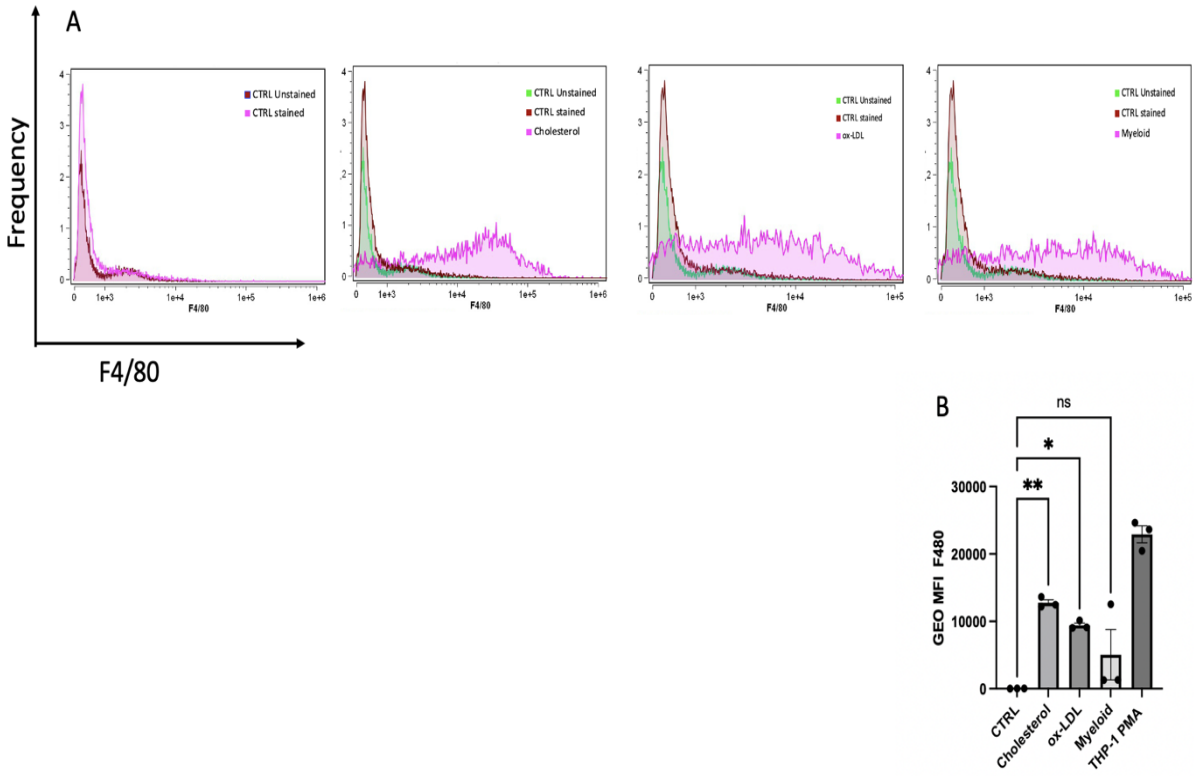

Figure 4.20 Flow cytometric analysis of F4/80expression in S100β SNEPs before and after treatment with myeloid inductive stimuli. Representative histogram plots for F4/80 staining of SNEPs with a F4/80-APC conjugated antibody in (A) CONTROL (CTRL - No treatment) and following treatment with media supplemented with cholesterol, oxidized low-density lipoprotein (ox-LDL) and myeloid differentiation media, and (B) geometric mean fluorescent intensity (GEO MFI) of F4/80 positive cells. THP-1 PMA macrophages were used as a positive control. F4/80 expression was analysed and compared by overlaying the histograms of unstained/stained control versus stained treated cells. Flow cytometry was performed using the Amnis™ Cellstream Flow Cytometer. Cell debris were excluded from the analysis based on scatter signals. Data are from the average of three independent experiments. Data are ± SEM **** $p<0.0001$ vs CTRL.

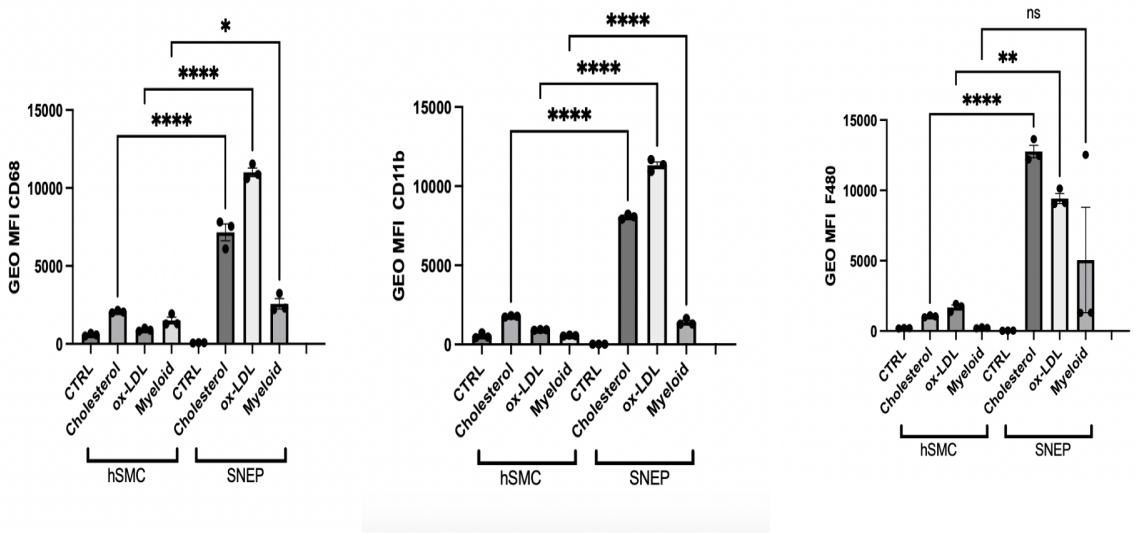

Figure 4.21. Comparison of the expression of CD68, CD11b and F4/80 in hSMC vs S100β SNEPs before and after treatment with myeloid inductive stimuli. Geometric mean fluorescent intensity (GEO MFI) of myeloid positive cells following treatments. The expression level of the CD68-PE, CD11b-Cynine7 and F4/80-APC was analysed and compared by overlaying the histograms of unstained/stained control versus stained treated cells. Flow cytometry was performed using the Amnis™ Cellstream Flow Cytometer. Cell debris were excluded from the analysis based on scatter signals. Data are the mean ± SEM from the average of three independent experiments * $p<0.05$ ** $p<0.01$ *** $p<0.001$ **** $p<0.0001$ vs hSMCs.

4.4 Summary

Human hiPSC-derived smooth muscle cells (hSMCs)

- Human hiPSC derived hSMC exhibited myogenic expression of Cnn1, a SMC differentiation marker, *in vitro.*
- There was lipid uptake of Oil Red O, and mRNA levels of myeloid genes only *CD68* expression levels increased significantly hSMC supplemented with myeloid differentiation media *in vitro*.
- Cholesterol and ox-LDL promoted CD68 and MACII protein expression in hSMC while flow cytometric analysis revealed increases in CD68 with cholesterol and myeloid differentiation media.

Human hiPSC-derived S100β NE progenitors (S100β SNEPs)

- S100β SNEPs exhibited stem cell expression of S100β, a neuroectoderm differentiation marker, *in vitro.*
- There was lipid uptake of Oil Red O and a significant increase in the myeloid gene expression of *CD68* in S100β SNEPs treated with myeloid differentiation media *in vitro.* There was an increase in the myeloid gene expression of *MAC II* in S100β SNEPs following treatment of cells with cholesterol and ox-LDL *in vitro*.
- S100β SNEPs treated with cholesterol, ox-LDL or myeloid differentiation media increased their expression of myeloid differentiation markers, CD68 and MAC II expression *in vitro* while flow cytometric analysis of myeloid differentiation marker expression revealed that only cholesterol and ox-LDL promoted a significant increase in all 3 myeloid markers.

Collectively the data suggest that S100β SNEPs have a greater propensity to undergo myeloid differentiation and transition to macrophage-like cells *in vitro.*

4.5 Discussion

The previous chapter of results have highlighted the capability of S100β mVSCs in differentiation into myeloid-like cells. The overall outcome of that transition was more convincing than the dedifferentiation of MOVAS SMC into myeloid-like cells as S100β mVSCs exhibited macrophage markers. This could be due to the state of MOVAS SMC known as immortalised cells that were bought commercially. This Chapter addressed whether HiPSC-derived NE progenitor cells (SNEP) and HiPSC-derived smooth muscle cells (hSMC) can undergo myeloid differentiation into macrophages-like cells.

Macrophage-like SMCs demonstrate low expression of contractile markers and possess functions similar to macrophages such as innate immune signalling, phagocytosis, and efferocytosis (Vengrenyuk et al., 2015). In 1997, Andreeva et al. identified cells co-expressing CD68 and α-SMA in human aorta atherosclerosis plaque, especially in lipid-rich regions (Andreeva et al., 1997). Subsequently, Allahverdian et al. estimated that these chimeric cells accounted for about 40 % of all CD68-positive cells in atherosclerotic lesions. However, these studies could not determine whether chimeric cells were vSMC-derived cells that activated macrophage markers, or macrophages that activated SMC markers, or neither, until the cell lineage tracing strategy confirmed that these chimeric cells are SMC-derived (Allahverdian et al., 2014).

The accumulation of SMC-like and non-SMCs [macrophage-like cells (MLCs), endothelial cells (ECs), osteoblasts (OBs), adipocytes (APs), mesenchymal stem cells (MSCs)] play an important role during vascular disease progression and lesion formation (Bonacina et al., 2023). Normal arterial vessels and lesions following injury or during arteriosclerotic (carotid ligation/wire-induced injury etc) and atherosclerosis (apolipoprotein E deficient mouse model (ApoE) or low-density lipoprotein receptor (LDL-R) deficient mice fed a high-fat diet) are heterogeneous with a variety of cellular phenotypes found in the adventitial, medial and intimal layers (Potente et al., 2017; Van Kuijk et al., 2019). Recent evidence suggests that most of the major cell types in atherosclerotic plaques, e.g. macrophages, endothelial cells, T-cells, and SMC-like cells are

heterogeneous and/or plastic to some extent. Although macrophages, endothelial cells, T cells, and SMCs are the most discussed cells relating to disease progression, recent research in the field has highlighted the role of S100β resident vascular stem cells (DiLuca et al., 2021, Molony et al., 2021, Liu et al., 2022) They may originate from a resident progenitor stem cell, which can give rise to various cell types like (myo)fibroblasts, SMC-like cells or non-SMCs (El Agha et al., 2017).

The major focus of this Chapter was to determine whether HiPSC-derived smooth muscle cells (hSMC) and/or HiPSC-derived NE progenitor cells (SNEP) in culture were capable of undergoing myeloid differentiation following treatment of cells with three myeloid differentiation inductive stimuli (cholesterol, ox-LDL and myeloid differentiation media). By using cultured S100β SNEPs, hSMC and cultured THP-1 PMA macrophages as a positive technical control. hSMC and S100β SNEPs demonstrate similar sporadic phenotypic characteristics but only S100β SNEPs differentiated into MLCs when loaded with cholesterol and ox-LDL by increasing CD68, CD11b and F4/80 expression.

While cholesterol and ox-LDL promoted CD68 and MAC II protein expression in hSMC and flow cytometric analysis revealed increases in CD68 with cholesterol and myeloid differentiation media, the expression of biomarkers of myeloid differentiation into MLCs was sporadic. At mRNA levels, only myeloid differentiation media promoted *CD68* expression levels in hSMC.

CD68 expression level in S100β SNEPs was only promoted with myeloid differentiation media. While *MAC-2* expression levels in S100β SNEPs were promoted with cholesterol and ox-LDL. This indicates that a 7-day treatment was enough to achieve transcriptional activity in S100β SNEPs. In addition, cholesterol, ox-LDL and myeloid differentiation media promoted CD68 and MacII protein expression in S100β SNEPs. Flow cytometric analysis revealed increases in CD68 with all three cholesterol, ox-LDL and myeloid differentiation media, while Cd11b and F4/80 expressions increased with cholesterol and ox-LDL in S100β SNEPs.

The differences between protein and mRNA levels can be explained by two main factors. Firstly, protein degradation might lower protein levels independently of mRNA levels, which are influenced by transcription. As a result, even if mRNA levels rise, the protein might be broken down before it accumulates, failing to reflect changes in transcription. Secondly, mRNA itself can be unstable and degraded before translation occurs. Therefore, an increase in mRNA might be misleading if the mRNA is broken down before it is used to produce protein. Similarly, variations in protein levels might not solely be due to translation efficiency but could also be affected by the dynamics of protein degradation (Belle et al., 2006; Y. Liu et al., 2016; Vogel & Marcotte, 2012).

The abundance of proteins and mRNA is governed by the balance between the rates of their production and degradation (Vogel & Marcotte, 2012). Recent advancements in single-cell techniques for measuring mRNA and protein levels have enabled detailed, high-throughput analyses of multiple genes. These findings often contrast with those from broader population studies. For instance, a recent extensive study of individual Escherichia coli cells found that bacterial protein and mRNA levels appear to be completely uncorrelated (Taniguchi et al., 2010). However, the measurements and their independent validation are still pending. Nonetheless, mRNA concentrations explain approximately 54–77% of the variation in average protein levels, and the average correlations observed across many single-cell measurements are comparable to those obtained from bulk measurements of cell populations. The limited lifespan of bacterial mRNAs and their low production rates per cell lead to greater fluctuations in mRNA concentrations within individual cells compared to the more stable proteins. This disparity in molecular lifetimes helps to explain the lack of correlation between RNA and protein levels in single cells.

When averaged across populations, these variations disappear, revealing a correlation between mRNA and protein levels (Vogel & Marcotte, 2012). The absence of correlation in single cells can partly be explained by the regulation of translation: while mRNA levels may not reflect this, the concentrations of proteins within the same complex tend to show less variation when comparing different gene classes across yeast cells (Fraser et al., 2004; Gandhi et al., 2011).

Collectively, several earlier *in vitro* studies provide a strong basis for understanding why protein levels might not always align with mRNA data, highlighting the complexities of post-transcriptional and post-translational regulation. (Belle et al. 2006) noted that variations in protein degradation rates can significantly affect protein abundance, meaning that protein levels may not always mirror changes in mRNA levels. (Vogel & Marcotte 2012) emphasized the importance of mRNA stability and degradation in determining protein levels, which can lead to discrepancies between mRNA and protein data. (Y. Liu et al. 2016) explored how post-transcriptional and translational controls, including mRNA degradation, contribute to the observed differences between mRNA and protein levels.

Additionally, it was clear that the cells underwent morphological changes, with some becoming more rounded as they developed into MLCs. Although this was not directly discussed in the thesis, it could indicate varying levels of apoptosis in response to the three different stimuli (cholesterol, oxLDL, myeloid differentiation media). These stimuli might induce different extents of apoptosis, and the observed shape changes could be related to cell death, potentially explaining some of the discrepancies.

Studies has demonstrated that cholesterol buildup in macrophages can induce endoplasmic reticulum (ER) stress, which may then trigger apoptosis. This stress can alter cell shape and disrupt normal cellular functions, such as protein synthesis, folding, and degradation, leading to discrepancies between mRNA levels and protein expression (Calaluce et al., 2010; Marcel et al., 2009). Cholesterol has been shown to promote apoptosis and cell rounding through pathways involving reactive oxygen species (ROS) and mitochondrial processes. Specifically, cholesterol can enhance the expression of apoptosis-related proteins like cleaved caspase-3 and Bax, while reducing levels of anti-apoptotic proteins such as Bcl-xL. This imbalance results in DNA/RNA fragmentation and cell death (K. Li et al., 2020). Another study has been demonstrated the link between cholesterol-induced cellular stress and cell death when the accumulation of oxidized LDL in cells occurs. This process leads to (ER) stress and apoptosis (Wu et al., 2021).

Several previous studies *in vitro* (Matsumoto et al., 2000; Rong et al., 2003) and *in vivo* (Feil et al.,2014; Allahverdian et al., 2014) highlighted the contribution and trans differentiation of medial SMC to myeloid-like cells, which is more convincing in this chapter than the previous one. However, data in this chapter suggest that S100β SNEPs are fully capable of differentiation into macrophage-like cells (MLCs) and acquiring the myeloid markers at protein levels. This confirms the findings from the previous results chapter.

Chapter 5

General Discussion

5.1 General Discussion

Cardiovascular Disease (CVD), such as atherosclerosis, is a chronic progressive inflammatory disease widely regarded as one of the leading causes of death (Lockhart et al., 2012). The accumulation of SMC-like and non-SMC neointimal cells leading to intimal medial thickening, lipid accumulation, plaque formation and the obstruction to blood flow is considered a hallmark of atherosclerosis (Benditt & Benditt, 1973). The origin of SMC-like and non-SMC neointimal cells is controversial. Recent lineage tracing studies, scRNA-seq and single-cell chromatin immunoprecipitation (ChIP) analysis *in situ* have provided compelling evidence in various animal models for the involvement of a rare population of differentiated Myh11/Sca1^{+} medial SMCs that undergo de-differentiation and phenotypic switching (Chappell et al., 2016; Gomez et al., 2013; (Pan et al., 2020). Contrasting lineage tracing studies from our lab and others suggest a role for resident S100β adventitial and/or mVSCs in contributing to the accumulatio of SMC-like cells within lesions (Kramann et al., 2016; Tang et al., 2012; Wan et al., 2012; Di Luca et al., 2021, Molony et al., 2021).

This thesis assessed whether S100β mVSCs in culture undergo myeloid differentiation following treatment of cells with three myeloid differentiation inductive stimuli (cholesterol, ox-LDL and myeloid differentiation media). In doing so, it addressed the likelihood of S100β resident mVSCs as an alternative source of non-SMC derived macrophage-like cells (MLCs) within vascular lesions in response to pro-atherogenic stimuli. Using quantitative SMC differentiation assays, lipid uptake, immunocytochemistry (ICC) and flow cytometry of myeloid differentiation markers, the data suggest that S100β mVSCs are capable of transitioning to MLCs, at least *in vitro* (Figure 5.1). Moreover, the data demonstrate strong parallels in the response of S100β mVSCs to atherogenic stimuli in both human and mouse cells, enhancing its translational impact in CVD.

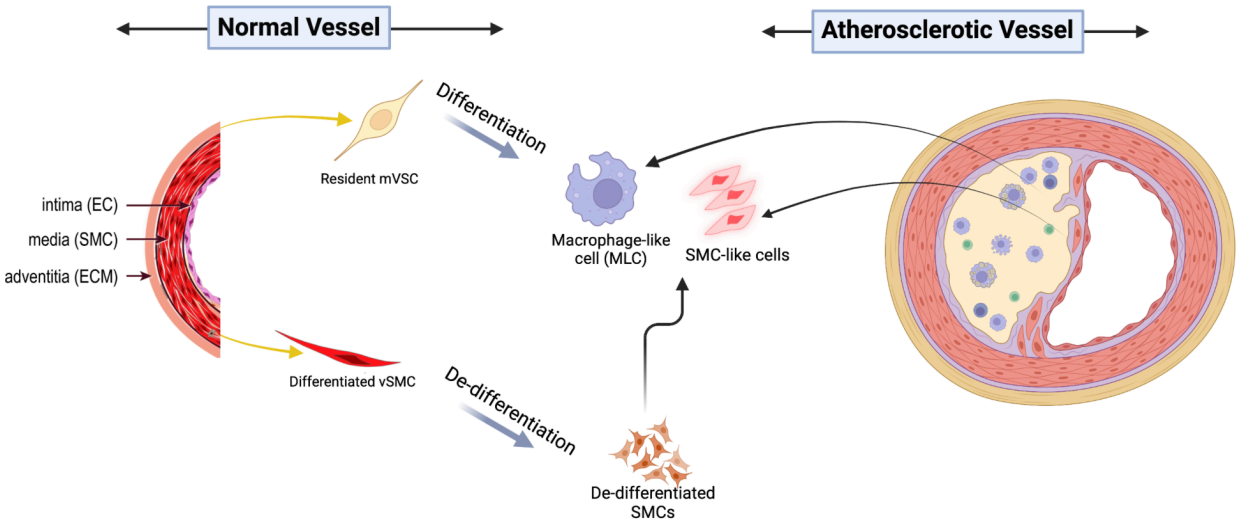

Figure 5.1 Schematic of arterial architecture in normal and atherosclerotic vessels. Illustrates that S100β mVSCs are capable of transitioning to MLCs. S100β resident mVSCs as an alternative source of non-SMC derived macrophage-like cells (MLCs) within vascular lesions in response to pro-atherogenic stimuli. Created with Biorender.

Monocyte and macrophage supply and recruitment are pivotal events in atherogenesis (Hoek et al., 2000). Indeed, the number of circulating monocytes correlates with lesion size in experimental atherosclerosis (Swirski et al., 2007). While many of the original studies on macrophage supply and recruitment within atherosclerotic lesions focused on circulating monocytes from bone marrow (Swirski et al., 2007), recent studies have provided strong evidence for local recruitment from cells within the vessel wall (Susser & Rayner, 2022). Classical (Ly6C^{high}) monocytes were considered the largest subset in mouse blood and were seen as the primary precursors for most macrophages within atherosclerotic lesions in mice (Swirski et al., 2007).) while Ly6C^{low} monocytes patrol the endothelium and support vessel wall repair (Auffray et al., 2007). Unlike the early stage of DIT during which medial cells are the only lipid-laden cells of intima, later stage lesions contain macrophage foam cells derived from activated monocytes. However, recent lineage tracing analysis have shown that upon switching to a synthetic phenotype, medial vSMCs progressively lose their expression of contractile proteins such as αSMA, MYH11 and SM22α and acquire macrophage and leukocyte specific markers such as CD68, CD11b, F4/80, HLA-DR and

LGALS3/MacII (Shankman et al., 2015; Albarrán-Juárez et al., 2016). As a result, the contribution of medial vSMC-derived cells to all SMC-like and non-SMC cells within atherosclerotic lesions based purely on immunohistochemical studies was considered underestimated.

Medial cells and not circulating macrophages are presumed the major cellular compartment responsive to lipid accumulation during early lesion formation (Pryma et al., 2019), in particular, within the intima of atherosclerosis-prone arteries *in utero* as well as in infants and children (Milei et al., 2008). In early studies on human coronary artery sections, at least 50% of total intimal foam cells were purported to be derived from vSMCs and that about 40% of $CD68^+$ cells were of vSMC rather than myeloid origin (Allahverdian et al., 2014). However, these studies relied on co-localization of the SMC marker, αSMA (ACTA-2) to confirm their myogenic origin which casts some doubt on these observations as αSMA is an unreliable marker for differentiated SMCs with *Acta2-Cre* expression routinely observed in SMC-like cells or myofibroblasts (Skalli et al., 1989) (Hautmann et al., 1999) (Chakraborty et al., 2019). In this context, stem cells or their immediate myogenic myofibroblast progeny can give rise to αSMA^+ cells, which could also be responsible for lipid accumulation during early lesion formation (Putra et al., 2020).

The source of αSMA^+ SMC-like cells contributing to subclinical atherosclerosis, in-stent restenosis and neointimal hyperplasia is controversial. To date, the sources reported based on lineage tracing studies are de-differentiated SMCs (Chappell et al., 2016), S100β resident vascular stem cells (Tang et al., 2012, Di Luca et al., 2021), bone marrow-derived stem cells (Sata, 2003; Shimizu et al., 2001) and endothelial mesenchymal transition (Cooley et al, 2014; Zeisberg et al., 2007). Irrespective of their origin, there are many possible mechanisms by which αSMA^+ cells accelerate foam cell accumulation in atherosclerosis. The secretory properties of intimal synthetic αSMA^+ cells contribute to ECM secretion by an increased proteoglycan production (Nakashima et al., 2007). ApoB100-containing lipoproteins including LDL particles are retained and modified within the proteoglycan network built by αSMA^+ via hydrophobic interactions (Ismail et al., 1994).

The recent application of scRNA-seq in mouse and human atherosclerosis has also provided novel insights regarding the biological functions and subset composition of macrophages in atherosclerotic lesions (Yu et al., 2023). Using a combination of scRNA-seq and lineage tracing to profile lesional cells derived from $CX3CR1^+$ precursors in mice during both progression and regression of

atherosclerosis, the analyses revealed a spectrum of macrophage activation states with greater complexity than the traditional M1 and M2 polarization states (Lin et al., 2019). Progression was associated with differentiation of $CXC3R1^{+}$ monocytes into more distinct states than during regression. Moreover, an unexpected cluster of proliferating monocytes with a stem cell-like signature was observed, suggesting that monocytes may persist in a proliferating self-renewal state in inflamed tissue, rather than differentiating immediately into macrophages after entering the tissue (Lin et al., 2019).

In addition, CD200, an inhibitory immune checkpoint known to control macrophage activation through interaction with its cognate receptor CD200R, has recently been implicated in controlling macrophage activation. Studies suggest that CD200 promotes arterial homeostasis by limiting excessive supply and activation of monocyte-macrophages during atherogenesis via both local and systemic cell-dependent mechanisms (Kassiteridi et al., 2021). Indeed, CD200 has now been shown to identify and mark αSMA^{+} SMC and non-SMCs in early to advanced mouse atherosclerotic lesions (Bashore et al., 2023).

Single-cell RNA sequencing and "omics" technologies have further shown that both neural stem cells (NPCs) and oligodendrocyte precursor cells (OPCs), both of which are $S100\beta^{+}$ (Raponi et al., 2007) ;(Deloulme et al., 2004), express genes that are typically attributed to immune cells (Falcão et al., 2018);(Dittmann et al., 2023). Importantly, S100β NPC- and OPC-derived progeny both act as phagocytes for dead neurons and myelin debris, respectively, properties typically attributed to microglia and macrophages (Lu et al., 2011);(Falcão et al., 2018); (Auguste et al., 2022). NPCs and OPCs also directly react to inflammatory environments through chemokine and cytokine receptors that they express, and actively participate in modulating the inflammatory environment by secreting chemokines and cytokines (Watson et al., 2020); (Belenguer et al., 2021); (Shariq et al., 2021); (Dittmann et al., 2023). Therefore, it is not surprising that S100β mVSCs can undergo myeloid differentiation to MLCs in response to an inflammatory environment induced by ox-LDL.

Previous studies had indicated that lipid loading induces the expression of macrophage markers and a gain of phagocytic activity by arterial vSMCs. Subendothelial vSMCs of human aorta express macrophage antigens *in situ* and *in vitro.* Cells, expressing αSMA^{+} and the macrophage CD68 antigen, were identified both in grossly normal aortic areas and in atherosclerotic lesions

(fatty streaks and atherosclerotic plaques (Andreeva et al., 1997). These seminal findings raised the possibility that some atherosclerotic lesion cells expressing macrophage markers, and assumed to be of monocyte origin, may be in fact be vSMCs and/or S100β mVSCs that change their phenotype following lipid loading. The extent of this phenotypic change in S100β mVSCs has not been previously investigated in mouse or human stem cells.

While previous studies have demonstrated the ability of S100β mVSCs to undergo trilineage specification (Tang et al., 2012), this study is one of the first to demonstrate the ability of aortic arch-derived S100β mVSCs to undergo myeloid differentiation, particularly in response to ox-LDL, to MLCs *in vitro*. Moreover, as the progeny of these cells are also αSMA^{+}, this population and not circulating macrophages, may also be responsible for the MLC population that accumulates locally within vascular lesions (Di Luca et al., 2021).

5.2 Conclusion

This thesis investigated whether mouse and human S100β mVSCs and Cnn1 vSMCs undergo myeloid differentiation in response to cholesterol, ox-LDL and myeloid differentiation media. Our findings suggest that S100β mVSCs are fully capable of differentiation into macrophage-like cells (MLCs) and acquiring myeloid markers to a greater extent than vSMCs in culture.

5.3 Future work

In order to validate the putative role of S100β mVSCs and/or their progeny in contributing to the accumulation of non-SMC MLCs *in situ*, there are a series of studies that could be undertaken.

Firstly, lineage tracing analysis of S100β mVSCs and interrogation of the marked cell population for MLC markers would confirm that αSMA^{+} MLCs are derived from an S100β parent cell population. This methodology relies on the conditional expression of reporter genes (e.g., GFP) exclusively in a specific cell line (e.g., S100β mVSCs), allowing identification of both parents and progeny cells. In the case of S100β tracing studies, Cre recombinase expression is under control

of the promoter of the S100β gene, which is exclusively expressed in the mVSCs. Consequently, Cre recombinase is expressed in the same way as S100β and then recognizes LoxP sites flanking a stop sequence located at a locus carrying the reporter gene. Once the stop sequence is irreversibly removed from the parent cell DNA by the Cre recombinase, the reporter gene can be expressed uninterrupted and independently of S100β expression. The transmission of this gene to each descendant cell allows identification of all S100β mVSC-derived cells by the signal resulting from the expression of the reporter gene (e.g., green fluorescence for GFP). In addition, Cre recombinase expression can be controlled by an inducible system permitting its activation at a given time upon the administration of an inducer such as tamoxifen. These conditional and inducible Cre recombinase systems would allow the study of mVSC fate independently of the expression of marker genes, which are often autoregulated in plaques. These lineage tracing studies have already confirmed that a significant number of αSMA$^+$ SMC-like cells are derived from an S100β parent cell (Di Luca et a., 2021, Yuan et al., 2017, Molony et al, 2021). It would be of interest to determine whether non-SMC αSMA$^+$ MLCs are derived from a marked S100β mVSC cell population following interrogation of these marked cells with antibodies against MLC markers (CD68, CD11b, F4/80, HLA-DR and LGALS3/MacII) using immunocytochemistry and/or flow cytometry.

Secondly, single-cell analysis of fate-mapped S100β mVSCs could reveal the heterogeneity, including stem-like properties, of cells during atherosclerosis progression and regression. Interrogation of scRNA-seq datasets from normal and atherosclerotic vessels would reveal discrete cluster(s) of cells that are derived from S100β stem cells using trajectory analysis. Preliminary data from murine models of atherosclerosis (LDL-R$^{-/-}$ and ApoE$^{-/-}$ deficient mice) reveal that a significant number (~50%) of atherosclerotic cells are derived from an S100β/Sca1 cell population present in normal vessels (unpublished data). Interrogation of these discrete cluster of cells and their progeny for MLC genes would confirm their abundance through the progression of atherosclerotic lesions.

Finally, the mechanisms and processes by which S100β mVSCs may facilitate foam cell accumulation in atherosclerosis could be addressed by initially examining the secretory properties of these cells and their progeny in contributing to ECM secretion via increased proteoglycan production. Indeed, ApoB100-containing lipoproteins including LDL particles are retained and

modified within the proteoglycan network built by cells via hydrophobic interactions. Other key questions that could be addressed include whether myeloid differentiation of mVSCs and foam cell formation can occur irrespective of oxidative or enzymatic LDL modifications, as reported for SMCs. In addition, an analysis of the expression of the cholesterol exporter protein ATP-Binding Cassette A1 (ABCA1) and lysosomal acid lipase (LAL), a key cytosolic enzyme which hydrolyzes cholesteryl esters (the main form of cholesterol storage) to free cholesterol, would reveal whether a significantly reduced expression of these key proteins in mVSC cells (but not in monocyte/macrophage derived-foam cells), is responsible for enhanced retention of lipid in mVSCs and their progeny when compared to monocyte/macrophage derived-foam cells. These data would reveal whether mVSCs may contain a much larger burden of lipids than macrophages, as they are unable to release excess lipid via ABCA1 and LAL.

Bibliography

A, Y., N, K., Bd, G., X, W., P, A., G, K., W, T., J, S., & I, T. (2021). ODC (Ornithine Decarboxylase)-Dependent Putrescine Synthesis Maintains MerTK (MER Tyrosine-Protein Kinase) Expression to Drive Resolution. *Arteriosclerosis, Thrombosis, and Vascular Biology*, *41*(3). https://doi.org/10.1161/ATVBAHA.120.315622

Afroze, T., Yang, L. L., Wang, C., Gros, R., Kalair, W., Hoque, A. N., Mungrue, I. N., Zhu, Z., & Husain, M. (2003). Calcineurin-independent regulation of plasma membrane Ca2+ ATPase-4 in the vascular smooth muscle cell cycle. *American Journal of Physiology-Cell Physiology*, *285*(1), C88–C95. https://doi.org/10.1152/ajpcell.00518.2002

Ailawadi, G., Moehle, C. W., Pei, H., Walton, S. P., Yang, Z., Kron, I. L., Lau, C. L., & Owens, G. K. (2009). Smooth muscle phenotypic modulation is an early event in aortic aneurysms. *The Journal of Thoracic and Cardiovascular Surgery*, *138*(6), 1392–1399. https://doi.org/10.1016/j.jtcvs.2009.07.075

Aird, W. C. (2007). Phenotypic Heterogeneity of the Endothelium. *Circulation Research*, *100*(2), 174–190. https://doi.org/10.1161/01.RES.0000255690.03436.ae

Akaki, T., Sato, K., Shimizu, T., Sano, C., Kajitani, H., Dekio, S., & Tomioka, H. (1997). Effector molecules In expression of the antimicrobial activity of macrophages against Mycobacterium avium complex: Roles of reactive nitrogen intermediates, reactive oxygen intermediates, and free fatty acids. *Journal of Leukocyte Biology*, *62*(6), 795–804. https://doi.org/10.1002/jlb.62.6.795

Albarrán-Juárez, J., Kaur, H., Grimm, M., Offermanns, S., & Wettschureck, N. (2016). Lineage tracing of cells involved in atherosclerosis. *Atherosclerosis*, *251*, 445–453. https://doi.org/10.1016/j.atherosclerosis.2016.06.012

Alberts, B., Johnson, A., Lewis, J., Raff, M., Roberts, K., & Walter, P. (2002). *Molecular Biology of the Cell* (4th ed.). Garland Science.

Alexander, M. R., & Owens, G. K. (2012). Epigenetic Control of Smooth Muscle Cell Differentiation and Phenotypic Switching in Vascular Development and Disease. *Annual Review of Physiology*, *74*(1), 13–40. https://doi.org/10.1146/annurev-physiol-012110-142315

Allahverdian, S., Chaabane, C., Boukais, K., Francis, G. A., & Bochaton-Piallat, M.-L. (2018). Smooth muscle cell fate and plasticity in atherosclerosis. *Cardiovascular Research*, *114*(4), 540–550. https://doi.org/10.1093/cvr/cvy022

Allahverdian, S., Chehroudi, A. C., McManus, B. M., Abraham, T., & Francis, G. A. (2014). Contribution of intimal smooth muscle cells to cholesterol accumulation and macrophage-like cells in human atherosclerosis. *Circulation*, *129*(15), 1551–1559. https://doi.org/10.1161/CIRCULATIONAHA.113.005015

Allingham, M. J., van Buul, J. D., & Burridge, K. (2007). ICAM-1-mediated, Src- and Pyk2-dependent vascular endothelial cadherin tyrosine phosphorylation is required for leukocyte transendothelial migration. *Journal of Immunology (Baltimore, Md.: 1950)*, *179*(6), 4053–4064. https://doi.org/10.4049/jimmunol.179.6.4053

Anderson, C. L., Shen, L., Eicher, D. M., Wewers, M. D., & Gill, J. K. (1990). Phagocytosis mediated by three distinct Fc gamma receptor classes on human leukocytes. *Journal of Experimental Medicine*, *171*(4), 1333–1345. https://doi.org/10.1084/jem.171.4.1333

Anderson, H. A., Maylock, C. A., Williams, J. A., Paweletz, C. P., Shu, H., & Shacter, E. (2003). Serum-derived protein S binds to phosphatidylserine and stimulates the phagocytosis of apoptotic cells. *Nature Immunology*, *4*(1), 87–91. https://doi.org/10.1038/ni871

Andreeva, E. R., Pugach, I. M., & Orekhov, A. N. (1997). Subendothelial smooth muscle cells of human aorta express macrophage antigen in situ and in vitro. *Atherosclerosis*, *135*(1), 19–27. https://doi.org/10.1016/s0021-9150(97)00136-6

Asmar, R. G., Brunel, P. C., Pannier, B. M., Lacolley, P. J., & Safar, M. E. (1988). Arterial distensibility and ambulatory blood pressure monitoring in essential hypertension. *The American Journal of Cardiology*, *61*(13), 1066–1070. https://doi.org/10.1016/0002-9149(88)90127-0

Atri, C., Guerfali, F. Z., & Laouini, D. (2018). Role of Human Macrophage Polarization in Inflammation during Infectious Diseases. *International Journal of Molecular Sciences*, *19*(6), Article 6. https://doi.org/10.3390/ijms19061801

Auffray, C., Fogg, D., Garfa, M., Elain, G., Join-Lambert, O., Kayal, S., Sarnacki, S., Cumano, A., Lauvau, G., & Geissmann, F. (2007). Monitoring of blood vessels and tissues by a population of monocytes with patrolling behavior. *Science (New York, N.Y.)*, *317*(5838), 666–670. https://doi.org/10.1126/science.1142883

Auguste, Y. S. S., Ferro, A., Kahng, J. A., Xavier, A. M., Dixon, J. R., Vrudhula, U., Nichitiu, A.-S., Rosado, D., Wee, T.-L., Pedmale, U. V., & Cheadle, L. (2022). Oligodendrocyte precursor

cells engulf synapses during circuit remodeling in mice. *Nature Neuroscience*, *25*(10), 1273–1278. https://doi.org/10.1038/s41593-022-01170-x

Babaev, V. R., Bobryshev, Y. V., Stenina, O. V., Tararak, E. M., & Gabbiani, G. (1990). Heterogeneity of smooth muscle cells in atheromatous plaque of human aorta. *The American Journal of Pathology*, *136*(5), 1031–1042.

Babaev, V. R., Bobryshev, Y. V., Sukhova, G. K., & Kasantseva, I. A. (1993). Monocyte/macrophage accumulation and smooth muscle cell phenotypes in early atherosclerotic lesions of human aorta. *Atherosclerosis*, *100*(2), 237–248. https://doi.org/10.1016/0021-9150(93)90210-l

Bacakova, L., Zarubova, J., Travnickova, M., Musilkova, J., Pajorova, J., Slepicka, P., Kasalkova, N. S., Svorcik, V., Kolska, Z., Motarjemi, H., & Molitor, M. (2018). Stem cells: Their source, potency and use in regenerative therapies with focus on adipose-derived stem cells - a review. *Biotechnology Advances*, *36*(4), 1111–1126. https://doi.org/10.1016/j.biotechadv.2018.03.011

Bain, C. C., Bravo-Blas, A., Scott, C. L., Gomez Perdiguero, E., Geissmann, F., Henri, S., Malissen, B., Osborne, L. C., Artis, D., & Mowat, A. M. (2014). Constant replenishment from circulating monocytes maintains the macrophage pool in the intestine of adult mice. *Nature Immunology*, *15*(10), 929–937. https://doi.org/10.1038/ni.2967

Baroja-Mazo, A., Martín-Sánchez, F., Gomez, A. I., Martínez, C. M., Amores-Iniesta, J., Compan, V., Barberà-Cremades, M., Yagüe, J., Ruiz-Ortiz, E., Antón, J., Buján, S., Couillin, I., Brough, D., Arostegui, J. I., & Pelegrín, P. (2014). The NLRP3 inflammasome is released

as a particulate danger signal that amplifies the inflammatory response. *Nature Immunology*, *15*(8), 738–748. https://doi.org/10.1038/ni.2919

Bashore, A. C., Chung, A., Ibikunle, C., Yan, H., Xue, C., Li, M., Bauer, R. C., & Reilly, M. P. (2023). *Single-cell multimodal profiling of atherosclerosis identifies CD200 as a cell surface lineage marker of vascular smooth muscle cells and their derived cells* (p. 2023.09.29.557779). bioRxiv. https://doi.org/10.1101/2023.09.29.557779

Baud, V., Chissoe, S. L., Viegas-Péquignot, E., Diriong, S., N'Guyen, V. C., Roe, B. A., & Lipinski, M. (1995). EMR1, an unusual member in the family of hormone receptors with seven transmembrane segments. *Genomics*, *26*(2), 334–344. https://doi.org/10.1016/0888-7543(95)80218-b

Bazzoni, G., & Dejana, E. (2004). Endothelial Cell-to-Cell Junctions: Molecular Organization and Role in Vascular Homeostasis. *Physiological Reviews*, *84*(3), 869–901. https://doi.org/10.1152/physrev.00035.2003

Beattie, L., Sawtell, A., Mann, J., Frame, T. C. M., Teal, B., de Labastida Rivera, F., Brown, N., Walwyn-Brown, K., Moore, J. W. J., MacDonald, S., Lim, E.-K., Dalton, J. E., Engwerda, C. R., MacDonald, K. P., & Kaye, P. M. (2016). Bone marrow-derived and resident liver macrophages display unique transcriptomic signatures but similar biological functions. *Journal of Hepatology*, *65*(4), 758–768. https://doi.org/10.1016/j.jhep.2016.05.037

Bekkering, S., Arts, R. J. W., Novakovic, B., Kourtzelis, I., van der Heijden, C. D. C. C., Li, Y., Popa, C. D., Ter Horst, R., van Tuijl, J., Netea-Maier, R. T., van de Veerdonk, F. L., Chavakis, T., Joosten, L. A. B., van der Meer, J. W. M., Stunnenberg, H., Riksen, N. P., & Netea, M. G.

(2018). Metabolic Induction of Trained Immunity through the Mevalonate Pathway. *Cell*, *172*(1–2), 135-146.e9. https://doi.org/10.1016/j.cell.2017.11.025

Belenguer, G., Duart-Abadia, P., Jordán-Pla, A., Domingo-Muelas, A., Blasco-Chamarro, L., Ferrón, S. R., Morante-Redolat, J. M., & Fariñas, I. (2021). Adult Neural Stem Cells Are Alerted by Systemic Inflammation through TNF-α Receptor Signaling. *Cell Stem Cell*, *28*(2), 285-299.e9. https://doi.org/10.1016/j.stem.2020.10.016

Belle, A., Tanay, A., Bitincka, L., Shamir, R., & O'Shea, E. K. (2006). Quantification of protein half-lives in the budding yeast proteome. *Proceedings of the National Academy of Sciences*, *103*(35), 13004–13009. https://doi.org/10.1073/pnas.0605420103

Benditt, E. P., & Benditt, J. M. (1973). Evidence for a monoclonal origin of human atherosclerotic plaques. *Proceedings of the National Academy of Sciences of the United States of America*, *70*(6), 1753–1756. https://doi.org/10.1073/pnas.70.6.1753

Bennett, M. R., Sinha, S., & Owens, G. K. (2016). Vascular Smooth Muscle Cells in Atherosclerosis. *Circulation Research*, *118*(4), 692–702. https://doi.org/10.1161/CIRCRESAHA.115.306361

Bentzon, J. F., & Majesky, M. W. (2018). Lineage tracking of origin and fate of smooth muscle cells in atherosclerosis. *Cardiovascular Research*, *114*(4), 492–500. https://doi.org/10.1093/cvr/cvx251

Berk, B. C., Abe, J.-I., Min, W., Surapisitchat, J., & Yan, C. (2001). Endothelial Atheroprotective and Anti-inflammatory Mechanisms. *Annals of the New York Academy of Sciences*, *947*(1), 93–111. https://doi.org/10.1111/j.1749-6632.2001.tb03932.x

Black, P. H., & Garbutt, L. D. (2002). Stress, inflammation and cardiovascular disease. *Journal of Psychosomatic Research*, *52*(1), 1–23. https://doi.org/10.1016/S0022-3999(01)00302-6

Bonacina, F., Di Costanzo, A., Genkel, V., Kong, X. Y., Kroon, J., Stimjanin, E., Tsiantoulas, D., & Grootaert, M. O. (2023). The heterogeneous cellular landscape of atherosclerosis: Implications for future research and therapies. A collaborative review from the EAS young fellows. *Atherosclerosis*, *372*, 48–56. https://doi.org/10.1016/j.atherosclerosis.2023.03.021

Borisenko, G. G., Matsura, T., Liu, S.-X., Tyurin, V. A., Jianfei, J., Serinkan, F. B., & Kagan, V. E. (2003). Macrophage recognition of externalized phosphatidylserine and phagocytosis of apoptotic Jurkat cells—Existence of a threshold. *Archives of Biochemistry and Biophysics*, *413*(1), 41–52. https://doi.org/10.1016/S0003-9861(03)00083-3

Bruikman, C. S., Vreeken, D., Zhang, H., van Gils, M. J., Peter, J., van Zonneveld, A. J., Hovingh, G. K., & van Gils, J. M. (2020). The identification and function of a Netrin-1 mutation in a pedigree with premature atherosclerosis. *Atherosclerosis*, *301*, 84–92. https://doi.org/10.1016/j.atherosclerosis.2020.02.015

Bruns, A. M., & Horvath, C. M. (2014). Antiviral RNA recognition and assembly by RLR family innate immune sensors. *Cytokine & Growth Factor Reviews*, *25*(5), 507–512. https://doi.org/10.1016/j.cytogfr.2014.07.006

Buchrieser, J., James, W., & Moore, M. D. (2017). Human Induced Pluripotent Stem Cell-Derived Macrophages Share Ontogeny with MYB-Independent Tissue-Resident Macrophages. *Stem Cell Reports*, *8*(2), 334–345. https://doi.org/10.1016/j.stemcr.2016.12.020

Burtenshaw, D. (2020). *Diagnostic potential of extracellular vesicles (EVs) and single-cell photonics (scPH) in subclinical atherosclerotic disease* [Doctoral, Dublin City University]. https://doras.dcu.ie/26580/

Calaluce, R., Gubin, M. M., Davis, J. W., Magee, J. D., Chen, J., Kuwano, Y., Gorospe, M., & Atasoy, U. (2010). The RNA binding protein HuR differentially regulates unique subsets of mRNAs in estrogen receptor negative and estrogen receptor positive breast cancer. *BMC Cancer*, *10*(1), 126. https://doi.org/10.1186/1471-2407-10-126

Campbell, J. H., & Campbell, G. R. (2012). Smooth muscle phenotypic modulation—A personal experience. *Arteriosclerosis, Thrombosis, and Vascular Biology*, *32*(8), 1784–1789. https://doi.org/10.1161/ATVBAHA.111.243212

Campbell, K. A., Lipinski, M. J., Doran, A. C., Skaflen, M. D., Fuster, V., & McNamara, C. A. (2012). Lymphocytes and the adventitial immune response in atherosclerosis. *Circulation Research*, *110*(6), 889–900. https://doi.org/10.1161/CIRCRESAHA.111.263186

Canfrán-Duque, A., Rotllan, N., Zhang, X., Andrés-Blasco, I., Thompson, B. M., Sun, J., Price, N. L., Fernández-Fuertes, M., Fowler, J. W., Gómez-Coronado, D., Sessa, W. C., Giannarelli, C., Schneider, R. J., Tellides, G., McDonald, J. G., Fernández-Hernando, C., & Suárez, Y. (2023). Macrophage-Derived 25-Hydroxycholesterol Promotes Vascular Inflammation, Atherogenesis, and Lesion Remodeling. *Circulation*, *147*(5), 388–408. https://doi.org/10.1161/CIRCULATIONAHA.122.059062

Canton, J. (2014). Phagosome maturation in polarized macrophages. *Journal of Leukocyte Biology*, *96*(5), 729–738. https://doi.org/10.1189/jlb.1MR0114-021R

Cao, T., Zhang, L., Yao, L.-L., Zheng, F., Wang, L., Yang, J.-Y., Guo, L.-Y., Li, X.-Y., Yan, Y.-W., Pan, Y.-M., Jiang, M., Chen, L., Tang, J.-M., Chen, S.-Y., & Wang, J.-N. (2017). S100B promotes injury-induced vascular remodeling through modulating smooth muscle phenotype. *Biochimica Et Biophysica Acta. Molecular Basis of Disease*, *1863*(11), 2772–2782. https://doi.org/10.1016/j.bbadis.2017.07.002

Caplice, N. M., Bunch, T. J., Stalboerger, P. G., Wang, S., Simper, D., Miller, D. V., Russell, S. J., Litzow, M. R., & Edwards, W. D. (2003). Smooth muscle cells in human coronary atherosclerosis can originate from cells administered at marrow transplantation. *Proceedings of the National Academy of Sciences of the United States of America*, *100*(8), 4754–4759. https://doi.org/10.1073/pnas.0730743100

Carr, I. (1973). *The macrophage; a review of ultrastructure and function*. Academic Press.

Catravas, J. D., Callow, A. D., & Ryan, U. S. (1999). *Vascular Endothelium: Mechanisms of Cell Signaling*. IOS Press.

Chakraborty, R., Saddouk, F. Z., Carrao, A. C., Krause, D. S., Greif, D. M., & Martin, K. A. (2019). Promoters to Study Vascular Smooth Muscle. *Arteriosclerosis, Thrombosis, and Vascular Biology*, *39*(4), 603–612. https://doi.org/10.1161/ATVBAHA.119.312449

Chamley-Campbell, J., Campbell, G. R., & Ross, R. (1979). The smooth muscle cell in culture. *Physiological Reviews*, *59*(1), 1–61. https://doi.org/10.1152/physrev.1979.59.1.1

Chang, M. K., Bergmark, C., Laurila, A., Hörkkö, S., Han, K. H., Friedman, P., Dennis, E. A., & Witztum, J. L. (1999). Monoclonal antibodies against oxidized low-density lipoprotein bind to apoptotic cells and inhibit their phagocytosis by elicited macrophages: Evidence that oxidation-specific epitopes mediate macrophage recognition. *Proceedings of the*

National Academy of Sciences of the United States of America, *96*(11), 6353–6358. https://doi.org/10.1073/pnas.96.11.6353

Chappell, J., Harman, J. L., Narasimhan, V. M., Yu, H., Foote, K., Simons, B. D., Bennett, M. R., & Jørgensen, H. F. (2016a). Extensive Proliferation of a Subset of Differentiated, yet Plastic, Medial Vascular Smooth Muscle Cells Contributes to Neointimal Formation in Mouse Injury and Atherosclerosis Models. *Circulation Research*, *119*(12), 1313–1323. https://doi.org/10.1161/CIRCRESAHA.116.309799

Chappell, J., Harman, J. L., Narasimhan, V. M., Yu, H., Foote, K., Simons, B. D., Bennett, M. R., & Jørgensen, H. F. (2016b). Extensive Proliferation of a Subset of Differentiated, yet Plastic, Medial Vascular Smooth Muscle Cells Contributes to Neointimal Formation in Mouse Injury and Atherosclerosis Models. *Circulation Research*, *119*(12), 1313–1323. https://doi.org/10.1161/CIRCRESAHA.116.309799

Chen, D., Zhang, C., Chen, J., Yang, M., Afzal, T. A., An, W., Maguire, E. M., He, S., Luo, J., Wang, X., Zhao, Y., Wu, Q., & Xiao, Q. (2021). miRNA-200c-3p promotes endothelial to mesenchymal transition and neointimal hyperplasia in artery bypass grafts. *The Journal of Pathology*, *253*(2), 209–224. https://doi.org/10.1002/path.5574

Chen, P.-Y., Qin, L., Baeyens, N., Li, G., Afolabi, T., Budatha, M., Tellides, G., Schwartz, M. A., & Simons, M. (2015). Endothelial-to-mesenchymal transition drives atherosclerosis progression. *The Journal of Clinical Investigation*, *125*(12), 4514–4528. https://doi.org/10.1172/JCI82719

Chen, W., Schilperoort, M., Cao, Y., Shi, J., Tabas, I., & Tao, W. (2022). Macrophage-targeted nanomedicine for the diagnosis and treatment of atherosclerosis. *Nature Reviews. Cardiology*, *19*(4), 228–249. https://doi.org/10.1038/s41569-021-00629-x

Cheng, M., Yang, L., Fan, M., An, S., & Li, J. (2019). Proatherogenic stimuli induce HuR in atherosclerosis through MAPK/ErK pathway. *American Journal of Translational Research*, *11*(4), 2317–2327.

Cherepanova, O. A., Gomez, D., Shankman, L. S., Swiatlowska, P., Williams, J., Sarmento, O. F., Alencar, G. F., Hess, D. L., Bevard, M. H., Greene, E. S., Murgai, M., Turner, S. D., Geng, Y.-J., Bekiranov, S., Connelly, J. J., Tomilin, A., & Owens, G. K. (2016). Activation of the pluripotency factor OCT4 in smooth muscle cells is atheroprotective. *Nature Medicine*, *22*(6), 657–665. https://doi.org/10.1038/nm.4109

Cherepanova, O. A., Srikakulapu, P., Greene, E. S., Chaklader, M., Haskins, R. M., McCanna, M. E., Bandyopadhyay, S., Ban, B., Leitinger, N., McNamara, C. A., & Owens, G. K. (2020). Novel Autoimmune IgM Antibody Attenuates Atherosclerosis in IgM Deficient Low-Fat Diet-Fed, but Not Western Diet-Fed Apoe-/- Mice. *Arteriosclerosis, Thrombosis, and Vascular Biology*, *40*(1), 206–219. https://doi.org/10.1161/ATVBAHA.119.312771

Cheung, C., Bernardo, A. S., Trotter, M. W. B., Pedersen, R. A., & Sinha, S. (2012). Generation of human vascular smooth muscle subtypes provides insight into embryological origin-dependent disease susceptibility. *Nature Biotechnology*, *30*(2), 165–173. https://doi.org/10.1038/nbt.2107

Chistiakov, D. A., Bobryshev, Y. V., Nikiforov, N. G., Elizova, N. V., Sobenin, I. A., & Orekhov, A. N. (2015). RETRACTED: Macrophage phenotypic plasticity in atherosclerosis: The

associated features and the peculiarities of the expression of inflammatory genes. *International Journal of Cardiology*, *184*, 436–445. https://doi.org/10.1016/j.ijcard.2015.03.055

Chistiakov, D. A., Bobryshev, Y. V., & Orekhov, A. N. (2016). Macrophage-mediated cholesterol handling in atherosclerosis. *Journal of Cellular and Molecular Medicine*, *20*(1), 17–28. https://doi.org/10.1111/jcmm.12689

Chistiakov, D. A., Orekhov, A. N., & Bobryshev, Y. V. (2015). Vascular smooth muscle cell in atherosclerosis. *Acta Physiologica (Oxford, England)*, *214*(1), 33–50. https://doi.org/10.1111/apha.12466

Chistiakov, D. A., Sobenin, I. A., & Orekhov, A. N. (2013). Vascular extracellular matrix in atherosclerosis. *Cardiology in Review*, *21*(6), 270–288. https://doi.org/10.1097/CRD.0b013e31828c5ced

Cho, H.-J., Cho, H.-J., Lee, H.-J., Song, M.-K., Seo, J.-Y., Bae, Y.-H., Kim, J.-Y., Lee, H.-Y., Lee, W., Koo, B.-K., Oh, B.-H., Park, Y.-B., & Kim, H.-S. (2013). Vascular Calcifying Progenitor Cells Possess Bidirectional Differentiation Potentials. *PLOS Biology*, *11*(4), e1001534. https://doi.org/10.1371/journal.pbio.1001534

Choi, H. Y., Rahmani, M., Wong, B. W., Allahverdian, S., McManus, B. M., Pickering, J. G., Chan, T., & Francis, G. A. (2009). ATP-binding cassette transporter A1 expression and apolipoprotein A-I binding are impaired in intima-type arterial smooth muscle cells. *Circulation*, *119*(25), 3223–3231. https://doi.org/10.1161/CIRCULATIONAHA.108.841130

Cines, D. B., Pollak, E. S., Buck, C. A., Loscalzo, J., Zimmerman, G. A., McEver, R. P., Pober, J. S., Wick, T. M., Konkle, B. A., Schwartz, B. S., Barnathan, E. S., McCrae, K. R., Hug, B. A.,

Schmidt, A. M., & Stern, D. M. (1998). Endothelial cells in physiology and in the pathophysiology of vascular disorders. *Blood*, *91*(10), 3527–3561.

Cohn, J. N. (2001). Arterial compliance to stratify cardiovascular risk: More precision in therapeutic decision making. *American Journal of Hypertension*, *14*(8 Pt 2), 258S-263S. https://doi.org/10.1016/s0895-7061(01)02154-9

Cooley, B. C., Nevado, J., Mellad, J., Yang, D., St Hilaire, C., Negro, A., Fang, F., Chen, G., San, H., Walts, A. D., Schwartzbeck, R. L., Taylor, B., Lanzer, J. D., Wragg, A., Elagha, A., Beltran, L. E., Berry, C., Feil, R., Virmani, R., … Boehm, M. (2014). TGF-β signaling mediates endothelial-to-mesenchymal transition (EndMT) during vein graft remodeling. *Science Translational Medicine*, *6*(227), 227ra34. https://doi.org/10.1126/scitranslmed.3006927

Covas, D. T., Panepucci, R. A., Fontes, A. M., Silva, W. A., Orellana, M. D., Freitas, M. C. C., Neder, L., Santos, A. R. D., Peres, L. C., Jamur, M. C., & Zago, M. A. (2008). Multipotent mesenchymal stromal cells obtained from diverse human tissues share functional properties and gene-expression profile with CD146+ perivascular cells and fibroblasts. *Experimental Hematology*, *36*(5), 642–654. https://doi.org/10.1016/j.exphem.2007.12.015

D'Arcy, M. S. (2019). Cell death: A review of the major forms of apoptosis, necrosis and autophagy. *Cell Biology International*, *43*(6), 582–592. https://doi.org/10.1002/cbin.11137

De Backer, G., Ambrosioni, E., Borch-Johnsen, K., Brotons, C., Cifkova, R., Dallongeville, J., Ebrahim, S., Faergeman, O., Graham, I., Mancia, G., Manger Cats, V., Orth-Gomér, K., Perk, J., Pyörälä, K., Rodicio, J. L., Sans, S., Sansoy, V., Sechtem, U., Silber, S., … Third

Joint Task Force of European and Other Societies on Cardiovascular Disease Prevention in Clinical Practice. (2003). European guidelines on cardiovascular disease prevention in clinical practice. Third Joint Task Force of European and Other Societies on Cardiovascular Disease Prevention in Clinical Practice. *European Heart Journal*, *24*(17), 1601–1610. https://doi.org/10.1016/s0195-668x(03)00347-6

DeBakey, M. E., & Glaeser, D. H. (2000). Patterns of atherosclerosis: Effect of risk factors on recurrence and survival—analysis of 11,890 cases with more than 25-year follow-up. *The American Journal of Cardiology*, *85*(9), 1045–1053. https://doi.org/10.1016/S0002-9149(00)00694-9

Decker, C., Sadhu, S., & Fredman, G. (2021). Pro-Resolving Ligands Orchestrate Phagocytosis. *Frontiers in Immunology*, *12*, 660865. https://doi.org/10.3389/fimmu.2021.660865

Deloulme, J. C., Raponi, E., Gentil, B. J., Bertacchi, N., Marks, A., Labourdette, G., & Baudier, J. (2004). Nuclear expression of S100B in oligodendrocyte progenitor cells correlates with differentiation toward the oligodendroglial lineage and modulates oligodendrocytes maturation. *Molecular and Cellular Neurosciences*, *27*(4), 453–465. https://doi.org/10.1016/j.mcn.2004.07.008

Deng, Y., Lin, C., Zhou, H. J., & Min, W. (2017). Smooth muscle cell differentiation: Mechanisms and models for vascular diseases. *Frontiers in Biology*, *12*(6), 392–405. https://doi.org/10.1007/s11515-017-1473-z

DeRuiter, M. c., Poelmann, R. e., VanMunsteren, J. c., Mironov, V., Markwald, R. r., & Gittenberger-de Groot, A. c. (1997). Embryonic Endothelial Cells Transdifferentiate Into

Mesenchymal Cells Expressing Smooth Muscle Actins In Vivo and In Vitro. *Circulation Research*, *80*(4), 444–451. https://doi.org/10.1161/01.RES.80.4.444

Di Luca, M. (2019). *The embryological origin of resident vascular stem cells – implications for vascular disease* [Doctoral, Dublin City University]. https://doras.dcu.ie/23734/

Di Luca, M., Fitzpatrick, E., Burtenshaw, D., Liu, W., Helt, J.-C., Hakimjavadi, R., Corcoran, E., Gusti, Y., Sheridan, D., Harman, S., Lally, C., Redmond, E. M., & Cahill, P. A. (2021). The calcium binding protein S100β marks hedgehog-responsive resident vascular stem cells within vascular lesions. *Npj Regenerative Medicine*, *6*(1), Article 1. https://doi.org/10.1038/s41536-021-00120-8

DiRenzo, D., Owens, G. K., & Leeper, N. J. (2017). "Attack of the Clones": Commonalities Between Cancer and Atherosclerosis. *Circulation Research*, *120*(4), 624–626. https://doi.org/10.1161/CIRCRESAHA.116.310091

Dittmann, N. L., Torabi, P., Watson, A. E. S., Yuzwa, S. A., & Voronova, A. (2023). Culture Protocol and Transcriptomic Analysis of Murine SVZ NPCs and OPCs. *Stem Cell Reviews and Reports*, *19*(4), 983–1000. https://doi.org/10.1007/s12015-022-10492-z

Dobnikar, L., Taylor, A. L., Chappell, J., Oldach, P., Harman, J. L., Oerton, E., Dzierzak, E., Bennett, M. R., Spivakov, M., & Jørgensen, H. F. (2018). Disease-relevant transcriptional signatures identified in individual smooth muscle cells from healthy mouse vessels. *Nature Communications*, *9*(1), 4567. https://doi.org/10.1038/s41467-018-06891-x

Dominici, M., Le Blanc, K., Mueller, I., Slaper-Cortenbach, I., Marini, F., Krause, D., Deans, R., Keating, A., Prockop, D., & Horwitz, E. (2006). Minimal criteria for defining multipotent

mesenchymal stromal cells. The International Society for Cellular Therapy position statement. *Cytotherapy*, *8*(4), 315–317. https://doi.org/10.1080/14653240600855905

Doran, A. C., Yurdagul, A., & Tabas, I. (2020). Efferocytosis in health and disease. *Nature Reviews. Immunology*, *20*(4), 254–267. https://doi.org/10.1038/s41577-019-0240-6

Dubland, J. A., Allahverdian, S., Besler, K. J., Ortega, C., Wang, Y., Pryma, C. S., Boukais, K., Chan, T., Seidman, M. A., & Francis, G. A. (2021). Low LAL (Lysosomal Acid Lipase) Expression by Smooth Muscle Cells Relative to Macrophages as a Mechanism for Arterial Foam Cell Formation. *Arteriosclerosis, Thrombosis, and Vascular Biology*, *41*(6), e354–e368. https://doi.org/10.1161/ATVBAHA.120.316063

Duffy, D., & Rader, D. J. (2009). Update on strategies to increase HDL quantity and function. *Nature Reviews Cardiology*, *6*(7), 455–463. https://doi.org/10.1038/nrcardio.2009.94

Dulak, J., Szade, K., Szade, A., Nowak, W., & Józkowicz, A. (2015). Adult stem cells: Hopes and hypes of regenerative medicine. *Acta Biochimica Polonica*, *62*(3), 329–337. https://doi.org/10.18388/abp.2015_1023

Ezekowitz, R. A., Sastry, K., Bailly, P., & Warner, A. (1990). Molecular characterization of the human macrophage mannose receptor: Demonstration of multiple carbohydrate recognition-like domains and phagocytosis of yeasts in Cos-1 cells. *Journal of Experimental Medicine*, *172*(6), 1785–1794. https://doi.org/10.1084/jem.172.6.1785

Fadok, V. A., Voelker, D. R., Campbell, P. A., Cohen, J. J., Bratton, D. L., & Henson, P. M. (1992). Exposure of phosphatidylserine on the surface of apoptotic lymphocytes triggers specific recognition and removal by macrophages. *The Journal of Immunology*, *148*(7), 2207–2216. https://doi.org/10.4049/jimmunol.148.7.2207

Falcão, A. M., van Bruggen, D., Marques, S., Meijer, M., Jäkel, S., Agirre, E., Samudyata, null, Floriddia, E. M., Vanichkina, D. P., Ffrench-Constant, C., Williams, A., Guerreiro-Cacais, A. O., & Castelo-Branco, G. (2018). Disease-specific oligodendrocyte lineage cells arise in multiple sclerosis. *Nature Medicine*, *24*(12), 1837–1844. https://doi.org/10.1038/s41591-018-0236-y

Feil, S., Fehrenbacher, B., Lukowski, R., Essmann, F., Schulze-Osthoff, K., Schaller, M., & Feil, R. (2014). Transdifferentiation of vascular smooth muscle cells to macrophage-like cells during atherogenesis. *Circulation Research*, *115*(7), 662–667. https://doi.org/10.1161/CIRCRESAHA.115.304634

Feng, J. Q., Ward, L. M., Liu, S., Lu, Y., Xie, Y., Yuan, B., Yu, X., Rauch, F., Davis, S. I., Zhang, S., Rios, H., Drezner, M. K., Quarles, L. D., Bonewald, L. F., & White, K. E. (2006). Loss of DMP1 causes rickets and osteomalacia and identifies a role for osteocytes in mineral metabolism. *Nature Genetics*, *38*(11), Article 11. https://doi.org/10.1038/ng1905

Fiorelli, S., Cosentino, N., Porro, B., Fabbiocchi, F., Niccoli, G., Fracassi, F., Capra, N., Barbieri, S., Crea, F., Marenzi, G., Cavalca, V., Tremoli, E., & Eligini, S. (2021). Netrin-1 in Atherosclerosis: Relationship between Human Macrophage Intracellular Levels and In Vivo Plaque Morphology. *Biomedicines*, *9*(2), 168. https://doi.org/10.3390/biomedicines9020168

Fishbein, G. A., & Fishbein, M. C. (2009). Arteriosclerosis: Rethinking the current classification. *Archives of Pathology & Laboratory Medicine*, *133*(8), 1309–1316. https://doi.org/10.5858/133.8.1309

Fishbein, M. C., & Fishbein, G. A. (2015). Arteriosclerosis: Facts and fancy. *Cardiovascular Pathology*, *24*(6), 335–342. https://doi.org/10.1016/j.carpath.2015.07.007

Fisher, E. A. (2016). Regression of Atherosclerosis: The Journey From the Liver to the Plaque and Back. *Arteriosclerosis, Thrombosis, and Vascular Biology*, *36*(2), 226–235. https://doi.org/10.1161/ATVBAHA.115.301926

Forrester, S. J., & Griendling, K. K. (2017). Mitochondrial Respiration and Atherosclerosis: R-E-S-P-I-R-E. Find Out What it Means to Mφ (and VSMC). *Arteriosclerosis, Thrombosis, and Vascular Biology*, *37*(12), 2229–2230. https://doi.org/10.1161/ATVBAHA.117.310298

Franklin, B. S., Bossaller, L., De Nardo, D., Ratter, J. M., Stutz, A., Engels, G., Brenker, C., Nordhoff, M., Mirandola, S. R., Al-Amoudi, A., Mangan, M. S., Zimmer, S., Monks, B. G., Fricke, M., Schmidt, R. E., Espevik, T., Jones, B., Jarnicki, A. G., Hansbro, P. M., … Latz, E. (2014). The adaptor ASC has extracellular and "prionoid" activities that propagate inflammation. *Nature Immunology*, *15*(8), 727–737. https://doi.org/10.1038/ni.2913

Fraser, H. B., Hirsh, A. E., Giaever, G., Kumm, J., & Eisen, M. B. (2004). Noise Minimization in Eukaryotic Gene Expression. *PLOS Biology*, *2*(6), e137. https://doi.org/10.1371/journal.pbio.0020137

Fredman, G., Hellmann, J., Proto, J. D., Kuriakose, G., Colas, R. A., Dorweiler, B., Connolly, E. S., Solomon, R., Jones, D. M., Heyer, E. J., Spite, M., & Tabas, I. (2016). An imbalance between specialized pro-resolving lipid mediators and pro-inflammatory leukotrienes promotes instability of atherosclerotic plaques. *Nature Communications*, *7*, 12859. https://doi.org/10.1038/ncomms12859

Frid, M. G., Kale, V. A., & Stenmark, K. R. (2002). Mature Vascular Endothelium Can Give Rise to Smooth Muscle Cells via Endothelial-Mesenchymal Transdifferentiation. *Circulation Research*, *90*(11), 1189–1196. https://doi.org/10.1161/01.RES.0000021432.70309.28

Galkina, E., Kadl, A., Sanders, J., Varughese, D., Sarembock, I. J., & Ley, K. (2006). Lymphocyte recruitment into the aortic wall before and during development of atherosclerosis is partially L-selectin dependent. *The Journal of Experimental Medicine*, *203*(5), 1273–1282. https://doi.org/10.1084/jem.20052205

Gammill, L. S., & Bronner-Fraser, M. (2003). Neural crest specification: Migrating into genomics. *Nature Reviews. Neuroscience*, *4*(10), 795–805. https://doi.org/10.1038/nrn1219

Gandhi, S. J., Zenklusen, D., Lionnet, T., & Singer, R. H. (2011). Transcription of functionally related constitutive genes is not coordinated. *Nature Structural & Molecular Biology*, *18*(1), 27–34. https://doi.org/10.1038/nsmb.1934

Gautier, E. L., Shay, T., Miller, J., Greter, M., Jakubzick, C., Ivanov, S., Helft, J., Chow, A., Elpek, K. G., Gordonov, S., Mazloom, A. R., Ma'ayan, A., Chua, W.-J., Hansen, T. H., Turley, S. J., Merad, M., & Randolph, G. J. (2012). Gene-expression profiles and transcriptional regulatory pathways that underlie the identity and diversity of mouse tissue macrophages. *Nature Immunology*, *13*(11), 1118–1128. https://doi.org/10.1038/ni.2419

Geng, S., Zhang, Y., Yi, Z., Lu, R., & Li, L. (2021). Resolving monocytes generated through TRAM deletion attenuate atherosclerosis. *JCI Insight*, *6*(20), e149651. https://doi.org/10.1172/jci.insight.149651

Gerlach, B. D., Ampomah, P. B., Yurdagul, A., Liu, C., Lauring, M. C., Wang, X., Kasikara, C., Kong, N., Shi, J., Tao, W., & Tabas, I. (2021). Efferocytosis induces macrophage proliferation to

help resolve tissue injury. *Cell Metabolism*, *33*(12), 2445-2463.e8. https://doi.org/10.1016/j.cmet.2021.10.015

Getz, G. S., & Reardon, C. A. (2012). Animal Models of Atherosclerosis. *Arteriosclerosis, Thrombosis, and Vascular Biology*, *32*(5), 1104–1115. https://doi.org/10.1161/ATVBAHA.111.237693

Gimbrone Jr., M. A., Topper, J. N., Nagel, T., Anderson, K. R., & Garcia-Cardeña, G. (2000). Endothelial Dysfunction, Hemodynamic Forces, and Atherogenesisa. *Annals of the New York Academy of Sciences*, *902*(1), 230–240. https://doi.org/10.1111/j.1749-6632.2000.tb06318.x

Gimona, M., Djinovic-Carugo, K., Kranewitter, W. J., & Winder, S. J. (2002). Functional plasticity of CH domains. *FEBS Letters*, *513*(1), 98–106. https://doi.org/10.1016/s0014-5793(01)03240-9

Ginhoux, F., & Guilliams, M. (2016). Tissue-Resident Macrophage Ontogeny and Homeostasis. *Immunity*, *44*(3), 439–449. https://doi.org/10.1016/j.immuni.2016.02.024

Glass, C. K., & Witztum, J. L. (2001). Atherosclerosis. The road ahead. *Cell*, *104*(4), 503–516. https://doi.org/10.1016/s0092-8674(01)00238-0

Gofman, J. W., & Lindgren, F. (1950). The role of lipids and lipoproteins in atherosclerosis. *Science (New York, N.Y.)*, *111*(2877), 166–171. https://doi.org/10.1126/science.111.2877.166

Gomez, D., Baylis, R. A., Durgin, B. G., Newman, A. A. C., Alencar, G. F., Mahan, S., St Hilaire, C., Müller, W., Waisman, A., Francis, S. E., Pinteaux, E., Randolph, G. J., Gram, H., & Owens, G. K. (2018). Interleukin-1β has atheroprotective effects in advanced atherosclerotic

lesions of mice. *Nature Medicine*, *24*(9), 1418–1429. https://doi.org/10.1038/s41591-018-0124-5

Gomez, D., & Owens, G. K. (2012). Smooth muscle cell phenotypic switching in atherosclerosis. *Cardiovascular Research*, *95*(2), 156–164. https://doi.org/10.1093/cvr/cvs115

Gomez, D., Shankman, L. S., Nguyen, A. T., & Owens, G. K. (2013). Detection of histone modifications at specific gene loci in single cells in histological sections. *Nature Methods*, *10*(2), 171–177. https://doi.org/10.1038/nmeth.2332

Gomez, D., Swiatlowska, P., & Owens, G. K. (2015). Epigenetic Control of Smooth Muscle Cell Identity and Lineage Memory. *Arteriosclerosis, Thrombosis, and Vascular Biology*, *35*(12), 2508–2516. https://doi.org/10.1161/ATVBAHA.115.305044

Gomez Perdiguero, E., Klapproth, K., Schulz, C., Busch, K., Azzoni, E., Crozet, L., Garner, H., Trouillet, C., de Bruijn, M. F., Geissmann, F., & Rodewald, H.-R. (2015). Tissue-resident macrophages originate from yolk-sac-derived erythro-myeloid progenitors. *Nature*, *518*(7540), 547–551. https://doi.org/10.1038/nature13989

Gonzalez, J. M., Franzke, C.-W., Yang, F., Romero, R., & Girardi, G. (2011). Complement activation triggers metalloproteinases release inducing cervical remodeling and preterm birth in mice. *The American Journal of Pathology*, *179*(2), 838–849. https://doi.org/10.1016/j.ajpath.2011.04.024

Gordon, S., & Martinez, F. O. (2010). Alternative Activation of Macrophages: Mechanism and Functions. *Immunity*, *32*(5), 593–604. https://doi.org/10.1016/j.immuni.2010.05.007

Gräbner, R., Lötzer, K., Döpping, S., Hildner, M., Radke, D., Beer, M., Spanbroek, R., Lippert, B., Reardon, C. A., Getz, G. S., Fu, Y.-X., Hehlgans, T., Mebius, R. E., van der Wall, M.,

Kruspe, D., Englert, C., Lovas, A., Hu, D., Randolph, G. J., … Habenicht, A. J. R. (2009). Lymphotoxin β receptor signaling promotes tertiary lymphoid organogenesis in the aorta adventitia of aged ApoE−/− mice. *Journal of Experimental Medicine*, *206*(1), 233–248. https://doi.org/10.1084/jem.20080752

Gronthos, S., Franklin, D. M., Leddy, H. A., Robey, P. G., Storms, R. W., & Gimble, J. M. (2001). Surface protein characterization of human adipose tissue-derived stromal cells. *Journal of Cellular Physiology*, *189*(1), 54–63. https://doi.org/10.1002/jcp.1138

Grover, S. P., & Mackman, N. (2020). Tissue factor in atherosclerosis and atherothrombosis. *Atherosclerosis*, *307*, 80–86. https://doi.org/10.1016/j.atherosclerosis.2020.06.003

Guenther, S., Vrekoussis, T., Heublein, S., Bayer, B., Anz, D., Knabl, J., Navrozoglou, I., Dian, D., Friese, K., Makrigiannakis, A., & Jeschke, U. (2012). Decidual Macrophages Are Significantly Increased in Spontaneous Miscarriages and Over-Express FasL: A Potential Role for Macrophages in Trophoblast Apoptosis. *International Journal of Molecular Sciences*, *13*(7), Article 7. https://doi.org/10.3390/ijms13079069

Guilliams, M., De Kleer, I., Henri, S., Post, S., Vanhoutte, L., De Prijck, S., Deswarte, K., Malissen, B., Hammad, H., & Lambrecht, B. N. (2013). Alveolar macrophages develop from fetal monocytes that differentiate into long-lived cells in the first week of life via GM-CSF. *Journal of Experimental Medicine*, *210*(10), 1977–1992. https://doi.org/10.1084/jem.20131199

Guilliams, M., Ginhoux, F., Jakubzick, C., Naik, S. H., Onai, N., Schraml, B. U., Segura, E., Tussiwand, R., & Yona, S. (2014). Dendritic cells, monocytes and macrophages: A unified

nomenclature based on ontogeny. *Nature Reviews Immunology*, *14*(8), 571–578. https://doi.org/10.1038/nri3712

Guilliams, M., & Scott, C. L. (2017). Does niche competition determine the origin of tissue-resident macrophages? *Nature Reviews Immunology*, *17*(7), 451–460. https://doi.org/10.1038/nri.2017.42

Gupta, D., Shah, H. P., Malu, K., Berliner, N., & Gaines, P. (2014). Differentiation and Characterization of Myeloid Cells. *Current Protocols in Immunology / Edited by John E. Coligan ... [et Al.]*, *104*, Unit-22F.5. https://doi.org/10.1002/0471142735.im22f05s104

Gusti, Y. S. Y. (2023). *Epigenetic profiling of mouse and human vascular smooth muscle cells, S100β resident vascular stem cells and their lineage-specific progeny in vitro* [Doctoral, Dublin City University]. https://doras.dcu.ie/28190/

Guzik, T. J., Hoch, N. E., Brown, K. A., McCann, L. A., Rahman, A., Dikalov, S., Goronzy, J., Weyand, C., & Harrison, D. G. (2007). Role of the T cell in the genesis of angiotensin II–induced hypertension and vascular dysfunction. *Journal of Experimental Medicine*, *204*(10), 2449–2460. https://doi.org/10.1084/jem.20070657

Haka, A. S., Grosheva, I., Chiang, E., Buxbaum, A. R., Baird, B. A., Pierini, L. M., & Maxfield, F. R. (2009). Macrophages create an acidic extracellular hydrolytic compartment to digest aggregated lipoproteins. *Molecular Biology of the Cell*, *20*(23), 4932–4940. https://doi.org/10.1091/mbc.e09-07-0559

Haldar, M., Kohyama, M., So, A. Y.-L., Kc, W., Wu, X., Briseño, C. G., Satpathy, A. T., Kretzer, N. M., Arase, H., Rajasekaran, N. S., Wang, L., Egawa, T., Igarashi, K., Baltimore, D., Murphy, T. L., & Murphy, K. M. (2014). Heme-Mediated SPI-C Induction Promotes Monocyte

Differentiation into Iron-Recycling Macrophages. *Cell*, *156*(6), 1223–1234. https://doi.org/10.1016/j.cell.2014.01.069

Hanayama, R., Tanaka, M., Miwa, K., Shinohara, A., Iwamatsu, A., & Nagata, S. (2002). Identification of a factor that links apoptotic cells to phagocytes. *Nature*, *417*(6885), 182–187. https://doi.org/10.1038/417182a

Hansson, G. K., & Hermansson, A. (2011). The immune system in atherosclerosis. *Nature Immunology*, *12*(3), 204–212. https://doi.org/10.1038/ni.2001

Hansson Göran K. (2005). Inflammation, Atherosclerosis, and Coronary Artery Disease. *New England Journal of Medicine*, *352*(16), 1685–1695. https://doi.org/10.1056/NEJMra043430

Hao, H., Gabbiani, G., & Bochaton-Piallat, M.-L. (2003). Arterial Smooth Muscle Cell Heterogeneity. *Arteriosclerosis, Thrombosis, and Vascular Biology*, *23*(9), 1510–1520. https://doi.org/10.1161/01.ATV.0000090130.85752.ED

Hara, H., & Yokoyama, S. (1991). Interaction of free apolipoproteins with macrophages. Formation of high density lipoprotein-like lipoproteins and reduction of cellular cholesterol. *Journal of Biological Chemistry*, *266*(5), 3080–3086. https://doi.org/10.1016/S0021-9258(18)49957-7

Harman, S. (2023). *Characterisation of extracellular vesicles (EVs) from dysfunctional endothelial cells following exposure to alcohol* [Masters, Dublin City University]. https://doras.dcu.ie/27999/

Hautmann, M. B., Adam, P. J., & Owens, G. K. (1999). Similarities and differences in smooth muscle alpha-actin induction by TGF-beta in smooth muscle versus non-smooth muscle

cells. *Arteriosclerosis, Thrombosis, and Vascular Biology*, *19*(9), 2049–2058. https://doi.org/10.1161/01.atv.19.9.2049

He, L., Li, Y., Li, Y., Pu, W., Huang, X., Tian, X., Wang, Y., Zhang, H., Liu, Q., Zhang, L., Zhao, H., Tang, J., Ji, H., Cai, D., Han, Z., Han, Z., Nie, Y., Hu, S., Wang, Q.-D., … Zhou, B. (2017). Enhancing the precision of genetic lineage tracing using dual recombinases. *Nature Medicine*, *23*(12), 1488–1498. https://doi.org/10.1038/nm.4437

Heidenreich, P. A., Trogdon, J. G., Khavjou, O. A., Butler, J., Dracup, K., Ezekowitz, M. D., Finkelstein, E. A., Hong, Y., Johnston, S. C., Khera, A., Lloyd-Jones, D. M., Nelson, S. A., Nichol, G., Orenstein, D., Wilson, P. W. F., & Woo, Y. J. (2011). Forecasting the Future of Cardiovascular Disease in the United States. *Circulation*, *123*(8), 933–944. https://doi.org/10.1161/CIR.0b013e31820a55f5

Hempleman, S. C., & Warburton, S. J. (2013). Comparative embryology of the carotid body. *Respiratory Physiology & Neurobiology*, *185*(1), 3–8. https://doi.org/10.1016/j.resp.2012.08.004

Herre, J., Marshall, A. S. J., Caron, E., Edwards, A. D., Williams, D. L., Schweighoffer, E., Tybulewicz, V., Sousa, C. R. e, Gordon, S., & Brown, G. D. (2004). Dectin-1 uses novel mechanisms for yeast phagocytosis in macrophages. *Blood*, *104*(13), 4038–4045. https://doi.org/10.1182/blood-2004-03-1140

Herrero-Fernandez, B., Gomez-Bris, R., Somovilla-Crespo, B., & Gonzalez-Granado, J. M. (2019). Immunobiology of Atherosclerosis: A Complex Net of Interactions. *International Journal of Molecular Sciences*, *20*(21), 5293. https://doi.org/10.3390/ijms20215293

Herring, B. P., Hoggatt, A. M., Burlak, C., & Offermanns, S. (2014). Previously differentiated medial vascular smooth muscle cells contribute to neointima formation following vascular injury. *Vascular Cell*, *6*, 21. https://doi.org/10.1186/2045-824X-6-21

Herzenberg, L. A., Tung, J., Moore, W. A., Herzenberg, L. A., & Parks, D. R. (2006). Interpreting flow cytometry data: A guide for the perplexed. *Nature Immunology*, *7*(7), 681–685. https://doi.org/10.1038/ni0706-681

Hiemstra, P. S. (2006). Defensins and cathelicidins in inflammatory lung disease: Beyond antimicrobial activity. *Biochemical Society Transactions*, *34*(2), 276–278. https://doi.org/10.1042/BST0340276

Higuchi, R., Fockler, C., Dollinger, G., & Watson, R. (1993). Kinetic PCR Analysis: Real-time Monitoring of DNA Amplification Reactions. *Bio/Technology*, *11*(9), 1026–1030. https://doi.org/10.1038/nbt0993-1026

Hirayama, D., Iida, T., & Nakase, H. (2017). The Phagocytic Function of Macrophage-Enforcing Innate Immunity and Tissue Homeostasis. *International Journal of Molecular Sciences*, *19*(1), 92. https://doi.org/10.3390/ijms19010092

Hoeffel, G., Chen, J., Lavin, Y., Low, D., Almeida, F. F., See, P., Beaudin, A. E., Lum, J., Low, I., Forsberg, E. C., Poidinger, M., Zolezzi, F., Larbi, A., Ng, L. G., Chan, J. K. Y., Greter, M., Becher, B., Samokhvalov, I. M., Merad, M., & Ginhoux, F. (2015). C-Myb+ Erythro-Myeloid Progenitor-Derived Fetal Monocytes Give Rise to Adult Tissue-Resident Macrophages. *Immunity*, *42*(4), 665–678. https://doi.org/10.1016/j.immuni.2015.03.011

Hoek, R. M., Ruuls, S. R., Murphy, C. A., Wright, G. J., Goddard, R., Zurawski, S. M., Blom, B., Homola, M. E., Streit, W. J., Brown, M. H., Barclay, A. N., & Sedgwick, J. D. (2000). Down-

regulation of the macrophage lineage through interaction with OX2 (CD200). *Science (New York, N.Y.)*, *290*(5497), 1768–1771. https://doi.org/10.1126/science.290.5497.1768

Hohsfield, L. A., Tsourmas, K. I., Ghorbanian, Y., Syage, A. R., Kim, S. J., Cheng, Y., Furman, S., Inlay, M. A., Lane, T. E., & Green, K. N. (2022). MAC2 is a long-lasting marker of peripheral cell infiltrates into the mouse CNS after bone marrow transplantation and coronavirus infection. *Glia*, *70*(5), 875–891. https://doi.org/10.1002/glia.24144

Holness, C. L., & Simmons, D. L. (1993). Molecular cloning of CD68, a human macrophage marker related to lysosomal glycoproteins. *Blood*, *81*(6), 1607–1613.

Hoofnagle, M. H., Thomas, J. A., Wamhoff, B. R., & Owens, G. K. (2006). Origin of Neointimal Smooth Muscle. *Arteriosclerosis, Thrombosis, and Vascular Biology*, *26*(12), 2579–2581. https://doi.org/10.1161/01.ATV.0000249623.79871.bc

Hu, Y., Zhang, Z., Torsney, E., Afzal, A. R., Davison, F., Metzler, B., & Xu, Q. (2004). Abundant progenitor cells in the adventitia contribute to atherosclerosis of vein grafts in ApoE-deficient mice. *The Journal of Clinical Investigation*, *113*(9), 1258–1265. https://doi.org/10.1172/JCI19628

Huang, H., Song, T.-J., Li, X., Hu, L., He, Q., Liu, M., Lane, M. D., & Tang, Q.-Q. (2009). BMP signaling pathway is required for commitment of C3H10T1/2 pluripotent stem cells to the adipocyte lineage. *Proceedings of the National Academy of Sciences*, *106*(31), 12670–12675. https://doi.org/10.1073/pnas.0906266106

Huang, S. X. L., Islam, M. N., O'Neill, J., Hu, Z., Yang, Y.-G., Chen, Y.-W., Mumau, M., Green, M. D., Vunjak-Novakovic, G., Bhattacharya, J., & Snoeck, H.-W. (2014). Efficient generation

of lung and airway epithelial cells from human pluripotent stem cells. *Nature Biotechnology*, *32*(1), 84–91. https://doi.org/10.1038/nbt.2754

Huang, Z., Nelson, E. R., Smith, R. L., & Goodman, S. B. (2007). The Sequential Expression Profiles of Growth Factors from Osteroprogenitors to Osteoblasts In Vitro. *Tissue Engineering*, *13*(9), 2311–2320. https://doi.org/10.1089/ten.2006.0423

Hutchins, P. M., & Heinecke, J. W. (2015). Cholesterol efflux capacity, macrophage reverse cholesterol transport and cardioprotective HDL. *Current Opinion in Lipidology*, *26*(5), 388. https://doi.org/10.1097/MOL.0000000000000209

Ihrie, R. A., & Alvarez-Buylla, A. (2008). Cells in the astroglial lineage are neural stem cells. *Cell and Tissue Research*, *331*(1), 179–191. https://doi.org/10.1007/s00441-007-0461-z

Ikari, Y., McManus, B. M., Kenyon, J., & Schwartz, S. M. (1999). Neonatal intima formation in the human coronary artery. *Arteriosclerosis, Thrombosis, and Vascular Biology*, *19*(9), 2036–2040. https://doi.org/10.1161/01.atv.19.9.2036

Insull, W. (2009). The pathology of atherosclerosis: Plaque development and plaque responses to medical treatment. *The American Journal of Medicine*, *122*(1 Suppl), S3–S14. https://doi.org/10.1016/j.amjmed.2008.10.013

Iqbal, A. J., McNeill, E., Kapellos, T. S., Regan-Komito, D., Norman, S., Burd, S., Smart, N., Machemer, D. E. W., Stylianou, E., McShane, H., Channon, K. M., Chawla, A., & Greaves, D. R. (2014). Human CD68 promoter GFP transgenic mice allow analysis of monocyte to macrophage differentiation in vivo. *Blood*, *124*(15), e33–e44. https://doi.org/10.1182/blood-2014-04-568691

Ismail, N. A., Alavi, M. Z., & Moore, S. (1994). Lipoprotein-proteoglycan complexes from injured rabbit aortas accelerate lipoprotein uptake by arterial smooth muscle cells. *Atherosclerosis*, *105*(1), 79–87. https://doi.org/10.1016/0021-9150(94)90010-8

Jago, R., Sebire, S. J., Wood, L., Pool, L., Zahra, J., Thompson, J. L., & Lawlor, D. A. (2014). Associations between objectively assessed child and parental physical activity: A cross-sectional study of families with 5–6 year old children. *BMC Public Health*, *14*, 655. https://doi.org/10.1186/1471-2458-14-655

Johnson, C. P., Baugh, R., Wilson, C. A., & Burns, J. (2001). Age related changes in the tunica media of the vertebral artery: Implications for the assessment of vessels injured by trauma. *Journal of Clinical Pathology*, *54*(2), 139–145. https://doi.org/10.1136/jcp.54.2.139

Johnson, J. L., & Newby, A. C. (2009). Macrophage heterogeneity in atherosclerotic plaques. *Current Opinion in Lipidology*, *20*(5), 370–378. https://doi.org/10.1097/MOL.0b013e3283309848

Ju, H., Gros, R., You, X., Tsang, S., Husain, M., & Rabinovitch, M. (2001). Conditional and targeted overexpression of vascular chymase causes hypertension in transgenic mice. *Proceedings of the National Academy of Sciences of the United States of America*, *98*(13), 7469–7474. https://doi.org/10.1073/pnas.131147598

Kassiteridi, C., Cole, J. E., Griseri, T., Falck-Hansen, M., Goddard, M. E., Seneviratne, A. N., Green, P. A., Park, I., Shami, A. G., Pattarabanjird, T., Upadhye, A., Taylor, A. M., Handa, A., Channon, K. M., Lutgens, E., McNamara, C. A., Williams, R. O., & Monaco, C. (2021).

CD200 Limits Monopoiesis and Monocyte Recruitment in Atherosclerosis. *Circulation Research*, *129*(2), 280–295. https://doi.org/10.1161/CIRCRESAHA.119.316062

Katsuda, S., & Kaji, T. (2003). Atherosclerosis and extracellular matrix. *Journal of Atherosclerosis and Thrombosis*, *10*(5), 267–274. https://doi.org/10.5551/jat.10.267

Kawai, T., & Akira, S. (2011). Toll-like receptors and their crosstalk with other innate receptors in infection and immunity. *Immunity*, *34*(5), 637–650. https://doi.org/10.1016/j.immuni.2011.05.006

Kennedy, E., Hakimjavadi, R., Greene, C., Mooney, C. J., Fitzpatrick, E., Collins, L. E., Loscher, C. E., Guha, S., Morrow, D., Redmond, E. M., & Cahill, P. A. (2014). Embryonic rat vascular smooth muscle cells revisited—A model for neonatal, neointimal SMC or differentiated vascular stem cells? *Vascular Cell*, *6*(1), 6. https://doi.org/10.1186/2045-824X-6-6

Kennedy, E., Mooney, C. J., Hakimjavadi, R., Fitzpatrick, E., Guha, S., Collins, L. E., Loscher, C. E., Morrow, D., Redmond, E. M., & Cahill, P. A. (2014). Adult vascular smooth muscle cells in culture express neural stem cell markers typical of resident multipotent vascular stem cells. *Cell and Tissue Research*, *358*(1), 203–216. https://doi.org/10.1007/s00441-014-1937-2

Kennedy, M. A., Barrera, G. C., Nakamura, K., Baldán, Á., Tarr, P., Fishbein, M. C., Frank, J., Francone, O. L., & Edwards, P. A. (2005). ABCG1 has a critical role in mediating cholesterol efflux to HDL and preventing cellular lipid accumulation. *Cell Metabolism*, *1*(2), 121–131. https://doi.org/10.1016/j.cmet.2005.01.002

Khatana, C., Saini, N. K., Chakrabarti, S., Saini, V., Sharma, A., Saini, R. V., & Saini, A. K. (2020). Mechanistic Insights into the Oxidized Low-Density Lipoprotein-Induced Atherosclerosis.

Oxidative Medicine and Cellular Longevity, *2020*, e5245308. https://doi.org/10.1155/2020/5245308

Khazen, W., M'Bika, J.-P., Tomkiewicz, C., Benelli, C., Chany, C., Achour, A., & Forest, C. (2005). Expression of macrophage-selective markers in human and rodent adipocytes. *FEBS Letters*, *579*(25), 5631–5634. https://doi.org/10.1016/j.febslet.2005.09.032

Kim, H.-A., Choi, B., Suh, C.-H., Han, M. H., Jung, J.-Y., Sayeed, H. M., Kim, Y. W., & Sohn, S. (2017). Highly Expression of CD11b and CD32 on Peripheral Blood Mononuclear Cells from Patients with Adult-Onset Still's Disease. *International Journal of Molecular Sciences*, *18*(1), 202. https://doi.org/10.3390/ijms18010202

Kim, K., Doi, A., Wen, B., Ng, K., Zhao, R., Cahan, P., Kim, J., Aryee, M. J., Ji, H., Ehrlich, L. I. R., Yabuuchi, A., Takeuchi, A., Cunniff, K. C., Hongguang, H., Mckinney-Freeman, S., Naveiras, O., Yoon, T. J., Irizarry, R. A., Jung, N., … Daley, G. Q. (2010). Epigenetic memory in induced pluripotent stem cells. *Nature*, *467*(7313), 285–290. https://doi.org/10.1038/nature09342

Kim, K., Zhao, R., Doi, A., Ng, K., Unternaehrer, J., Cahan, P., Hongguang, H., Loh, Y.-H., Aryee, M. J., Lensch, M. W., Li, H., Collins, J. J., Feinberg, A. P., & Daley, G. Q. (2011). Donor cell type can influence the epigenome and differentiation potential of human induced pluripotent stem cells. *Nature Biotechnology*, *29*(12), 1117–1119. https://doi.org/10.1038/nbt.2052

Klappacher, G. W., & Glass, C. K. (2002). Roles of peroxisome proliferator-activated receptor γ in lipid homeostasis and inflammatory responses of macrophages. *Current Opinion in Lipidology*, *13*(3), 305.

Klatt, D., Cheng, E., Philipp, F., Selich, A., Dahlke, J., Schmidt, R. E., Schott, J. W., Büning, H., Hoffmann, D., Thrasher, A. J., & Schambach, A. (2019). Targeted Repair of p47-CGD in iPSCs by CRISPR/Cas9: Functional Correction without Cleavage in the Highly Homologous Pseudogenes. *Stem Cell Reports*, *13*(4), 590–598. https://doi.org/10.1016/j.stemcr.2019.08.008

Klebanoff, S. J. (1968). Myeloperoxidase-halide-hydrogen peroxide antibacterial system. *Journal of Bacteriology*, *95*(6), 2131–2138. https://doi.org/10.1128/jb.95.6.2131-2138.1968

Kohyama, M., Ise, W., Edelson, B. T., Wilker, P. R., Hildner, K., Mejia, C., Frazier, W. A., Murphy, T. L., & Murphy, K. M. (2009). Role for Spi-C in the development of red pulp macrophages and splenic iron homeostasis. *Nature*, *457*(7227), 318–321. https://doi.org/10.1038/nature07472

Kolodgie, F. D., Burke, A. P., Nakazawa, G., & Virmani, R. (2007). Is Pathologic Intimal Thickening the Key to Understanding Early Plaque Progression in Human Atherosclerotic Disease? *Arteriosclerosis, Thrombosis, and Vascular Biology*, *27*(5), 986–989. https://doi.org/10.1161/ATVBAHA.0000258865.44774.41

Koopman, R., Schaart, G., & Hesselink, M. K. (2001). Optimisation of oil red O staining permits combination with immunofluorescence and automated quantification of lipids. *Histochemistry and Cell Biology*, *116*(1), 63–68. https://doi.org/10.1007/s004180100297

Korshunov, V. A., & Berk, B. C. (2003). Flow-Induced Vascular Remodeling in the Mouse. *Arteriosclerosis, Thrombosis, and Vascular Biology*, *23*(12), 2185–2191. https://doi.org/10.1161/01.ATV.0000103120.06092.14

Kovacs, S. B., & Miao, E. A. (2017). Gasdermins: Effectors of Pyroptosis. *Trends in Cell Biology*, *27*(9), 673–684. https://doi.org/10.1016/j.tcb.2017.05.005

Koyanagi-Aoi, M., Ohnuki, M., Takahashi, K., Okita, K., Noma, H., Sawamura, Y., Teramoto, I., Narita, M., Sato, Y., Ichisaka, T., Amano, N., Watanabe, A., Morizane, A., Yamada, Y., Sato, T., Takahashi, J., & Yamanaka, S. (2013). Differentiation-defective phenotypes revealed by large-scale analyses of human pluripotent stem cells. *Proceedings of the National Academy of Sciences*, *110*(51), 20569–20574. https://doi.org/10.1073/pnas.1319061110

Kramann, R., Schneider, R. K., DiRocco, D. P., Machado, F., Fleig, S., Bondzie, P. A., Henderson, J. M., Ebert, B. L., & Humphreys, B. D. (2015). Perivascular Gli1+ Progenitors Are Key Contributors to Injury-Induced Organ Fibrosis. *Cell Stem Cell*, *16*(1), 51–66. https://doi.org/10.1016/j.stem.2014.11.004

Kurushima, H., Ramprasad, M., Kondratenko, N., Foster, D. M., Quehenberger, O., & Steinberg, D. (2000). Surface expression and rapid internalization of macrosialin (mouse CD68) on elicited mouse peritoneal macrophages. *Journal of Leukocyte Biology*, *67*(1), 104–108. https://doi.org/10.1002/jlb.67.1.104

Lampiasi, N., Russo, R., & Zito, F. (2016). The Alternative Faces of Macrophage Generate Osteoclasts. *BioMed Research International*, *2016*, e9089610. https://doi.org/10.1155/2016/9089610

Lan, T.-H., Huang, X.-Q., & Tan, H.-M. (2013). Vascular fibrosis in atherosclerosis. *Cardiovascular Pathology: The Official Journal of the Society for Cardiovascular Pathology*, *22*(5), 401–407. https://doi.org/10.1016/j.carpath.2013.01.003

Lee, C. Z. W., Kozaki, T., & Ginhoux, F. (2018). Studying tissue macrophages in vitro: Are iPSC-derived cells the answer? *Nature Reviews. Immunology*, *18*(11), 716–725. https://doi.org/10.1038/s41577-018-0054-y

Lemaitre, B., Nicolas, E., Michaut, L., Reichhart, J. M., & Hoffmann, J. A. (1996). The dorsoventral regulatory gene cassette spätzle/Toll/cactus controls the potent antifungal response in Drosophila adults. *Cell*, *86*(6), 973–983. https://doi.org/10.1016/s0092-8674(00)80172-5

Levin, R., Grinstein, S., & Canton, J. (2016). The life cycle of phagosomes: Formation, maturation, and resolution. *Immunological Reviews*, *273*(1), 156–179. https://doi.org/10.1111/imr.12439

Li, J., Huang, N. F., Zou, J., Laurent, T. J., Lee, J. C., Okogbaa, J., Cooke, J. P., & Ding, S. (2013). Conversion of Human Fibroblasts to Functional Endothelial Cells by Defined Factors. *Arteriosclerosis, Thrombosis, and Vascular Biology*, *33*(6), 1366–1375. https://doi.org/10.1161/ATVBAHA.112.301167

Li, K., Deng, Y., Deng, G., Chen, P., Wang, Y., Wu, H., Ji, Z., Yao, Z., Zhang, X., Yu, B., & Zhang, K. (2020). High cholesterol induces apoptosis and autophagy through the ROS-activated AKT/FOXO1 pathway in tendon-derived stem cells. *Stem Cell Research & Therapy*, *11*(1), 131. https://doi.org/10.1186/s13287-020-01643-5

Li, Y., Zhu, H., Zhang, Q., Han, X., Zhang, Z., Shen, L., Wang, L., Lui, K. O., He, B., & Zhou, B. (2021). Smooth muscle-derived macrophage-like cells contribute to multiple cell lineages in the atherosclerotic plaque. *Cell Discovery*, *7*(1), 111. https://doi.org/10.1038/s41421-021-00328-4

Liang, G., & Zhang, Y. (2013). Genetic and Epigenetic Variations in iPSCs: Potential Causes and Implications for Application. *Cell Stem Cell*, *13*(2), 149–159. https://doi.org/10.1016/j.stem.2013.07.001

Liao, J., Chen, X., Li, Y., Ge, Z., Duan, H., Zou, Y., & Ge, J. (2012). Transfer of Bone-Marrow-Derived Mesenchymal Stem Cells Influences Vascular Remodeling and Calcification after Balloon Injury in Hyperlipidemic Rats. *BioMed Research International*, *2012*, e165296. https://doi.org/10.1155/2012/165296

Libby, P. (2003). Vascular biology of atherosclerosis: Overview and state of the art. *The American Journal of Cardiology*, *91*(3A), 3A-6A. https://doi.org/10.1016/s0002-9149(02)03143-0

Libby, P. (2021). Inflammation during the life cycle of the atherosclerotic plaque. *Cardiovascular Research*, *117*(13), 2525–2536. https://doi.org/10.1093/cvr/cvab303

Libby, P., Loscalzo, J., Ridker, P. M., Farkouh, M. E., Hsue, P. Y., Fuster, V., Hasan, A. A., & Amar, S. (2018). Inflammation, Immunity, and Infection in Atherothrombosis: JACC Review Topic of the Week. *Journal of the American College of Cardiology*, *72*(17), 2071–2081. https://doi.org/10.1016/j.jacc.2018.08.1043

Lin, J.-D., Nishi, H., Poles, J., Niu, X., Mccauley, C., Rahman, K., Brown, E. J., Yeung, S. T., Vozhilla, N., Weinstock, A., Ramsey, S. A., Fisher, E. A., & Loke, P. (2019). Single-cell analysis of fate-mapped macrophages reveals heterogeneity, including stem-like properties, during atherosclerosis progression and regression. *JCI Insight*, *4*(4), e124574, 124574. https://doi.org/10.1172/jci.insight.124574

Liu, F.-T., & Rabinovich, G. A. (2005). Galectins as modulators of tumour progression. *Nature Reviews Cancer*, *5*(1), 29–41. https://doi.org/10.1038/nrc1527

Liu, M., Espinosa-Diez, C., Mahan, S., Du, M., Nguyen, A. T., Hahn, S., Chakraborty, R., Straub, A. C., Martin, K. A., Owens, G. K., & Gomez, D. (2021). H3K4 di-methylation governs smooth muscle lineage identity and promotes vascular homeostasis by restraining plasticity. *Developmental Cell*, *56*(19), 2765-2782.e10. https://doi.org/10.1016/j.devcel.2021.09.001

Liu, W., Harman, S., DiLuca, M., Burtenshaw, D., Corcoran, E., Cahill, P. A., & Redmond, E. M. (2020). Moderate Alcohol Consumption Targets S100β+ Vascular Stem Cells and Attenuates Injury-Induced Neointimal Hyperplasia. *Alcoholism, Clinical and Experimental Research*, *44*(9), 1734–1746. https://doi.org/10.1111/acer.14415

Liu, W., Redmond, E. M., Morrow, D., & Cullen, J. P. (2011). Differential effects of daily-moderate versus weekend-binge alcohol consumption on atherosclerotic plaque development in mice. *Atherosclerosis*, *219*(2), 448–454. https://doi.org/10.1016/j.atherosclerosis.2011.08.034

Liu, X., Guo, J.-W., Lin, X.-C., Tuo, Y.-H., Peng, W.-L., He, S.-Y., Li, Z.-Q., Ye, Y.-C., Yu, J., Zhang, F.-R., Ma, M.-M., Shang, J.-Y., Lv, X.-F., Zhou, A.-D., Ouyang, Y., Wang, C., Pang, R.-P., Sun, J.-X., Ou, J.-S., … Liang, S.-J. (2021). Macrophage NFATc3 prevents foam cell formation and atherosclerosis: Evidence and mechanisms. *European Heart Journal*, *42*(47), 4847–4861. https://doi.org/10.1093/eurheartj/ehab660

Liu, Y., Beyer, A., & Aebersold, R. (2016). On the Dependency of Cellular Protein Levels on mRNA Abundance. *Cell*, *165*(3), 535–550. https://doi.org/10.1016/j.cell.2016.03.014

Logovskaya, L. V., Bukharova, T. B., Volkov, A. V., Vikhrova, E. B., Makhnach, O. V., & Goldshtein, D. V. (2013). Induction of Osteogenic Differentiation of Multipotent Mesenchymal Stromal Cells from Human Adipose Tissue. *Bulletin of Experimental Biology and Medicine*, *155*(1), 145–150. https://doi.org/10.1007/s10517-013-2100-x

Lu, Z., Elliott, M. R., Chen, Y., Walsh, J. T., Klibanov, A. L., Ravichandran, K. S., & Kipnis, J. (2011). Phagocytic activity of neuronal progenitors regulates adult neurogenesis. *Nature Cell Biology*, *13*(9), 1076–1083. https://doi.org/10.1038/ncb2299

Luca, M. di, Hakimjavadi, R., Burtenshaw, D., Fitzpatrick, E., Mathiue, P., Lally, C., Cahill, E. M. R. and P. A., Luca, M. di, Hakimjavadi, R., Burtenshaw, D., Fitzpatrick, E., Mathiue, P., Lally, C., & Cahill, E. M. R. and P. A. (2018). The Dichotomy of Vascular Smooth Muscle Differentiation/De- Differentiation in Health and Disease. In *Muscle Cell and Tissue—Current Status of Research Field*. IntechOpen. https://doi.org/10.5772/intechopen.76812

Luque-Martin, R., Mander, P. K., Leenen, P. J. M., & Winther, M. P. J. (2021). Classic and new mediators for in vitro modelling of human macrophages. *Journal of Leukocyte Biology*, *109*(3), 549–560. https://doi.org/10.1002/JLB.1RU0620-018R

Luscinskas, F. W., Gerszten, R. E., Garcia-Zepeda, E. A., Lim, Y. C., Yoshida, M., Ding, H. A., Gimbrone, M. A., Luster, A. D., & Rosenzweig, A. (2000). C-C and C-X-C chemokines trigger firm adhesion of monocytes to vascular endothelium under flow conditions. *Annals of the New York Academy of Sciences*, *902*, 288–293. https://doi.org/10.1111/j.1749-6632.2000.tb06324.x

Lyadova, I., Gerasimova, T., & Nenasheva, T. (2021). Macrophages Derived From Human Induced Pluripotent Stem Cells: The Diversity of Protocols, Future Prospects, and Outstanding Questions. *Frontiers in Cell and Developmental Biology*, *9*, 640703. https://doi.org/10.3389/fcell.2021.640703

Maherali, N., Sridharan, R., Xie, W., Utikal, J., Eminli, S., Arnold, K., Stadtfeld, M., Yachechko, R., Tchieu, J., Jaenisch, R., Plath, K., & Hochedlinger, K. (2007). Directly Reprogrammed Fibroblasts Show Global Epigenetic Remodeling and Widespread Tissue Contribution. *Cell Stem Cell*, *1*(1), 55–70. https://doi.org/10.1016/j.stem.2007.05.014

Maiseyeu, A., Di, L., Ravodina, A., Barajas-Espinosa, A., Sakamoto, A., Chaplin, A., Zhong, J., Gao, H., Mignery, M., Narula, N., Finn, A. V., & Rajagopalan, S. (2022). Plaque-targeted, proteolysis-resistant, activatable and MRI-visible nano-GLP-1 receptor agonist targets smooth muscle cell differentiation in atherosclerosis. *Theranostics*, *12*(6), 2741–2757. https://doi.org/10.7150/thno.66456

Majesky, M. W. (2007). Developmental Basis of Vascular Smooth Muscle Diversity. *Arteriosclerosis, Thrombosis, and Vascular Biology*, *27*(6), 1248–1258. https://doi.org/10.1161/ATVBAHA.107.141069

Majesky, M. W., Dong, X. R., Hoglund, V., Mahoney, W. M., & Daum, G. (2011). The Adventitia. *Arteriosclerosis, Thrombosis, and Vascular Biology*, *31*(7), 1530–1539. https://doi.org/10.1161/ATVBAHA.110.221549

Majesky, M. W., Horita, H., Ostriker, A., Lu, S., Regan, J. N., Bagchi, A., Dong, X. R., Poczobutt, J., Nemenoff, R. A., & Weiser-Evans, M. C. M. (2017). Differentiated Smooth Muscle Cells Generate a Subpopulation of Resident Vascular Progenitor Cells in the Adventitia

Regulated by Klf4. *Circulation Research*, *120*(2), 296–311. https://doi.org/10.1161/CIRCRESAHA.116.309322

Mantovani, A., Biswas, S. K., Galdiero, M. R., Sica, A., & Locati, M. (2013). Macrophage plasticity and polarization in tissue repair and remodelling. *The Journal of Pathology*, *229*(2), 176–185. https://doi.org/10.1002/path.4133

Mantovani, A., Sica, A., Sozzani, S., Allavena, P., Vecchi, A., & Locati, M. (2004). The chemokine system in diverse forms of macrophage activation and polarization. *Trends in Immunology*, *25*(12), 677–686. https://doi.org/10.1016/j.it.2004.09.015

Marcel, Y. L., Ouimet, M., & Wang, M.-D. (2009). Cellular Lipid Traffic and Lipid Transporters: Regulation of Efflux and HDL Formation. In C. Ehnholm (Ed.), *Cellular Lipid Metabolism* (pp. 73–106). Springer. https://doi.org/10.1007/978-3-642-00300-4_3

Margariti, A., Winkler, B., Karamariti, E., Zampetaki, A., Tsai, T., Baban, D., Ragoussis, J., Huang, Y., Han, J.-D. J., Zeng, L., Hu, Y., & Xu, Q. (2012). Direct reprogramming of fibroblasts into endothelial cells capable of angiogenesis and reendothelialization in tissue-engineered vessels. *Proceedings of the National Academy of Sciences*, *109*(34), 13793–13798. https://doi.org/10.1073/pnas.1205526109

Martinez, F. O., & Gordon, S. (2014). The M1 and M2 paradigm of macrophage activation: Time for reassessment. *F1000Prime Reports*, *6*, 13. https://doi.org/10.12703/P6-13

Martinon, F., Mayor, A., & Tschopp, J. (2009). The inflammasomes: Guardians of the body. *Annual Review of Immunology*, *27*, 229–265. https://doi.org/10.1146/annurev.immunol.021908.132715

Mass, E., & Lachmann, N. (2021). From macrophage biology to macrophage-based cellular immunotherapies. *Gene Therapy*, *28*(9), 473–476. https://doi.org/10.1038/s41434-021-00221-5

Masui, S., Nakatake, Y., Toyooka, Y., Shimosato, D., Yagi, R., Takahashi, K., Okochi, H., Okuda, A., Matoba, R., Sharov, A. A., Ko, M. S. H., & Niwa, H. (2007). Pluripotency governed by Sox2 via regulation of Oct3/4 expression in mouse embryonic stem cells. *Nature Cell Biology*, *9*(6), 625–635. https://doi.org/10.1038/ncb1589

Maul, T. M., Chew, D. W., Nieponice, A., & Vorp, D. A. (2011a). Mechanical stimuli differentially control stem cell behavior: Morphology, proliferation, and differentiation. *Biomechanics and Modeling in Mechanobiology*, *10*(6), 939–953. https://doi.org/10.1007/s10237-010-0285-8

Maul, T. M., Chew, D. W., Nieponice, A., & Vorp, D. A. (2011b). Mechanical stimuli differentially control stem cell behavior: Morphology, proliferation, and differentiation. *Biomechanics and Modeling in Mechanobiology*, *10*(6), 939–953. https://doi.org/10.1007/s10237-010-0285-8

McClellan, M., Brown, N., Califf, R. M., & Warner, J. J. (2019). Call to Action: Urgent Challenges in Cardiovascular Disease: A Presidential Advisory From the American Heart Association. *Circulation*, *139*(9), e44–e54. https://doi.org/10.1161/CIR.0000000000000652

McDonald, O. G., & Owens, G. K. (2007). Programming Smooth Muscle Plasticity With Chromatin Dynamics. *Circulation Research*, *100*(10), 1428–1441. https://doi.org/10.1161/01.RES.0000266448.30370.a0

McDonald, O. G., Wamhoff, B. R., Hoofnagle, M. H., & Owens, G. K. (2006). Control of SRF binding to CArG box chromatin regulates smooth muscle gene expression in vivo. *The Journal of Clinical Investigation*, *116*(1), 36–48. https://doi.org/10.1172/JCI26505

Meijer, K., Weening, D., de Vries, M. P., Priebe, M. G., Vonk, R. J., & Roelofsen, H. (2015). Quantitative proteomics analyses of activation states of human THP-1 macrophages. *Journal of Proteomics*, *128*, 164–172. https://doi.org/10.1016/j.jprot.2015.07.013

Mi, Z., Rogers, D. A., Mirnics, Z. K., & Schor, N. F. (2009). p75NTR-dependent modulation of cellular handling of reactive oxygen species. *Journal of Neurochemistry*, *110*(1), 295–306. https://doi.org/10.1111/j.1471-4159.2009.06137.x

Milei, J., Ottaviani, G., Lavezzi, A. M., Grana, D. R., Stella, I., & Matturri, L. (2008). Perinatal and infant early atherosclerotic coronary lesions. *The Canadian Journal of Cardiology*, *24*(2), 137–141. https://doi.org/10.1016/s0828-282x(08)70570-1

Milioti, N., Bermudez-Fajardo, A., Penichet, M. L., & Oviedo-Orta, E. (2008). Antigen-induced immunomodulation in the pathogenesis of atherosclerosis. *Clinical & Developmental Immunology*, *2008*, 723539. https://doi.org/10.1155/2008/723539

Mills, C. D., Kincaid, K., Alt, J. M., Heilman, M. J., & Hill, A. M. (2000). M-1/M-2 macrophages and the Th1/Th2 paradigm. *Journal of Immunology (Baltimore, Md.: 1950)*, *164*(12), 6166–6173. https://doi.org/10.4049/jimmunol.164.12.6166

Milutinović, A., Šuput, D., & Zorc-Pleskovič, R. (2020). Pathogenesis of atherosclerosis in the tunica intima, media, and adventitia of coronary arteries: An updated review. *Bosnian Journal of Basic Medical Sciences*, *20*(1), 21–30. https://doi.org/10.17305/bjbms.2019.4320

Molony, C., King, D., Di Luca, M., Kitching, M., Olayinka, A., Hakimjavadi, R., Julius, L. A. N., Fitzpatrick, E., Gusti, Y., Burtenshaw, D., Healy, K., Finlay, E. K., Kernan, D., Llobera, A., Liu, W., Morrow, D., Redmond, E. M., Ducrée, J., & Cahill, P. A. (2021). Disease-Relevant Single Cell Photonic Signatures Identify S100β Stem Cells and their Myogenic Progeny in Vascular Lesions. *Stem Cell Reviews and Reports*, *17*(5), 1713–1740. https://doi.org/10.1007/s12015-021-10125-x

Moore, K. J., Koplev, S., Fisher, E. A., Tabas, I., Björkegren, J. L. M., Doran, A. C., & Kovacic, J. C. (2018). Macrophage Trafficking, Inflammatory Resolution, and Genomics in Atherosclerosis: JACC Macrophage in CVD Series (Part 2). *Journal of the American College of Cardiology*, *72*(18), 2181–2197. https://doi.org/10.1016/j.jacc.2018.08.2147

Moore, K. J., Sheedy, F. J., & Fisher, E. A. (2013). Macrophages in atherosclerosis: A dynamic balance. *Nature Reviews. Immunology*, *13*(10), 709–721. https://doi.org/10.1038/nri3520

Moore, K. J., & Tabas, I. (2011). Macrophages in the pathogenesis of atherosclerosis. *Cell*, *145*(3), 341–355. https://doi.org/10.1016/j.cell.2011.04.005

Moriya, J. (2019). Critical roles of inflammation in atherosclerosis. *Journal of Cardiology*, *73*(1), 22–27. https://doi.org/10.1016/j.jjcc.2018.05.010

Mulder, R., Banete, A., & Basta, S. (2014). Spleen-derived macrophages are readily polarized into classically activated (M1) or alternatively activated (M2) states. *Immunobiology*, *219*(10), 737–745. https://doi.org/10.1016/j.imbio.2014.05.005

Muller, P. A., Koscsó, B., Rajani, G. M., Stevanovic, K., Berres, M.-L., Hashimoto, D., Mortha, A., Leboeuf, M., Li, X.-M., Mucida, D., Stanley, E. R., Dahan, S., Margolis, K. G., Gershon, M.

D., Merad, M., & Bogunovic, M. (2014). Crosstalk between Muscularis Macrophages and Enteric Neurons Regulates Gastrointestinal Motility. *Cell*, *158*(2), 300–313. https://doi.org/10.1016/j.cell.2014.04.050

Murray, C. J., Lopez, A. D., & World Health Organization. (1996). *The global burden of disease: A comprehensive assessment of mortality and disability from diseases, injuries, and risk factors in 1990 and projected to 2020: Summary*. World Health Organization.

Murray, P. J. (2017). Macrophage Polarization. *Annual Review of Physiology*, *79*(Volume 79, 2017), 541–566. https://doi.org/10.1146/annurev-physiol-022516-034339

Murry, C. E., & Keller, G. (2008). Differentiation of embryonic stem cells to clinically relevant populations: Lessons from embryonic development. *Cell*, *132*(4), 661–680. https://doi.org/10.1016/j.cell.2008.02.008

Muse, E. D., Yu, S., Edillor, C. R., Tao, J., Spann, N. J., Troutman, T. D., Seidman, J. S., Henke, A., Roland, J. T., Ozeki, K. A., Thompson, B. M., McDonald, J. G., Bahadorani, J., Tsimikas, S., Grossman, T. R., Tremblay, M. S., & Glass, C. K. (2018). Cell-specific discrimination of desmosterol and desmosterol mimetics confers selective regulation of LXR and SREBP in macrophages. *Proceedings of the National Academy of Sciences of the United States of America*, *115*(20), E4680–E4689. https://doi.org/10.1073/pnas.1714518115

Nakagawa, M., Koyanagi, M., Tanabe, K., Takahashi, K., Ichisaka, T., Aoi, T., Okita, K., Mochiduki, Y., Takizawa, N., & Yamanaka, S. (2008). Generation of induced pluripotent stem cells without Myc from mouse and human fibroblasts. *Nature Biotechnology*, *26*(1), 101–106. https://doi.org/10.1038/nbt1374

Nakagawa, M., Takizawa, N., Narita, M., Ichisaka, T., & Yamanaka, S. (2010). Promotion of direct reprogramming by transformation-deficient Myc. *Proceedings of the National Academy of Sciences*, *107*(32), 14152–14157. https://doi.org/10.1073/pnas.1009374107

Nakamura, K., Kennedy, M. A., Baldán, Á., Bojanic, D. D., Lyons, K., & Edwards, P. A. (2004). Expression and Regulation of Multiple Murine ATP-binding Cassette Transporter G1 mRNAs/Isoforms That Stimulate Cellular Cholesterol Efflux to High Density Lipoprotein *. *Journal of Biological Chemistry*, *279*(44), 45980–45989. https://doi.org/10.1074/jbc.M408652200

Nakashima, Y., Fujii, H., Sumiyoshi, S., Wight, T. N., & Sueishi, K. (2007). Early human atherosclerosis: Accumulation of lipid and proteoglycans in intimal thickenings followed by macrophage infiltration. *Arteriosclerosis, Thrombosis, and Vascular Biology*, *27*(5), 1159–1165. https://doi.org/10.1161/ATVBAHA.106.134080

Nakashima, Y., Plump, A. S., Raines, E. W., Breslow, J. L., & Ross, R. (1994). ApoE-deficient mice develop lesions of all phases of atherosclerosis throughout the arterial tree. *Arteriosclerosis and Thrombosis: A Journal of Vascular Biology*, *14*(1), 133–140. https://doi.org/10.1161/01.atv.14.1.133

Nakashima, Y., Wight, T. N., & Sueishi, K. (2008). Early atherosclerosis in humans: Role of diffuse intimal thickening and extracellular matrix proteoglycans. *Cardiovascular Research*, *79*(1), 14–23. https://doi.org/10.1093/cvr/cvn099

Nam, D., Ni, C.-W., Rezvan, A., Suo, J., Budzyn, K., Llanos, A., Harrison, D., Giddens, D., & Jo, H. (2009). Partial carotid ligation is a model of acutely induced disturbed flow, leading to rapid endothelial dysfunction and atherosclerosis. *American Journal of Physiology. Heart*

and Circulatory Physiology, *297*(4), H1535-1543. https://doi.org/10.1152/ajpheart.00510.2009

Nemenoff, R. A., Horita, H., Ostriker, A. C., Furgeson, S. B., Simpson, P. A., VanPutten, V., Crossno, J., Offermanns, S., & Weiser-Evans, M. C. M. (2011). SDF-1α induction in mature smooth muscle cells by inactivation of PTEN is a critical mediator of exacerbated injury-induced neointima formation. *Arteriosclerosis, Thrombosis, and Vascular Biology*, *31*(6), 1300–1308. https://doi.org/10.1161/ATVBAHA.111.223701

New, S. E. P., Alvarez-Gonzalez, C., Vagaska, B., Gomez, S. G., Bulstrode, N. W., Madrigal, A., & Ferretti, P. (2015a). A matter of identity—Phenotype and differentiation potential of human somatic stem cells. *Stem Cell Research*, *15*(1), 1–13. https://doi.org/10.1016/j.scr.2015.04.003

New, S. E. P., Alvarez-Gonzalez, C., Vagaska, B., Gomez, S. G., Bulstrode, N. W., Madrigal, A., & Ferretti, P. (2015b). A matter of identity—Phenotype and differentiation potential of human somatic stem cells. *Stem Cell Research*, *15*(1), 1–13. https://doi.org/10.1016/j.scr.2015.04.003

Nimmerjahn, F., & Ravetch, J. V. (2008). Fcγ receptors as regulators of immune responses. *Nature Reviews Immunology*, *8*(1), 34–47. https://doi.org/10.1038/nri2206

Niwa, H., Ogawa, K., Shimosato, D., & Adachi, K. (2009). A parallel circuit of LIF signalling pathways maintains pluripotency of mouse ES cells. *Nature*, *460*(7251), 118–122. https://doi.org/10.1038/nature08113

North, R. J., & Mackaness, G. B. (1963). Electronmicroscopical Observations on the Peritoneal Macrophages of Normal Mice and Mice Immunised with Listeria monocytogenes. *British Journal of Experimental Pathology*, *44*(6), 608–611.

Okabe, Y., & Medzhitov, R. (2016). Tissue biology perspective on macrophages. *Nature Immunology*, *17*(1), 9–17. https://doi.org/10.1038/ni.3320

O'Shea, J. J., & Paul, W. E. (2010). Mechanisms Underlying Lineage Commitment and Plasticity of Helper CD4+ T Cells. *Science*, *327*(5969), 1098–1102. https://doi.org/10.1126/science.1178334

Ouimet, M., Barrett, T. J., & Fisher, E. A. (2019). HDL and Reverse Cholesterol Transport. *Circulation Research*, *124*(10), 1505–1518. https://doi.org/10.1161/CIRCRESAHA.119.312617

Ouimet, M., & Marcel, Y. L. (2012). Regulation of lipid droplet cholesterol efflux from macrophage foam cells. *Arteriosclerosis, Thrombosis, and Vascular Biology*, *32*(3), 575–581. https://doi.org/10.1161/ATVBAHA.111.240705

Ouyang, S., You, J., Zhi, C., Li, P., Lin, X., Tan, X., Ma, W., Li, L., & Xie, W. (2021). Ferroptosis: The potential value target in atherosclerosis. *Cell Death & Disease*, *12*(8), 782. https://doi.org/10.1038/s41419-021-04054-3

Owens, G. K. (1995). Regulation of differentiation of vascular smooth muscle cells. *Physiological Reviews*, *75*(3), 487–517. https://doi.org/10.1152/physrev.1995.75.3.487

Owens, G. K., Kumar, M. S., & Wamhoff, B. R. (2004). Molecular regulation of vascular smooth muscle cell differentiation in development and disease. *Physiological Reviews*, *84*(3), 767–801. https://doi.org/10.1152/physrev.00041.2003

Palinski, W., Hörkkö, S., Miller, E., Steinbrecher, U. P., Powell, H. C., Curtiss, L. K., & Witztum, J. L. (1996). Cloning of monoclonal autoantibodies to epitopes of oxidized lipoproteins from apolipoprotein E-deficient mice. Demonstration of epitopes of oxidized low density lipoprotein in human plasma. *The Journal of Clinical Investigation*, *98*(3), 800–814. https://doi.org/10.1172/JCI118853

Pan, H., Xue, C., Auerbach, B. J., Fan, J., Bashore, A. C., Cui, J., Yang, D. Y., Trignano, S. B., Liu, W., Shi, J., Ihuegbu, C. O., Bush, E. C., Worley, J., Vlahos, L., Laise, P., Solomon, R. A., Connolly, E. S., Califano, A., Sims, P. A., … Reilly, M. P. (2020). Single-Cell Genomics Reveals a Novel Cell State During Smooth Muscle Cell Phenotypic Switching and Potential Therapeutic Targets for Atherosclerosis in Mouse and Human. *Circulation*, *142*(21), 2060–2075. https://doi.org/10.1161/CIRCULATIONAHA.120.048378

Papakonstanti, E. a., & Stournaras, C. (2008). Cell responses regulated by early reorganization of actin cytoskeleton. *FEBS Letters*, *582*(14), 2120–2127. https://doi.org/10.1016/j.febslet.2008.02.064

Parhami, F., Mody, N., Gharavi, N., Ballard, A. J., Tintut, Y., & Demer, L. L. (2002). Role of the cholesterol biosynthetic pathway in osteoblastic differentiation of marrow stromal cells. *Journal of Bone and Mineral Research: The Official Journal of the American Society for Bone and Mineral Research*, *17*(11), 1997–2003. https://doi.org/10.1359/jbmr.2002.17.11.1997

Park, W. S., Heo, S. C., Jeon, E. S., Hong, D. H., Son, Y. K., Ko, J.-H., Kim, H. K., Lee, S. Y., Kim, J. H., & Han, J. (2013). Functional expression of smooth muscle-specific ion channels in TGF-β1-treated human adipose-derived mesenchymal stem cells. *American Journal of*

Physiology-Cell Physiology, *305*(4), C377–C391. https://doi.org/10.1152/ajpcell.00404.2012

Parkhurst, C. N., Yang, G., Ninan, I., Savas, J. N., Yates, J. R., Lafaille, J. J., Hempstead, B. L., Littman, D. R., & Gan, W.-B. (2013). Microglia Promote Learning-Dependent Synapse Formation through Brain-Derived Neurotrophic Factor. *Cell*, *155*(7), 1596–1609. https://doi.org/10.1016/j.cell.2013.11.030

Passman, J. N., Dong, X. R., Wu, S.-P., Maguire, C. T., Hogan, K. A., Bautch, V. L., & Majesky, M. W. (2008). A sonic hedgehog signaling domain in the arterial adventitia supports resident Sca1+ smooth muscle progenitor cells. *Proceedings of the National Academy of Sciences*, *105*(27), 9349–9354. https://doi.org/10.1073/pnas.0711382105

Patel, U., Rajasingh, S., Samanta, S., Cao, T., Dawn, B., & Rajasingh, J. (2017). Macrophage polarization in response to epigenetic modifiers during infection and inflammation. *Drug Discovery Today*, *22*(1), 186–193. https://doi.org/10.1016/j.drudis.2016.08.006

Peiser, L., Gough, P. J., Kodama, T., & Gordon, S. (2000). Macrophage Class A Scavenger Receptor-Mediated Phagocytosis of Escherichia coli: Role of Cell Heterogeneity, Microbial Strain, and Culture Conditions In Vitro. *Infection and Immunity*, *68*(4), 1953–1963. https://doi.org/10.1128/iai.68.4.1953-1963.2000

Phillips, M. C. (2014). Molecular Mechanisms of Cellular Cholesterol Efflux *. *Journal of Biological Chemistry*, *289*(35), 24020–24029. https://doi.org/10.1074/jbc.R114.583658

Plump, A. S., Smith, J. D., Hayek, T., Aalto-Setälä, K., Walsh, A., Verstuyft, J. G., Rubin, E. M., & Breslow, J. L. (1992). Severe hypercholesterolemia and atherosclerosis in apolipoprotein

E-deficient mice created by homologous recombination in ES cells. *Cell*, *71*(2), 343–353. https://doi.org/10.1016/0092-8674(92)90362-g

Poduri, A., Rateri, D. L., Howatt, D. A., Balakrishnan, A., Moorleghen, J. J., Cassis, L. A., & Daugherty, A. (2015). Fibroblast Angiotensin II Type 1a Receptors Contribute to Angiotensin II–Induced Medial Hyperplasia in the Ascending Aorta. *Arteriosclerosis, Thrombosis, and Vascular Biology*, *35*(9), 1995–2002. https://doi.org/10.1161/ATVBAHA.115.305995

Poole, K. E. S., van Bezooijen, R. L., Loveridge, N., Hamersma, H., Papapoulos, S. E., Löwik, C. W., & Reeve, J. (2005). Sclerostin is a delayed secreted product of osteocytes that inhibits bone formation. *FASEB Journal: Official Publication of the Federation of American Societies for Experimental Biology*, *19*(13), 1842–1844. https://doi.org/10.1096/fj.05-4221fje

Porta, C., Riboldi, E., Ippolito, A., & Sica, A. (2015). Molecular and epigenetic basis of macrophage polarized activation. *Seminars in Immunology*, *27*(4), 237–248. https://doi.org/10.1016/j.smim.2015.10.003

Potter, C. M. F., Lao, K. H., Zeng, L., & Xu, Q. (2014). Role of Biomechanical Forces in Stem Cell Vascular Lineage Differentiation. *Arteriosclerosis, Thrombosis, and Vascular Biology*, *34*(10), 2184–2190. https://doi.org/10.1161/ATVBAHA.114.303423

Poznyak, A. V., Wu, W.-K., Melnichenko, A. A., Wetzker, R., Sukhorukov, V., Markin, A. M., Khotina, V. A., & Orekhov, A. N. (2020). Signaling Pathways and Key Genes Involved in Regulation of foam Cell Formation in Atherosclerosis. *Cells*, *9*(3), Article 3. https://doi.org/10.3390/cells9030584

Pryma, C. S., Ortega, C., Dubland, J. A., & Francis, G. A. (2019). Pathways of smooth muscle foam cell formation in atherosclerosis. *Current Opinion in Lipidology*, *30*(2), 117–124. https://doi.org/10.1097/MOL.0000000000000574

Psaltis, P. J., Harbuzariu, A., Delacroix, S., Witt, T. A., Holroyd, E. W., Spoon, D. B., Hoffman, S. J., Pan, S., Kleppe, L. S., Mueske, C. S., Gulati, R., Sandhu, G. S., & Simari, R. D. (2012). Identification of a monocyte-predisposed hierarchy of hematopoietic progenitor cells in the adventitia of postnatal murine aorta. *Circulation*, *125*(4), 592–603. https://doi.org/10.1161/CIRCULATIONAHA.111.059360

Pugsley, M. K., & Tabrizchi, R. (2000). The vascular system. An overview of structure and function. *Journal of Pharmacological and Toxicological Methods*, *44*(2), 333–340. https://doi.org/10.1016/s1056-8719(00)00125-8

Putra, A., Alif, I., Hamra, N., Santosa, O., Kustiyah, A. R., Muhar, A. M., & Lukman, K. (2020). MSC-released TGF-β regulate α-SMA expression of myofibroblast during wound healing. *Journal of Stem Cells & Regenerative Medicine*, *16*(2), 73–79. https://doi.org/10.46582/jsrm.1602011

Que, X., Hung, M.-Y., Yeang, C., Gonen, A., Prohaska, T. A., Sun, X., Diehl, C., Määttä, A., Gaddis, D. E., Bowden, K., Pattison, J., MacDonald, J. G., Ylä-Herttuala, S., Mellon, P. L., Hedrick, C. C., Ley, K., Miller, Y. I., Glass, C. K., Peterson, K. L., … Witztum, J. L. (2018). Oxidized phospholipids are proinflammatory and proatherogenic in hypercholesterolaemic mice. *Nature*, *558*(7709), 301–306. https://doi.org/10.1038/s41586-018-0198-8

Rabinovitch, M. (1995). Professional and non-professional phagocytes: An introduction. *Trends in Cell Biology*, *5*(3), 85–87. https://doi.org/10.1016/s0962-8924(00)88955-2

Rahman, K., Vengrenyuk, Y., Ramsey, S. A., Vila, N. R., Girgis, N. M., Liu, J., Gusarova, V., Gromada, J., Weinstock, A., Moore, K. J., Loke, P., & Fisher, E. A. (2017). Inflammatory Ly6Chi monocytes and their conversion to M2 macrophages drive atherosclerosis regression. *The Journal of Clinical Investigation*, *127*(8), 2904–2915. https://doi.org/10.1172/JCI75005

Ramprasad, M. P., Terpstra, V., Kondratenko, N., Quehenberger, O., & Steinberg, D. (1996). Cell surface expression of mouse macrosialin and human CD68 and their role as macrophage receptors for oxidized low density lipoprotein. *Proceedings of the National Academy of Sciences of the United States of America*, *93*(25), 14833–14838. https://doi.org/10.1073/pnas.93.25.14833

Raponi, E., Agenes, F., Delphin, C., Assard, N., Baudier, J., Legraverend, C., & Deloulme, J.-C. (2007). S100B expression defines a state in which GFAP-expressing cells lose their neural stem cell potential and acquire a more mature developmental stage. *Glia*, *55*(2), 165–177. https://doi.org/10.1002/glia.20445

Rasheed, A., & Rayner, K. J. (2021). Macrophage Responses to Environmental Stimuli During Homeostasis and Disease. *Endocrine Reviews*, *42*(4), 407–435. https://doi.org/10.1210/endrev/bnab004

Raymond, C. K., Pownder, T. A., & Sexson, S. L. (1999). General method for plasmid construction using homologous recombination. *BioTechniques*, *26*(1), 134–138, 140–141. https://doi.org/10.2144/99261rr02

Redheuil, A., Yu, W.-C., Wu, C. O., Mousseaux, E., de Cesare, A., Yan, R., Kachenoura, N., Bluemke, D., & Lima, J. A. C. (2010). Reduced Ascending Aortic Strain and Distensibility. *Hypertension*, *55*(2), 319–326. https://doi.org/10.1161/HYPERTENSIONAHA.109.141275

Reinert, R. B., Kantz, J., Misfeldt, A. A., Poffenberger, G., Gannon, M., Brissova, M., & Powers, A. C. (2012). Tamoxifen-Induced Cre-loxP Recombination Is Prolonged in Pancreatic Islets of Adult Mice. *PLOS ONE*, *7*(3), e33529. https://doi.org/10.1371/journal.pone.0033529

Robbins, C. S., Hilgendorf, I., Weber, G. F., Theurl, I., Iwamoto, Y., Figueiredo, J.-L., Gorbatov, R., Sukhova, G. K., Gerhardt, L. M. S., Smyth, D., Zavitz, C. C. J., Shikatani, E. A., Parsons, M., van Rooijen, N., Lin, H. Y., Husain, M., Libby, P., Nahrendorf, M., Weissleder, R., & Swirski, F. K. (2013). Local proliferation dominates lesional macrophage accumulation in atherosclerosis. *Nature Medicine*, *19*(9), 1166–1172. https://doi.org/10.1038/nm.3258

Rong, J. X., Shapiro, M., Trogan, E., & Fisher, E. A. (2003). Transdifferentiation of mouse aortic smooth muscle cells to a macrophage-like state after cholesterol loading. *Proceedings of the National Academy of Sciences of the United States of America*, *100*(23), 13531–13536. https://doi.org/10.1073/pnas.1735526100

Roos, D. (1991). The involvement of oxygen radicals in microbicidal mechanisms of leukocytes and macrophages. *Klinische Wochenschrift*, *69*(21), 975–980. https://doi.org/10.1007/BF01645142

Roostalu, U., Aldeiri, B., Albertini, A., Humphreys, N., Simonsen-Jackson, M., Wong, J. K. F., & Cossu, G. (2018). Distinct Cellular Mechanisms Underlie Smooth Muscle Turnover in Vascular Development and Repair. *Circulation Research*, *122*(2), 267–281. https://doi.org/10.1161/CIRCRESAHA.117.312111

Rosamond, W., Flegal, K., Friday, G., Furie, K., Go, A., Greenlund, K., Haase, N., Ho, M., Howard, V., Kissela, B., Kittner, S., Lloyd-Jones, D., McDermott, M., Meigs, J., Moy, C., Nichol, G., O'Donnell, C. J., Roger, V., Rumsfeld, J., … Hong, Y. (2007). Heart Disease and Stroke Statistics—2007 Update. *Circulation*, *115*(5), e69–e171. https://doi.org/10.1161/CIRCULATIONAHA.106.179918

Ross Russell. (1999). Atherosclerosis—An Inflammatory Disease. *New England Journal of Medicine*, *340*(2), 115–126. https://doi.org/10.1056/NEJM199901143400207

Rothermundt, M., Peters, M., Prehn, J. H. M., & Arolt, V. (2003). S100B in brain damage and neurodegeneration. *Microscopy Research and Technique*, *60*(6), 614–632. https://doi.org/10.1002/jemt.10303

Sage, A. P., & Mallat, Z. (2014). Multiple potential roles for B cells in atherosclerosis. *Annals of Medicine*, *46*(5), 297–303. https://doi.org/10.3109/07853890.2014.900272

Sage, A. P., Tsiantoulas, D., Binder, C. J., & Mallat, Z. (2019). The role of B cells in atherosclerosis. *Nature Reviews. Cardiology*, *16*(3), 180–196. https://doi.org/10.1038/s41569-018-0106-9

Sainz, J., Al Haj Zen, A., Caligiuri, G., Demerens, C., Urbain, D., Lemitre, M., & Lafont, A. (2006). Isolation of "Side Population" Progenitor Cells From Healthy Arteries of Adult Mice. *Arteriosclerosis, Thrombosis, and Vascular Biology*, *26*(2), 281–286. https://doi.org/10.1161/01.ATV.0000197793.83391.91

Sakamoto, A., Torii, S., Jinnouchi, H., Finn, A. V., Virmani, R., & Kolodgie, F. D. (2018). Pathologic intimal thickening: Are we any closer to understand early transitional plaques that lead

to symptomatic disease? *Atherosclerosis*, *274*, 227–229. https://doi.org/10.1016/j.atherosclerosis.2018.04.033

Sanchez, L. A., & Veith, F. J. (1998). Diagnosis and treatment of chronic lower extremity ischemia. *Vascular Medicine (London, England)*, *3*(4), 291–299. https://doi.org/10.1177/1358836X9800300405

Sartore, S., Chiavegato, A., Faggin, E., Franch, R., Puato, M., Ausoni, S., & Pauletto, P. (2001). Contribution of adventitial fibroblasts to neointima formation and vascular remodeling: From innocent bystander to active participant. *Circulation Research*, *89*(12), 1111–1121. https://doi.org/10.1161/hh2401.100844

Sata, M. (2003). Circulating Vascular Progenitor Cells Contribute to Vascular Repair, Remodeling, and Lesion Formation. *Trends in Cardiovascular Medicine*, *13*(6), 249–253. https://doi.org/10.1016/S1050-1738(03)00106-3

Sawai, C. M., Babovic, S., Upadhaya, S., Knapp, D. J. H. F., Lavin, Y., Lau, C. M., Goloborodko, A., Feng, J., Fujisaki, J., Ding, L., Mirny, L. A., Merad, M., Eaves, C. J., & Reizis, B. (2016). Hematopoietic Stem Cells Are the Major Source of Multilineage Hematopoiesis in Adult Animals. *Immunity*, *45*(3), 597–609. https://doi.org/10.1016/j.immuni.2016.08.007

Schaftenaar, F., Frodermann, V., Kuiper, J., & Lutgens, E. (2016). Atherosclerosis: The interplay between lipids and immune cells. *Current Opinion in Lipidology*, *27*(3), 209–215. https://doi.org/10.1097/MOL.0000000000000302

Schenkel, A. R., Mamdouh, Z., & Muller, W. A. (2004). Locomotion of monocytes on endothelium is a critical step during extravasation. *Nature Immunology*, *5*(4), 393–400. https://doi.org/10.1038/ni1051

Schenten, D., & Medzhitov, R. (2011). The control of adaptive immune responses by the innate immune system. *Advances in Immunology*, *109*, 87–124. https://doi.org/10.1016/B978-0-12-387664-5.00003-0

Schiele, T. M. (2005). Current understanding of coronary in-stent restenosis. Pathophysiology, clinical presentation, diagnostic work-up, and management. *Zeitschrift Fur Kardiologie*, *94*(11), 772–790. https://doi.org/10.1007/s00392-005-0299-x

Schlegel, M., Sharma, M., Brown, E. J., Newman, A. A. C., Cyr, Y., Afonso, M. S., Corr, E. M., Koelwyn, G. J., van Solingen, C., Guzman, J., Farhat, R., Nikain, C. A., Shanley, L. C., Peled, D., Schmidt, A. M., Fisher, E. A., & Moore, K. J. (2021). Silencing Myeloid Netrin-1 Induces Inflammation Resolution and Plaque Regression. *Circulation Research*, *129*(5), 530–546. https://doi.org/10.1161/CIRCRESAHA.121.319313

Schmitz, B., Vischer, P., Brand, E., Schmidt-Petersen, K., Korb-Pap, A., Guske, K., Nedele, J., Schelleckes, M., Hillen, J., Rötrige, A., Simmet, T., Paul, M., Cambien, F., & Brand, S.-M. (2013). Increased monocyte adhesion by endothelial expression of VCAM-1 missense variation in vitro. *Atherosclerosis*, *230*(2), 185–190. https://doi.org/10.1016/j.atherosclerosis.2013.07.039

Schneider, C. A., Rasband, W. S., & Eliceiri, K. W. (2012). NIH Image to ImageJ: 25 years of image analysis. *Nature Methods*, *9*(7), Article 7. https://doi.org/10.1038/nmeth.2089

Schonkeren, D., van der Hoorn, M.-L., Khedoe, P., Swings, G., van Beelen, E., Claas, F., van Kooten, C., de Heer, E., & Scherjon, S. (2011). Differential distribution and phenotype of decidual macrophages in preeclamptic versus control pregnancies. *The American Journal of Pathology*, *178*(2), 709–717. https://doi.org/10.1016/j.ajpath.2010.10.011

Schulz, C., Perdiguero, E. G., Chorro, L., Szabo-Rogers, H., Cagnard, N., Kierdorf, K., Prinz, M., Wu, B., Jacobsen, S. E. W., Pollard, J. W., Frampton, J., Liu, K. J., & Geissmann, F. (2012). A Lineage of Myeloid Cells Independent of Myb and Hematopoietic Stem Cells. *Science*, *336*(6077), 86–90. https://doi.org/10.1126/science.1219179

Schwartz, S. M., deBlois, D., & O'Brien, E. R. (1995). The intima. Soil for atherosclerosis and restenosis. *Circulation Research*, *77*(3), 445–465. https://doi.org/10.1161/01.res.77.3.445

Scott, C. L., Zheng, F., De Baetselier, P., Martens, L., Saeys, Y., De Prijck, S., Lippens, S., Abels, C., Schoonooghe, S., Raes, G., Devoogdt, N., Lambrecht, B. N., Beschin, A., & Guilliams, M. (2016). Bone marrow-derived monocytes give rise to self-renewing and fully differentiated Kupffer cells. *Nature Communications*, *7*(1), 10321. https://doi.org/10.1038/ncomms10321

Serhan, C. N. (2014). Pro-resolving lipid mediators are leads for resolution physiology. *Nature*, *510*(7503), 92–101. https://doi.org/10.1038/nature13479

Seri, B., García-Verdugo, J. M., Collado-Morente, L., McEwen, B. S., & Alvarez-Buylla, A. (2004). Cell types, lineage, and architecture of the germinal zone in the adult dentate gyrus. *Journal of Comparative Neurology*, *478*(4), 359–378. https://doi.org/10.1002/cne.20288

Shankman, L. S., Gomez, D., Cherepanova, O. A., Salmon, M., Alencar, G. F., Haskins, R. M., Swiatlowska, P., Newman, A. A. C., Greene, E. S., Straub, A. C., Isakson, B., Randolph, G. J., & Owens, G. K. (2015). KLF4-dependent phenotypic modulation of smooth muscle cells has a key role in atherosclerotic plaque pathogenesis. *Nature Medicine*, *21*(6), 628–637. https://doi.org/10.1038/nm.3866

Shapouri-Moghaddam, A., Mohammadian, S., Vazini, H., Taghadosi, M., Esmaeili, S.-A., Mardani, F., Seifi, B., Mohammadi, A., Afshari, J. T., & Sahebkar, A. (2018). Macrophage plasticity, polarization, and function in health and disease. *Journal of Cellular Physiology*, *233*(9), 6425–6440. https://doi.org/10.1002/jcp.26429

Shariq, M., Sahasrabuddhe, V., Krishna, S., Radha, S., Nruthyathi, null, Bellampalli, R., Dwivedi, A., Cheramangalam, R., Reizis, B., Hébert, J., & Ghosh, H. S. (2021). Adult neural stem cells have latent inflammatory potential that is kept suppressed by Tcf4 to facilitate adult neurogenesis. *Science Advances*, *7*(21), eabf5606. https://doi.org/10.1126/sciadv.abf5606

Sharma, M., Schlegel, M. P., Afonso, M. S., Brown, E. J., Rahman, K., Weinstock, A., Sansbury, B. E., Corr, E. M., van Solingen, C., Koelwyn, G. J., Shanley, L. C., Beckett, L., Peled, D., Lafaille, J. J., Spite, M., Loke, P., Fisher, E. A., & Moore, K. J. (2020). Regulatory T Cells License Macrophage Pro-Resolving Functions During Atherosclerosis Regression. *Circulation Research*, *127*(3), 335–353. https://doi.org/10.1161/CIRCRESAHA.119.316461

Shaw, L. J., Bairey Merz, C. N., Pepine, C. J., Reis, S. E., Bittner, V., Kelsey, S. F., Olson, M., Johnson, B. D., Mankad, S., Sharaf, B. L., Rogers, W. J., Wessel, T. R., Arant, C. B., Pohost, G. M., Lerman, A., Quyyumi, A. A., & Sopko, G. (2006). Insights From the NHLBI-Sponsored Women's Ischemia Syndrome Evaluation (WISE) Study: Part I: Gender Differences in Traditional and Novel Risk Factors, Symptom Evaluation, and Gender-Optimized Diagnostic Strategies. *Journal of the American College of Cardiology*, *47*(3, Supplement), S4–S20. https://doi.org/10.1016/j.jacc.2005.01.072

Shi, C., & Pamer, E. G. (2011). Monocyte recruitment during infection and inflammation. *Nature Reviews. Immunology*, *11*(11), 762–774. https://doi.org/10.1038/nri3070

Shi, H., Wang, Q., Zhang, Q., Leng, L., & Li, H. (2010). Tissue expression characterization of chicken adipocyte fatty acid-binding protein and its expression difference between fat and lean birds in abdominal fat tissue. *Poultry Science*, *89*(2), 197–202. https://doi.org/10.3382/ps.2009-00397

Shi, L., Jiang, Q., Bushkin, Y., Subbian, S., & Tyagi, S. (2019). Biphasic Dynamics of Macrophage Immunometabolism during Mycobacterium tuberculosis Infection. *mBio*, *10*(2), e02550-18. https://doi.org/10.1128/mBio.02550-18

Shi, N., & Chen, S.-Y. (2016). Smooth Muscle Cell Differentiation: Model Systems, Regulatory Mechanisms, and Vascular Diseases. *Journal of Cellular Physiology*, *231*(4), 777–787. https://doi.org/10.1002/jcp.25208

Shibata, Y., Abiko, Y., & Takiguchi, H. (1991). Macrophage Membrane: Structure and Function. In J. R. Harris (Ed.), *Megakaryocytes, Platelets, Macrophages, and Eosinophils* (pp. 209–236). Springer US. https://doi.org/10.1007/978-1-4757-9531-8_8

Shikatani, E. A., Chandy, M., Besla, R., Li, C. C., Momen, A., El-Mounayri, O., Robbins, C. S., & Husain, M. (2016). C-Myb Regulates Proliferation and Differentiation of Adventitial Sca1+ Vascular Smooth Muscle Cell Progenitors by Transactivation of Myocardin. *Arteriosclerosis, Thrombosis, and Vascular Biology*, *36*(7), 1367–1376. https://doi.org/10.1161/ATVBAHA.115.307116

Shimizu, K., Sugiyama, S., Aikawa, M., Fukumoto, Y., Rabkin, E., Libby, P., & Mitchell, R. N. (2001). Host bone-marrow cells are a source of donor intimal smooth- muscle-like cells

in murine aortic transplant arteriopathy. *Nature Medicine*, *7*(6), 738–741. https://doi.org/10.1038/89121

Sica, A., & Mantovani, A. (2012). Macrophage plasticity and polarization: In vivo veritas. *The Journal of Clinical Investigation*, *122*(3), 787–795. https://doi.org/10.1172/JCI59643

Sinha, S., Iyer, D., & Granata, A. (2014). Embryonic origins of human vascular smooth muscle cells: Implications for in vitro modeling and clinical application. *Cellular and Molecular Life Sciences: CMLS*, *71*(12), 2271–2288. https://doi.org/10.1007/s00018-013-1554-3

Skalli, O., Pelte, M. F., Peclet, M. C., Gabbiani, G., Gugliotta, P., Bussolati, G., Ravazzola, M., & Orci, L. (1989). Alpha-smooth muscle actin, a differentiation marker of smooth muscle cells, is present in microfilamentous bundles of pericytes. *The Journal of Histochemistry and Cytochemistry: Official Journal of the Histochemistry Society*, *37*(3), 315–321. https://doi.org/10.1177/37.3.2918221

Soehnlein, O., & Libby, P. (2021). Targeting inflammation in atherosclerosis—From experimental insights to the clinic. *Nature Reviews Drug Discovery*, *20*(8), 589–610. https://doi.org/10.1038/s41573-021-00198-1

Sorokin, V., Vickneson, K., Kofidis, T., Woo, C. C., Lin, X. Y., Foo, R., & Shanahan, C. M. (2020). Role of Vascular Smooth Muscle Cell Plasticity and Interactions in Vessel Wall Inflammation. *Frontiers in Immunology*, *11*, 599415. https://doi.org/10.3389/fimmu.2020.599415

Souilhol, C., Serbanovic-Canic, J., Fragiadaki, M., Chico, T. J., Ridger, V., Roddie, H., & Evans, P. C. (2020). Endothelial responses to shear stress in atherosclerosis: A novel role for

developmental genes. *Nature Reviews. Cardiology*, *17*(1), 52–63. https://doi.org/10.1038/s41569-019-0239-5

Spann, N. J., Garmire, L. X., McDonald, J. G., Myers, D. S., Milne, S. B., Shibata, N., Reichart, D., Fox, J. N., Shaked, I., Heudobler, D., Raetz, C. R. H., Wang, E. W., Kelly, S. L., Sullards, M. C., Murphy, R. C., Merrill, A. H., Brown, H. A., Dennis, E. A., Li, A. C., … Glass, C. K. (2012). Regulated accumulation of desmosterol integrates macrophage lipid metabolism and inflammatory responses. *Cell*, *151*(1), 138–152. https://doi.org/10.1016/j.cell.2012.06.054

Spin, J. M., Maegdefessel, L., & Tsao, P. S. (2012). Vascular smooth muscle cell phenotypic plasticity: Focus on chromatin remodelling. *Cardiovascular Research*, *95*(2), 147–155. https://doi.org/10.1093/cvr/cvs098

Spin, J. M., Nallamshetty, S., Tabibiazar, R., Ashley, E. A., King, J. Y., Chen, M., Tsao, P. S., & Quertermous, T. (2004). Transcriptional profiling of in vitro smooth muscle cell differentiation identifies specific patterns of gene and pathway activation. *Physiological Genomics*, *19*(3), 292–302. https://doi.org/10.1152/physiolgenomics.00148.2004

Spin, J. M., Quertermous, T., & Tsao, P. S. (2010). Chromatin Remodeling Pathways in Smooth Muscle Cell Differentiation, and Evidence for an Integral Role for p300. *PLOS ONE*, *5*(12), e14301. https://doi.org/10.1371/journal.pone.0014301

Spitznagel, J. K. (1990). Antibiotic proteins of human neutrophils. *Journal of Clinical Investigation*, *86*(5), 1381–1386. https://doi.org/10.1172/JCI114851

Susser, L. I., & Rayner, K. J. (2022). Through the layers: How macrophages drive atherosclerosis across the vessel wall. *The Journal of Clinical Investigation*, *132*(9). https://doi.org/10.1172/JCI157011

Swirski, F. K., Libby, P., Aikawa, E., Alcaide, P., Luscinskas, F. W., Weissleder, R., & Pittet, M. J. (2007). Ly-6Chi monocytes dominate hypercholesterolemia-associated monocytosis and give rise to macrophages in atheromata. *The Journal of Clinical Investigation*, *117*(1), 195–205. https://doi.org/10.1172/JCI29950

Swirski, F. K., & Nahrendorf, M. (2014). Do vascular smooth muscle cells differentiate to macrophages in atherosclerotic lesions? *Circulation Research*, *115*(7), 605–606. https://doi.org/10.1161/CIRCRESAHA.114.304925

Tabas, I., & Bornfeldt, K. E. (2016). Macrophage Phenotype and Function in Different Stages of Atherosclerosis. *Circulation Research*, *118*(4), 653–667. https://doi.org/10.1161/CIRCRESAHA.115.306256

Takahashi, K., & Yamanaka, S. (2006). Induction of Pluripotent Stem Cells from Mouse Embryonic and Adult Fibroblast Cultures by Defined Factors. *Cell*, *126*(4), 663–676. https://doi.org/10.1016/j.cell.2006.07.024

Takata, K., Kozaki, T., Lee, C. Z. W., Thion, M. S., Otsuka, M., Lim, S., Utami, K. H., Fidan, K., Park, D. S., Malleret, B., Chakarov, S., See, P., Low, D., Low, G., Garcia-Miralles, M., Zeng, R., Zhang, J., Goh, C. C., Gul, A., … Ginhoux, F. (2017). Induced-Pluripotent-Stem-Cell-Derived Primitive Macrophages Provide a Platform for Modeling Tissue-Resident Macrophage Differentiation and Function. *Immunity*, *47*(1), 183-198.e6. https://doi.org/10.1016/j.immuni.2017.06.017

Takayanagi, H., Kim, S., Koga, T., Nishina, H., Isshiki, M., Yoshida, H., Saiura, A., Isobe, M., Yokochi, T., Inoue, J., Wagner, E. F., Mak, T. W., Kodama, T., & Taniguchi, T. (2002). Induction and activation of the transcription factor NFATc1 (NFAT2) integrate RANKL signaling in terminal differentiation of osteoclasts. *Developmental Cell*, *3*(6), 889–901. https://doi.org/10.1016/s1534-5807(02)00369-6

Tamoutounour, S., Guilliams, M., Montanana Sanchis, F., Liu, H., Terhorst, D., Malosse, C., Pollet, E., Ardouin, L., Luche, H., Sanchez, C., Dalod, M., Malissen, B., & Henri, S. (2013). Origins and Functional Specialization of Macrophages and of Conventional and Monocyte-Derived Dendritic Cells in Mouse Skin. *Immunity*, *39*(5), 925–938. https://doi.org/10.1016/j.immuni.2013.10.004

Tanabe, K., Nakamura, M., Narita, M., Takahashi, K., & Yamanaka, S. (2013). Maturation, not initiation, is the major roadblock during reprogramming toward pluripotency from human fibroblasts. *Proceedings of the National Academy of Sciences*, *110*(30), 12172–12179. https://doi.org/10.1073/pnas.1310291110

Tang, J., Wang, H., Huang, X., Li, F., Zhu, H., Li, Y., He, L., Zhang, H., Pu, W., Liu, K., Zhao, H., Bentzon, J. F., Yu, Y., Ji, Y., Nie, Y., Tian, X., Zhang, L., Gao, D., & Zhou, B. (2020). Arterial Sca1+ Vascular Stem Cells Generate De Novo Smooth Muscle for Artery Repair and Regeneration. *Cell Stem Cell*, *26*(1), 81-96.e4. https://doi.org/10.1016/j.stem.2019.11.010

Tang, Z., Wang, A., Yuan, F., Yan, Z., Liu, B., Chu, J. S., Helms, J. A., & Li, S. (2012). Differentiation of multipotent vascular stem cells contributes to vascular diseases. *Nature Communications*, *3*(1), Article 1. https://doi.org/10.1038/ncomms1867

Taniguchi, Y., Choi, P. J., Li, G.-W., Chen, H., Babu, M., Hearn, J., Emili, A., & Xie, X. S. (2010). Quantifying E. coli Proteome and Transcriptome with Single-Molecule Sensitivity in Single Cells. *Science*, *329*(5991), 533–538. https://doi.org/10.1126/science.1188308

Tarling, E. J., & Edwards, P. A. (2011). ATP binding cassette transporter G1 (ABCG1) is an intracellular sterol transporter. *Proceedings of the National Academy of Sciences*, *108*(49), 19719–19724. https://doi.org/10.1073/pnas.1113021108

Tasnim, F., Xing, J., Huang, X., Mo, S., Wei, X., Tan, M.-H., & Yu, H. (2019). Generation of mature kupffer cells from human induced pluripotent stem cells. *Biomaterials*, *192*, 377–391. https://doi.org/10.1016/j.biomaterials.2018.11.016

Taura, D., Noguchi, M., Sone, M., Hosoda, K., Mori, E., Okada, Y., Takahashi, K., Homma, K., Oyamada, N., Inuzuka, M., Sonoyama, T., Ebihara, K., Tamura, N., Itoh, H., Suemori, H., Nakatsuji, N., Okano, H., Yamanaka, S., & Nakao, K. (2009). Adipogenic differentiation of human induced pluripotent stem cells: Comparison with that of human embryonic stem cells. *FEBS Letters*, *583*(6), 1029–1033. https://doi.org/10.1016/j.febslet.2009.02.031

Tellides, G., & Pober, J. S. (2015). Inflammatory and immune responses in the arterial media. *Circulation Research*, *116*(2), 312–322. https://doi.org/10.1161/CIRCRESAHA.116.301312

Tesfamariam, B., & Cohen, R. A. (1992). Free radicals mediate endothelial cell dysfunction caused by elevated glucose. *American Journal of Physiology-Heart and Circulatory Physiology*, *263*(2), H321–H326. https://doi.org/10.1152/ajpheart.1992.263.2.H321

Thelin, N., Holmberg, S., & Thelin, A. (2006). Knee injuries account for the sports-related increased risk of knee osteoarthritis. *Scandinavian Journal of Medicine & Science in Sports*, *16*(5), 329–333. https://doi.org/10.1111/j.1600-0838.2005.00497.x

Theofilis, P., Oikonomou, E., Tsioufis, K., & Tousoulis, D. (2023). The Role of Macrophages in Atherosclerosis: Pathophysiologic Mechanisms and Treatment Considerations. *International Journal of Molecular Sciences*, *24*(11), Article 11. https://doi.org/10.3390/ijms24119568

Thomas, C. A., Li, Y., Kodama, T., Suzuki, H., Silverstein, S. C., & El Khoury, J. (2000). Protection from Lethal Gram-Positive Infection by Macrophage Scavenger Receptor–Dependent Phagocytosis. *Journal of Experimental Medicine*, *191*(1), 147–156. https://doi.org/10.1084/jem.191.1.147

Tieu, B. C., Lee, C., Sun, H., Lejeune, W., Recinos, A., Ju, X., Spratt, H., Guo, D.-C., Milewicz, D., Tilton, R. G., & Brasier, A. R. (2009). An adventitial IL-6/MCP1 amplification loop accelerates macrophage-mediated vascular inflammation leading to aortic dissection in mice. *The Journal of Clinical Investigation*, *119*(12), 3637–3651. https://doi.org/10.1172/JCI38308

Tintut, Y., Alfonso, Z., Saini, T., Radcliff, K., Watson, K., Boström, K., & Demer, L. L. (2003). Multilineage potential of cells from the artery wall. *Circulation*, *108*(20), 2505–2510. https://doi.org/10.1161/01.CIR.0000096485.64373.C5

Tirkkonen, L., Haimi, S., Huttunen, S., Wolff, J., Pirhonen, E., Sándor, G. K., & Miettinen, S. (2013). Osteogenic medium is superior to growth factors in differentiation of human

adipose stem cells towards bone-forming cells in 3D culture. *European Cells & Materials*, *25*, 144–158. https://doi.org/10.22203/ecm.v025a10

Tokumoto, Y., Ogawa, S., Nagamune, T., & Miyake, J. (2010). Comparison of efficiency of terminal differentiation of oligodendrocytes from induced pluripotent stem cells versus embryonic stem cells in vitro. *Journal of Bioscience and Bioengineering*, *109*(6), 622–628. https://doi.org/10.1016/j.jbiosc.2009.11.013

Torsney, E., Hu, Y., & Xu, Q. (2005). Adventitial progenitor cells contribute to arteriosclerosis. *Trends in Cardiovascular Medicine*, *15*(2), 64–68. https://doi.org/10.1016/j.tcm.2005.02.003

Trinick, T. R., & Duly, E. B. (2013). Hyperlipidemia: Overview. In B. Caballero (Ed.), *Encyclopedia of Human Nutrition (Third Edition)* (pp. 442–452). Academic Press. https://doi.org/10.1016/B978-0-12-375083-9.00148-3

Tsai, T.-N., Kirton, J. P., Campagnolo, P., Zhang, L., Xiao, Q., Zhang, Z., Wang, W., Hu, Y., & Xu, Q. (2012). Contribution of stem cells to neointimal formation of decellularized vessel grafts in a novel mouse model. *The American Journal of Pathology*, *181*(1), 362–373. https://doi.org/10.1016/j.ajpath.2012.03.021

Tsuchiya, S., Kobayashi, Y., Goto, Y., Okumura, H., Nakae, S., Konno, T., & Tada, K. (1982). Induction of maturation in cultured human monocytic leukemia cells by a phorbol diester. *Cancer Research*, *42*(4), 1530–1536.

Ueno, N., & Wilson, M. E. (2012). Receptor-mediated phagocytosis of Leishmania: Implications for intracellular survival. *Trends in Parasitology*, *28*(8), 335–344. https://doi.org/10.1016/j.pt.2012.05.002

Underhill, D. M., & Goodridge, H. S. (2012). Information processing during phagocytosis. *Nature Reviews Immunology*, *12*(7), 492–502. https://doi.org/10.1038/nri3244

Uribe-Querol, E., & Rosales, C. (2020). Phagocytosis: Our Current Understanding of a Universal Biological Process. *Frontiers in Immunology*, *11*, 1066. https://doi.org/10.3389/fimmu.2020.01066

van de Laar, L., Saelens, W., De Prijck, S., Martens, L., Scott, C. L., Van Isterdael, G., Hoffmann, E., Beyaert, R., Saeys, Y., Lambrecht, B. N., & Guilliams, M. (2016). Yolk Sac Macrophages, Fetal Liver, and Adult Monocytes Can Colonize an Empty Niche and Develop into Functional Tissue-Resident Macrophages. *Immunity*, *44*(4), 755–768. https://doi.org/10.1016/j.immuni.2016.02.017

van der Laan, L. J. W., Döpp, E. A., Haworth, R., Pikkarainen, T., Kangas, M., Elomaa, O., Dijkstra, C. D., Gordon, S., Tryggvason, K., & Kraal, G. (1999). Regulation and Functional Involvement of Macrophage Scavenger Receptor MARCO in Clearance of Bacteria In Vivo. *The Journal of Immunology*, *162*(2), 939–947. https://doi.org/10.4049/jimmunol.162.2.939

van Furth, R., Cohn, Z. A., Hirsch, J. G., Humphrey, J. H., Spector, W. G., & Langevoort, H. L. (1972). The mononuclear phagocyte system: A new classification of macrophages, monocytes, and their precursor cells. *Bulletin of the World Health Organization*, *46*(6), 845–852.

van Gils, J. M., Derby, M. C., Fernandes, L. R., Ramkhelawon, B., Ray, T. D., Rayner, K. J., Parathath, S., Distel, E., Feig, J. L., Alvarez-Leite, J. I., Rayner, A. J., McDonald, T. O., O'Brien, K. D., Stuart, L. M., Fisher, E. A., Lacy-Hulbert, A., & Moore, K. J. (2012). The

neuroimmune guidance cue netrin-1 promotes atherosclerosis by inhibiting the emigration of macrophages from plaques. *Nature Immunology*, *13*(2), 136–143. https://doi.org/10.1038/ni.2205

van Gils, J. M., Ramkhelawon, B., Fernandes, L., Stewart, M. C., Guo, L., Seibert, T., Menezes, G. B., Cara, D. C., Chow, C., Kinane, T. B., Fisher, E. A., Balcells, M., Alvarez-Leite, J., Lacy-Hulbert, A., & Moore, K. J. (2013). Endothelial expression of guidance cues in vessel wall homeostasis dysregulation under proatherosclerotic conditions. *Arteriosclerosis, Thrombosis, and Vascular Biology*, *33*(5), 911–919. https://doi.org/10.1161/ATVBAHA.112.301155

Velican, C., & Velican, D. (1981). Coronary intimal necrosis occurring as an early stage of atherosclerotic involvement. *Atherosclerosis*, *39*(4), 479–496. https://doi.org/10.1016/0021-9150(81)90006-X

Vengrenyuk, Y., Nishi, H., Long, X., Ouimet, M., Savji, N., Martinez, F. O., Cassella, C. P., Moore, K. J., Ramsey, S. A., Miano, J. M., & Fisher, E. A. (2015). Cholesterol loading reprograms the microRNA-143/145-myocardin axis to convert aortic smooth muscle cells to a dysfunctional macrophage-like phenotype. *Arteriosclerosis, Thrombosis, and Vascular Biology*, *35*(3), 535–546. https://doi.org/10.1161/ATVBAHA.114.304029

Virani, S. S., Alonso, A., Aparicio, H. J., Benjamin, E. J., Bittencourt, M. S., Callaway, C. W., Carson, A. P., Chamberlain, A. M., Cheng, S., Delling, F. N., Elkind, M. S. V., Evenson, K. R., Ferguson, J. F., Gupta, D. K., Khan, S. S., Kissela, B. M., Knutson, K. L., Lee, C. D., Lewis, T. T., … null, null. (2021). Heart Disease and Stroke Statistics—2021 Update. *Circulation*, *143*(8), e254–e743. https://doi.org/10.1161/CIR.0000000000000950

Virmani, R., Kolodgie, F. D., Burke, A. P., Farb, A., & Schwartz, S. M. (2000). Lessons from sudden coronary death: A comprehensive morphological classification scheme for atherosclerotic lesions. *Arteriosclerosis, Thrombosis, and Vascular Biology*, *20*(5), 1262–1275. https://doi.org/10.1161/01.atv.20.5.1262

Vogel, C., & Marcotte, E. M. (2012). Insights into the regulation of protein abundance from proteomic and transcriptomic analyses. *Nature Reviews Genetics*, *13*(4), 227–232. https://doi.org/10.1038/nrg3185

Wagner, D. E., & Klein, A. M. (2020). Lineage tracing meets single-cell omics: Opportunities and challenges. *Nature Reviews. Genetics*, *21*(7), 410–427. https://doi.org/10.1038/s41576-020-0223-2

Wakil, S. J. (1989). Fatty acid synthase, a proficient multifunctional enzyme. *Biochemistry*, *28*(11), 4523–4530. https://doi.org/10.1021/bi00437a001

Waller, B. F., Orr, C. M., Slack, J. D., Pinkerton, C. A., Van Tassel, J., & Peters, T. (1992). Anatomy, histology, and pathology of coronary arteries: A review relevant to new interventional and imaging techniques--Part I. *Clinical Cardiology*, *15*(6), 451–457. https://doi.org/10.1002/clc.4960150613

Wang, D., Wang, Z., Zhang, L., & Wang, Y. (2017). Roles of Cells from the Arterial Vessel Wall in Atherosclerosis. *Mediators of Inflammation*, *2017*, 1–9. https://doi.org/10.1155/2017/8135934

Wang, G., Jacquet, L., Karamariti, E., & Xu, Q. (2015). Origin and differentiation of vascular smooth muscle cells. *The Journal of Physiology*, *593*(14), 3013–3030. https://doi.org/10.1113/JP270033

Wang, N., Lan, D., Chen, W., Matsuura, F., & Tall, A. R. (2004). ATP-binding cassette transporters G1 and G4 mediate cellular cholesterol efflux to high-density lipoproteins. *Proceedings of the National Academy of Sciences*, *101*(26), 9774–9779. https://doi.org/10.1073/pnas.0403506101

Wang, N., Liang, H., & Zen, K. (2014). Molecular mechanisms that influence the macrophage m1-m2 polarization balance. *Frontiers in Immunology*, *5*, 614. https://doi.org/10.3389/fimmu.2014.00614

Wang, Y., Dubland, J. A., Allahverdian, S., Asonye, E., Sahin, B., Jaw, J. E., Sin, D. D., Seidman, M. A., Leeper, N. J., & Francis, G. A. (2019). Smooth Muscle Cells Contribute the Majority of Foam Cells in ApoE (Apolipoprotein E)-Deficient Mouse Atherosclerosis. *Arteriosclerosis, Thrombosis, and Vascular Biology*, *39*(5), 876–887. https://doi.org/10.1161/ATVBAHA.119.312434

Wang, Y., Nanda, V., Direnzo, D., Ye, J., Xiao, S., Kojima, Y., Howe, K. L., Jarr, K.-U., Flores, A. M., Tsantilas, P., Tsao, N., Rao, A., Newman, A. A. C., Eberhard, A. V., Priest, J. R., Ruusalepp, A., Pasterkamp, G., Maegdefessel, L., Miller, C. L., … Leeper, N. J. (2020). Clonally expanding smooth muscle cells promote atherosclerosis by escaping efferocytosis and activating the complement cascade. *Proceedings of the National Academy of Sciences of the United States of America*, *117*(27), 15818–15826. https://doi.org/10.1073/pnas.2006348117

Wang, Y., Zhao, Y., Ye, T., Yang, L., Shen, Y., & Li, H. (2021). Ferroptosis Signaling and Regulators in Atherosclerosis. *Frontiers in Cell and Developmental Biology*, *9*, 809457. https://doi.org/10.3389/fcell.2021.809457

Weisser, S. B., McLarren, K. W., Kuroda, E., & Sly, L. M. (2013). Generation and characterization of murine alternatively activated macrophages. *Methods in Molecular Biology (Clifton, N.J.)*, *946*, 225–239. https://doi.org/10.1007/978-1-62703-128-8_14

Weissman, I. L. (2000). Stem cells: Units of development, units of regeneration, and units in evolution. *Cell*, *100*(1), 157–168. https://doi.org/10.1016/s0092-8674(00)81692-x

Williams, J. W., Zaitsev, K., Kim, K.-W., Ivanov, S., Saunders, B. T., Schrank, P. R., Kim, K., Elvington, A., Kim, S. H., Tucker, C. G., Wohltmann, M., Fife, B. T., Epelman, S., Artyomov, M. N., Lavine, K. J., Zinselmeyer, B. H., Choi, J.-H., & Randolph, G. J. (2020). Limited proliferation capacity of aortic intima resident macrophages requires monocyte recruitment for atherosclerotic plaque progression. *Nature Immunology*, *21*(10), 1194–1204. https://doi.org/10.1038/s41590-020-0768-4

Williams, K. J., & Tabas, I. (1995). The response-to-retention hypothesis of early atherogenesis. *Arteriosclerosis, Thrombosis, and Vascular Biology*, *15*(5), 551–561. https://doi.org/10.1161/01.atv.15.5.551

Williams, N. C., & O'Neill, L. A. J. (2018). A Role for the Krebs Cycle Intermediate Citrate in Metabolic Reprogramming in Innate Immunity and Inflammation. *Frontiers in Immunology*, *9*, 141. https://doi.org/10.3389/fimmu.2018.00141

Winkels, H., Ehinger, E., Vassallo, M., Buscher, K., Dinh, H. Q., Kobiyama, K., Hamers, A. A. J., Cochain, C., Vafadarnejad, E., Saliba, A.-E., Zernecke, A., Pramod, A. B., Ghosh, A. K., Anto Michel, N., Hoppe, N., Hilgendorf, I., Zirlik, A., Hedrick, C. C., Ley, K., & Wolf, D. (2018). Atlas of the Immune Cell Repertoire in Mouse Atherosclerosis Defined by Single-

Cell RNA-Sequencing and Mass Cytometry. *Circulation Research*, *122*(12), 1675–1688. https://doi.org/10.1161/CIRCRESAHA.117.312513

Wu, L., Lv, Y., Lv, Y., Xiang, S., Zhao, Z., Tang, Z., Ou, L., Yan, B., Xiao, X., Wen, G., Cao, R., & Yang, J. (2021). A novel secretagogin/ATF4 pathway is involved in oxidized LDL-induced endoplasmic reticulum stress and islet β-cell apoptosis. *Acta Biochimica et Biophysica Sinica*, *53*(1), 54–62. https://doi.org/10.1093/abbs/gmaa142

Xi, J., Khalil, M., Shishechian, N., Hannes, T., Pfannkuche, K., Liang, H., Fatima, A., Haustein, M., Suhr, F., Bloch, W., Reppel, M., Šarić, T., Wernig, M., Jänisch, R., Brockmeier, K., Hescheler, J., & Pillekamp, F. (2010). Comparison of contractile behavior of native murine ventricular tissue and cardiomyocytes derived from embryonic or induced pluripotent stem cells. *The FASEB Journal*, *24*(8), 2739–2751. https://doi.org/10.1096/fj.09-145177

Xiao, L., Liu, Y., & Wang, N. (2014). New paradigms in inflammatory signaling in vascular endothelial cells. *American Journal of Physiology-Heart and Circulatory Physiology*, *306*(3), H317–H325. https://doi.org/10.1152/ajpheart.00182.2013

Xu, F., Ji, J., Li, L., Chen, R., & Hu, W. (2007). Activation of adventitial fibroblasts contributes to the early development of atherosclerosis: A novel hypothesis that complements the “Response-to-Injury Hypothesis” and the “Inflammation Hypothesis.” *Medical Hypotheses*, *69*(4), 908–912. https://doi.org/10.1016/j.mehy.2007.01.062

Xu, F., Liu, Y., Shi, L., Liu, W., Zhang, L., Cai, H., Qi, J., Cui, Y., Wang, W., & Hu, Y. (2015). NADPH oxidase p47phox siRNA attenuates adventitial fibroblasts proliferation and migration in

apoE(-/-) mouse. *Journal of Translational Medicine*, *13*, 38. https://doi.org/10.1186/s12967-015-0407-2

Xu, H., Manivannan, A., Crane, I., Dawson, R., & Liversidge, J. (2008). Critical but divergent roles for CD62L and CD44 in directing blood monocyte trafficking in vivo during inflammation. *Blood*, *112*(4), 1166–1174. https://doi.org/10.1182/blood-2007-06-098327

Xu, Y.-J., Zheng, L., Hu, Y.-W., & Wang, Q. (2018). Pyroptosis and its relationship to atherosclerosis. *Clinica Chimica Acta; International Journal of Clinical Chemistry*, *476*, 28–37. https://doi.org/10.1016/j.cca.2017.11.005

Yan, F., Liu, Y.-F., Liu, Y., & Zhao, Y.-X. (2008). KLF4: A novel target for the treatment of atherosclerosis. *Medical Hypotheses*, *70*(4), 845–847. https://doi.org/10.1016/j.mehy.2007.07.031

Yan, H.-F., Zou, T., Tuo, Q.-Z., Xu, S., Li, H., Belaidi, A. A., & Lei, P. (2021). Ferroptosis: Mechanisms and links with diseases. *Signal Transduction and Targeted Therapy*, *6*(1), 49. https://doi.org/10.1038/s41392-020-00428-9

Yao, Y., Xu, X.-H., & Jin, L. (2019). Macrophage Polarization in Physiological and Pathological Pregnancy. *Frontiers in Immunology*, *10*. https://doi.org/10.3389/fimmu.2019.00792

Yap, C., Mieremet, A., de Vries, C. J. M., Micha, D., & de Waard, V. (2021). Six Shades of Vascular Smooth Muscle Cells Illuminated by KLF4 (Krüppel-Like Factor 4). *Arteriosclerosis, Thrombosis, and Vascular Biology*, *41*(11), 2693–2707. https://doi.org/10.1161/ATVBAHA.121.316600

Yeung, A. T. Y., Hale, C., Lee, A. H., Gill, E. E., Bushell, W., Parry-Smith, D., Goulding, D., Pickard, D., Roumeliotis, T., Choudhary, J., Thomson, N., Skarnes, W. C., Dougan, G., & Hancock,

R. E. W. (2017). Exploiting induced pluripotent stem cell-derived macrophages to unravel host factors influencing Chlamydia trachomatis pathogenesis. *Nature Communications*, *8*, 15013. https://doi.org/10.1038/ncomms15013

Ylä-Herttuala, S., Palinski, W., Rosenfeld, M. E., Parthasarathy, S., Carew, T. E., Butler, S., Witztum, J. L., & Steinberg, D. (1989). Evidence for the presence of oxidatively modified low density lipoprotein in atherosclerotic lesions of rabbit and man. *The Journal of Clinical Investigation*, *84*(4), 1086–1095. https://doi.org/10.1172/JCI114271

You, X.-M., Mungrue, I. N., Kalair, W., Afroze, T., Ravi, B., Sadi, A. M., Gros, R., & Husain, M. (2003). Conditional expression of a dominant-negative c-Myb in vascular smooth muscle cells inhibits arterial remodeling after injury. *Circulation Research*, *92*(3), 314–321. https://doi.org/10.1161/01.res.0000056758.73215.5a

Yu, E. P. K., Reinhold, J., Yu, H., Starks, L., Uryga, A. K., Foote, K., Finigan, A., Figg, N., Pung, Y.-F., Logan, A., Murphy, M. P., & Bennett, M. (2017). Mitochondrial Respiration Is Reduced in Atherosclerosis, Promoting Necrotic Core Formation and Reducing Relative Fibrous Cap Thickness. *Arteriosclerosis, Thrombosis, and Vascular Biology*, *37*(12), 2322–2332. https://doi.org/10.1161/ATVBAHA.117.310042

Yu, L., Zhang, Y., Liu, C., Wu, X., Wang, S., Sui, W., Zhang, Y., Zhang, C., & Zhang, M. (2023). Heterogeneity of macrophages in atherosclerosis revealed by single-cell RNA sequencing. *FASEB Journal: Official Publication of the Federation of American Societies for Experimental Biology*, *37*(3), e22810. https://doi.org/10.1096/fj.202201932RR

Yu, X.-H., Fu, Y.-C., Zhang, D.-W., Yin, K., & Tang, C.-K. (2013). Foam cells in atherosclerosis. *Clinica Chimica Acta; International Journal of Clinical Chemistry*, *424*, 245–252. https://doi.org/10.1016/j.cca.2013.06.006

Yu, X.-H., Zhang, D.-W., Zheng, X.-L., & Tang, C.-K. (2019). Cholesterol transport system: An integrated cholesterol transport model involved in atherosclerosis. *Progress in Lipid Research*, *73*, 65–91. https://doi.org/10.1016/j.plipres.2018.12.002

Yuan, F., Wang, D., Xu, K., Wang, J., Zhang, Z., Yang, L., Yang, G.-Y., & Li, S. (2017). Contribution of Vascular Cells to Neointimal Formation. *PLOS ONE*, *12*(1), e0168914. https://doi.org/10.1371/journal.pone.0168914

Yunna, C., Mengru, H., Lei, W., & Weidong, C. (2020). Macrophage M1/M2 polarization. *European Journal of Pharmacology*, *877*, 173090. https://doi.org/10.1016/j.ejphar.2020.173090

Yurdagul, A. (2021). Metabolic Consequences of Efferocytosis and its Impact on Atherosclerosis. *Immunometabolism*, *3*(2), e210017. https://doi.org/10.20900/immunometab20210017

Yurdagul, A., Subramanian, M., Wang, X., Crown, S. B., Ilkayeva, O. R., Darville, L., Kolluru, G. K., Rymond, C. C., Gerlach, B. D., Zheng, Z., Kuriakose, G., Kevil, C. G., Koomen, J. M., Cleveland, J. L., Muoio, D. M., & Tabas, I. (2020). Macrophage Metabolism of Apoptotic Cell-Derived Arginine Promotes Continual Efferocytosis and Resolution of Injury. *Cell Metabolism*, *31*(3), 518-533.e10. https://doi.org/10.1016/j.cmet.2020.01.001

Yusuf, S., Reddy, S., Ôunpuu, S., & Anand, S. (2001). Global Burden of Cardiovascular Diseases. *Circulation*, *104*(22), 2746–2753. https://doi.org/10.1161/hc4601.099487

Zachary, I., & Morgan, R. D. (2011). Therapeutic angiogenesis for cardiovascular disease: Biological context, challenges, prospects. *Heart*, *97*(3), 181–189. https://doi.org/10.1136/hrt.2009.180414

Zadelaar, S., Kleemann, R., Verschuren, L., de Vries-Van der Weij, J., van der Hoorn, J., Princen, H. M., & Kooistra, T. (2007). Mouse models for atherosclerosis and pharmaceutical modifiers. *Arteriosclerosis, Thrombosis, and Vascular Biology*, *27*(8), 1706–1721. https://doi.org/10.1161/ATVBAHA.107.142570

Zarbock, A., Abram, C. L., Hundt, M., Altman, A., Lowell, C. A., & Ley, K. (2008). PSGL-1 engagement by E-selectin signals through Src kinase Fgr and ITAM adapters DAP12 and FcR gamma to induce slow leukocyte rolling. *The Journal of Experimental Medicine*, *205*(10), 2339–2347. https://doi.org/10.1084/jem.20072660

Zhang, D.-D., Song, Y., Kong, P., Xu, X., Gao, Y.-K., Dou, Y.-Q., Weng, L., Wang, X.-W., Lin, Y.-L., Zhang, F., Zhang, H., & Han, M. (2021). Smooth muscle 22 alpha protein inhibits VSMC foam cell formation by supporting normal LXRα signaling, ameliorating atherosclerosis. *Cell Death & Disease*, *12*(11), 982. https://doi.org/10.1038/s41419-021-04239-w

Zhang, F., Guo, X., Xia, Y., & Mao, L. (2021). An update on the phenotypic switching of vascular smooth muscle cells in the pathogenesis of atherosclerosis. *Cellular and Molecular Life Sciences*, *79*(1), 6. https://doi.org/10.1007/s00018-021-04079-z

Zhang, H., Shi, J., Hachet, M. A., Xue, C., Bauer, R. C., Jiang, H., Li, W., Tohyama, J., Millar, J., Billheimer, J., Phillips, M. C., Razani, B., Rader, D. J., & Reilly, M. P. (2017). CRISPR/Cas9-Mediated Gene Editing in Human iPSC-Derived Macrophage Reveals Lysosomal Acid

Lipase Function in Human Macrophages-Brief Report. *Arteriosclerosis, Thrombosis, and Vascular Biology*, *37*(11), 2156–2160. https://doi.org/10.1161/ATVBAHA.117.310023

Zhang, L., Xue, S., Ren, F., Huang, S., Zhou, R., Wang, Y., Zhou, C., & Li, Z. (2021). An atherosclerotic plaque-targeted single-chain antibody for MR/NIR-II imaging of atherosclerosis and anti-atherosclerosis therapy. *Journal of Nanobiotechnology*, *19*(1), 296. https://doi.org/10.1186/s12951-021-01047-4

Zhang, X., McDonald, J. G., Aryal, B., Canfrán-Duque, A., Goldberg, E. L., Araldi, E., Ding, W., Fan, Y., Thompson, B. M., Singh, A. K., Li, Q., Tellides, G., Ordovás-Montanes, J., García Milian, R., Dixit, V. D., Ikonen, E., Suárez, Y., & Fernández-Hernando, C. (2021). Desmosterol suppresses macrophage inflammasome activation and protects against vascular inflammation and atherosclerosis. *Proceedings of the National Academy of Sciences of the United States of America*, *118*(47), e2107682118. https://doi.org/10.1073/pnas.2107682118

Zhou, J., Li, Y.-S., & Chien, S. (2014). Shear stress-initiated signaling and its regulation of endothelial function. *Arteriosclerosis, Thrombosis, and Vascular Biology*, *34*(10), 2191–2198. https://doi.org/10.1161/ATVBAHA.114.303422

Zorc-Pleskovič, R., Pleskovič, A., Vraspir-Porenta, O., Zorc, M., & Milutinović, A. (2018). Immune cells and vasa vasorum in the tunica media of atherosclerotic coronary arteries. *Bosnian Journal of Basic Medical Sciences*, *18*(3), 240–245. https://doi.org/10.17305/bjbms.2018.2951